Stony Brook University

OFFICIAL COPY

The official electronic file of this thesis or dissertation is maintained by the University Libraries on behalf of The Graduate School at Stony Brook University.

© All Rights Reserved by Author.

Using Direct Measurements of Submarine Groundwater Discharge to Investigate the Coupling Between Surface and Pore Waters

A Dissertation Presented

by

John Paul Rapaglia

to

The Graduate School

In Partial Fulfillment of the

Requirements

for the Degree of

Doctor of Philosophy

in

Marine and Atmospheric Science

Stony Brook University

December 2007

Stony Brook University

The Graduate School

John Paul Rapaglia

We, the dissertation committee for the above candidate for the

doctor of philosophy degree, hereby recommend

acceptance of this dissertation

Dr. Henry Bokuniewicz-Dissertation Advisor
Full Professor, Marine Sciences Research Center

Dr. James Kirk Cochran-Chairperson of Defense
Full Professor, Marine Sciences Research Center

Dr. Sergio Sañudo-Wilhemy
Full Professor, Marine Sciences Research Center

Dr. Teng-Fong Wong
Department Chair, Geosciences

Dr. Luca Zaggia
Research Scientist, National Research Council of Italy (CNR-ISMAR)

This dissertation is accepted by the Graduate School

Lawrence Martin
Dean of the graduate School

Abstract of the Dissertation

Using Direct Measurements of Submarine Groundwater Discharge to Investigate the Coupling Between Surface and Pore Waters

by

John Paul Rapaglia

Doctor of Philosophy

in

Marine and Atmospheric Science

Stony Brook University

2007

Submarine groundwater discharge (SGD) and its associated impact on coastal ecosystems was investigated at the sediment-water interface using diverse methods. This intercomparison of methods was the objective of a major project carried out in 5 diverse hydrogeological settings (Cockburn Sound, Australia; Donnalucata, Sicily; Shelter Island, USA; Ubatuba Bay, Brazil; and Flic-en-Flac Bay, Mauritius). Small-scale sedimentary processes were deemed very important in the control of local hydrogeological characteristics. Seepage meters were used to directly measure the flow of water across the sediment-sea interface. Coincident measurements of bulk ground conductivity (BGC) were made alongside seepage meters at four of these locations. An inverse relationship between BGC and SGD allowed for the extrapolation of point measurements of SGD to larger areas using BGC data. SGD estimates made using this method compared favorably with those obtained using other techniques.

Using seepage meters to measure flow rates, along with a manual drive point piezometer to measure pore water profiles, the coupling between pore water composition and advection due to SGD was investigated. The process of dispersion was found to determine both the shape and depth of salinity, nutrient, and radium profiles in the sediment. Dispersion may be controlled by biological or physical processes including the rate of advection itself, all of which change over time. Dispersion coefficients ranging from 0.02 m^2d^{-1} to 2.8 m^2d^{-1} were estimated from direct measurements.

This data also allowed for the investigation of anthropogenic impacts on the signature of SGD in coastal lagoons. At Shelter Island, the pilings of a pier altered the flow of groundwater into the sea by piercing a confining layer and allowing for a large influx of fresh groundwater from below. In the Venice Lagoon, the difference in water elevation between the lagoon and the sea has been investigated as a possible

driver of SGD beneath the barrier lands, which separate the two bodies of water. A strong correlation was found between water level difference and SGD. This suggested that the hydraulic gradient caused by this difference drives a flow beneath the barrier island. The flow is enhanced by the presence of artificial conduits created when former inlets were in-filled. If the inlets are closed by storm surge barriers, as proposed, a groundwater exchange beneath the barriers could potentially be as large as 1.0×10^6 m^3 d^{-1}.

Dedication

This thesis is dedicated to my father, Joseph James Rapaglia. My father, who earned three master's degrees himself, was one of the biggest influences on my life. Although he was never able to finish his PhD, a fact that disturbed him for many years, he was a wonderful teacher who changed the future of many a young student until he tragically fell into a coma on November 6th, 1996. He remained in a coma for eight long years before passing away on December 24th 2004. He was the most remarkable, intelligent man I have ever encountered, In life and beyond he always taught me to reach for the stars and to never settle. I know that, wherever he is, today he is smiling. Dad I know you were with me all the way through this process. This PhD belongs as much to you as it does to me. Thank you for everything. I miss you terribly.

Table of Contents

List of symbols..... ix
List of figures xi
List of tables..... xiii
Acknowledgements..... xiv
CV, publications and field of study..... xvi
Chapter 1: The study of submarine groundwater discharge in urban and pristine lagoons
A: Introduction..... 1
B Outline of the thesis..... 3
C Comparison of methods utilized to measure SGD..... 3
D. Mixing in the sediment-the process of dispersion..... 9
E. Anthropogenic perturbation of SGD signature..... 10
F. Previous work and the impetus for this study..... 12
G. Brief introduction into the chapters of this thesis..... 14
References..... 17

Chapter II: Improved understanding of spatial patterns of submarine groundwater discharge from bulk ground electrical conductivity measurement
1. Introduction. 23
A. Methods to investigate Submarine Groundwater Discharge.. 23
B. Application of geoelectric (conductivity / resistivity) techniques in SGD studies..... 25
2. Methods..... 32
A. Conductivity Survey & Seepage Meter Deployments..... 32
B. Study Sites..... 34
3. Results..... 38
A. Cockburn Sound, Australia..... 39
B. Shelter Island, USA..... 39
C. Ubatuba Bay, Brazil..... 42
D. Flic-en-Flac Bay, Mauritius..... 43
E. Interpretation of BGC results..... 46
F. Interpretation of SGD results..... 47
4. Discussion..... 48
A. Extrapolation of SGD from BGC measurements..... 48
B. Quantifying SGD using the empirical relationship..... 50
C. Independent estimates at the SGD study sites..... 51
D. Determination of the freshwater fraction of discharge..... 55
5. Conclusion..... 56
References..... 57
Tables..... 65
Figures..... 68

Chapter III. Submarine Groundwater Discharge Modification: An Effect of Pier Pilings on Near-Shore Submarine Groundwater Discharge From a (Partially) Confined Aquifer
1. Introduction..... 82
2. Methods..... 83
A. Study Site..... 83
B. Bulk ground conductivity measurement..... 84
C. Seepage Meter..... 86
3. Results..... 89
A. Spatial variation of bulk ground conductivity..... 89
B. Seepage rates and salinity of SGD..... 90
4. Discussion..... 91
A. Aquifer Confinement..... 91
B. Effect of pilings on SGD rate and salinity..... 92
C. Anthropogenic Modification of SGD..... 94
5. Conclusions..... 96
References..... 96
Figures..... 100

Chapter IV The impact of groundwater advection on salinity, nutrients, and radium in pore waters of permeable sediments.
1. Introduction..... 104
A. Theory..... 106
B. Site Description..... 109
2. Methods..... 113
3. Results..... 115
A. Mattituck, NY..... 116
B. Jamaica Bay, NY..... 116
C. The Venice Lagoon..... 119
4. Discussion..... 121
A. Interpretation of the salinity profiles..... 121
B. Magnitude of dispersion (mass balance of salt)..... 125
C Magnitude of dispersion: steady-state, one-dimensional analytical solutions..... 126
1. A “slab” solution (Martin et al. 2007)..... 126
2. Exploration of the relationship between BGC and SGD as explained by dispersion coefficients; a steady-state, one-dimensional, semi-infinite analytical solution..... 128
D. Characteristics of dispersion..... 132
E. A comment on the ecological implications of dispersion..... 134
5. Conclusions..... 136
References..... 137
Tables..... 143
Figures..... 145

Chapter 5. A Previously Undocumented Source of Water Into Venice Lagoon, Italy
1. Introduction..... 162
A. Previous work..... 164
B. Site Description..... 168
C. The Module Sperimentale Elettrodinamico “MOSE” Project... 171
2. Methods..... 172
3. Results..... 174
4. Discussion..... 177
A. Explanation of high discharge rates at Treporti..... 177
B. possible impacts of the “Moses Project”..... 179
C. Ecological significance of the transport of water through barrier islands..... 182
5. Conclusions..... 183
References..... 184
Tables..... 188
Figures..... 190

Chapter 6. Summary and future work..... 198
A. Overview of the main objectives of the thesis 198
B. A closer look at the intercomparison experiment, and how to utilize the knowledge obtained..... 201
C. SGD and its impact on a small scale, what we have learned, and where to go from here..... 203
D. Understanding of anthropogenic modification on the SGD signature of coastal lagoons..... 205
References..... 207

Appendices:
Appendix A: List of seepage meter measurements..... 209
Appendix B: Discussion of error in SGD measurements made using seepage meters..... 220
Appendix C: Evolution of the Venice Lagoon..... 225

List of symbols by chapter

In Chapter II:
F*=** formation factor. (unitless)
***m*=** empirical constant determined by the tortuosity of the sediiment (unitless)
***Φ*=** porosity (unitless)
$\sigma_{b=}$ bulk ground conductivity (mS cm^{-1})
***A*=** properties of the sediment matrix (unitless)ρ_w= pore water resistivity (ohm-m)
α=numerical value of sediment characteristics
***Q*=** total discharge (cm^3 d^{-1})
q_s= discharge of salt water (cm^3 d^{-1})
q_f= discharge of freshwater (cm^3 d^{-1})
σ_w= conductivity of pore water (mS cm^{-1})
σ_s= maximum bulk ground conductivity (mS cm^{-1})
σ_f= minimum bulk ground (mS cm^{-1})

In Chapter III:
σ_b =bulk ground conductivity
σ_w= interstitial water conductivity

In Chapter IV:
σ_w= interstitial water conductivity
σ_b =bulk ground conductivity
***A*=** area (m^2)
***D*=** dispersion coefficient (m^2 s^{-1})
***dc/dz*=** the salinity gradient in the sediment (g cm^{-1})
***q*=** specific discharge of water (cm^3 cm^{-2} d^{-1})
***qs*=** is the flux of salt into the sediment (cm^3 d^{-1})
***t*=** time (d)
***Φ*=** porosity (unitless)
***ω*=** upward velocity of water (SGD velocity) (cm d^{-1})
S_0= concentration of salt at the surface (g cm^{-1})
z_1= depth of the profile (cm)
z_2= depth if not at y-intercept (cm)
S_2= concentration of salt at depth if not 0 (g cm^{-1})
S_L= salinity at lower limit of profile (unitless)
***L*=** depth at lower limit of the profile (cm)
S_U= salinity at upper limit of the profile (unitless)
ϑ= Variable describing salinity relationship
***F*=** flux of salt (g/cm3)
***t*=** time (d)

In Chapter V
q=specific discharge (m d^{-1})
***k*=** hydraulic conductivty (m d^{-1})
***dh/dl*=** hydraulic gradient (unitless)
V_p= Tidal prism (m^3)

***Q*= discharge (m^3 d^{-1})**
***A*= area (m^2)**

List Of Figures

Chapter II.
Figure 1. Maps of study sites..... 68
Figure 2. Bulk ground conductivity at Shelter Island..... 69
Figure 3. SGD vs. Tidal elevation Shelter Island..... 70
Figure 4. Time series of SGD in seepage meter, Shelter Island..... 71
Figure 5. BGC transects, Brazil..... 72
Figure 6. Temporal variation of BGC, Brazil..... 74
Figure 7. Map of seepage meter transect, Brazil..... 74
Figure 8. Time series of SGD as measured by seepage meters, Brazil..... 75
Figure 9. BGC transects, Mauritius..... 77
Figure 10. SGD transect, Mauritius..... 78
Figure 11. SGD vs. salinity, Mauritius..... 79
Figure 12. Multi-site empirical relationship between BGC and SGD..... 80
Figure 13. Contour maps of SGD from interpolated BGC..... 81

Chapter III.
Figure 1. Maps of Shelter Island Study Site..... 100
Figure 2. Bulk ground conductivity at Shelter Island..... 101
Figure 3. Influence of pier on BGC..... 102
Figure 4. Seepage meter measurements..... 103

Chapter IV.
Figure 1. Maps of study sites..... 145
Figure 2. Photo of seepage meters and novel piezometer use..... 146
Figure 3. SGD vs. Tidal elevation, Jamaica Bay, NY..... 146
Figure 4. Salinity vs cumulative flow..... 147
Figure 5. Salinity profile Mattituck..... 147
Figure 6. SGD and salinity profile, Jamaica Bay..... 148
Figure 7. SGD and salinity profile, Jamaica Bay..... 149
Figure 8. SGD and salinity profile, Jamaica Bay 150
Figure 9. SGD and salinity profile, Jamaica Bay..... 151
Figure 10. SGD and salinity profile, Jamaica Bay..... 152
Figure 11. Nutrient profiles, Jamaica Bay..... 153
Figure 12. Salinity and Radium profiles, Venice..... 154
Figure 13. SGD and salinity profile Venice..... 155
Figure 14. DIN vs. Depth Venice..... 156
Figure 15. DIN vs. Salinity Venice..... 156
Figure 16. Shallow and deep salinity profiles, Jamaica Bay..... 157
Figure 17: Advection dispersion model at four sites..... 158
Figure 18. Correlation between curves produced using 2 equations..... 160
Figure 19. Multi-site relationship between BGC and SGD..... 162

Chapter V.
Figure 1. Map of Venice Lagoon..... 190
Figure 2. Picture of the study site..... 191
Figure 3. Historic Map of the Venice Lagoon..... 192
Figure 4. SGD vs. water elevation difference..... 193
Figure 5. SGD vs. water elevation P. Sabbioni..... 194
Figure 6. Salinity profiles..... 195
Figure 7. Tidal cycles in the Venice Lagoon..... 196
Figure 8. Historical record of the frequency..... 196
Figure 9. Subsurface conductivity and nutrient sample locations..... 197

Appendix B.
Figure 1. Duplication of SGD measurements Jamaica Bay..... 222
Figure 2. Duplication of SGD measurements Shelter Island..... 222
Figure 3. Duplication of SGD measurements Mattituck..... 223
Figure 4. Replication of SGD measurements Mauritius..... 223
Figure 5. Variance in seepage meter measurements..... 224

List of Tables

Chapter II.
Table 1. Site characteristics..... 65
Table 2. SGD and BGC comparison..... 66
Table 3. Values of A and α for each of the study sites..... 67
Table 4. SGD data..... 67

Chapter IV.
Table 1. Dispersion Coefficients in the literature..... 143
Table 2. Calculated dispersion coefficients..... 143

Chapter V
Table 1. Seepage measurements at Treporti..... 188
Table 2. Theoretical volume flux into the Venice Lagoon..... 189
Table 3. DIN and PO_4 loading into the Venice Lagoon..... 189

Acknowledgements

A PhD is a process that involves many people, and when your PhD takes you around the globe it becomes even more difficult to acknowledge everyone. In fact, if I were to try I may miss my dissertation deadline. There are a few people, however, whom I must mention.

First and foremost I need to thank my advisor Dr. Henry Bokuniewicz. I can not imagine a better advisor. Henry has always been the perfect combination of a hands-off advisor yet there for you whenever you need him. I think with any other advisor I would never have been able to finish. I am, forever indebted to you, and as I am a quarter Sicilian, that means you can feel free to ask me for a favor whenever it is necessary.

I'd also like to thank my thesis committee Drs. Kirk Cochran, Sergio Sañudo-Wilhelmy, Teng-Fong Wong, and Luca Zaggia for all of their thoughtful comments and suggestions regarding this manuscript.

I need to give a special mention to Dr. Thomas Stieglitz who provided much of the bulk ground conductivity data used within this manuscript as well as some of the interpretation. I look forward to working with you in the Australian mangroves, whether it involves taking samples or being on crocodile watch if necessary.

I would like to thank the staff of MSRC especially Eileen Doyle, Eileen Goldsmith, and Bonnie Stephens. Each of you have kept me from jumping off a cliff. We are so lucky here at MSRC to have such a wonderful staff, it is something I will always miss.

I need to thank my fellow students and friends here at MSRC, specifically Drs. Brian Batten and Frank Buonaiuto for showing me the way, as well as Lora Clarke, Ruth Coffey, and Owen Doherty for their help with this manuscript.

On that note I need to thank the staff and students of the National Research Council of Italy and the University of Venice, including Franco Costa for keeping me out of jail, Gianfranco Magris, Andrea Pesce, Flaviano Collavini, Eloisa DiSipio, Virginia Barros, and especially my Muranese boat instructor Italo Ongaro.

I'd like to thank Professore Gian Maria Zuppi for his infinite wisdom and his many spritzes.

I would also like to give a special mention to my other friends, especially Federica Bellutti, Sophie Copeland, Gordon Davis, Takashi Kanno, Marc Neveu, and Sean Otten who have kept the alcohol flowing at a constant level in order to help my creativity a la Ernest Hemingway.

A special thanks goes to Ester Garcia-Solsona and her colleagues at the University of Barcelona who have made my life more interesting as well as joined me in the endless headaches that is research in Venice

I need to mention, once again, Dr. Luca Zaggia who has been my boss, my mentor, and especially my friend. I hope that we have many more chances to explore the world looking for black pearls together.

How can I ever offer enough thanks to my family whose support has never wavered and my mother whose strength and faith is palpable. There is no one more important to me.

Finally, I need to acknowledge two incredible friends. We've been through a lot. It all started back in Venice in 2002, a 31 day period in which we learned that the three of us could do anything together. Michael Finiguerra you have been our support. I can never thank you enough, remember there is a Nil in your future. Dr. Aaron Beck; Venice, Mauritius, Germany, Great South Bay, Mattituck, and Jamaica Bay, man have we seen the world, including salads with high conductivity. Remember you are the scientist, I'll deal with the people. Good luck my friends.

John Rapaglia – PhD Candidate

61 Ridgeland Manor Rye, NY 10580 (914) 967-7508 jrapagli@ic.sunysb.edu

EDUCATION:

5/2004-Present: Marine Sciences Research Center, SUNY Stony Brook
Stony Brook, NY 11794

Ph.D Student

1/2002-5/2004: Marine Sciences Research Center, SUNY Stony Brook
Stony Brook, NY 11794

Master's of Science: Marine Environmental and Atmospheric Sciences
G.P.A. 3.8 (4.0 scale)
Thesis: *Distribution of Submarine Groundwater Discharge at Coastlines*

8/1997-5/2001: Mary Washington College; Fredericksburg, VA 22401

Bachelor's of Science: Environmental Science
Graduated Magna Cum Laude from Mary Washington College with a BS in Environmental Science as well as completing the Geography major.
Environmental Science G.P.A. 3.65 (4.0 scale)
Geography G.P.A. 3.94 (4.0 scale)

RELEVANT WORK EXPERIENCE:

6/2006-Present: Consiglio Nazionale della Ricerca
S.Polo 1364 Venezia 30125, Italy

Researcher
Primary field researcher on a project concerning the flow of groundwater and the total water budget of the Venice Lagoon Italy. In charge of laboratory analysis of radium isotopes as well as inorganic nutrients.

6/2006-Present: Universita' Ca' Foscari di Venezia
Dorsoduro 2137 Venezia 30123, Italy

Researcher
Primary field researcher on a project concerning the flow of groundwater into the Porto Marghera industrial zone using various measurement techniques.

8/2002-6/2006: Marine Sciences Research Center
Stony Brook, NY 11794

Research Assistant
Assistant to Professor Henry Bokuniewicz with his research as part of SCOR/LOICZ working group 112 and their research on submarine groundwater discharge and its viability as a possible pathway for nutrients and contaminants. In addition I perform bi-weekly analysis of beach volume on Long Island's south shore

1/2005-6/2005: Suffolk County Community College
Selden, NY 11783

Adjunct Faculty
Instructor of Marine Biology lecture and lab material for second year students.

6/2002-8/2002 Research Education for Undergraduate Program
Marine Sciences Research Center, Stony Brook, NY 11794

Teaching Assistant
Graduate student assistant for the prestigious REU program which this past year spent a month in Venice, Italy on a collaborative project with the Consiglia Nazionale della Richerche and the Universita ca Foscari di Venezia.

1/2002-6/2002 SUNY Stony Brook, Stony Brook, NY 11794

Teaching Assistant

Lab instructor for undergraduate introductory biology course. Introduced several new lecture topics as well as laboratory procedures and safety

AWARDS AND HONORS:

2003-2004 **Fulbright Scholarship (Italy)**
2002 **August A. Guerrera Award** (for excellence in groundwater hydrology)
2002-2003 **New York Sea Grant Scholar**
2001 **Meriwether Lewis and William Clark Award** (for excellence in geography discipline Mary Washington College)
2001 **Magna cum Laude** (Mary Washington College)
Fall 1998, Spring 2001 **President's List** (4.0 GPA (4.0 scale)) Mary Washington
Fall 1997, 1999, Spring 1999,2000 **Dean's List** (3.5-3.99 GPA)

PRESENTATIONS AND PUBLICATIONS:

Rapaglia, J.P. 2005. Submarine groundwater discharge into the Venice Lagoon, Italy. Estuaries 28(5): 705-713.

Stieglitz, T., **Rapaglia, J.**, and Krupa, S. 2007. An effect of pier pilings on near-shore submarine groundwater discharge from a confined aquifer. Estuaries and Coasts. 30 (3): 1-8.

Beck, A.J., **Rapaglia, J.P.,** Cochran, J.K., and Bokuniewicz, H.B. 2007. Radium mass-balance in Jamaica Bay, NY:Evidence for a substantial flux of submarine groundwater. Marine Chemistry. In Press.

Bokuniewicz, H., **Rapaglia, J.,** and Beck, A. 2007. Submarine Groundwater Discharge from a Volcanic Island: A case study of Mauritius Island. International Journals of Oceans and Oceanography. In Press.

Beck A.J., **Rapaglia J**.P., Cochran J.K., and Bokuniewicz H.B. Submarine groundwater discharge to Great South Bay, NY, estimated using Ra isotopes. Marine Chemistry. Submitted.

Rapaglia J., DiSipio E., Zuppi G.M., Zaggia L., Galgaro T., and Bokuniewicz H. Salinization of the Venice Lagoon from groundwater discharge. Nature. Submitted.

Stieglitz, T., and **Rapaglia, J**. Improved understanding of spatial patterns of submarine groundwater discharge from bulk ground electrical conductivity measurements. Journal of Geophysical Research. Submitted.

Garcia-Solsona, E., Masqué, P., Cochran, J.K., Garcia-Orellana, J., **Rapaglia, J.,** Beck, A., Zaggia, L., Collavini, F., and Bokuniewicz, H. Estimating submarine groundwater discharge into the northern Venice Lagoon, Italy by using the radium quartet. Marine Chemistry. Submitted.

Rapaglia J. Garcia-Solsona E. Garcia-Orellana J. Bokuniewicz H. Zaggia L. Collavini F. Masque P. Zuppi G.M. Cochran J.K. Beck A. 2006. Submarine Groundwater Discharge into the Venice Lagoon, its Magnitude and Implications. International Conference on Coastal Engineering (ICCE) September 3-8 2006. San Diego, CA.

Rapaglia J. Bokuniewicz H. Zaggia L. Collavini F. Masque P. Garcia-Solsona E. Zuppi G.M. Cochran J.K. and Beck A. 2005. Measurement of Submarine Groundwater Discharge and Associated Contaminants into the Venice Lagoon, Italy. Land Ocean Interactions in the Coastal Zone (LOICZ) inaugural meeting. June 23-29 2005. Egmond aan Zee, Netherlands.

Rapaglia J. and Bokuniewicz H. 2003. Assessment of direct measurements of submarine ground-water discharge. Long Island Ground-Water Symposium June 6, 2003. Brookhaven National Laboratory

Beck A. **Rapaglia J.** Cochran J.K. and Bokuniewicz H. 2005. Multiple geochemical tracers of submarine groundwater discharge to Jamaica Bay, NY. Long Island Geologists Conference. April 21-22 2005. Stony Brook, NY.

Garcia-Solsona, E., Masqué, P., **Rapaglia J**., Bokuniewicz, H., Zaggia, L., Collavini, F., Cochran, J. K., Zuppi, G. M., Sanchez-Cabeza, J. A., and Beck, A. 2004. Radium Isotopic Tracers of Submarine Groundwater Discharge into the Venice Lagoon. International Atomic Energy Agency (IAEA) Isotopes in the Aquatic environment. 25-29 October 2004. Monte-Carlo Monaco.

FUNDED PROJECTS

2006-2008 A.P.A.T. (Associazione per il Proteggio L'ambiente). *Seasonal fluxes of groundwater into the Venice Lagoon Italy.* €190,000. CO-Principal Investigator.

2006-2007 ALCOA Foundation. *Quantifying submarine groundwater discharge into the canals of the Porto Marghera Industrial Zone.* $100,000. CO-Principal investigator, grant writer.

CHAPTER I: The study of submarine groundwater discharge in urban and pristine lagoons

A. Introduction

Groundwater encompasses more than 90% of the available freshwater on earth (Hiscock 2005). This water, stored from hours to many centuries, will eventually return to the sea. Some of the groundwater may intersect stream channels while other groundwater discharges directly into the sea. Until recently the process of groundwater discharging directly into the sea, referred to as submarine groundwater discharge (SGD), was ignored as an important process in both the hydrological and chemical cycles of local, regional, and global systems (Burnett et al. 2006). This is no longer the case. Studies of SGD have now been completed in many coastal systems around the world. At the time of the first review of the subject in 2002 (Taniguchi et al. 2002), 45 study sites were compiled, and in the years since several new locations have been investigated (Burnett et al. 2006). SGD, while providing only a small percentage of the average daily fluvial flux on the global scale, has been shown to be an important component of the hydrological budget in local and regional systems (Burnett et al. 2001). However, when the recirculation of seawater is considered, SGD is also likely to play a major role in the global biogeochemical cycles as well (i.e. Taniguchi et al. 2002). In this thesis, SGD includes the discharge of fresh water, the recirculation of salt water or both (Taniguchi et al. 2002, 2006, Martin et al. 2006). Even though SGD probably accounts for less than 10% of the total freshwater flux into the world's ocean, the associated flow of saltwater can increase the total discharge by an order of magnitude in many locations (Moore 1996, Li et al. 1999). Although recirculated seawater is not a component of the

hydrological budget, it is SGD, and may be important for the flux of contaminants to coastal oceans (Moore 1999, Taniguchi et al 2006). Often, in these cases, total SGD can be on par with the total fluvial input, or may, in fact, be much greater (Charette et al. 2005).

Anytime water enters into and discharges from the sediment beneath the sea, processes take place which change the chemical signature of this water. Groundwater is often elevated in the concentration of certain constituents, such as nitrates and, formerly, phosphates from fertilizers. Therefore when SGD occurs, whether it be fresh SGD or saline SGD, it presents a pathway for chemicals to enter into the coastal system. Moore (1999) likened the transition zone between interstitial fresh and salty groundwater to an estuary and, hence, called the zone the "subterranean estuary". Analogous to a surface estuary, when fresh water mixes with salt water chemical processes including desorption, adsorption, chemical reactions (e.g. redox induced solubility), and mixing take place (Charette et al. 2005). These processes are collectively termed as dispersion and can be dependent on the advection of water itself as will be discussed in Chapter IV of this thesis.

Unfortunately the ability to accurately measure both SGD and associated constituents has eluded us. One of the major inhibitors, when it comes to reducing uncertainty, is that the flow itself is very variable on both spatial and temporal scales and depends on many factors including permeability, pressure gradients, and preferential conduits (e.g. Bokuniewicz et al. 2004, 2007, Paulsen et al. 2004). In light of this complexity, the basis of SGD must be unraveled for numerous case studies encompassing a wide variety of situations. One approach to resolving the issue of

understanding SGD processes and flux is to look at the phenomenon on the small scale (~1 m). SGD is variable on very small scales, perhaps due to sediment characteristics. Site-specific investigations of SGD patterns and small scale sedimentary process in Venice (Chapters IV and V) and Long Island (Chapters II, III, and IV) are a major part of this thesis. Site-specific studies from Australia, Mauritius and Brazil are also included as part of this body of work. If we can begin to determine these characteristics and the processes that are occurring within the sediment, perhaps we can increase the accuracy with which we estimate the quantity and impact of SGD on coastal systems.

B. Outline of this thesis

Herein I investigate SGD on the scale of meters, including within the sediment, and attempt to make some statements about SGD on a larger scale using this knowledge. In addition, I look at data from a very diverse group of study sites to attempt to see how site-dependent characteristics on a small scale affect SGD flow in different lagoons. Site specific SGD at Cockburn Sound, Australia, Shelter Island, NY, Ubatuba Bay, Brazil and Flic-en-Flac Bay, Mauritius are discussed in Chapters II and III. Herein, the utility of employing bulk ground conductivity on the sub-meter scale in order to extrapolate point measurements of SGD to wider systems is examined. In the fourth chapter, I examine sites in Venice and Long Island to quantify the dispersion process and how the rate of advection of SGD, itself, affects pore water chemistry. In Chapters III and V, the impact of small and large scale anthropogenic modifications on SGD processes is investigated using case studies in Long Island and Venice.

C. Comparison of methods utilized to measure SGD

The ability to measure SGD has only come about with technological advances in the last few decades, which is one of the reasons for the lack of attention to SGD, historically, in the study of coastal systems (Kohout 1966). In recent years, however, the study of SGD has achieved the status of a distinct discipline; there is a "critical mass" of scientists around the world perusing common questions with a widely accepted arsenal of methods. Methods to measure SGD include point measurements using vented benthic chambers, integrated estimates using chemical tracers, and theoretical estimates using hydrological models based on piezometric measurements (Burnett et al. 2006). At this point I will not go into an in-depth explanation of the different techniques as they will be discussed in detail in the following chapters. Each of these technologies is still in the process of being developed and evaluated. As SGD is variable on both spatial and temporal scales, we can use integrated measurements to obtain an average discharge rate of a large area while point measurements help to define the variability in coastal systems (Bokuniewicz et al. 2004). Geochemical tracers often fill this role but, as will be discussed in Chapters II and III, geophysical parameters can be used as well.

With the emergence of different SGD measurement technologies, it became clear that there was a need for an intercomparison of these methods. Under the framework of a joint UNESCO-International Atomic Energy Agency (IAEA)-Intergovernmental Oceanographic Commission-(IOC) venture, five sites (Cockburn Sound, Australia; Donnalucata, Italy; Shelter Island, USA; Ubatuba, Brazil; and Flic-en-Flac, Mauritius) in different hydrogeological settings were chosen as locations for a large project to

compare different methods (Burnett et al. 2001, 2006). The project was comprised of a group of scientists from six U.S. and 5 international institutes, including the Australia Institute of Marine Sciences; Florida State University, U.S.A.; Istitut de Pesquicas Energeticas e Nuclearas, Brazil; James Cook University, Australia; the Marine Environmental Laboratory, International Atomic Energy Agency, Monaco; The Research Institute for Humanity and Nature, Japan; San Jose State University, U.S.A.; Shirsov Institute of Oceanology, Russia, South Florida Water Management District, U.S.A.; Stony Brook University, U.S.A.; The University of South Carolina, U.S.A., and Woods Hole Oceanographic Institution, U.S.A. In addition, many scientists and students from local institutions participated at each of the study sites. The project was completed in 2005 and produced a plethora of information, some of which is highlighted by Burnett et al. (2006). The objective of this project was to compare how the different techniques performed in various hydrogeological settings, and to be able to determine which technique or combination of techniques should be used when studying SGD flux into certain systems. I personally participated in the field work at two of these study sites (Shelter Island and Mauritius) and was engaged in the data analysis and interpretation for all sites.

The first study site was Cockburn Sound, Australia. Measurements were taken there from November 25 - December 6, 2000 (Linderfelt and Turner 2001, Smith and Nield 2003, Taniguchi et al. 2003, Loveless 2006 as cited in Burnett et al. 2006). Cockburn Sound was chosen as it had been extensively studied to determine the environmental impact of waste discharges into the Perth Sound (Burnett et al. 2006). It was representative of a coastal plain with unconsolidated sediments underlain by

unconfined aquifers. Previous work attempting to model the flow of groundwater within the area had been accomplished (Nield 1999, as cited in Smith and Nield 2003). Both manual and automated seepage meters were used to collect point measurements of SGD. In addition, the measurement of both radium and radon were employed as natural tracers to get integrated SGD estimates. Measurements of bulk ground conductivity to a depth of 1 m in the sediment were made in order to obtain a 3-dimensional map of the subsurface distribution of salt water. In Cockburn Sound, as expected from a coastal plain setting, discharge was limited to a small area, about 60 m from the shoreline. Discharge estimates produced from different techniques compared fairly well with one another. I have incorporated a new, independent assessment of these data in Chapter II of this thesis.

The second major study site was Donnalucata, Italy. Measurements were carried out in Donnalucata during two field campaigns (June 2001 and March 2002) and results were published in a special issue of Continental Shelf Research (Burnett and Dulaiova 2006, Kontar and Ozorovich 2006, Moore 2006, Povinec et al. 2006, Schiavo et al. 2006, Taniguchi et al. 2006). This site was chosen as representative of karstic aquifers. The sediment is underlain by several meters of carbonate sands as well as carbonate aquifers. The specific study area is known to be the location of many submarine springs from which a large amount of freshwater is entering the coastal sea (Burnett et al. 2006). At this site, stable isotopes of oxygen and hydrogen were used to determine the origin of the discharging water. SGD fluxes were measured using both manual seepage meters for point measurements and radium and radon for integrated tracers. Unfortunately, during both sampling periods, the presence of high winds and waves precluded the possibility of

using either seepage meters or radon measurements in the open sea and therefore the comparison between the methods was poor. Though it is important to give mention to this site, in order to understand the whole scheme of the project, it will not be discussed in the proceeding chapters of this dissertation. Instead, my research in Venice, which was not one of the intercomparison sites, will be discussed in Chapters IV and V.

The third major study site was located in Shelter Island, NY, U.S.A. Measurements were made during the week of May 17-25, 2002 (Paulsen et al. 2004). Long Island is a comprised of a series of glacial moraines including a terminal moraine from the last glacial maximum (Pouyat et al. 2002). Here, on the eastern end of Long Island, the unconsolidated, upper glacial aquifer extends about 30 m below the sediment-sea interface (Paulsen et al. 2001). The site was chosen as representative of a glacial till setting, and a previous study of discharge from Shelter Island implicated SGD as a cause of harmful algal blooms (Paulsen et al. 2004, Laroche et al. 1997). At this site, both manual and automated seepage meters were utilized in order to make point measurements of SGD flowing into the bay. In addition, radium and radon were once again utilized to integrate SGD over a large area. As in Australia, a 3D map of bulk ground conductivity in the sediment was produced for the study site, in order to gain a better understanding of the subsurface fresh/salt water distribution. A comparison of the fluxes estimated by the integrated and point measurements showed similar discharge patterns (i.e. controlled by tidal elevation) but different overall flux calculations. The distribution of SGD at this site has been determined to be dominated by the drilling of pier pilings into the sediment which will be further discussed in Chapter III. My

participation in the investigation at this site was the basis of my master's thesis and additional interpretation of these results is included in Chapters II and III.

The fourth study site was Flamengo Bay, Ubatuba Brazil. Measurements were made at Ubatuba from November 16-22, 2003 (Oliveira et al. 2003, Bokuniewicz et al 2004, Burnett et al. 2007, Stieglitz et al. 2007b). Ubatuba was chosen as representative of a fractured crystalline rock aquifer, as the local hydrology had been previously studied (Mahiques 1995 as cited in Oliveira et al. 2003) and the oceanographic institute of the University of Sao Paolo was located nearby. The backdrop of the site consisted of a mountain range with an average precipitation rate of 1800 mm yr^{-1} (Oliveira et al. 2003). Once again, both automated and manual seepage meters were used for point measurements, with radium and radon used as tracers for integrated discharge measurements. Conductivity maps of the sediment were created using a manual method as well as by deploying an electrode array to automatically measure conductivity in transects. Discharge seemed to be dominated by the location of the fractures which explains the high variability among the different types of SGD measurement techniques. I did not participate in the field work at this site, but a new interpretation of some of the data collected here is incorporated in the analysis in Chapter II.

The final site, Flic-en-Flac Bay, Mauritius was investigated from March 18-26 2005 (Oberdorfer 2005, Bokuniewicz et al. 2007). Mauritius was chosen as representative of a volcanic island setting with high average precipitation rates (~2000 mm yr^{-1}). In addition, there were some well known submarine freshwater springs which could be seen "boiling" on the surface. In Mauritius, a suite of 12 manual seepage meters as well as a few automated seepage meters were used to obtain point

measurements of discharge into Flic-en-Flac Bay. Measurements of radon were used to calculate the integrated flux of SGD into the lagoon. Radium measurements were limited and mostly done offshore, outside of the lagoon, but, a systematic survey of ground conductivity was performed from which several detailed sediment conductivity distribution maps were created. I participated in this field work and will discuss the use of geophysical results in the interpretation of direct measurements of SGD in Chapter II. Discharge at the site was dominated by the presence of the large spring and could be clearly seen in both the seepage meter data and the conductivity measurements.

Though comparisons were made between all methods at each site the most promising comparison may have been between measurements made of flow rates using seepage meters (SGD) and bulk ground conductivity (BGC). This comparison was completed in four of the five sites (with the exception of Sicily). I partook in two of these experiments: Shelter Island U.S.A. (2002) and Mauritius (2005). Data from the Mauritius site, were published by Bokuniewicz et al. (2007) data from Shelter Island were published by Stieglitz et al. (2007a) and only the data directly concerned with relation to electrical conductivity will be discussed here in Chapters II and III.

D. Mixing in the sediment- the process of dispersion

Differences in the relationship between SGD and BGC among the different site is likely due to sediment characteristics and the various processes of dispersion. Dispersion is an important phenomenon, which occurs in both surface and subterranean

estuaries. In Chapter IV I will investigate dispersion, and the various mechanisms of dispersion to understand how the process affects the profiles of salinity in the sediment.

Utilizing simultaneous measurements of salinity in the sediment and SGD in benthic chambers I will quantify dispersion in my study sites. Different methods will be used for this quantification and they will be tested against one another as well as values found in the literature. An understanding of dispersion may help to quantify the relationship between BGC and SGD discussed in Chapter II.

E. Anthropogenic perturbation of SGD signature

The main impetus for the study of SGD has always been the attempt to understand the process in order to better advise coastal zone managers as to how to minimize the negative effects of SGD (Johannes 1980). Ecosystem changes, such as eutrophication, often can not be explained by fluvial inputs of nutrients alone (Paerl 1997). Anthropogenic perturbations of both the chemical signature of groundwater as well as its prevalent flow paths must be fundamentally changing the import of SGD in coastal systems (e.g. Nakayama et al. 2007). Even before the industrial revolution, humans had already left an indelible footprint on the environment. In the case of Venice, for example, Venetians diverted the course of two major rivers in the 1300's away from the lagoon; they drilled hundreds of millions of tree trunks into the sediment in order to stabilize the islands; they dredged channels for navigational purpose; etc. As I will discuss in Chapters II and V, each of these modifications likely impacted the flow of groundwater in the area.

In the 20th century humans began to change the chemical signature of many groundwaters. Fertilizers and pesticides used in agricultural practices, often infiltrated into the aquifers thereby contaminating them and in many cases making them unsafe to use (Valiela et al. 1992). Elevated concentrations of metals have been found in groundwater down gradient from industrial plants (Critto et al. 2003). Unlined landfills have become a major point source of pollution (Gobler and Boniello 2003). Technological advances in medicine and pharmaceuticals have led to pollution as medicinal waste products often find their way into the groundwater. (Swartz et al. 2006) It is possible, for instance, that increasing levels of estrogen in discharging groundwater may be causing transgender modifications in fish and other animals (Parrot and Wood 2002, Atkinson et al. 2003). MTBE and other byproducts of the petroleum industry are known to be seeping into the Upper Glacial Aquifer on Long Island, NY from gas station leaks and oil spills (Wilson and Kohaltkar 2002). Caffeine levels have risen sharply in surface aquifers to the point where some investigators believe they may be a good tracer of septic-system plumes in groundwater flow (Swartz et al. 2006).

One of the objectives of this thesis is to shed light on the possible impacts that anthropogenic modifications have on SGD flow paths and expected discharge rates. Chapter III will discuss, in detail, the impact of driving pilings into a confining layer to produce local areas of high discharge. Meanwhile, Chapter V will make some predictions as to the possible impacts to SGD caused by the largest public works project in the history of Venice (The “MOSE” Project).

F. The Venice Lagoon

As the teaching assistant in the National Science Foundation's Research Education for Undergraduates (REU) program, I was able visit the Venice Lagoon, Italy in order to collect the first measurements of SGD using manual seepage meters. Here, I collaborated with the University of Venice as well as the National Research Council of Italy's marine research institute. Previously, the institutes had completed a large project to determine, accurately, the input of water and associated contaminants into the Venice Lagoon from the drainage basin (Zuliani et al. 2005). At the completion of the project it was determined that there was at least a 15% deficit between the input of precipitation surplus (i.e. minus evapotranspiration) and the amount of water discharging into the lagoon from the rivers. It was hypothesized that this deficit could be accounted for through the discharge of groundwater, however, at the time, SGD was considered unlikely due to the lack of a known hydraulic gradient towards the lagoon in the upper unconfined aquifer (Zonta et al. 2005). To test this hypothesis measurements were made in several locations to determine if there was a flow of water into the lagoon. The preliminary results were surprising. Not only was there a flow of water into the lagoon, but this flow was of a large volume. With the support of a Fulbright grant, I was able to return to Venice in order to continue the study of SGD into the Venice Lagoon on a much larger scale. The objectives of the investigation in Venice were to reconcile the budget deficit and determine the flux of SGD and, possibly, associated nutrients into the Venice Lagoon, as well as to describe the difference in SGD flow in different parts of the lagoon. A series of over 300 measurements were performed using manual seepage meters in two different locations in the lagoon. One of these locations was adjacent to

the Porto Marghera Industrial Zone (the third largest industrial zone in Italy) while the other was in the relatively pristine northern lagoon. With these measurements, I demonstrated that SGD is an important source of water into the Venice Lagoon. The average flow rate among the study sites was 20 cm d^{-1} which if extrapolated over the entire lagoon floor would equal a flow of about 900 m^3 s^{-1}, or 25 times greater than the river discharge. However, it seems that the majority of this discharge is re-circulated sea water (Rapaglia 2005) and the sites chosen probably overestimate the total discharge into the lagoon. If the budget deficit previously estimated by the National Research Council of Italy (Zonta et al. 2005) is any indication, the discharge of freshwater into the Venice Lagoon is probably on the order of 15% of the total freshwater discharge into the lagoon. Measurements of nitrate, nitrite, ammonium and phosphate suggest that SGD can be an important source of nutrients in the area, as concentrations of these nutrients are highly elevated in groundwater compared to the ambient lagoon water. Eutrophication can be a problem during summer months in the Venice Lagoon, and, therefore, this previously undocumented source of nutrients could be a major factor contributing to eutrophication. Another interesting result of this study was, to determine how the drivers of SGD vary in the two main study sites in the lagoon. In the industrial zone, low rates of SGD seem to be controlled by the hydraulic gradient of the unconfined aquifer's water table, and respond very quickly to precipitation events. Meanwhile, in the northern lagoon, much higher flow rates composed of mostly saline water are found. Here, I have hypothesized that the flow is driven by an (artesian) vertical hydraulic gradient, and is induced by the dredging of channels which may have pierced confining layers in the sediment. During the period between 2004 and the present, I have participated in a study in concert with

the Universitat Autonoma de Barcelona. This investigation has found, so far, elevated radium concentrations which support the idea that flow rates are high in certain areas of the lagoon (Garcia-Solsona et al. 2007).

Most of the SGD in the lagoon seemed to be driven by a hydraulic gradient from a multi-tiered aquifer system to depths of 1000 m. Natural and anthropogenic modification of the morphology of the lagoon led to specialized conduits of high discharge. However, it was likely in the case of the lagoon, that a large proportion of the SGD was of a marine origin. As much as 90% of the water discharging had similar salinities to either the ambient lagoon or Adriatic Sea water. Still, total nitrogen concentrations were elevated in the discharging water. Much of this data were presented in my master's thesis and will not be discussed here. It is important to note that this research has led to current research projects to expand the understanding of SGD in the Venice Lagoon.

Beginning in June of 2006 point measurements of SGD using vented benthic chambers were combined with a full lagoon survey of radium performed every three months in order to look at seasonal patterns of discharge into the Venice Lagoon. This work is scheduled to be completed in June of 2008. As of June 2007, a year of data have been collected and is currently in the process of analysis.

G. Brief introduction to the chapters of this thesis

This thesis is written as a collection of 4 articles, one of which has already been published, two others have been submitted, and the fourth shall be submitted by late

September. Each chapter, therefore, is a self-contained article in which the problem is described and the site characteristics are discussed. Hence, there may be some overlap of information between chapters. The chapters are organized thematically rather than chronologically. As described earlier, the research over the past five years has been a collaboration among many other investigators. The results embodied in this thesis represent my contribution to the effort in terms of both direct measurements of SGD and of the integration and interpretation of results, especially the geophysical measurement of electrical conductivity made by Dr. Thomas Stieglitz.

Chapter II of this thesis is dedicated to the comparison of two diverse methods utilized in the study of SGD. The first method involves the use of vented benthic chambers, commonly known as "seepage meters", to measure SGD through a specified area of sediment. These devices have been used for over 30 years (Lee, 1977) and are commonly employed in the study of SGD worldwide (Bokuniewicz 1980, Cable et al. 1997, 2006, Paulsen et al. 2004, Burnett et al. 2006). I personally have made many hundreds of measurements using these devices (Appendix A.)

As the flow of groundwater is very variable on small spatial scales, the utility of seepage meters is limited only to the area of sediment they cover. Therefore, it is very important to extrapolate measurements made with seepage meters to a larger scale in order to better understand the flow of water into the investigated system. This is done by the measurement of bulk ground conductivity (BGC) as an indicator of salinity in the interstitial water. Areas where the BGC are low can be sites of freshwater discharge. Though this BGC alone cannot quantify rates of SGD it can be a good gauge as to locations where it is occurring. As it is relatively easy and quick to utilize this method,

if a correlation can be found between SGD and BGC, we can therefore use the BGC to extrapolate measurements of SGD over a much larger area. In Chapter II, data are presented from four diverse locations to suggest that this extrapolation is possible in sites dominated by freshwater discharge. The BGC data used here had been collected by Dr. Stieglitz. I participated in its collection at Shelter Island and Mauritius. All BGC data are used here with permission of Dr. Stieglitz.

Chapter III has been accepted for the June 2007 issue of Estuaries and Coasts (Stieglitz et al. 2007a). It is a specific look at one of the sites outlined in Chapter II. Here we explain, using both seepage meter and BGC measurements, the effect of the drilling of pier pilings through a semi-confining layer of an aquifer. The data discusses the impact of human modification on the SGD signature of a coastal system. Artificial conduits created by the pilings may be sites of very high discharge and may have completely changed the SGD signature of the lagoon. I contributed the collection of data from the use of manual seepage meters and participated in the collection of BGC and the direct measurements made by the South Florida Water Management District. I served as corresponding author for this article.

The fourth chapter investigates the effect of SGD itself on the profile of salinity in the sediment in an attempt to better understand the import of SGD in the transport of pollutants into a system. This is traditionally modeled as an advection-diffusion process. The "diffusion", however is actually a parameterization of, potentially, multiple processes of vertical dispersion. The notion that SGD may be an important pathway for chemical constituents has been voiced in the past, but to understand the import of this flow we must understand how the flow itself changes the concentrations found in the

sediment. In addition many estimates have been made considering both stable flow rates and consistent sources. Herein I investigate and quantify the process of dispersion and its effect on salinity in the sediment in three diverse sites. The methods utilized in this study include seepage meters in order to measure the in situ flow rate and a retract-a-tip piezometer to measure the pore water profiles of salinity, nutrients, and radium isotopes.

The final chapter brings the study back to the Venice lagoon where I investigate a possibly important transport of salt water through the barrier lands to the east of the lagoon. Currently, the city of Venice is constructing massive barriers to separate the lagoon from the sea in the event of high water, in order to protect this world heritage site from damaging floods. This project, known as MOSE, involves the modification of the inlets and, for that reason, it is extremely controversial. A large amount of money (>20 million euros) has already been spent to determine the impact of these projects on the ecosystem of the lagoon. However, until this dissertation, no researcher has considered how the gates will impact the exchange of water beneath the barrier islands caused by the increased gradient between the sea and the lagoon when the gates are in use. The study of SGD along these barrier lands can help to clarify the process of exchange. Combined with a wealth of information concerning the character of the tides, the methods utilized in this study include seepage meters in order to measure the in situ flow rate and a retract-a-tip piezometer to measure the pore water profiles of salinity.

References:

Atkinson, S., Atkinson, M.J., and Tarrant, M. 2003. Estrogens from sewage in coastal marine environments. Environmental Health Perspectives. 111 (4): 531-535.

Bokuniewicz, H., 1980. Groundwater Seepage into Great South Bay, New-York. Estuarine and Coastal Marine Science . 10 (4): 437-444.

Bokuniewicz, H.J., Kontar, E., Rodriguez, M., and Klein, P.A. 2004. Submarine groundwater discharge patterns through a fractured rock aquifer: a case study in the Ubatuba coastal area, Brazil. Revista de la Asociacion Argentina de Sedimentologia. 11: 9-16.

Bokuniewicz, H., Rapaglia, J., and Beck, A. 2007. Submarine Groundwater Discharge from a Volcanic Island: A case study of Mauritius Island. International Journals of Oceans and Oceanography. In press.

Burnett, W. C., and Dulaiova, H. 2006. Radon as a tracer of submarine groundwater discharge into a boat basin in Donnalucata, Sicily. Continental Shelf Research. 26(7): 862-873.

Burnett, W. C., Taniguchi, M., and Oberdorfer, J. 2001. Measurement and significance of the direct discharge of groundwater into the coastal zone. Journal of Sea Research. 46 (2): 109-116.

Burnett, W.C., Aggarwal, P.K., Bokuniewicz, H., Cable, J.E., Charette, M.A., Kontar, E., Krupa, S., Kulkarni, K. M., Loveless, A., Moore, W.S., Oberdorfer, J.A., Oliveira, J., Ozyurt, N., Povinec, P., Privitera, A.M.G., Rajar, R., Ramessur, R.T., Scholten, J., Stieglitz, T., Taniguchi, and M.,Turner, J.V. 2006. Quantifying submarine groundwater discharge in the coastal zone via multiple methods. Science of the Total Environment 367 (2-3): 498-543.

Burnett, W.C., Peterson, R., Moore, W.S., and Oliveira, J. 2007. Radon and radium isotopes as tracers of submarine groundwater discharge — results from the Ubatuba, Brazil SGD assessment intercomparison. Estuarine, Coastal, and Shelf Science. submitted for publication.

Cable, J. E., Burnett, W. C., Chanton, J. P., Corbett, D. R., and Cable, P. H. 1997. Field Evaluation of Seepage Meters in the Coastal Marine Environment. Estuarine, Coastal, and Shelf Science. 45: 367-375.

Cable, J.E., Martin J.B., and Jaeger J. 2006. Exonerating Bernoulli? On evaluating the physical and biological processes affecting marine seepage meters. Limnology and Oceanography Methods. 4: 172-183.

Charette, M.A., Sholkovitz, E.R. and Hansel, C.M. 2005. Trace element cycling in a subterranean estuary: part 1. Geochemistry of permeable sediments. Geochimica et Cosmochimica Acta. 69 (8): 2095-2109.

Critto, A., Marcomini, A., and Carlon, C. 2003. Characterization of contaminated soil and groundwater surrounding an illegal landfill (S. Giuliano, Venice, Italy) by principal component analysis and kriging. Environmental Pollution. 122: 235-244.

Garcia-Solsona, E., Masqué, P., Cochran, J.K., Garcia-Orellana, J., Rapaglia, J., Beck, A., Zaggia, L., Collavini, F., and Bokuniewicz H. 2007. Estimating submarine groundwater discharge into the northern Venice Lagoon, Italy by using the radium quartet. Marine Chemistry. Submitted.

Gobler, C.J., and Boneillo, G.E. 2003. Impacts of anthropogenically influenced groundwater seepage on water chemistry and phytoplankton dynamics within a coastal marine system. Marine Ecology Progress-Series. 255: 101-114.

Hiscock, K. 2005. *Hydrogeology: Principles and Practice*. Blackwell Publishing, England, 408p.

Johannes, R.E. 1980 The ecological significance of the submarine discharge of groundwater. Marine Ecolological Progress Series. 3: 365-373.

Kohout, F.A. 1966. A neglected phenomenon of coastal hydrology. Hydrology. 26: 391-413.

Kontar, E., and Ozorovich, Y. 2006: Geo-electromagnetic survey of the fresh/salt water interface in the coastal southeastern Sicily. Continental Shelf Research. 26 (7): 843-851.

LaRoche, J., Nuzzi R., Waters R., Wyman K., Falkowski P. G., and Wallace D. W. R. 1997. Brown Tide Blooms in Long Island's Coastal Waters Linked to Interannual Variability in Groundwater Flow. Global Climate Change. 3: 397-410.

Lee, D. R. 1977. A Device for Measuring Seepage Flux in Lakes and Estuaries. Limnology and Oceanography. 22 (1): 140-147.

Li, L., Barry, D. A., Stagnitti, F. and Parlange, J. Y. 1999. Submarine groundwater discharge and associated chemical input to a coastal sea. Water Resources Research. 35 (11): 3253–3259.

Linderfelt, W.R., and Turner, J.V. 2001. Interaction between shallow groundwater, saline surface water and nutrient discharge in a seasonal estuary: the Swan-Canning River and estuary system, Western Australia. Hydrological processes special issue: integrating research and management for an urban estuarine system: the Swan-Canning Estuary. Western Australia. Hydrological Processes. 15:2631–53.

Loveless, A.M. 2006. Biogeochemical, spatial and temporal dynamics of submarine groundwater discharge in an oligotrophic semi enclosed coastal embayment. PhD thesis, University of Western Australia, Perth, Australia.

Mahiques, M.M. 1995. Sedimentary dynamics of the bays off Ubatuba, State of São Paulo. Bolletino Instituto Oceanografia, São Paulo. 43(2): 111–22.

Martin, J.B., Cable, J.E., Jaeger ,J., Hartl, K., and Smith, C.G. 2006. Therman and chemical evidence for rapid water exchange across the sediment water interface by bioirrigation in the Indian River Lagoon, Florida. Limnology and Oceanography. 51 (3): 1332-1341.

Moore, W. S. 1996. Large Groundwater Inputs to Coastal Waters revealed by Radium-226 Enrichments. Nature. 380: 612-614.

Moore, W.S. 1999. The subterranean estuary: a reaction zone of ground water and sea water. Marine Chemistry. 65 (1-2): 111-125.

Moore, W.S. 2006. Radium isotopes as tracers of submarine groundwater discharge in Sicily. Continental Shelf Research. 26 (7): 852-861.

Oberdorfer, J. 2005. Fresh groundwater discharge to the coastline of the Curepipe Aquifer, Mauritius. Submarine Groundwater Discharge Assessment Intercomparison Experiment, Mauritius; Report to UNESCO.

Oliveira, J., Burnett, W.C., Mazzilli, B.P., Braga, E.S., Farias, L.A., Christoff, J., and Furtado, V.V. 2003. Reconnaissance of submarine groundwater discharge at Ubatuba coast, Brazil using 222-Rn as a natural tracer. Journal of Environmental Radioactivity. 69: 37-52.

Nakayama, T., Watanabe, M., Tanji, K., and Moriuka, T. 2007. Effect of underground urban structures on eutrophic coastal environments. Science of the Total Environment. In press.

Nield, S.P., 1999. Modelling of the superficial aquifer of the Cockburn groundwater area. Prepared for Water and Rivers Commission and Kwinana Industries Council. Western Australia.

Paerl, H. 1997. Coastal eutrophication and harmful algal blooms: Importance of atmospheric deposition and groundwater as “new” nitrogen and other nutrient sources. Limnology and Oceanography. 42 (5): 1154-1165.

Parrot, J.L., and Wood, C.S. 2002. Fathead minnow life cycle tests for detection of endocrine disrupting substances in effluents. Water Quality Research Journal of Canada. 37 (3): 651-657.

Paulsen R.J., Smith, C.F., O'Rourke, D., and Wong, T.F., 2001 Development and Evaluation of an Ultrasonic Ground Water Seepage Meter, Ground Water 39 (6): 904-911.

Paulsen, R.J., O'Rourke, D., Smith, C.F., and Wong, T.F. 2004. Tidal load and salt water influences on submarine groundwater discharge. Ground Water. 42 (7): 990-999.

Povinec, P.P., Commanduci, J.F., Levy-Palomo, I., and Oregioni, B. 2006. Monitoring of submarine groundwater discharge along the Donnalucata coast in the south-eastern Sicily using underwater gamma-ray spectrometry. Continental Shelf Research. 26(7): 874-884.

Pouyat, R. Groffman, P. Yesilonis, I. and Hernandez, L. 2002. Soil carbon pools and fluxes in urban ecosystems. Environmental Pollution. 116: 107-118.

Rapaglia, J.P. 2005. Submarine groundwater discharge into the Venice Lagoon, Italy. Estuaries. 28 (5): 705-713.

Schiavo, M.A., Hauser, S., Cusimano, G., and Gatto, L. 2006. Geochemical characterization of groundwater and submarine discharge in the south-eastern Sicily. Continental Shelf Research. 26 (7): 826-834.

Smith, A.J., and Nield, S.P. 2003. Groundwater discharge from the superficial aquifer into Cockburn Sound Western Australia: estimation by inshore water balance. Biogeochemistry. 66: 125–44.

Stieglitz, T., Rapaglia, J., and Krupa, S. 2007a. Submarine Groundwater Discharge Modification: An Effect of Pier Pilings on Near-Shore Submarine Groundwater Discharge From a (Partially) Confined Aquifer. Estuaries and Coasts. In press.

Stieglitz, T., Taniguchi, M., and Neylon, S. 2007b. Spatial variability of submarine groundwater discharge, Ubatuba, Brazil. Estuarine, Coastal, and Shelf Science submitted for publication.

Swartz, C.H., Reddy, S., Benotti, M.J., Yin, H., Barber, L.B., Brownawell, B.J., and Rudell, R.A. 2006. Steroid estrogens, nonylphenol ethoxylate metabolites, and other wastewater contaminants in groundwater affected by a residential septic system on Cape Cod, MA. Environmental Science and Technology. 40: 4894-4902.

Taniguchi, M.; Burnett, W.C., Cable, J.E., and Turner, J.V. 2002. Investigation of submarine groundwater discharge. Hydrological Processes. 16: 2115-2129.

Taniguchi, M., Turner, J.V., Smith, A. 2003 Evaluations of groundwater discharge rates from subsurface temperature in Cockburn Sound, Western Australia. Biogeochemistry. 66:111–24.

Taniguchi, M., Burnett, W.C., Dulaiova, H., Kontar, E.A., Povinic, P.P., and Moore, W.S. 2006. Submarine groundwater discharge measured by seepage meters in Sicilian coastal waters. Continental Shelf Research. 26 (7): 835–42.

Wilson, J.T. and Kohaltkar, R. 2002. Role of natural attenuation in life cycle of MTBE plumes. Journal of Environmental Engineering. 128 (9): 876-882.

Valiela, I., Foreman, K., LaMontagne, M., Hersh, D., Costa, J., Peckol, P., Demeo-Andersen, B., D'Avanzo, C., Babione, M., Sham, C.H., Brawley, J., and Lajtha, K. 1992. Coupling of watersheds and coastal waters: sources and consequences of nutrient enrichment in Waquoit Bay, Massachusetts. Estuaries. 15 (4) 443-457.

Zuliani, A., Zaggia, L., Collavini, F., and Zonta, R. 2005. Freshwater discharge from the drainage basin to the Venice Lagoon, Italy. Environment International. 31: 929-938.

Zonta, R., Cochran, J.K., Collavini, F., Costa, F., Scattolin, M., and Zaggia, L. 2005. Sediment and heavy metal accumulation in a small canal, Venice, Italy. Aquatic Ecosystem Health & Management. 8 (1): 63-71.

CHAPTER II .Improved understanding of spatial patterns of submarine groundwater discharge from bulk ground electrical conductivity measurements*

1. Introduction

A. Methods to investigate submarine groundwater discharge

Submarine groundwater discharge (SGD) is considered of vital importance to the water balance and the ecology of many parts of the world's coastal zone (e.g. Johannes 1980, Slomp and Van Capellen 2004, Crusius et al. 2005, Kaleris 2005, Mulligan and Charette 2006, Moore 2006, Schiavo et al. 2006). Though the study of SGD has been actively pursued for decades (e.g. Kohout 1966), the impact of the findings has, and continues to be, limited by uncertainty in both accurately quantifying flow rates as well as separating the terrestrial and marine components of SGD (Burnett et al. 2001, Taniguchi et al. 2002, Burnett and Dulaiova 2006). There remains much debate as to the magnitude of this discharge and to whether and where the total flux of SGD (all water which discharges across the sediment sea-interface) or only fresh SGD affects the coastal zone (Taniguchi and Iwakawa 2004, Crusius et al. 2005).

To date, a number of fundamentally different techniques have been used to measure these volume fluxes across the sediment-water interface, *via* (1) the use of tracers for integrated measurements over large areas, (2) direct point measurements using benthic chambers, and (3) mathematical models based on traditional hydrogeologic parameters. The use of tracers has become increasingly popular in the last decade (Moore, 1996, 2006, Krest et al. 2000, Kelly and Moran 2002, Burnett and Dulaoiva 2003, Charette et al. 2003, Hwang et al. 2005, Beck et al. 2007). Frequently applied tracers are the quartet of radium isotopes (223,224,226,228) and ^{222}Rn, the

concentrations of which are elevated in groundwater over surface water. Using these tracers allows for determination of the integrated discharge of SGD into a water body (Charette et al. 2003, Burnett and Dulaiova 2006). Quantitative measurements of fluxes from tracer studies can be confounded by the problem of accurately defining end members in the mixing model. Still, radionuclide tracer studies have successfully been applied in small bays in e.g. Massachusetts and South Korea (Charette et al 2003, Hwang et al. 2005). An important limitation of such tracer studies is their inability to separate fresh groundwater and discharge of recirculated seawater, i.e. water of a marine origin which displays an isotopic signature similar to terrestrially-derived groundwater.

Seepage meters are the primary tool for the direct measurement of the movement of fluids across the seafloor (Lee 1977, Bokuniewicz 1980, Taniguchi and Fukuo 1993, Bokuniewicz et al. 2003, Paulsen et al. 2004, Taniguchi et al. 2005, Taniguchi 2006). Although these chambers display artifacts which may over- or underestimate SGD flow rates (Shaw and Prepas 1989, Libelo and Macintyre 1994, Cable et al. 1997, Shinn et al. 2002), they remain a commonly utilized apparatus because of their simplicity.

SGD has been shown to be highly variable on both spatial scales and time scales (Bokuniewicz et al. 2003, Paulsen et al. 2004, Rapaglia 2005, Burnett et al. 2006, Stieglitz et al. 2007a.). Where flow patterns are inhomogeneous, chamber measurements can only be considered representative of the small part of the sea floor which they cover, and their utility for estimation of total flux into, e.g. an embayment, may be compromised. Therefore, flow estimates obtained with different methods (e.g. tracers and seepage meters) may not compare well at such sites or regions (e.g. Shelter Island, NY: Burnett et al. 2006)

Some of the, to date, incompletely addressed problems in the accurate quantification of SGD fluxes, including separating the salt and freshwater components of SGD, reconciling the differences between point measurements and integrated measurements, and characterizing the variability in discharge between and within locations. A combination of different measuring techniques, both integrated and direct, may complement one another to better constrain SGD measurements. To address this issue, a series of intercomparison experiments were carried out by an international working group partially funded by SCOR (Scientific Committee on Oceanic Research), LOICZ (Land-Ocean Interactions in the Coastal Zone), IOC (Intergovernmental Oceanographic Commission) and the IAEA (International Atomic Energy Agency) (Burnett et al. 2001). Here we summarize investigations of the application of (electrical) ground conductivity measurements aimed at improving the quantification of SGD, carried out within the framework of the intercomparison experiments. We discuss the use of combining indirect and direct SGD measurements (made using conductivity and seepage meter measurements) in the context of improving the accuracy of SGD flux estimates, and elucidating the origin of terrestrial or marine groundwaters.

B. Application of geoelectric (conductivity/resistivity) techniques in SGD studies

Whilst SGD has been successfully located, mapped and/or quantified with various water column tracers including salinity (e.g. Milham and Howes, 1994), relatively few studies have used pore water salinity or conductivity as a means of determining the location and rate of SGD. Where terrestrially-derived fresh or brackish

groundwater is of interest, salinity and conductivity can be used as a tracer. Although salinity is conservative, the bulk ground conductivity (BGC) of sediment is a function of porosity and salinity of the interstitial water. As porosity increases, the amount of (conducting) interstitial water increases, raising BGC. In addition, an increase in the salinity of the interstitial water will raise BGC. In practice, variations of porewater salinity are significantly greater than variations of porosity (or porewater fraction), and it is this relationship that can be used in studies of fresh SGD. An advantage in the use of BGC is found in the remote applicability of these measurements. Whereas salinity in the pore water has to be measured directly, BGC can be measured without laborious sample collection (Zohdy and Jackson 1969). However, conductivity measurements are limited by the difficulty of separating pore water conductivity from sediment influences on bulk conductivity (Manheim et al. 2004a). Note that the term 'conductivity' is used throughout this paper. Other authors sometimes use the inverse of conductivity, or 'resistivity'.

In previous work, a number of different sensor designs have been employed. Kermabon et al. (1969) created a probe for measuring electrical resistivity, in order to determine the porosity and density of the sediments. The probe was large, 13 m long and had a mass of 700 kg in water. They related the resistivity of the brine to the resistivity of the saturated sands and a formation factor, in order to constrain the differences in sediment resistivity not accounted for by porosity alone. The formation resistivity factor is a function of the type and character of the sediment matrix, and varies with porosity. The sampling took place in deep sea sediments off the coast of Sicily, where the porosities ranged from 0.7 to 0.9. Hesslein (1976) created an instrument

which can measure pore water conductivity as well as take samples at close intervals (<10cm). Though he does not mention its utility in locating SGD, it is the model for later pore water samplers.

Lee (1985) used a temperature-sensitive transducer system to identify anomalies in bottom/sediment conductivity. This instrument included a conductivity probe attached to a rig which allowed the drag to remain in contact with the sediment-sea interface when towed behind a boat. Using the sediment drag, he was able to locate possible areas of discharge with both higher ground conductivity measurements (from 0.1 mS cm^{-1} to 0.4 mS cm^{-1}) and higher sediment temperature; however the time it took for the transducers to reach equilibrium severely limited the utility of the drag over large areas. He found that deep pore water in lake beds had a noticeably higher conductivity than that of ambient waters due both to higher temperature in the pore water as well as containing more dissolved salts. Vanek and Lee (1991) used a combination of the aforementioned conductivity probe, a pore water sampler, and bulk ground conductivity measurements to map zones likely to have fresh ground water discharge in Sweden. At this site, the bottom sediments were generally sandy. To measure pore water conductivity they dragged a continuously recording probe similar to the one used by Lee (1985), while they utilized a suction sampler to sample the pore water to determine the accuracy in the probe. They measured conductivity in a 300 x 350 m grid. By measuring conductivity during two different seasons in ambient sea water (28.2 mS cm^{-1}/39.8 mS cm^{-1}), wells (0.6 mS cm^{-1}/0.6 mS cm^{-1}), and pore water (21.05 mS cm^{-1}/24.7mS cm^{-1}) they deduced that pore water is comprised of a 70:30 or 60:40 sea water-fresh water mix dependent upon season, as the conductivity of the pore water changed with temperature.

They also used a well-flushed seepage meter and compared its water with that of wells, piezometers, and ambient sea water, showing that when well-flushed it consisted of greater than 90% sea water, which is slightly higher than what they measured in the pore water.

Seplow (1991) discussed the impact of SGD on pore water salinities with a focus on Great South Bay, NY. She used both laboratory and field experiments to test her hypothesis that the growth of density driven salt fingers will be reduced in the face of upward advection due to SGD. At a flow rate of 45 cm d^{-1}, salt fingers were still able to penetrate into the sediment, although the penetration rate was greatly reduced (~0.13 cm d^{-1}). The laboratory analysis used dye to trace the development of salt fingers in homogenous sediment while water was being pumped upward at different flow rates. In the field, a small, hand driven, conductivity probe, developed by Lee, was used to search for variation in BGC on the scale of centimeters. Some evidence for salt-fingering structures was found. The importance of Vanek and Lee's and Seplow's work was to use small scale conductivity measurements (both with the sediment drag as well as with a small conductivity cell attached to a rod which could measure conductivity every 2 cm to a depth of 14 cm) to look at in-homogeneities that may have been indicative of centimeter scale advective flows of pore water. The phenomenon, referred to as salt fingering, is one of the processes implicated in the penetration of salt downward into the sediment in the face of upward advection (Wooding 1969 as cited in Seplow 1991).

Further work using bulk ground conductivity patterns as a proxy for fresh pore water has been attempted in several sites in which the use of a conductivity probe was employed in locating sites of SGD. This method includes the use of a Wenner array of

electrodes through which induced voltage is amplified, and both current and voltage are measured with conventional multimeters (Stieglitz 2005, Stieglitz et al. 2000, 2007a,b).

In Australia, using this method, sediment was measured in which BGC was significantly reduced near "wonky holes" (Stieglitz and Ridd 2002, Stieglitz 2005) Scouring, possibly created by the high rates of advection of fresh groundwater, led to the existence of these features. In these studies BGC seemed site-dependent with a sharp interface between high and low BGC at the sediment surface on one beach, while at another beach there was a non-uniform BGC distribution. Near the "wonky holes" at a depth of about 20 m, BGC seemed to be lowest near the bottom of the scour (Stieglitz 2005). In the next chapter, we discuss the possibility that pier pilings may have punctured a confining layer allowing for an anomalously high advection of fresh groundwater (Stieglitz et al. 2007a). BGC measurements detected this influx of groundwater as BGC was lower in a five meter zone around the pilings. At this site, BGC was inversely correlated with flow rates taken with seepage meters. It seems the importance of this data is to show that these measurements can be a good first approximation as to the location of upward advection of SGD. However, low BGC in the sediment may not necessarily require the existence of SGD and the technique should be used in conjunction with seepage meters, which will be described below.

Cores have also been used in Belfast Bay, Maine (Ussler et al 2003) in the hopes of finding a low chloride signature (which is also a proxy for salinity in the sediment) indicative of fluid discharge which could lead to the scouring of pockmarks. However of the 42 cores taken, no clear signal of low chlorinity could be found suggesting that the pockmarks were not caused by SGD, or a least the discharge of fresh groundwater.

Greenwood et al. (2004) state that the use of surface electromagnetic and resistivity measurements could be utilized to map shallow porewater salinity as resistivity (similarly to conductivity) is based on both the porosity of the alluvium as well as the ionic content of the porewater (Breusse 1963). An advantage to the use of resistivity is found in the remote applicability of these measurements. Whereas salinity in the porewater has to be measured directly, resistivity can be measured without direct contact with the water column (Zohdy and Jackson 1969). Problems with resistivity measurements are discussed in Manheim et al. (2004a,b) and include the difficult process of establishing electrode contact and of making multiple measurements, the complexity of inversion modeling, and the difficulty of separating pore water conductivity from sediment influences on bulk resistivity.

Detailed analyses of the possibility of mapping SGD by using streaming resistivity surveys were reported by Manheim et al. (2004a,b), in which streamer cables were towed behind a boat in transects across coastal bays of the Delmarva Peninsula. The resistivity data were collected with a Zonge GDP-32 multifunction resistivity/induced polarization receiver. The data were then processed using Surfer software into three profile plots which calibrate the calculated resistivity to the observed resistivity. The investigators report high quality results when trying to locate areas of fresh groundwater discharge along transects of 8 to 30 km in length. Low conductivity (inverse of resistivity) zones from tens of meters to several kilometers in length were discriminated from high conductivity regions elsewhere. The results were ground-truthed with in-situ conductivity measurements taken with a manual Orion 140 conductimeter, and were found to correspond to a porewater salinity of 0.5 at the ambient temperature.

In the coastal lagoons along the Delmarva Peninsula, studied by Mannheim et al. 2004a,b several, 10 km long survey lines of resistivity were taken which allowed for the observation of two types of SGD. The first indicated an area of fresh water in the sediment at a depth of up to 3 m between 10 and 500 m offshore. The second was thicker and located further offshore. Both layers have a resistivity of greater than 10 ohm-m. Nowroozi et al. (1999) used a similar system to detect saltwater intrusion in Chesapeake Bay. Kruse et al. (1998) utilized this same technique to trace seawater intrusion along the gulf coast of Florida. It seems that the utility of these surveys is to quickly (at speeds up to 5 kts) test for the presence of fresh water in the sediment by measuring resistivities over large areas, although the existence of a low resistivity area does not prove the upward advection of freshwater and cannot provide estimates of discharge rates.

Breier et al. (2005) compared radium and resistivity measurements along a 17 km transect near Corpus Christi, Texas. Their survey was done after a rainstorm when surface salinity in the bay ranged from 2 to 7. Resistivity measurements (which they converted to conductivity measurements) showed an area of low sediment conductivity (<8 mS cm^{-1}) in the center of the bay. They also show a good correlation between water column radium and resistivity measurements, however radium desorbs from particles at a salinity of about 5, therefore this data should viewed with caution.

Greenwood et al. (2006) tested the feasibility of using electromagnetic (EM) methods in addition to resistivity surveys to map pore water salinity in shallow waters. This method proved useful at water depths of less than 1.5 m. They were able to clearly reproduce images of the high salinity pore water found around the roots of mangroves.

This method succeeded in detecting anomalies in brackish to hypersaline waters, but only if the difference in conductivity between the anomaly and the surrounding area was greater than 1 mS cm^{-1}. They suggest that this tool may not be useful in determining diffuse SGD as the change in conductivity may not be great, however in certain areas known to have high SGD the EM system was able to locate the low conductivity anomaly. A known or calculated formation factor was used to correlate area conductivity to pore water conductivity, but the authors point out that the formation factor is site dependent. Earlier, Hoefel and Evans (2001) also discussed the possibility of using EM data as a means of detecting SGD. They demonstrated that the method is feasible but that BGC depends not only on the pore water conductivity but on the porosity of the sediment matrix. The system utilized in this study consists of an EM transmitter and three receivers towed behind the transmitter. The change in the strength of the magnetic field are sensitive to changes in seafloor properties. The system, however, has a resolution of 10 m which is likely to miss the small scale variability in SGD noted in several studies mentioned earlier.

2. Methods

A. Conductivity survey and seepage meter deployments

Conductivity was recorded in-situ using a high resolution conductivity probe, consisting of four ring electrodes (2 cm diameter) configured in a Wenner array with an equal electrode vertical spacing of 1 cm. The ratio of current to induced voltage is proportional to ground conductivity. Vertical conductivity profiles were recorded by

inserting the probe into the ground, taking a reading at a particular depth, and then successively pushing the probe further into the ground. At each site a series of transects were surveyed in which measurements were taken several meters apart, with higher spatial resolution in areas with significant conductivity gradients. Measurements were taken at depth intervals of 10 cm to a maximum depth of 1 m to 1.5 m below the sediment interface. At each depth, the probe was left in place until readings stabilized. Transect data were interpolated by kriging using SURFER 6.0, taking spatial anisotropy in data points into account. The greatest source of error in these measurements is in the record of depth in the sediment.

When low BGC (<3 mS cm^{-1}) is found in saturated sediment, the assumption is made that there is a significant presence of fresh interstitial water. If BGC is higher than this value, there must be some conducting salts in the sediment. Bulk ground conductivity is converted to interstitial water conductivity by multiplying by the formation factor *(F*)* (Ullman and Aller 1982, Maerki et al. 2004) which according to Kermabon (1969) is equal to the porosity (Φ) times an exponent related to tortuosity $^{(m)}$;

$$F^* = \Phi^{-m} \qquad (1)$$

Concurrently with the conductivity measurements, manual seepage meters, first described by Lee (1977), were used to directly measure flow. Water which entered the chamber displaced the water within the chamber into a plastic bag attached to an outlet spigot. Measuring volume and time, a flow rate can be determined. Bags are usually pre-filled with 500 ml of ambient water (except when samples were collected for water quality measurements) to reduce artifacts (Shaw and Prepas 1989, Shaw et al. 1990, Libelo and MacIntyre 1994) and to allow for the measurement of flow rates into the

sediment (saltwater intrusion). Chambers were arranged in shore-perpendicular and, if possible, shore-parallel transects in an attempt to observe spatial discharge patterns. Where possible, the chambers were left in place for 24 hours prior to the first measurement. Samples were collected approximately every thirty minutes for periods between six and twelve hours. Near a submarine spring in Mauritius and at some locations in Ubatuba, Brazil samples were collected every ten minutes as flow rates were very high and the bag filled quickly. At Shelter Island and Brazil, in addition, a comparison was made with three types of automated seepage meters (Burnett et al. 2006, Stieglitz et al. 2007a). A discussion of error associated with seepage meters is found in Appendix B, here we have determined that the error is ±12%.

B. Study sites:

Five study sites were utilized by the SCOR-LOICZ working group 112 for the intercomparison of SGD measuring techniques. They were chosen for their diverse hydrogeological conditions, which are considered representative of many other coastal systems (Burnett et al. 2006). At four of these sites, coincident measurements of ground conductivity and SGD flow rates through seepage meters were made. The sites are briefly introduced here; more detailed information is found in Burnett et al (2006).

Cockburn Sound, Australia:

Cockburn Sound is a large (150 km^2), sheltered, marine embayment on the western coast of Australia (Figure 1a, Table 1). Much of Cockburn Sound is adjacent to a low-lying, drained sandy coastal plain (Burnett et al. 2006). The tidal range in

Cockburn Sound is 0.3 – 1.0 m (Taniguchi et al. 2003). The study site overlies an unconfined, coastal plain aquifer with high permeability which is recharged by seasonal rainfall of 0.85 m annual average of which 15-28% infiltrates the aquifer (Smith and Nield 2003). This aquifer is underlain by a layer of low permeability sediments as well as the confining Osborne formation (Smith and Nield 2003). The region is underlain by ~12000 m of marine and continental sediments, which are covered by a thin layer of Quaternary age deposits that act as a largely unconfined aquifer. Groundwater in the area generally flows in a westerly direction towards Cockburn Sound. There are virtually no surface streams as the soil is extremely permeable. Hydraulic conductivity in the area is large (20-1000 m^3 d^{-1}) but the hydraulic gradient is relatively low, ranging from 0.001 to 0.003 (Smith and Nield 2003). It has been hypothesized that over 70% of the nitrogen input into the bay is through groundwater discharge as much of the groundwater in the adjacent plain is characterized by a high nitrogen load (Kendrick et al. 2002).

Shelter Island, NY:

Shelter Island was chosen as representative of a glacial outwash plain setting located in Peconic Bay at the eastern end of Long Island (Figure 1b, Table 1). It is underlain by a highly permeable (conductivity ~100 m d^{-1}), homogenous but anisotrophic, unconsolidated aquifer representative of many coastlines located at the edge of the last glacial maximum. Shelter Island is a small (29.8 km^2) island whose glacial deposits lead to moderate relief (~60 m, Soren 1978). Here a marine influence

leads to a local annual precipitation of 1.17 m, about half of which recharges the aquifer system. Surface runoff is ephemeral and insignificant (Paulsen 1996). Freshwater in the upper glacial aquifer discharges directly into the surrounding coastal water, lowering the salinity in the open coastal waters around the island (Soren 1978, LaRoche 1997, Schubert 1999). Below the unconfined aquifer lie the Magothy and Lloyd Sand Member aquifers both of which contain groundwater with brackish salinities 2-10: (Soren 1978, Paulsen et al. 2001).

At the study area, West Neck Bay (Figure 1b), a narrow fringing marsh separates the bay from the coast. The tide is semi-diurnal and varies from 0.7 to 1.1 m. The sediment in the bay is variable, with fine to medium-grained sand located near the pier and pockets of silt found away from the pier. The bay is sheltered from the open sea, and therefore non-nautical wave action is minimal. Seepage of fresh groundwater above the water line can be observed in the intertidal zone in the form of rivulets of fresh water. Previous observations of seepage rates with a continuous seepage meter deployed close to a pier at the study site indicated seepage flow rates of up to 160 cm d^{-1}, displaying a strong correlation with tidal water level (O'Rourke 2000). Such flow rates are considered high for an unconfined aquifer system; at nearby sites on the same coastal-plain aquifer, SGD had been measured at rates much lower than 50 cm d^{-1} (Bokuniewicz 1980).

Ubatuba, Brazil:

Flamengo Bay near Ubatuba, Brazil (Figure 1c) was chosen as representative of a fractured rock aquifer which is likely to display highly variable SGD. Fractured rock would create preferential conduits through which groundwater would flow. Granitic and magmatic mountains, over 1000 m in elevation, spill down into the bay forming the basement for groundwater flow. Groundwater flow occurs in fractures of these pre-Cambrian rocks. These rocks are overlain by moderately permeable fine grained sands (4-5Φ). Hydraulic conductivities range from 2.5 to 50 m d-1 depending on location above the fractured rocks. The tidal range in Flamengo Bay ranges from 0.6-1.2 m. Here freshwater discharge is sufficient to reduce the salinity of local waters as seen at Shelter Island (Oberdorfer et al. 2007). Precipitation in the area is one of the highest in Brazil, averaging about 1.8 m yr^{-1} (Oliveira et al. 2003). Relevant site characteristics are located in table 1.

Flic-en-Flac Bay, Mauritius:

Mauritius was chosen as a site representative of volcanic island settings in which steep elevations are likely to create substantial onshore hydraulic gradients. The island of Mauritius covers 1865 km^2, and reaches elevations of up to 600 m. The average annual precipitation varies from 1.13 m on the east coast, to 0.90 m on the west coast, to 4.0 m on the central plateau (Burnett et al. 2006)**.** The coastal zone largely comprises lagoons created by the formation of either barrier reefs or fringing reefs. Lagoons are estimated to cover an area of 243 km^2. In some places along the western and eastern coasts, groundwater discharges are clearly visible. The coast has experienced algae blooms

(occasionally red tides), confirming the impact of contaminants in the lagoons and their deleterious influence on the health of the coral reefs in the lagoons (Bokuniewicz et al. 2007). Much of the coast is underlain with fractured volcanic basalts leading to conduits for discharge (J. Oberdorfer 2005, personal communication).

Flic-en-Flac Bay is on the eastern coast of the island of Mauritius (Figure 1d, Table 1). The embayment is partially enclosed by a fringing coral reef and is blanketed offshore with a layer (~1 m) of medium-large grained, coral sand (0-2Φ). Much of the lagoon is covered with patchy coral. The tidal range in the bay is less than 0.5 m. A well-known submarine spring is found in the area. Freshwater discharge from this submarine spring, and possibly others, is sufficient to reduce the salinity of coastal waters from oceanic salinities of 35 to salinities of 33 in the lagoon.

3. Results

The results presented here represent data on the SGD and BGC collected simultaneously at the different study sites. In the following analysis time-averaged values of these measurements will be used; although both SGD and BGC are temporally variable, the measurable changes tend to be on different scales. Fluctuations in SGD are typically much more rapid than the response of the BGC. As a result, I consider BGC as a natural filter, averaging out higher frequency fluctuations in SGD. Data from West Neck Bay, Ubatuba, and Mauritius have been reported previously (Stieglitz et al. 2007a, Stieglitz et al. 2007b, Bokuniewicz et al. 2007), and are here used in combination with data from Cockburn Sound, Australia. Data are presented in chronological order.

A. Cockburn Sound, Australia

Data were collected in Cockburn Sound from November 27-December 6, 2000. Three shore-normal transects (10 m) and one shore-parallel transect (85 m) of BGC show fresh groundwater close to the shoreline being replaced by increasingly salty groundwater with distance from the high tide mark. The transition occurs along a well-defined, shallow vertical gradient typical of unconfined aquifers (Stieglitz 2005). BGC increased from ~1 mS cm^{-1} near the shore to over 15 mS cm^{-1} less than 10 m from shore.

Two shore-parallel transects consisting of four manual seepage meters each were deployed up to 70 m from shore. These manual seepage meters show an offshore decrease in average SGD; however these drums were deployed offshore from the conductivity transects and therefore no direct relationship can be ascertained from these seepage meter deployments. Alongside one of the conductivity transects, an automated seepage meter was placed. Here seepage rates ranging from 4.05 to 60.88 cm d^{-1} were found, with a mean seepage rate of 32 cm d^{-1}. In addition, there was a strong inverse correlation between water elevation and SGD. This drum was deployed at a site with a medium value of BGC (6 mS cm^{-1}).

B. Shelter Island, NY USA

Data were collected in Shelter Island from May 17-24, 2002. Bulk ground conductivity measurements show fresh groundwater in the sediment surrounding a pier (Figures 2a and 2b). Here, two shore-normal transects and one shore-parallel transect of

BGC measurements were taken extending from the high water mark to 30 m offshore, at depths of up to two meters. In addition, a shore-normal transect of manual seepage meters measured coincident flow rates at 8, 11, and 15 m from the high tide mark. At 15 m from the high tide mark a shore-parallel transect of seepage meters (manual and automated) was placed 0, 2, 3, and 4 m from the pier.

Sediment BGC values were less than 2 mS cm^{-1} directly beneath the pier, indicating porewater with very low salinity. East of the pier there was a mixing zone about 2 m wide in which BGC values increase from 2 mS cm^{-1} to 9 mS cm^{-1}. At the ambient temperature of 14°C and a seawater conductivity of 34 mS cm^{-1} (both measured directly) salinity equals 28, or using (1), 9 mS cm^{-1}. The mixing zone width (or the area in which there was a large gradient in BGC) was negatively correlated with tide and ranged from 2.5 m at high tide to 5 m at low tide. All manual seepage meter measurements showed a strong negative correlation with tide ranging from about 32.5 cm d^{-1} at low tide to less than 5 cm d^{-1} at high tide along a transect 2 m away from a pier (Figure 3). This is an expected pattern in situations where SGD is driven by onshore hydraulic gradients. However, other expected patterns, such as an exponential decrease in SGD with distance from the shoreline, were not seen (Bokuniewicz 1980; Stieglitz et al. 2007a). Seepage rates did, however, decrease with (alongshore) distance from the pier (Figure 4). The highest average seepage rates of 65 cm d^{-1}, with a peak flow of 190 cm d^{-1}, were recorded directly under the pier, which is consistent with previous measurements close to the pier (O'Rourke 2000, Paulsen et al. 2004). Moving away from the pier, seepage rates of 25 cm d^{-1} with peak flow of 37 cm d^{-1} were recorded 2 m away. At 3 and 4 m from the pier, the seepage rates were further reduced to 6 cm d^{-1}

(peak 12 cm d^{-1}) and 2 cm d^{-1} (peak 6 cm d^{-1}) respectively (Sholkovitz et al. 2003) (Figure 4a and Table 1).

The salinity of water collected by the seepage meters increased with distance from the pier. When the devices were flushed, salinity averaged 10, 19, and 27 in the chambers located 2, 3, and 4 m from the pier respectively.

SGD decreased exponentially with increasing BGC, and with distance from the pier (figure 4a, and b). At sites of high BGC, the discharge was low, though not zero suggesting that even without freshwater discharge, there is an amount of water originating from the bay present. This water is, perhaps, driven into the sediment by tidal pumping, due to the presence of a considerable tidal excursion (> 1 m), or other mechanisms, which will be discussed in Chapter IV. Both the magnitude of the SGD and the width of the "low BGC" zone seem to be related to the tidal elevation. During ebb tide, the SGD in each of the devices increased by a factor of 2-4 while the "low BGC" zone widened by a factor of 2. This is likely to be due to a greater water table hydraulic gradient present at low tide. BGC at this site is averaged over time, as the BGC in certain locations changes with changing tidal elevation. Therefore the relationship discussed here only considers the average BGC value. Directly under the pier, for instance, the flow rate is negative at high tide, while BGC remains low. The reason for this may be that SGD does not remain negative long enough for sufficient salt penetration into the sediments directly under the pier, although it does on the fringe of the "low BGC" zone.

C. Ubatuba, Brazil

Data were collected in Brazil from November 16th to 22nd 2003. BGC profile data were collected along a shore-normal transect in Flamengo Bay (Figure 5). In figure 5, the slope of the beach and the water level at the time of recording are included.

In Flamengo Bay, it was difficult to push the probe into the sediment. A change in physical resistance is commonly associated with a change in density/porosity of the sediment and hence is likely to mark a change in sediment type. Locations of pronounced changes in physical resistance are marked in figure 5 (orange crosses)

A time series of BGC measurements was recorded at 35 cm and 45 cm below the sediment surface at site S6, alongside a manual seepage meter and an automated seepage meter (the latter from Woods Hole Oceanographic Institution). The depths at which the conductivity time series were recorded are indicated in figure 6 (top). The depth of 35 cm coincides with the change in sediment type at this location. Conductivity was burst-recorded for ca. 15 s every 10 min.

Manual seepage meters were placed along both shore-parallel and shore-normal transects. The shore-parallel transect consisted of three seepage meters at the low tide line. Seepage meters in the shore-normal transect were located at distances of 5, 10, 18, 32 and 44 m from the low-tide shoreline at (water) depths of 0.33 m, 0.71 m, 1.07 m, 1.46 m and 1.65 m respectively (Figure 7). Though the highest discharge (268 cm d^{-1}) was measured close to shore, SGD in the shore-parallel transect was variable over small distances. Indeed, discharge decreased with distance from shore, although the 5th and 6th locations also displayed significant flow rates (Bokuniewicz et al. 2004) (Figure 8). The

lowest salinity (~20) was measured in the seepage meter with the highest flow rate (Table 2).

As on Shelter Island, measured flow rates were highly dependent on location. Salinity in the chambers did show a correlation with flow rates, though the range of salinity (20-30) was not nearly as great as in Shelter Island (6-28). Conductivity measurements showed that a layer separating high from low BGC sediments was present about 50 cm beneath the surface, (Figure 5). Where this low conductivity fraction extends towards the surface, higher flow rates are measured within the chambers. As the location of advection of fresh water in this site is likely to be controlled by the spacing of fractures, the pool of lower conductivity water was probably affected by the presence of one of these fractures.

D. Flic-en-Flac Bay, Mauritius

Data were collected from March 18th to 25th 2005. BGC was measured in a 20,000 m^2 grid surrounding a known point of freshwater discharge (Figure 9). Here measurements were taken every 5 m in 100 m long offshore transects every 10 m along the beach. At each location, BGC was measured at 5 depths up to a maximum of 2 m in the sediment. Between locations in which there was a comparatively large gradient in BGC, additional profiles were recorded to achieve higher resolution. Maximum BGC was about 14 mS cm^{-1} corresponding to average surface water salinity in the area (~33). BGC in the sediment directly next to the spring was 0-1 mS cm^{-1}. The influence of the spring was widespread, as low BGC values were found within a 25 m radius of the

spring. Outside of this radius, we measured a sharp transition zone (5 m) between low (<3 mS cm^{-1}) and high (>10 mS cm^{-1}) BGC (Figure 9).

Nine chambers were placed at a total of 24 locations (Figure 1d). These seepage devices were deployed in three shore-normal transects (one adjacent to the spring, one in a cove 1000 m north of the spring, and one about 500 m south of the spring), as well as in a 1500 m shore-parallel transect (Figure 1d), corresponding to areas of low BGC as were measured on the first day of the experiment.

The first shore-normal transect consisted of five devices located adjacent to the known submarine spring. The shoreward device (M1) was placed at a water depth of 50 cm. The other four devices (M3, M6, M5, and M4) were placed at distances of 20, 50, 80, and 150 m from the low-tide shoreline. The respective water depths at low tide were 1.6 m, 1.9 m, 1.4 m, and 1.6 m. The tops of the devices were between 0.04 and 0.1 m above the sea floor. Measurements were taken at this transect over a period of 72 hours. The other two shore-normal transects will not be discussed in this paper.

The shore-parallel transect consisted of measurements taken at various times from devices deployed within 15 m of the low tide line. This transect consisted of 18 devices which were in place for a period of 10 hours to 5 days. Not all measurements along this transect were made simultaneously; however, at least six devices along this transect measured SGD throughout the sampling period.

The measured seepage rates were variable over the entire study area, ranging from negative seepage (i.e. flow of lagoon water into the sediment) to SGD of >490 cm d^{-1}. However, SGD showed a predictable pattern in the vicinity of the spring. Devices

placed near the spring recorded high rates while devices placed away from the spring recorded consistently lower flow rates.

The presence of the spring precluded the observation of an offshore decrease in SGD, and was evident in the alongshore transect (Figure 10). All of the devices in the alongshore transect were deployed in permeable, and presumably homogeneous, carbonate sands. SGD was 216 cm d^{-1} 15 m south and shoreward of the spring. At the same distance north of the spring, SGD was found to occur at a value of between 5 and 15 cm d^{-1}, more typical of the rest of the Flic-en-Flac Lagoon.

Only in the vicinity of the spring did the benthic chambers collect water with a significantly different salinity than the ambient lagoon water. Here waters with a salinity as low as 5 were collected by the benthic chambers. In addition, a linear inverse correlation was seen between salinity and SGD rates (Figure 11).

Below a flow rate of 200 cm d^{-1}, a negative, linear correlation between BGC and SGD in the chambers was observed. At flow rates greater than 200 cm d^{-1}, SGD had the same salinity as the water coming directly out of the spring. Average flow rates increased to close to 400 cm d^{-1} at this site and therefore it will be difficult to distinguish flows above 200 cm d^{-1} with BGC measurements alone. Salinities inside the chambers were inversely correlated with BGC measurements as well. At this site the flow rates, though variable, showed no correlation with tide. This suggests that flow was driven primarily by the submarine spring. Of the 24 meters which recorded ambient salinity and high BGC, the average flow rate was 10 cm d^{-1} but reached as high as 30 cm d^{-1} (Table 2). The values seemed to depend on beach slope, with the higher SGD occurring

near steeper gradients. The fairly large recirculated component of SGD at this site suggests enhanced mixing processes within the upper few centimeters of sediment.

E. Interpretation of BGC results

In these studies, BGC seemed site-dependent with a sharp interface between high and low BGC at the sediment surface at certain sites, while at other sites there is a non-uniform BGC distribution. In Cockburn Sound, BGC distribution was likely controlled by the discharge of fresh groundwater close to the shoreline as BGC increased rapidly from less than 1 mS cm^{-1} (fresh porewater) to more than 15 mS cm^{-1} (saltwater) within 10 m of the shore. In Shelter Island, BGC was high except along the shoreline as well as the immediate vicinity of the pier. In both of these cases, the transition zone was sharp, the gradient being between <1 mS cm^{-1} and 10 mS cm^{-1}. It is likely, then that at this site BGC was controlled by processes involving the emplacement of the pier. This idea will be fully discussed in the following chapter. In Ubatuba Bay, BGC is hypothesized to be dependent on fractures in the basaltic rock below the sandy sediment. Once again we found sharp gradients in the BGC from less than 1 mS cm^{-1} to greater 14 mS cm^{-1}. In Mauritius, BGC was clearly controlled by the location of the freshwater spring as abrupt transitions were found in every direction about 10-15 m from the center of the visible spring. In addition, along the beach there was a small zone of low BGC, where higher flow rates were found.

F. Interpretation of seepage meter results

SGD as recorded by seepage meters also seemed dependent on location in the area and, in general, corresponded very well with zones of low BGC (A discussion of the uncertainty associated with seepage meters is found in Appendix B). However, the negative correlation between BGC and SGD was site-dependent, and seemed to be based on several factors which will be explained in the next section (Table 3). In Cockburn Sound, high rates of seepage were located in the vicinity of the shoreline, and therefore characteristic of a coastal zone site in which SGD is driven by the onshore hydraulic gradient. Exponential decrease has previously been seen in similar sites (i.e. Bokuniewicz 1980) and follows basic hydrogeological theory (Hubbert 1940). Meanwhile in Shelter Island, average seepage decreased exponentially from 65 to 2 cm d^{-1} within a distance of 4 m from the pier. Evidence suggests that this pattern is due to the piercing of an apparent confining layer, as will be discussed in the next chapter of this thesis. In Ubatuba, discharge followed an apparently random pattern, with rates varying from 8 to 280 cm d^{-1}, most likely explained by fractures in the basaltic basement. If the seepage meters were placed near or above such fractures in the aquifer, high flow rates may be measured. Discharge of great magnitude was found near and above the spring in Mauritius (>490 cm d^{-1}). At this site a large lava tube may have served as a conduit (or underground river) of large flow. There are many examples of this type of feature on the island of Mauritius. Discharge was relatively low elsewhere at this site, but not insignificant, suggesting that in the absence of freshwater discharge there is still some re-circulated water discharging, perhaps driven into the sediment by bioirrigation, tidal pumping or wave set-up.

4. Discussion

A. Extrapolation of SGD values from BGC measurements

A family of curves is plotted in figure 12 showing BGC as a function of SGD (Table 2). The ability to extrapolate SGD values from BGC would be advantageous because it requires less labor to collect BGC data than to take many accurate SGD measurements, and it is more feasible to cover a large area. Using an empirical relationship between BGC and SGD:

$$\sigma_b = Ae^{-\alpha SGD} \qquad (2)$$

where σ_b is bulk ground conductivity. The parameter A is the value of BGC when there is no SGD. Presumably, this is the conductivity of the sediment matrix with the pore fluid at the ambient, oceanic salinity. Because the open water salinity and the (low) matrix conductivity is similar at the coastal sites, the value of A is also similar averaging 14.6 mS cm^{-1}. Because the value of A is similar for all sites, this site-specific, empirical relationship can be determined with even one measurement, as I have done for Cockburn Sound, although with a relatively low the degree of confidence.

When α increases the curve relating SGD and BGC becomes steeper, Shelter Island has an α of 0.0492 while Mauritius has an α of 0.0063. The value of α therefore represents the ability of SGD to flush the sediment with fresh water. When α is a large a small increase in SGD drives salt from the pore water lowering the BGC rapidly. Considering the data from Mauritius, for example, a BGC measurement corresponding to a salinity of 15 would be proportional to a discharge of 100 cm d^{-1}, while at Shelter Island this same BGC measurement would suggest a discharge of 20 cm d^{-1}. I will show later that α might be directly correlated to the freshwater fraction of the SGD.

The value of α may be associated with large-scale aquifer characteristics. The more homogeneous aquifers of Shelter Island and Cockburn Sound have the highest values for α. The volcanic rock, with its lava tubes in Mauritius, had the lowest value of α, and the fractured-rock aquifer in Brazil had intermediate values. I hypothesize that other unconsolidated aquifers would be characterized by large values of α, and that heterogeneous aquifers, karsts for example, would be represented by low values of α. On a small scale, processes such as bioturbation, tidal pumping, wave set-up, and density-driven salt fingers have been previously discussed, in addition to differences among the sediment matrix, such as porosity and tortuosity (Ataie-Ashtiani et al. 1999, Li et al. 1999, Taniguchi et al. 2005, Jaeger et al. 2005). Qualitatively as porosity, porewater salinity, and temperature increase, BGC increases. As tortuosity and grain size increase BGC decreases. Meanwhile SGD is directly correlated with hydraulic conductivity and tidal elevation. Table 1 is a partial list of relevant, physical parameters. As there is no clear pattern between individual site characteristics listed in Table 1and the empirical parameters A and α; it seems that no single characteristic controls this relationship. For example larger grain size, which allows for higher permeability, could produce the differences seen between Mauritius (1-0Φ) and Shelter Island (7-5 Φ), but not between Brazil (5-4 Φ) and Cockburn Sound (3-1 Φ) (These numbers are based on grain size descriptions in the literature Table 1). Porosity, as reported in the literature, does not change much from site to site. Hydraulic conductivity is generally inversely correlated with α, though it does not hold true for all sites. Meanwhile, tidal range has no apparent correlation with the slope of the relationship curve. It is likely, therefore, that the relationship is a function of a combination of these, and, perhaps, other

characteristics. The mechanisms which affect this relationship and a quantitative relationship between BGC and SGD will be discussed further in Chapter IV. In any event, we can largely reproduce the correlation between SGD and BGC at the various sites (Figure 12) pending different values of A and α with this empirical relationship alone.

B. Quantifying SGD using the empirical relationship

Based upon the site specific correlation between BGC and SGD as well as the area covered by BGC measurements we can approximate total discharge per kilometer of shoreline into the study areas. Using the Cockburn Sound BGC data to interpolate SGD throughout the study site (3200 m^2), and assuming high magnitude SGD occurs only in the vicinity of the shoreline (Burnett et al. 2006) the total discharge into Cockburn Sound is 2.91 x 10^3 m^3 d^{-1} km^{-1} of shoreline. For Shelter Island, interpolating the BGC data throughout the study site (3000 m^2) and, assuming the high discharge only occurs at the immediate shoreline and in the vicinity of the pier pilings, the total discharge into West Neck Bay is 1.59 x 10^3 m^3 d^{-1} km^{-1} of shoreline (Table 4). In Brazil, the interpolation of BGC data throughout the study area (1200 m^2) yields a total discharge into Ubatuba Bay of 7.16 x 10^3 m^3 d^{-1} km^{-1} of shoreline. In Mauritius, the BGC data throughout the study site (12,000 m^2) yields a total discharge into Flic-en-Flac bay of 2.45 x 10^5 m^3 d^{-1} km^{-1} of shoreline. These data are reported graphically in figure 13.

C. Independent estimates of SGD at the study sites

Independent estimates were produced at each of the study sites using a variety of techniques. I have examined the use of the relationship between point measurements of SGD and BGC as an integrated measurement of SGD, now I will compare it to other integrated estimates made using radium and radon isotopes, including mathematical modeling estimates where possible.

In Cockburn Sound, measurements made using radium (3.2×10^3 m^3 km^{-1} d^{-1}) and radon ($2.0\text{-}2.7 \times 10^3$ m^3 km^{-1} d^{-1}) correspond very well to the estimate stated above, suggesting that the relationship between BGC and seepage meter SGD could be very successful in the quantification of SGD. All of these numbers compared well with estimates of $2.5\text{-}4.8 \times 10^3$ m^3 km^{-1} d^{-1}made using mathematical models (Burnett et al. 2006).

In Shelter Island, integrated estimates of SGD (Burnett et al. 2006) using radium and radon were $8\text{-}20 \times 10^3$ and $16\text{-}26 \times 10^3$ m^3 km^{-1} d^{-1} respectively These were an order of magnitude higher than the estimated discharge using the method described here. However, a revision of the calculation using the same data but considering a different geometry of the study area significantly lowered the SGD. As discussed by Dulaiova et al. (2006), the longitudinal Ra gradient out of West neck bay was measured to be -0.84 dpm m^{-3} km^{-1} or -0.84×10^{-3} dpm m^{-3} m^{-1}. With a horizontal mixing coefficient of 30.7 m^2 sec^{-1} (Dulaiova et al. 2006), the flux of radium leaving the bay would be 25.8×10^{-3} dpm m^{-2} sec^{-1}. The calculation of SGD cited above was based on this flux leaving a

straight shoreline along which radium-enriched SGD was being added over the first 50 meters from shore.

These assumptions would be most appropriate for a straight open coastline, but West Neck Bay might be better represented by as more-or-less circular bay whose circumference (shoreline length) is *L*. Radium-enriched groundwater enters the Bay in a band, with a width, *d*, of 50m, around the parameter and leaves through an inlet channel of cross-sectional area *(A)* at the specific flux of 25.8 x 10^{-3} dpm m^{-2} sec^{-1} as calculated above. (The "m^{-2}" is a square meter of the cross-sectional area through which the horizontal flux occurs). SGD would be the product of the specific flux and the cross-sectional area (*A*=192 m^2) of the inlet, divided by length of the bay shoreline (*L*=2450 m), times the width of the seepage face (*d*=50m), divided again by the concentration of Ra in groundwater (220 dpm m^{-3}). When calculated with this geometry the estimated SGD will be reduced by a factor of *A/ (L*d),* or 0.035, relative to the value calculated assuming a straight shoreline. The radium-estimated SGD would then be between 0.280 and 0.700 x 10^3 m^3 km^{-1} d^{-1} compared to 1.59 x 10^3 m^3 km^{-1} d^{-1} calculated from the BGC. Mathematical models also displayed considerable variation in estimates ranging from 0.230-10 x 10^3 m^3 km^{-1} d^{-1}. The estimate using BGC is within the ranges estimated by these independent methods.

In Flamengo Bay, Brazil, there was, once again, large variation seen in the radon estimates which were from 2-15 x 10^3 m^3 km^{-1} d^{-1}. The value estimated from BGC of 7.16x 10^3 m^3 km^{-1} d^{-1} was near this independent estimate. Modeling estimates, however, were lower, ranging from 0.17-1.6 x10^3 m^3 km^{-1} d^{-1} (Oberdorfer, et al. 2007).

In Mauritius, a radon estimate of the area near the spring suggested that there was a discharge of 56 x 10^3 m^3 km^{-1} d^{-1}, which is lower than the estimate of 245 x 10^3 m^3 km^{-1} d^{-1} calculated in the previous sub-section, but this could depend on the area used in the calculation of the radon estimate (Burnett et al. 2006). The radon estimate likely integrated a larger area than was studied with the BGC-SGD comparison, and was, therefore less influenced by the presence of the spring. The various estimates of SGD in Mauritius might be reconciled by separating the total SGD, as measured with the radon method, into two parts, that supplied by the submerged spring and that supplied, at a lower rate, across the rest of the lagoon floor. Therefore,

$$SGD_{Rn} = SGD_{spring} + SGD_{lagoon} \quad (2)$$

Where SGD_{Rn} is the total SGD into the lagoon as calculated by the radon estimate multiplied by the length of the shoreline; SGD_{spring} is the SGD in the vicinity of the spring as calculated by the extrapolated BGC measurements; and SGD_{lagoon} must be the discharge remaining in the rest of the lagoon or the difference between the total SGD as calculated to by the radon minus the spring discharge. The radon estimate for the entire 8-km length of the lagoon was 26 m^3 m^{-1} d^{-1} (Burnett et al. 2006) corresponding to a total input of SGD of 208,000 cubic meters per day. Radon activities directly over the spring which yielded SGD rates between 0.65 and 1.1 m d^{-1}. Taking the average discharge of the spring to be 1 m d^{-1} for a distance of 100 m from shore (Figure 13b) then the discharge in this meter length of shoreline is 100 m^3 m^{-1} d^{-1}. The spring encompasses a swath 100 m along shore (Figure 13b), and, therefore, in this swath there is an average of 100 m^3 m^{-1} d^{-1} and a total discharge of 1.0 x 10^4 m^3 d^{-1}. In order to

account for the total SGD, therefore, 19.8 x 10^4 m^3 d^{-1} must be supplied from the remaining 7,900 m of shoreline. The average width of the lagoon is 500 m, giving a surface area (not including the spring) of 395 x 10^4 m^2. Dividing the total discharge by the surface area of the lagoon, the average flow rate would need to be 0.05 m d^{-1} or 5 cm d^{-1}away from the spring. According to the BGC-SGD relationship there is a small flow of 10 cm d^{-1} within 5 m of the shore, so a diffuse flow throughout the rest of the lagoon floor of 5 cm d^{-1} is reasonable and would account for the flow rates suggested by the Radon measurements reported in Burnett et al. (2006). A water budget model for the area resulted in an estimated a freshwater SGD between 26 m^3 m^{-1} d^{-1}(Oberdorfer, 2005, San Jose State University, personal communication); the total SGD would, of course, be higher.

With the exception of Mauritius, this method seems to provide an accurate estimate of the discharge within the investigated area when compared with independent tracer estimates. As calculations of SGD using tracers are complicated by the difficulty in accurately determining end-members, the method utilized in this chapter may provide a reliable check of tracer estimates. In addition, these measurements are often cheaper to make then those using tracers and, therefore, may have wider applicability especially in developing nations. Meanwhile, mathematical models often disregard the flow of re-circulated seawater, which may be an important component of the total SGD budget.

D. Determination of the freshwater fraction of discharge

The correlation between BGC and SGD data can also be used to determine the relative inputs of fresh and recirculated seawater by the following simple calculation.

$$q_s = \sigma_b / (\sigma_s - \sigma_f) * Q \quad (4)$$

and $$q_f = Q - q_s \quad (5)$$

Where: q_s=discharge of saltwater in cm d^{-1}, q_f =discharge of freshwater in cm d^{-1}, Q=total discharge in cm d^{-1}, σ_b=measured BGC in mS cm^{-1}, σ_s=max BGC of saline water in mS cm^{-1}, σ_f=min BGC of water in mS cm^{-1}. Using the Mauritius example if we have a σ_b of 9 corresponding to a Q of 110 cm d^{-1} (Figure 12) with a σ_s of 15 and σ_f of 0. The fresh water discharge should be: 44 cm d^{-1} and the salt water discharge is 66 cm d^{-1}. This relationship assumes a linear correlation between BGC and SGD and does not consider how the process of mixing in the subterranean estuary would affect the values, in order to facilitate understanding of the determination of the freshwater fraction.

Taking the correlation between BGC and SGD, we can extrapolate BGC measurements from the entire study site to determine the freshwater fraction of SGD in each of the sites. In other words, using the discharge estimates from the previous section as well as (3) and (4), we can determine the freshwater fraction of the SGD into our four study areas and therefore the total freshwater discharge. The freshwater fraction of SGD in Cockburn Sound is 41% yielding a total fresh discharge of 1.2 x 10^3 m^3 d^{-1} km^{-1} of shoreline. In Shelter Island, the freshwater fraction is 24% of the total discharge or 0.38 x 10^3 m^3 d^{-1} km^{-1}. In Brazil, the freshwater fraction is 29% of the total discharge or 2.08 x 10^3 m^3 d^{-1} km^{-1}. Meanwhile in Mauritius, the freshwater fraction is 63% of the total

discharge or 1.54 x 10^5 m^3 d^{-1} km^{-1} (Table 4). At this stage, such calculations should be viewed with caution but I consider them to be good approximations.

Because the empirical parameter α is interpreted as the capacity of SGD to flush salt from the sediments, the value of α might be expected to be related to the percentage of freshwater in the SGD. From these limited measurements, it appeared that, approximately, α = -0.004 (% of freshwater SGD) +0.0372. If this relation withstands further tests, it may provide the independent correlation of BGC from estimates of freshwater SGD.

5.Conclusion

A strong relationship between SGD and BGC should be expected in sites where fresh water discharge is important, as is demonstrated here in a variety of settings. If site specific characteristics can be determined, it appears possible to extrapolate SGD values to large areas from BGC data. BGC can then be used to interpolate and extrapolate point SGD measurements. Point measurements are generally considered valid but have the restriction of covering only small areas as well as being highly labor intensive. BGC measurements are relatively quicker to make and therefore can cover larger areas. Using the correlation between BGC and SGD measurements with seepage meters, both the total discharge and freshwater fraction of SGD have been estimated in four diverse hydrogeological settings. These numbers agree well with previously reported values, suggesting that this is a good method for accurately determining SGD in an area. This

method for accurately quantifying SGD may have a wide applicability if physical parameters are determined. It seems that the relationship between the two variables must be controlled by this set of parameters and, therefore, if we can understand how this relationship works we can begin to make statements about the SGD signature of a site through knowledge of BGC alone. Until these characteristics are fully understood, future studies of BGC and seepage meter measurements should be intertwined in order to provide a larger data set from which to establish the relationship between the two methods and to better understand the processes occurring at specific study sites.

References

Ataie-Ashtiani, B., Volker, R. E., and Lockington, D. A. 1999. Tidal effects on sea water intrusion in unconfined aquifers. Journal of Hydrology. 216: 17–31.

Beck, A.J., Rapaglia, J.P., Cochran, J.K., and Bokuniewicz H.B. 2007. Radium mass-balance in Jamaica Bay, NY: Evidence for a substantial flux of submarine groundwater. Marine Chemistry. in press.

Bokuniewicz, H. 1980. Groundwater Seepage into Great South Bay, New-York. Estuarine and Coastal Marine Science. 10 (4): 437-444.

Bokuniewicz, H., Buddemeier, R., Maxwell, B., and Smith, C. 2003. The typological approach to submarine groundwater discharge (SGD). Biogeochemistry. 66 (1-2): 145-158.

Bokuniewicz, H.J., Kontar, E., Rodriguez, M., and Klein, P.A., 2004. Submarine groundwater discharge patterns through a fractured rock aquifer: a case study in the Ubatuba coastal area, Brazil. Revista de la Asociacion Argentina de Sedimentologia. 11: 9-16.

Bokuniewicz, H., Rapaglia, J., and Beck. A., 2007. Submarine Groundwater Discharge from a Volcanic Island: A case study of Mauritius Island. International Journals of Oceans and Oceanography. Accepted.

Breusse, J.J. 1963. Modern geophysical methods for subsurface water exploration. Geophysics. 28 (4): 633-657.

Breier, J.A., Breier, C.F., and Edmonds, H.N., 2005. Detecting submarine groundwater discharge with synoptic surveys of sediment resistivity, radium, and salinity. Geophysical Research Letters. 32: DOI 10.1029/2005GL024639.

Burnett, W.C. and Dulaiova, H. 2006. Radon as a tracer of submarine groundwater discharge into a boat basin in Donnalucata, Sicily. Continental Shelf Research. 26: 862-873.

Burnett, W.C., and Dulaiova, H. 2003. Estimating the dynamics of groundwater input into the coastal zone via continuous radon-222 measurements. Journal of Environmental Radioactivity. 691 (1-2): 21-35.

Burnett, W.C., Taniguchi, M., and Oberdorfer, J. 2001. Measurement and significance of the direct discharge of groundwater into the coastal zone. Journal of Sea Research. 46 (2): 109-116.

Burnett, W.C., Aggarwal, P.K., Bokuniewicz, H., Cable, J.E., Charette, M.A., Kontar, E., Krupa, S., Kulkarni, K.M., Loveless, A., Moore, W.S., Oberdorfer, J.A., Oliveira, J., Ozyurt, N., Povinec, P., Privitera, A.M.G., Rajar, R., Ramessur, R.T., Scholten, J., Stieglitz, T., Taniguchi, M., and Turner, J.V., 2006. Quantifying submarine groundwater discharge in the coastal zone via multiple methods. Science of the Total Environment. 367 (2-3): 498-543.

Cable, J. E., Burnett, W. C., Chanton, J. P., Corbett, D. R. and Cable P. H., 1997. Field Evaluation of Seepage Meters in the Coastal Marine Environment. Estuarine, Coastal, and Shelf Science. 45: 367-375.

Charette, M.A., Splivallo, R., Herbold, C., Bollinger, M.S., and Moore, W.S., 2003. Salt marsh submarine groundwater discharge as traced by radium isotopes. Marine Chemistry. 84 (1-2): 113-121.

Crusius, J., Koopmans, D., Brattons, J.F., Charette, M.A., Kroeger, K., Henderson, P., Ryckman, L., Halloran, K., and Colman, J.A. 2005. Submarine groundwater discharge to a small estuary estimated from radon and salinity measurements and a box model. Biogeosciences. 2: 141-175.

Dulaiova, H., Burnett, W.C., Chanton, J.P., Moore, W.S., Bokuniewicz, H.J., Charette, M.A., and Sholkovitz, E. 2006, Assessment of groundwater discharges into West Neck Bay, New York, via natural tracers. Continental Shelf Research. 26: 1971-1983.

Greenwood, W.J., Kruse, S.E., Swarzenski, P.W., and Meunier J.K., 2004. Mapping porewater salinity with electromagnetic methods in shallow coastal environments:

Tampa Bay, Florida. Abstract to American Geophysical Union (AGU) 05/24/04. #NS31A-09.

Greenwood, W.J., Kruse, S.E., and Swarzenski, P.W. 2006. Extending electromagnetic methods to map coastal pore water salinities. Ground Water 44 (2): 292-299.

Hesslein, R.H. 1976. An in situ sampler for close interval pore water studies. Limnology and Oceanography. 21 (6): 912-914.

Hoefel, F.G., and Evans, R.L. 2001. Impact of low salinity porewater on seafloor electromagnetic data: A means of detecting submarine groundwater discharge. Estuarine Coastal and Shelf Science. 52: 179-189.

Hubbert, M.K. 1940. The theory of ground water motion. Journal of Geology. 48 (8): 785-944.

Hwang, D.W., Kim, G., Lee, Y.W., and Yang, H.S. 2005. Estimating submarine inputs of groundwater and nutrients to a coastal bay using radium isotopes. Marine Chemistry. 96: 61-71.

Jaeger, J., Hartl, K., Cable, J., and Martin, J. B. 2005. Evaluating the role of bioirrigation in submarine groundwater discharge. Abstract to Geological Society of America annual meeting. Salt Lake City. October 16-19.

Johannes, R.E. 1980. The ecological significance of the submarine discharge of groundwater. Marine Ecological Progress Series. 3: 365-373.

Kaleris, V. 2005. Submarine groundwater discharge: effects on hydrogeology and of near shore surface water bodies. Journal of Hydrology. 325: 96-117.

Kelly, R.P., and Moran, S.B., 2002. Seasonal changes in groundwater input to a well-mixed estuary estimated using radium isotopes and implications for coastal nutrient budgets. Limnology and Oceanography. 47: 1796-1807.

Kendrick, G.A., Aylward, M.J., Hegge, B.J., Cambridge, M.L., Hillman, K., Wyllie, A., and Lord, D.A. 2002. Changes in seagrass coverage in Cockburn Sound, Western Australia between 1967 and 1999. Aquatic Botany. 73: 75-87.

Kermabon, A., Gehin, C., and Blavier, P. 1969. A deep-sea electrical resistivity probe for measuring porosity and density of unconsolidated sediments. Geophysics. 34 (4): 554-571.

Krest, J.M., Moore, W.S., Gardner, L.R., and Morris, J.T., 2000. Marsh nutrient export supplied by groundwater discharge: Evidence from radium measurements. Global Biogeochemical Cycles. 14 (1): 167-176.

Kohout, F.A. 1966. A neglected phenomenon of coastal hydrology. Hydrology. 26: 391-413.

Kruse, S.E., Brodziski, M.P., and Geib, T.L. 1998. Use of electrical and electromagnetic techniques to map seawater intrusion near the Cross-Florida Barge Canal. Environmental and Engineering Geoscience. 4 (3): 331-340.

LaRoche, J., Nuzzi, R., Waters, R., Wyman, K., Falkowski, P. G., and Wallace, D. W. R. 1997. Brown Tide Blooms in Long Island's Coastal Waters Linked to Interannual Variability in Groundwater Flow. Global Climate Change. 3: 397-410.

Lee, D. R., 1977. A Device for Measuring Seepage Flux in Lakes and Estuaries. Limnology and Oceanography. 22 (1): 140-147.

Lee, D.R. 1985. Method for locating sediment anomalies in lakebeds that can be caused by groundwater flow. Journal of Hydrology. 79: 187-193.

Li, L., Barry, D. A., Stagnitti, F. and Parlange, J. Y., 1999. Submarine groundwater discharge and associated chemical input to a coastal sea. Water Resources Research. 35 (11): 3253–3259.

Libelo, E. L., and Macintyre, W. G. 1994. Effects of Surface-Water Movement on Seepage-Meter Measurements of Flow Through the Sediment Water Interface. Applied Hydrology. 4 (94): 49-54.

Maerki, M., Wehrli, B., Dinkel, C., and Muller, B. 2004. The influence of tortuosity on molecular diffusion in freshwater sediments of high porosity. Geochimica et Cosmochimica Acta. 68 (7): 1519–1528.

Manheim, F.T., Krantz, D.E.. Snyder, D.D., and Sturgis, B. 2004a. Streamer resistivity surveys in Delmarva coastal bays. In: Proceedings of the Symposium on the Application of Geophysics to Environmental and Engineering Problems. February 10-14, Las Vegas, Nevada.

Manheim, F.T. Krantz, D.E. and Bratton, J.F. 2004b. Studying ground water under Delmarva coastal bays using electrical resistivity. Ground Water. 42 (7): 1052-1068.

Martin, J.B., Cable, J.E., Jaeger, J., Hartl, K., and Smith, C.G. 2006. Thermal and chemical evidence for rapid water exchange across the sediment water interface by bioirrigation in the Indian River Lagoon, Florida. Limnology and Oceanography. 51 (3): 1332-1341.

Millham, N.P. and Howes, B.L. 1994. Freshwater flow into a coastal embayment: groundwater and surface water inputs. Limnology and Oceanography. 39 (8): 1928-1944.

Moore, W. S., 1996. Large Groundwater Inputs to Coastal Waters revealed by Radium-226 Enrichments. Nature. 380: 612-614.

Moore, W.S. 2006. The role of submarine groundwater discharge in coastal biogeochemistry. Journal of geochemical exploration. 88: 389-393.

Mulligan, A.E. and Charette, M.A. 2006. Intercomparison of submarine groundwater discharge estimates from a sandy unconfined aquifer. Journal of Hydrology. 327: 411-425.

Nowroozi, A.A., Horrocks, B., and Henderson, P. 1999. Saltwater intrusion into the freshwater aquifer in the eastern shore of Virginia: a reconnaissance electrical resistivity survey. Journal of Applied Goephysics. 42: 1-22.

Oberdorfer, J.A., Charette, M.A., Allen, M., Martin, J.B., and Cable, J.E. 2007. Hydrogeology and geochemistry of near-shore submarine groundwater discharge at Flamengo Bay, Ubatuba, Brazil. Estuarine, Coastal, and Shelf Science. submitted.

Oliveira, J., Burnett, W.C., Mazzilli, B.P., Braga, E.S., Farias, L.A., Christoff, J., and Furtado, V.V., 2003. Reconnaissance of submarine groundwater discharge at Ubatuba coast, Brazil using 222-Rn as a natural tracer. Journal of Environmental Radioactivity. 69: 37-52.

O'Rourke, D. 2000 Quantifying specific discharge into West Neck Bay, Shelter Island, New York, using a three-dimensional finite-difference groundwater flow model and continuous measurements with an ultrasonic seepage meter, MSc Thesis, State University of New York at Stony Brook. 80 pages.

Paulsen, R.J. 1996 Analysis of the coastal groundwater/saltwater interface and continuous measurements of specific discharge into Coecles Harbor, Shelter Island, NY, MSc Thesis, State University of New York at Stony Brook. 35 pages.

Paulsen R.J., Smith, C.F., O'Rourke, D., and Wong, T.F., 2001 Development and Evaluation of an Ultrasonic Ground Water Seepage Meter, Ground Water 39 (6): 904-911.

Paulsen, R.J., O'Rourke, D., Smith, C.F., and Wong, T.F., 2004. Tidal load and salt water influences on submarine groundwater discharge. Ground Water. 42 (7): 990-999.

Rapaglia, J.P. 2005. Submarine groundwater discharge into the Venice Lagoon, Italy. Estuaries. 28 (5): 705-713.

Schiavo, M.A., Hauser, S., Cusimano, G., and Gatto, L. 2006. Geochemical characterization of groundwater and submarine discharge in the south-eastern Sicily. Continental Shelf Research. 26 (7): 826-834.

Schlucter, M., Sauter, E., Hansen, H.P., and Suess, E. 2000. Seasonal variations of bioirrigation in coastal sediments: Modeling of field data. Geochimica et Cosmochimica Acta. 61 (5): 821-834.

Schubert, C.E., 1999. Ground-Water Flow Paths and Travel time to Three Small Embayments within the Peconic Estuary, Eastern Suffolk County, New York, *USGS Water-Resources Investigation Report* 98-4181, 41p.

Seplow, M.S. 1991. The influences of groundwater seepage on the pore water salinity of Great South Bay. M.S. Thesis State University of New York at Stony Brook. 80 pages.

Shaw, R.D., and Prepas, E.E., 1989. Anomalous, short term influx of water into seepage meters. Limnology and Oceanography. 34 (7) 1343-1351.

Shaw, R.D., Shaw, J.F.H., Fricker, H., and Prepas, E.E., 1990. An Integrated Approach to Quantify Groundwater Transport of Phosphorous to Narrow Lake, Alberta. Limnology and Oceanography. 35 (4): 870-886.

Shinn, E.A., Reich, C.D., and Hickey, D.T., 2002. Seepage Meters and Bernoulli's Revenge. Estuaries. 25 (1): 126-132.

Sholkovitz, E.R., Herbold, C., and Charette, M. A., 2003. An automated dye-dilution based seepage meter for the time-series measurement of submarine groundwater discharge. Limnology & Oceanography Methods. 1, 16–28.

Slomp, C.P., Van Cappellen, P. 2004. Nutrient inputs to the coastal ocean through submarine groundwater discharge: controls and potential impact. Journal of Hydrology. 295 (1-4): 64-86.

Smith, A.J., and Nield, S.P. 2003. Groundwater discharge from the superficial aquifer into Cockburn Sound Western Australia: estimation by inshore water balance. Biogeochemistry. 66: 125–44.

Soren, J., 1978. Hydrogeologic Conditions in the Town of Shelter Island, Suffolk County Long Island, New York, *USGS Water-Resources Investigations Report* 77-77, 22p.

Stieglitz, T. 2005. Submarine groundwater discharge into the near-shore zone of the Great Barrier Reef, Australia. Marine Pollution Bulletin. 51: 51-59.

Stieglitz, T., Ridd, P.V., and Hollins, S., 2000 A small sensor for detecting animal burrows and monitoring water conductivity. Wetlands Ecology and Management. 8: 1-7.

Stieglitz, T. and Ridd, P. 2002. Submarine groundwater discharge from paleochannel "Wonky Holes" on the inner shelf of the Great Barrier Reef, Australia. Australian Geographic Magazine .66: 28.

Stieglitz, T., Rapaglia, J., and Krupa, S. 2007a. An effect of pier pilings on near-shore submarine groundwater discharge from a confined aquifer. Estuaries. In press.

Stieglitz, T., Taniguchi, M., and Neylon, S. 2007b. Spatial variability of submarine groundwater discharge, Ubatuba, Brazil. Estuarine, Coastal, and Shelf Science. submitted.

Taniguchi, M. 2006. Submarine groundwater discharge measured by seepage meters in Sicilian coastal waters. Continental Shelf Research. 26 (7): 835-842.

Taniguchi, M., and Fukuo, Y. 1993. Continuous Measurements of groundwater seepage using an automatic seepage meter. Ground Water. 31: 675-679.

Taniguchi, M.; Burnett, W.C., Cable, J.E., and Turner, J.V. 2002. Investigation of submarine groundwater discharge. Hydrological Processes. 16: 2115-2129.

Taniguchi, M., Turner, J.V., Smith, A. 2003 Evaluations of groundwater discharge rates from subsurface temperature in Cockburn Sound, Western Australia. Biogeochemistry. 66:111–24.

Taniguchi, M., and Iwakawa, H. 2004. Submarine groundwater discharge in Osaka Bay, Japan. Limnology. 5 (1): 25-32.

Taniguchi, M., Ishitobi, T., and Seaki, K., 2005. Evaluation of time-space distribution of submarine ground water discharge. Ground Water. 43 (3): 336-342.

Ullman, W.J., and Aller, R.C., 1982. Diffusion coefficients in nearshore marine sediments. Limnology and Oceanography. 27 (3) 552-556.

Ussler, III W., Paull, C.K., Boucher, J., Frederich, G.E., and Thomas, D.J. 2003. Submarine pockmarks: a case study from Belfast Bay, Maine. Marine Geology. 202: 175-192.

Vanek, V. and Lee, D.R. 1991. Mapping submarine groundwater discharge areas-an example from Laholm Bay, Southwest Sweden. Limnology and Oceanography: 36(6): 1250-1262.

Wooding, R.A. 1969. Growth of fingers at an unstable diffusing interface in a porous medium or Hele-Shaw cell. Journal of Fluid Mechanics. 39: 477-495.

Zohdy, A.A.R. and Jackson, D.B. 1969. Application of deep electrical soundings for groundwater exploration in Hawaii. Geophysics. 34 (4): 584-600.

Tables for Chapter II

Table 1. Site characteristics from each of the study locations

Site	Pore size (Φ)#*	Porosity	Conduc-tivity (m d^{-1})	Hydraulic gradient	Tidal range (m)*	Avg. Salinity*	Avg. Temp. (˚C)*	α x10^{-2}
Cockburn Sound[1,2]	1-3	0.3	20-1000	0.002	0.3-1.0		20	2.95
Shelter Island [1,3,4]	4-6	0.3	60-83	0.0073	0.7-1.1	28	15	4.93
Flamengo Bay [5]	4-5	0.5	2.5-49	0.031	0.6-1.2	34	29	1.29
Mauritius [6]	0-1	0.5	0.5-86	0.011	0.2-0.5	33	23	0.63

#determined from descriptions of the sediment characteristics in the literature, *affects the BGC measurement; ** affects SGD rates; *** is important for both the BGC and SGD.

[1] Burnett et al. (2006), [2] Smith and Nield (2003), [3] Paulsen et al. (2001), [4] O' Rourke (2000), [5] Oberdorfer et al. (2007), [6] Bokuniewicz et al. (2007)

Table 2. SGD data from each of the study sites as measured by seepage meters

Site	Seepage Meter	AVG. SGD cm d^{-1}	AVG BGC mS cm^{-1}
Cockburn Sound	AUTO1	32	6.0
Shelter Island	MSRC1	22	4.2
Shelter Island	MSRC2	24	4.1
Shelter Island	MSRC3	25	4.0
Shelter Island	WHOI	6	9.0
Shelter Island	USFM	65	0.5
Shelter Island	SFWMD	2	11.0
Ubatuba Bay	S1	40	10.0
Ubatuba Bay	S2	10	7.0
Ubatuba Bay	S8	70	15.0
Mauritius	M1	216	0.5
Mauritius	M2	18	15.0
Mauritius	M3	108	9.0
Mauritius	M4	21	14.5
Mauritius	M5	14	0.5
Mauritius	M6	301	15.5
Mauritius	M7	11	14.5
Mauritius	M8	20	15.0
Mauritius	M9	8	15.0
Mauritius	M10	6	15.0
Mauritius	M11	8	15.5
Mauritius	M12	3	15.0
Mauritius	M13	166	5.0
Mauritius	M14	124	8.0
Mauritius	M15	362	0.5
Mauritius	M16	5	15.5
Mauritius	M17	6	15.5
Mauritius	M18	10	15.0
Mauritius	M19	32	14.0
Mauritius	M20	4	15.0
Mauritius	M21	16	15.0
Mauritius	M22	9	15.0
Mauritius	M23	8	15.5
Mauritius	M24	4	15.5
Mauritius	M25	3	15.5
Mauritius	M26	17	15.5

Table 3. Values of A and α for each of the study sites derived from the empirical relationship between BGC and SGD

Site	A= sediment characteristics and conductivity	α=
Cockburn Sound	14.96	0.030
Shelter Island	11.99	0.049
Flamengo Bay	16.67	0.013
Mauritius	16.11	0.006

Table 4. Total and freshwater SGD in the four different study locations.

Site	Total SGD (10^3 m^3 d^{-1} km^{-1})	Freshwater Fraction	Fresh SGD (10^3 m^3 d^{-1} km^{-1})
Cockburn Sound	2.91	41%	1.2
Shelter Island	1.59	24%	0.38
Brazil	7.16	29%	2.08
Mauritius	245.0	63%	154.0

Figures for Chapter II.

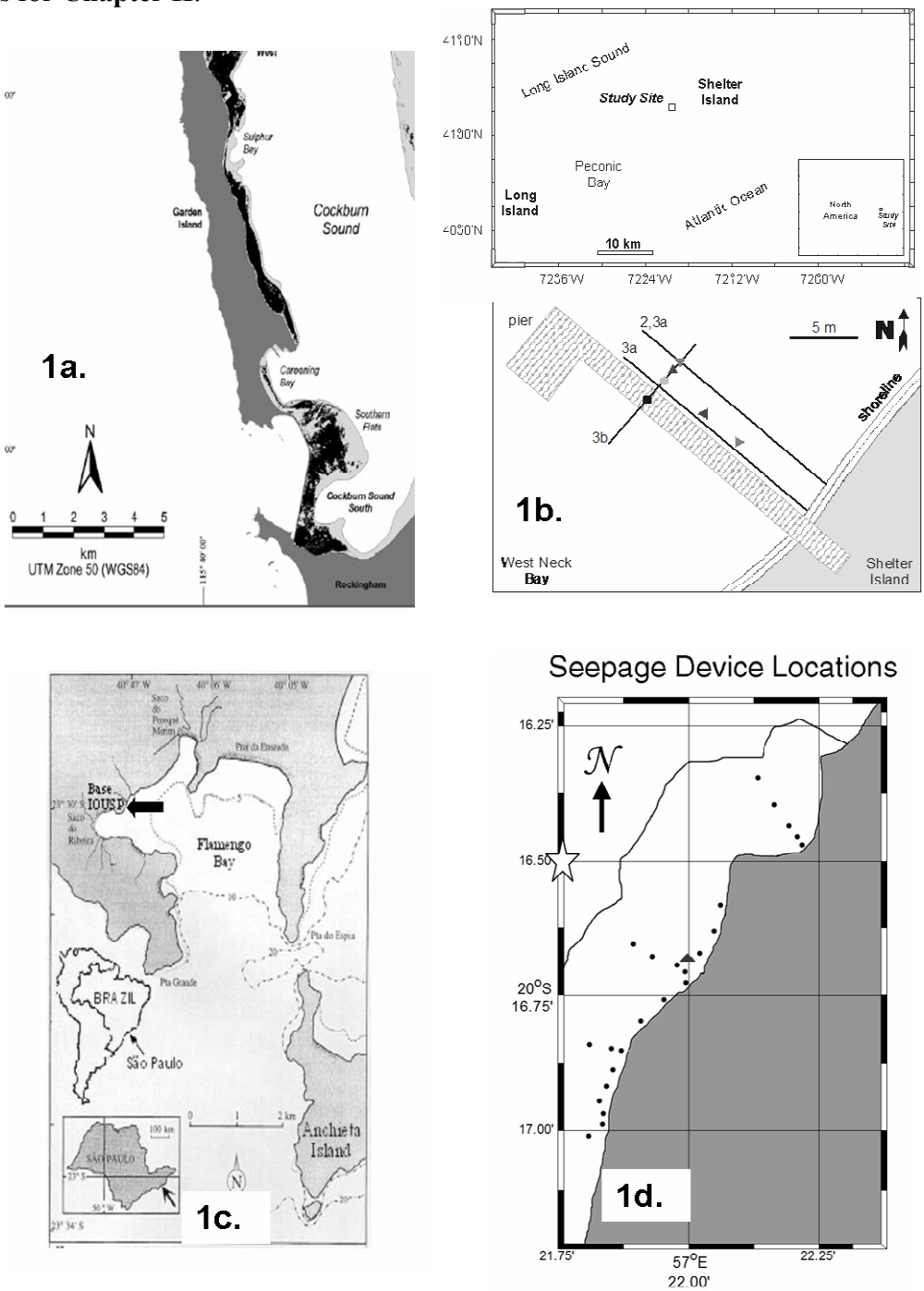

Figure 1. (a) Cockburn Sound, Australia (reproduced from Kendrick et al. 2002) (b) Location map of the study site at Shelter Island and overview of the study site with conductivity transects (lines) and seepage meters (dots) are marked. (Satellite Image: New York GIS & Google Earth). (c) Location map of Ubatuba and Flamengo bay Brazil (d) Location of seepage meters used in Flic-en-Flac Bay, Mauritius. The triangle denotes the location of a spring.

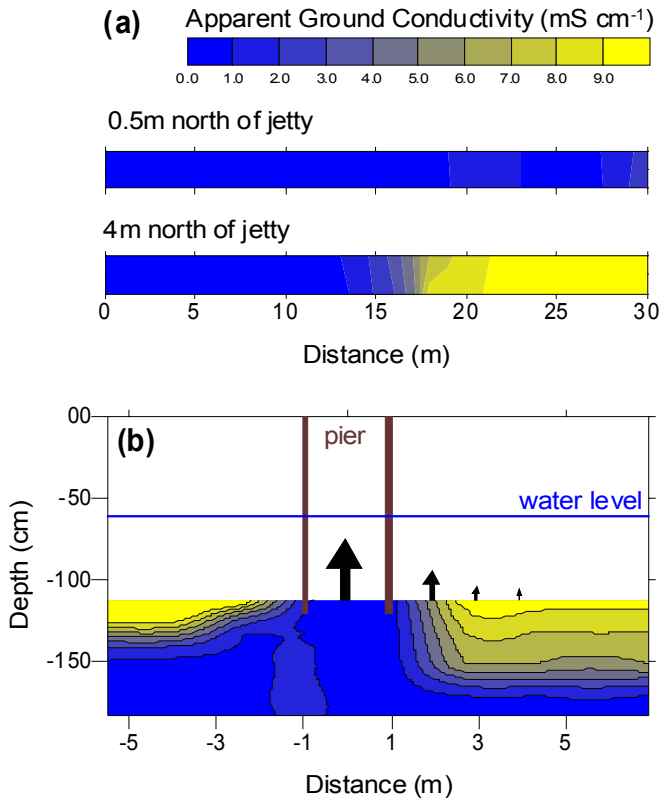

Figure 2. (a) Bulk ground conductivity at low tide of the top 10 cm of the seabed (top) along the pier and (bottom) 4 m north of the pier at Shelter Island, NY; (b) bulk ground conductivity along a shore-parallel transect below the pier, approximately 17 m from the mean high water level. The pilings are shown in brown. The length of the black arrows is approximately proportional to the average seepage flux measured at the respective location. A decrease in flow with increasing distance from the pier is apparent.

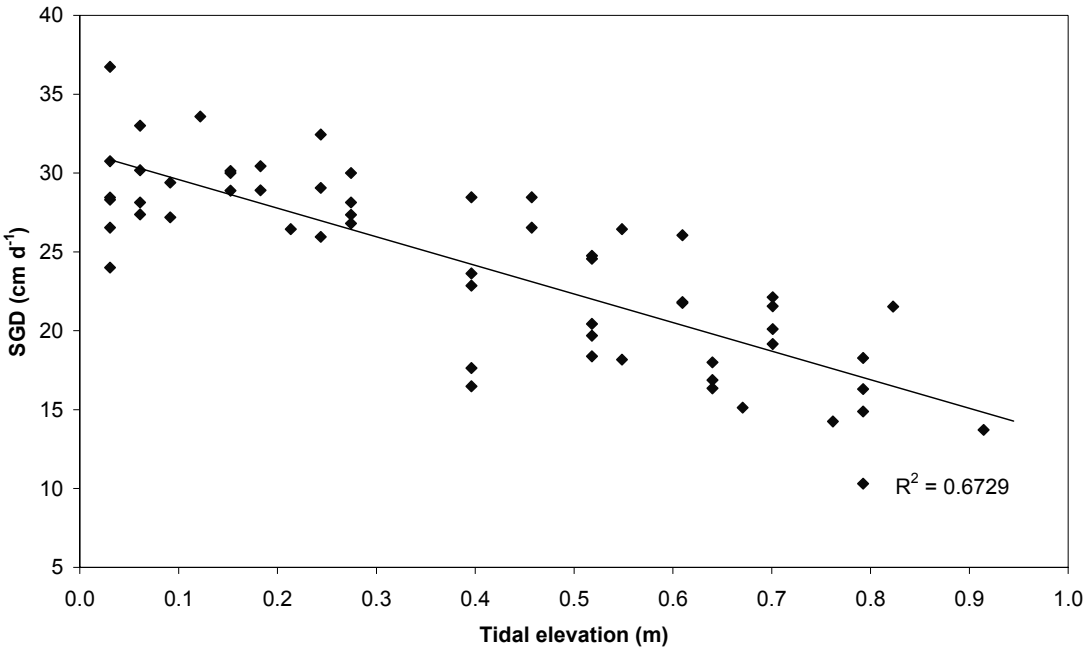

Figure 3. Seepage rates vs. tidal elevation measured along a transect parallel to the pier, showing distance to the pier center (locations of the seepage meters are indicated in Figure 1).

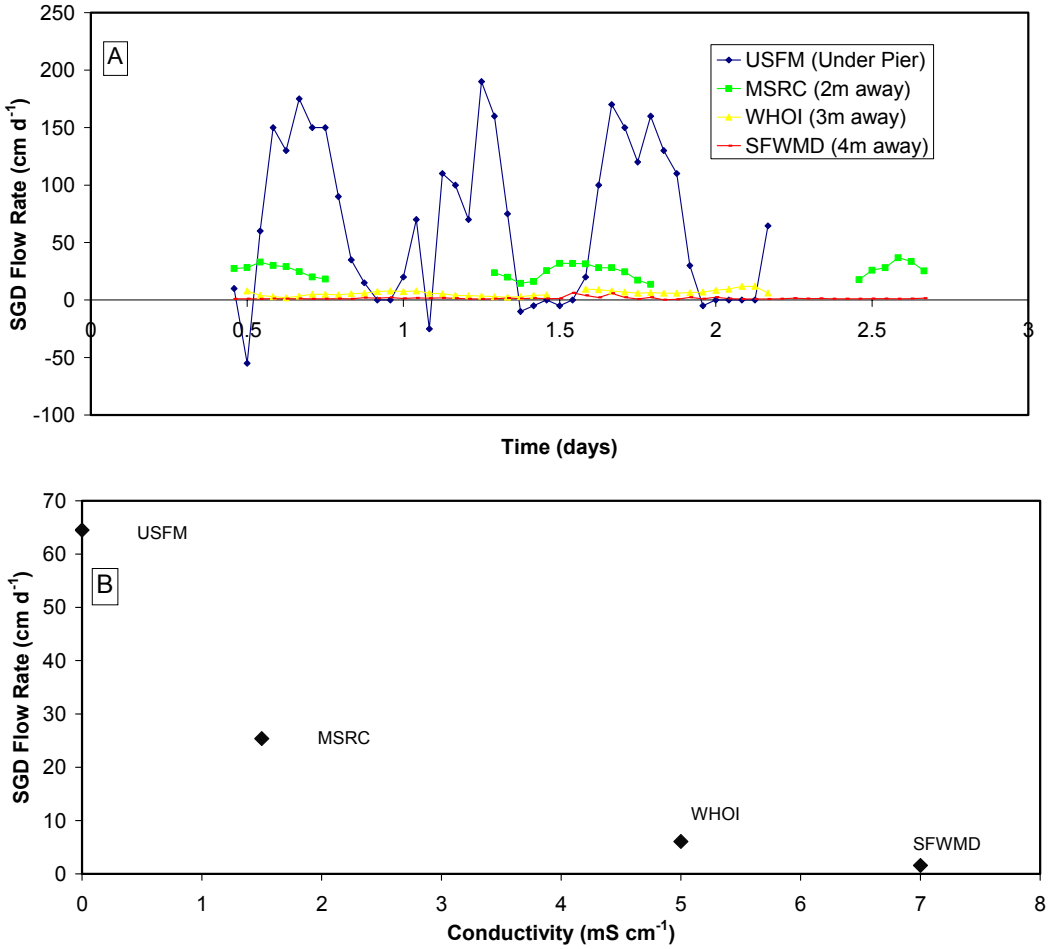

Figure 4a.. Time series of SGD measurements made with seepage meters at varying distances from the pier. 4b. Relationship between BGC and SGD in pier perpendicular transect.

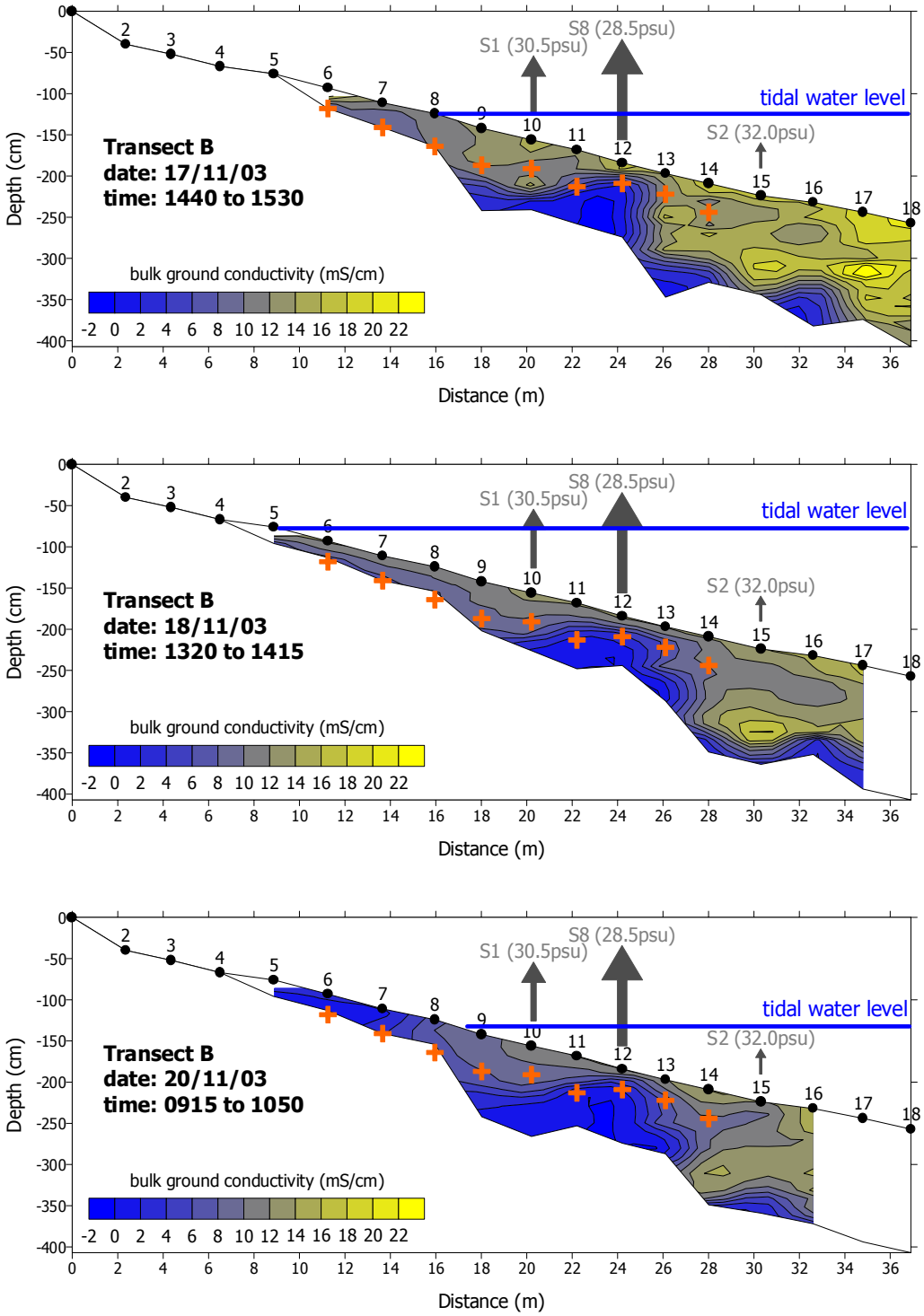

Figure 5: *Ground conductivity transect B at different times*. At each of the stations along the transect (indicated by numbers on the sediment surface), a profile of ground conductivity was recorded, and data was subsequently contoured. In addition, the tidal water level at

time of recording each transect is indicated. The arrows at stations 10, 12 and 15 mark the locations of the manual seepage meters S1, S8 and S2 respectively. The length of the arrows is proportional to the average flux of SGD into each of these seepage meters, and the average salinity of the SGD is also given. Note that the time of recording of each profile is marked in consecutive order in the time series of rainfall and water level in figure 6.

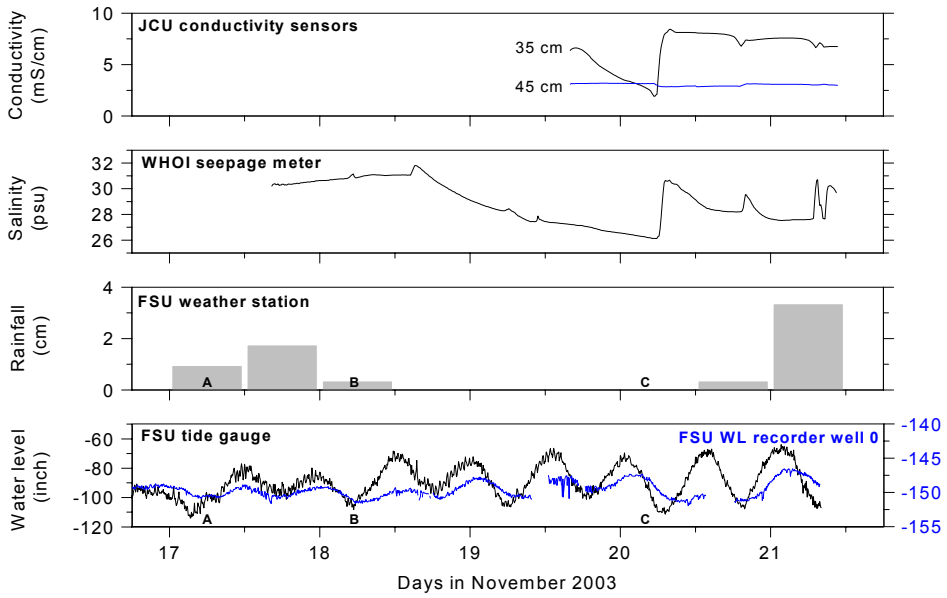

Figure 6: *Temporal variation of bulk ground conductivity.* Time series of bulk ground conductivity at 35 cm and 45 cm of depth below the sediment surface at site S6 (see Figure 5 top), together with salinity recorded in the dome of the WHOI automated seepage meter and FSU rainfall and water level data. The rainfall data is given

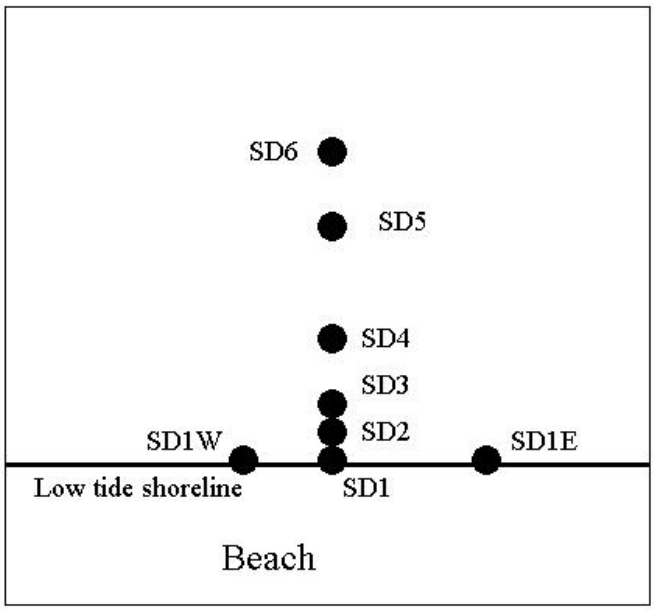

Figure 7. Shore normal transect of seepage meters in Flamengo Bay, Brazil

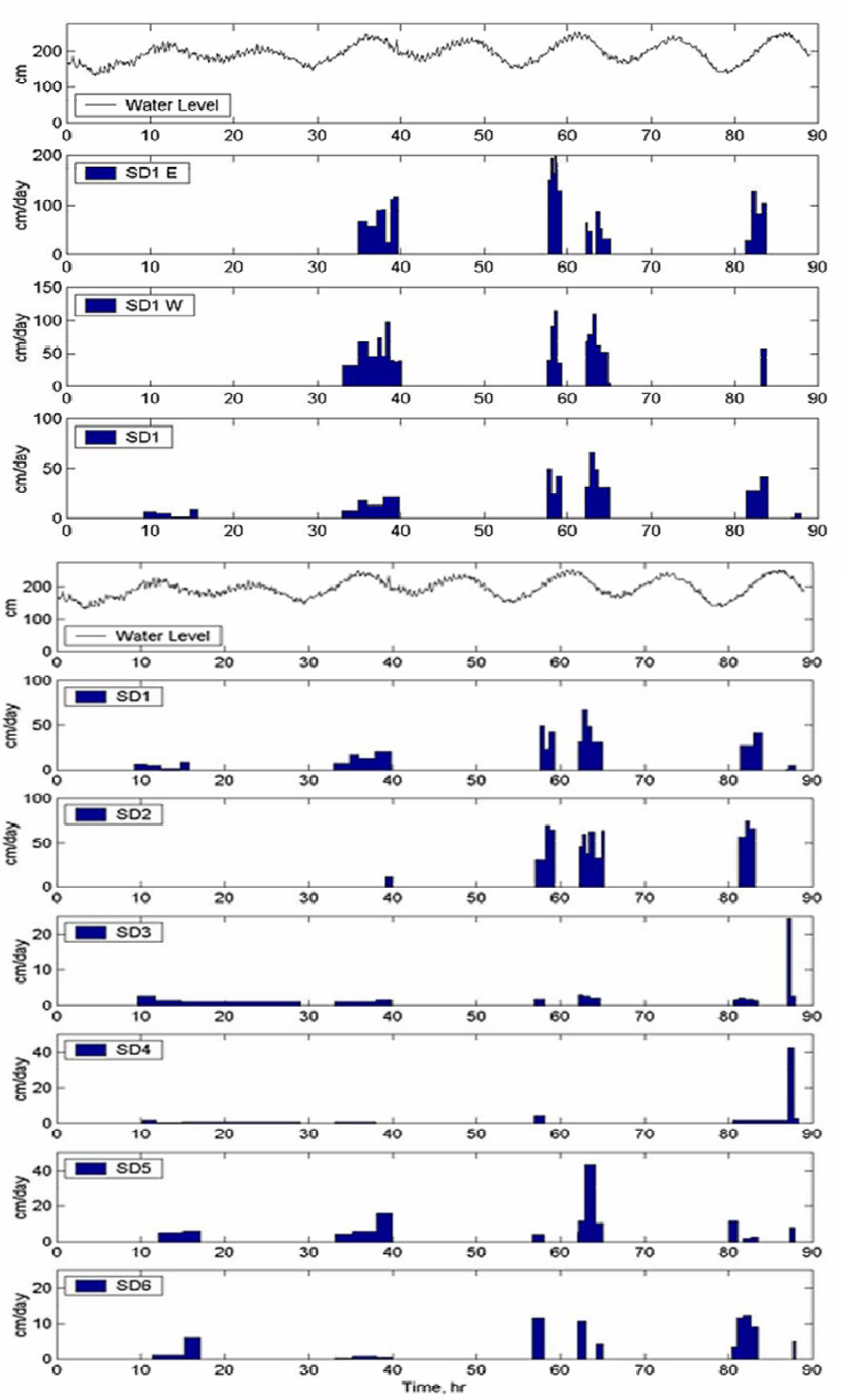
cm
Water Level
cm/day
SD1 E
SD1 W
SD1
SD2
SD3
SD4
SD5
SD6
Time, hr

Figure 8. Time series of SGD at different seepage meter locations in Brazil (Bokuniewicz et al. 2004). Blank areas represent periods of time in which seepage was not measured using benthic chambers. Tide level for the time period is also shown.

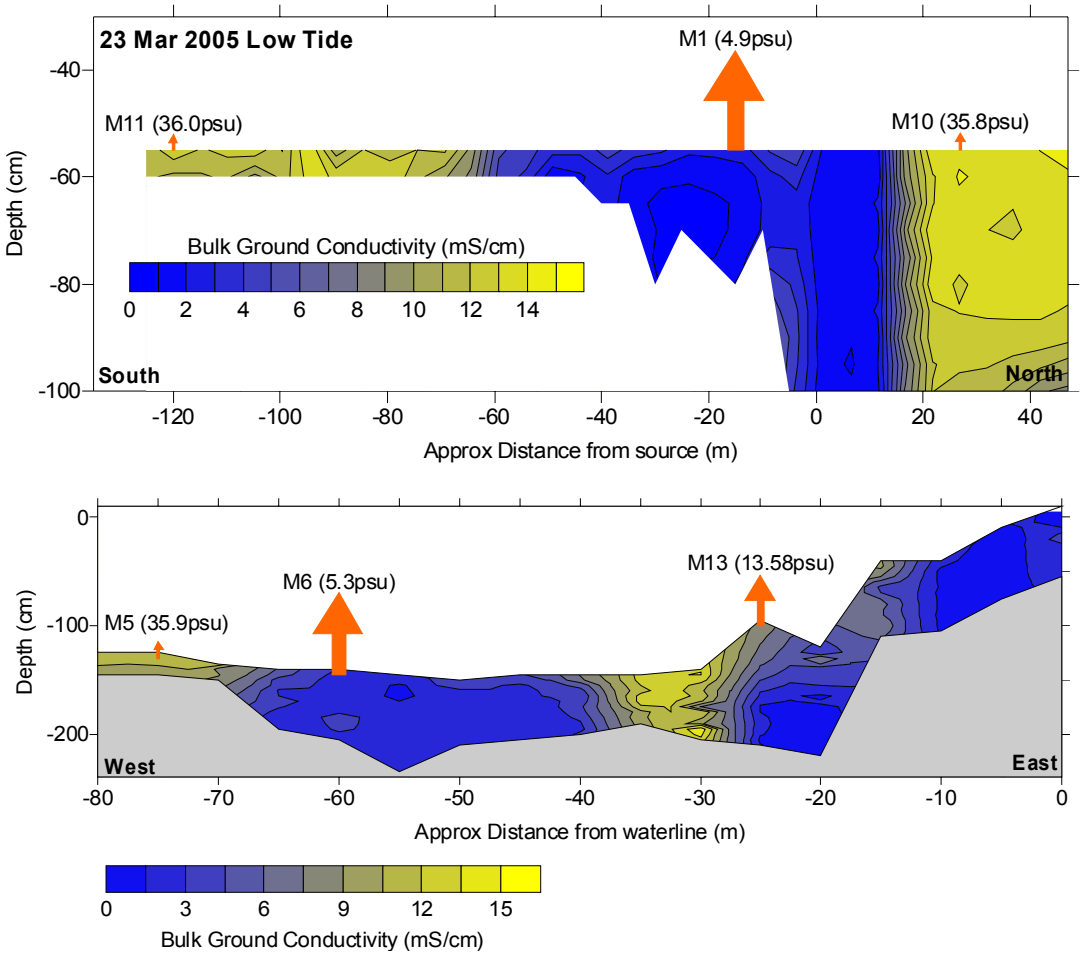

Figure 9. Along shore and shore normal transects of conductivity in the vicinity of the freshwater spring (Flic-en-Flac bay, Mauritius). The orange arrows represent relative SGD rates as measured in benthic chambers (as well as there average salinity).

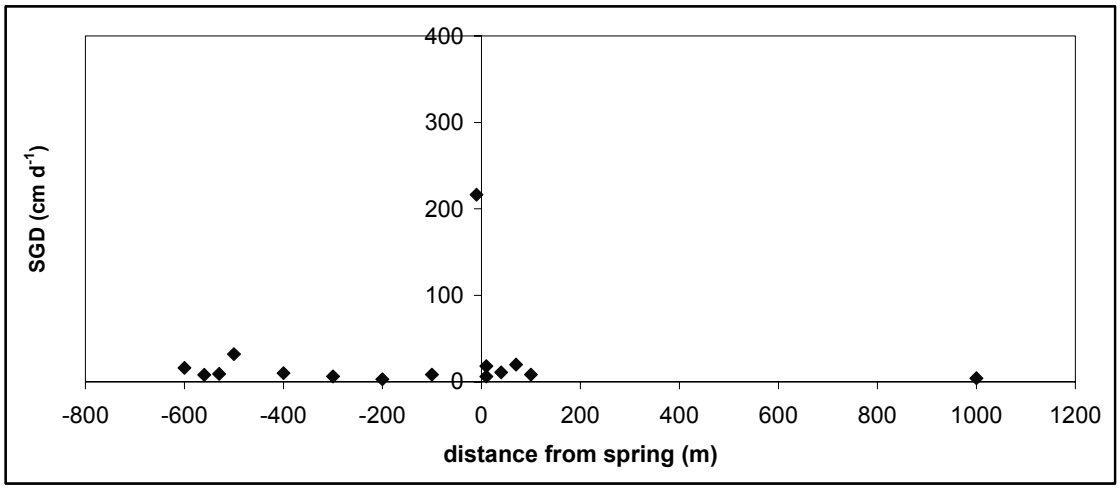

Figure 10. Alongshore pattern of discharge around the spring in Mauritius

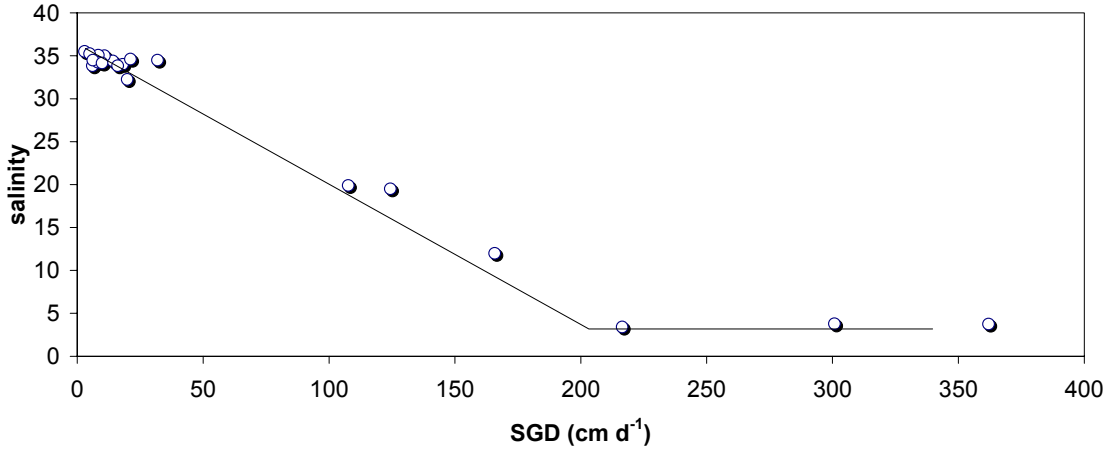

Figure 11. Relationship between the average flow rates measured at 28 different locations and the average salinity of the water in the chambers at the Mauritius site.

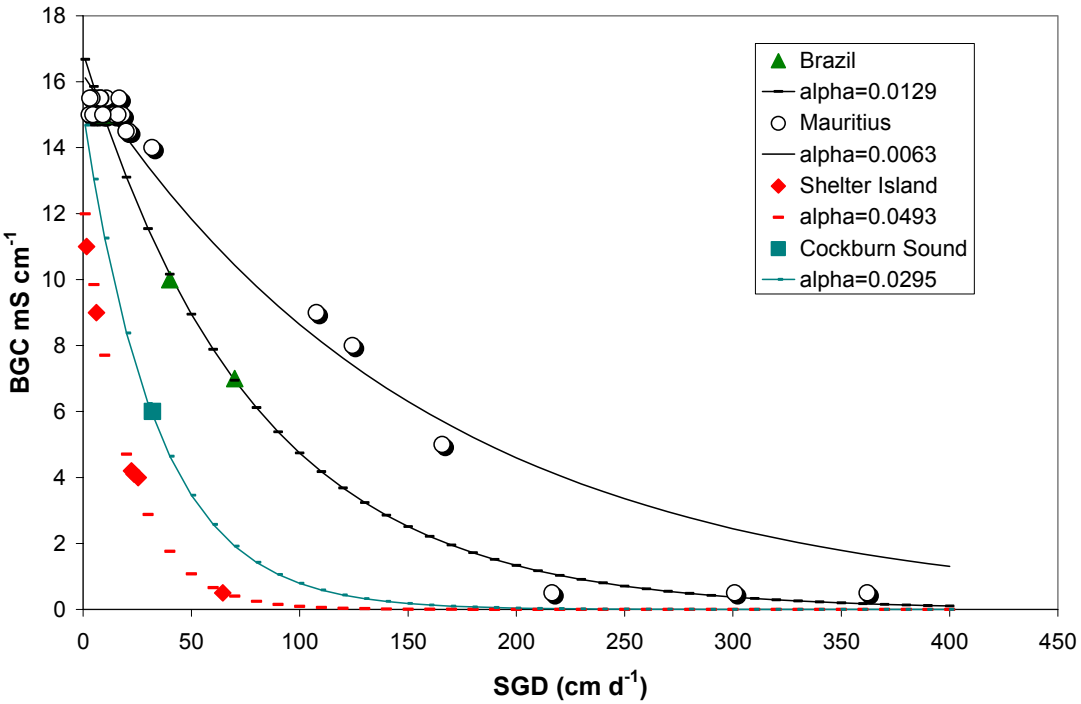

Figure 12. The relationship BGC and SGD at the four sites. Actual data from Cockburn Sound, Shelter Island, Ubatuba, and Mauritius are denoted by blue squares, red diamonds, green triangles, and hollow circles respectively. The other curves represent what the relationship is expected to look like plotting different values of the dispersion coefficient D.

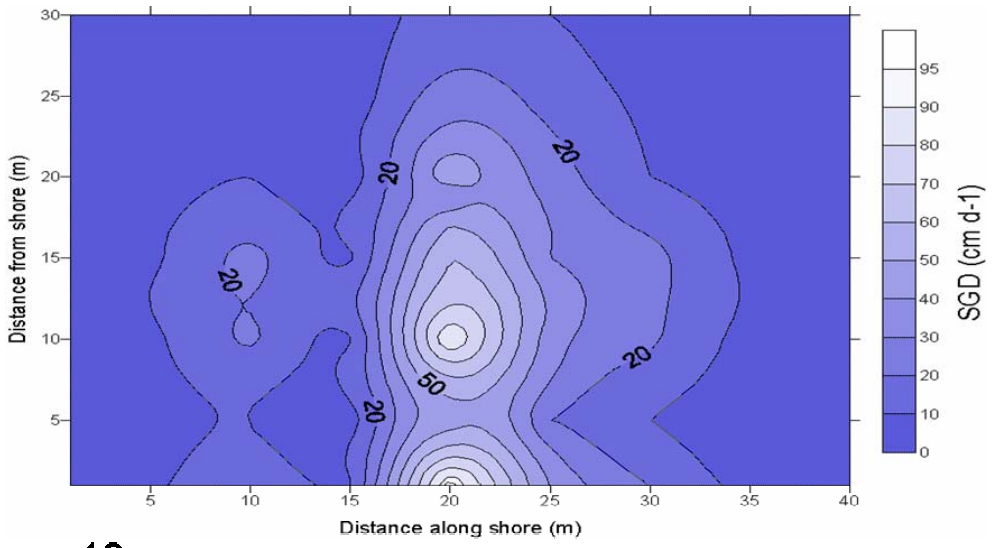
Distance from shore (m)
Distance along shore (m)
SGD (cm d-1)
20
50

13a.

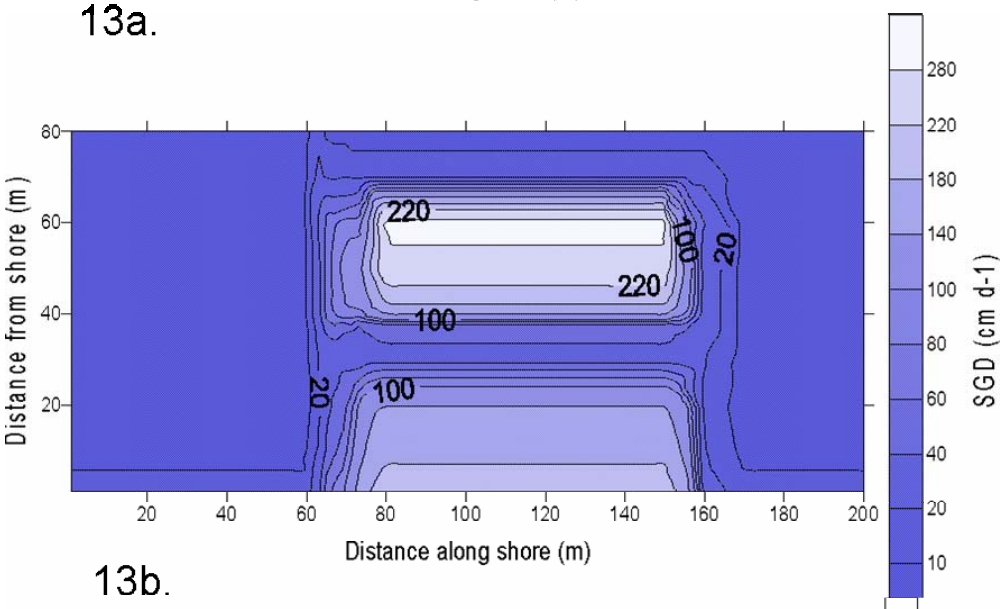
Distance from shore (m)
Distance along shore (m)
SGD (cm d-1)
220
100
20

13b.

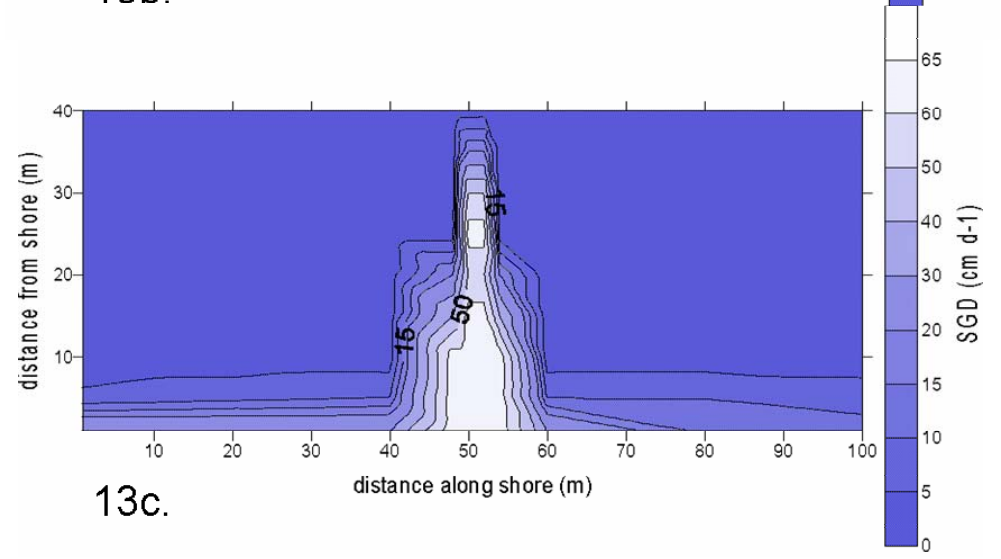
distance from shore (m)
distance along shore (m)
SGD (cm d-1)
15
50

13c.

Figure 13. A. Contour map of SGD at the Brazil site. B. Contour map of SGD at the Mauritius site. C. Contour map of SGD at the Shelter Island site. SGD values are extrapolated from BGC data and the model relating SGD and BGC.

CHAPTER III. Submarine Groundwater Discharge Modification: An Effect of Pier Pilings on Near-Shore Submarine Groundwater Discharge From a (Partially) Confined Aquifer*[1]

1. Introduction

In order to gain an understanding of the contribution of submarine groundwater discharge (SGD) to coastal water and solute budget, the SGD fluxes across the interface between sediment and water need to be accurately quantified. Vented benthic chambers (seepage meters) are routinely employed to measure SGD fluxes volumetrically (Lee 1977, Bokuniewicz 1980, Sholkovitz et al. 2003, Rapaglia 2005, Cable et al. 2006). These instruments provide a direct spot measurement of seepage or discharge flux in an area on the order of one square meter or less. Total-area fluxes are then commonly inferred by multiplying point measurements of flux per unit area by total expected discharge area. Where flow paths are simple and flow patterns homogeneous, directly measured total flow rates compare well with modeled total flow (Burnett et al. 2002, Burnett et al. 2006). But where aquifer confinement or preferential flow paths exist, such extrapolation may not be realistic, or even possible, without taking into account the spatial distribution of the confinement and flow paths. Such preferential flowpaths may be natural (e.g. Gaswirth et al. 2000, Mulligan and Uchupi 2003, Stieglitz 2005), or, unintentionally, man-made (Nakayama et al. 2007, Guswa et al. 1996).

The present study documents subsurface ground electrical conductivity as a pointer toward groundwater salinity levels at Shelter Island, USA, in the vicinity of a

*A version of this chapter has been published in Estuaries and Coasts as: Stieglitz T.C., Rapaglia J., and Krupa S.C. 2007. An effect of pier pilings on near-shore submarine groundwater discharge from a (partially) confined aquifer. Estuaries and Coasts. 30 (3) This chapter is embedded in the thesis as it appears in Estuaries and Coasts and therefore some overlap may occur between Chapters II and III. I contributed the manual seepage meter measurements and the interpretation of the entire set of seepage meter measurements. I also assisted with the geophysical measurements.

pier. In addition, concurrent directly observed submarine groundwater discharge flux was measured using benthic chambers or "seepage meters." The study demonstrates the alteration to the submarine groundwater discharge zone caused by the piercing of a shallow (partial) confining unit by pier pilings, resulting in a highly non-homogeneous spatial submarine groundwater discharge pattern. The experiments were carried out from May 17 to 24th, 2002, as part of a SCOR/LOICZ/IOC program concerned with SGD quantification.

2. Methods

A. Study site

Shelter Island lies in Peconic Bay between the north and south forks of Long Island (Figure 1a). It covers an area of 29.8 km^2 and consists of glacial deposits with moderate relief (less than 60 m). A temperate marine climate prevails, with an average annual precipitation of 117 cm. About half of the precipitation is estimated to be lost through evapotranspiration (Soren 1978), and thus the average recharge for Shelter Island is estimated to be 1.5x 10^6 L km^{-2}d^{-1} (Paulsen et al. 2001). No significant surface streams exist on Shelter Island. Shallow groundwater typically discharges directly into the surrounding coastal water (Schubert 1999). Despite the lack of surface discharge, a reduced-salinity signature is observed around the island (Soren 1978).

The unconfined fresh upper glacial aquifer consists of sands, silts, and gravels and is restricted in depth by the Gardiner's Clay aquitard at about 27 meters below ground surface (Paulsen et al. 2001). In the Magothy and Lloyd Sand Member aquifers

below the clay unit, the groundwater is brackish, with salinity ranging from about 2 to 10 (Soren 1978).

At the study area in West Neck Bay, a narrow fringing marsh separates the bay from the coast. The tidal range varies from 0.7 to 1.1 m. The pier extends ~30 m into the bay, and is 2 m wide. A set of pilings was driven into the sediment at intervals of 2.3 m. Although no records were found which described the exact depth these pilings were driven into the sediment, other piers in the area are known to have pilings which reach depths of 2-2.5 m (Ronald Paulsen, Suffolk County Department of Health Services. Per. Comm.). Seepage of fresh groundwater above the water line can be observed in the intertidal zone in the form of rivulets of fresh water. Previous observations of seepage rates with a continuous ultrasonic seepage meter deployed close to a pier at the study site indicated seepage flow rates of up to 160 cm d^{-1}, displaying a strong correlation with tidal water level (Paulsen et al. 2004). Such flow rates are unusually high for an unconfined aquifer system; at nearby sites on the same coastal-plain aquifer SGD had been measured at rates lower then 50 cm d^{-1} (Bokuniewicz 1980).

B. Bulk ground conductivity measurement

In marine sediments, electrical bulk ground conductivity is a measure of how much (conducting) salt is present in the ground. This is a function of two variables: (a) porewater fraction and (b) porewater conductivity, the latter in turn being a function of porewater salinity and temperature. The high-resolution conductivity probe used in this experiment is modified from Stieglitz et al. (2000) and consists of a series of four ring electrodes (2 cm diameter) configured in a Wenner array with an equal electrode spacing

of 1 cm, measuring the bulk ground conductivity in a sphere of approximately 4 cm diameter around the electrodes (Keller and Frischknecht, 1966). The principle probe design is described in detail in Stieglitz et al (2000). The probe is calibrated by immersing it into seawater of known conductivity, and relative errors in conductivity are less than 5 percent (Stieglitz et al. 2000). In this experiment, the source of greatest error lies in the inexactitude ($< \pm 5$ cm) of the measurement depth at which conductivity was recorded.

Bulk ground conductivity is dependent on sediment porosity, which in turn is dependent both on particle size and sorting. Less porous, saturated sediments have a smaller bulk ground conductivity when compared to sediments with higher porosity at constant conductivity of the porewater, resulting from the presence of non-conducting particles. Commonly, marine sediments saturated with water with a conductivity (σ_w) have a ground conductivity (σ_b) reduced by a factor of 2 to 3.5 compared to σ_w (e.g. Kermabon et al. 1969). Thus, variations of bulk ground conductivity up to a factor of approximately 2 can be explained by variations in sediment type at constant porewater conductivity. However, commonly significant variations in bulk ground conductivity are associated with variations in porewater conductivity (e.g. Stieglitz, 2005).

At the time of the experiments, seawater in West Neck Bay had a conductivity of approximately 34 mS cm^{-1} (salinity of 28 at temperature of 14°C). Therefore, sediments with a bulk ground conductivity of >10 mS cm^{-1} can be assumed to be saturated with seawater. Sediments of the same type with a bulk ground conductivity of significantly less than 10 mS cm^{-1} can be assumed to be saturated with brackish water or - at values close to zero - with fresh water.

Vertical conductivity profiles were recorded by inserting the probe into the ground, taking a reading at a particular depth, and then successively pushing the probe further into the ground for subsequent measurements. A vertical depth profile consisted of readings taken every 5 or 10 cm, to a maximum depth of approximately 1 m below the underwater ground surface. Conductivity profiles were recorded along transects parallel and perpendicular to the (shore-normal) pier at the study site (Figure 1b). Relative ground surface levels were recorded with a theodolite. Transect data were interpolated, taking spatial anisotropy in data distribution into account. In addition, the relative resistance to penetration was noted, to qualitatively assess the degree of sediment consolidation and to identify variations in sediment structure. A change in physical resistance commonly results from density/porosity variability in soft sediments and hence is likely to mark a change in sediment type.

In addition to the bulk ground conductivity measurements, a make-shift piezometer (steel pipe) was driven into the sediment to a depth of approximately 1 m below the sediment surface 5 m below the high water mark, and water level in the piezometer was qualitatively observed at low tide.

C. Seepage meters

The flux of SGD was directly measured with 3 manual and 3 different types of automated benthic chambers, inserted open-end down into the sediment. All measurements were made between May 17th and 24th 2002. All 4 types of seepage meters were simultaneously recording flow from May 21st to 23rd.

The manual seepage meters were installed along a transect 2 m to the north of the pier and perpendicular to the shore, at distances of approximately 8, 11, and 15 m from the shore. The manual meter furthest from shore and 3 automated seepage meters form a transect perpendicular to the pier at a distance of 15 m from shore (Figure. 1b). In addition to seepage rates, salinity of the discharge was recorded periodically.

The manual or "Lee type" seepage meter consisted of a benthic chamber made from a steel drum with a base area of 0.255 m^2, vented to a plastic bag (Lee, 1977). A pipe fitting was placed into the top, to which the plastic bag was connected. Water discharge across the sediment-water interface displaces the water in the chamber and exits through the pipe fitting into the plastic bag. The change in volume of water in the bag over a measured time interval provides a direct flux measurement (Lee 1977). Each collection bag was pre-filled with 500ml of water (Cable et al. 1997, 2006), and the bags were left on the chamber for between 30 and 60 minutes.

A second seepage meter ("Krupaseep") measured bidirectional flow across the sediment-water interface using heat pulse technology. A flow tube is connected to a polycarbonate benthic chamber covering a surface area of 0.29 m^2. A heat pulse is generated by a heater in the flow tube. The dissipation of the heat pulse is dependent on the water flow through the tube and is measured with temperature sensors at the ends of the tube (Krupa et al.1998). The Krupaseep seepage meter system is unique because it collects water quality data (temperature, salinity, conductivity, pH, ORP, and DO; inside and outside the seepage meters) concurrently with seepage rates.

An ultrasonic flow meter connected to a third benthic chamber with an area of 0.21 m^2 continuously measured the SGD rate from the perturbation of fluid flow through

a flow tube on sound propagation. SGD flow rates are determined from a comparison of acoustic velocities in both directions in the tube (Paulsen et al. 2001). Like the Krupaseep, this flow meter can record groundwater discharge and recharge. The measurements used in this comparison have been reported previously in a report by SCOR working group 112 (Anonymous 2002). Use has also been made of data recorded with a dye-dilution seepage meter published earlier by Sholkovitz et al. (2003). This seepage meter measures the seepage rate by injecting dye into a mixing chamber and then determining the time-integrated dilution of the dye to obtain the groundwater seepage rate. This seepage meter covers an area of 0.29 m^2.

Fluxes measured with all devices are normalized to unit area of seafloor. All automated flow meters were calibrated in the laboratory prior to the taking of measurements (as described in Krupa et al. 1998, Paulsen et al. 2001, Sholkovitz et al. 2003). Generally, the results obtained with the different types of flow meters are in close agreement with each other when the meters are deployed in comparable conditions (Taniguchi et al. 2003). Ambient surface water salinity and salinity of the water collected from the manual seepage chambers were measured using a refractometer, and the salinity inside the chambers of the heat-pulse and dye-dilution seepage meters was measured with a YSI sensor. No salinity data were available from the ultrasonic seepage meter.

3. Results

A. Spatial variation of bulk ground conductivity

From the high-water mark to approximately 15 m offshore, bulk ground conductivity was less than 2 mS cm^{-1}, indicating the presence of relatively fresh porewater (Figure. 2). In the narrow mixing zone (fresh porewater and seawater), ground conductivity at the sediment surface increased from 2 to > 9 mS cm^{-1} within a distance of 5 m during low tide and within 2.5 m during high tide. Further offshore, a steep gradient in bulk ground conductivity persisted with depth; the conductivity decreased sharply from >9 mS cm^{-1} at the surface to <1 mS cm^{-1} within no more than 60 cm of depth. With respect to vertical bulk ground conductivity as related to tidal variation, the spatial extent of the mixing zone varied little with time (Figure 2). Seawater did not intrude into depths below the hard sediment layer at either low or high tide.

Bulk ground conductivity varied considerably with distance from the pier (Figure 3). At the sediment surface along the entire extent of the pier, ground conductivity was significantly reduced close to the pier compared to 4 m away from the pier. The reduction was also evident in sediment below the surface: the conductivity in the near vicinity of the pier was less than 1 mS cm^{-1} throughout the sediment column, whereas steep vertical conductivity gradients were observed further than 1.5 m away from the pier center. At most stations along the transect, a relatively hard sediment layer of 5 to 10 cm thickness was identified less than 50 cm below the sediment from the relatively high pressure that was required to push the probe into the sediment. In comparison, less pressure was required above and below this sedimentary unit. A significant discharge of

water was observed at the open top of the make-shift piezometer pipe approximately 40 cm above the sediment.

B. Seepage rates and salinity of SGD

The seepage rate observed with the seepage meters varied significantly with distance from the pier, but not along the pier (Figure 4). The highest average seepage rates of 65 cm d^{-1}, with a peak flow of 190 cm d^{-1}, were recorded directly under the pier, which is consistent with previous measurements close to the pier (O'Rourke 2000). The highest temporal variability of seepage rate was also recorded directly under the pier. Further away from the pier, the seepage rate was greatly reduced, averaging 25 cm d^{-1} with peak flow of 37 cm d^{-1} at 2 m distance. At 3 and 4 m from the pier, the seepage rate was reduced to 6 cm d^{-1} (peak 12 cm d^{-1}) and 2 cm d^{-1} (peak 6 cm d^{-1}) respectively (Anonymous 2002, Sholkovitz et al. 2003). A systematic decrease of flow rate with distance from the pier is apparent (Figure 4a). Manual seepage devices deployed 2 m from the pier at 8 m and 11 m from shore recorded average flow rates of 24 and 23 cm d^{-1} respectively - comparable to results from the seepage meter 15 m offshore at a similar distance from the pier (Figure 4b).

A tidal modulation of the seepage rate was evident in all seepage meter records (Figure 4a, Figure 4b). Two meters away from the pier, for example, seepage flux was inversely correlated with tidal height (Figure 4d). This indicates that there is no significant time lag between variation in discharge and tidal forcing of the aquifer, which

is a pattern frequently observed in SGD studies (Paulsen et al. 2001, Kim and Hwang 2002, Taniguchi 2002).

During the experiment, the ambient salinity varied only slightly, within 1 m of the pier (i.e. between 27 and 28). Salinity in the manual seepage devices located 2 m from the pier was found to be between 8 and 10 when the instruments were flushed. In the dye injection seepage meter 3 m from the pier, a salinity of 19 was recorded when flushed (Sholkovitz et al. 2003). At 4 m from the pier, the salinity in the seepage meter was 27, similar to full seawater concentration at the time of measurement. A systematic increase in salinity of SGD with distance from the pier is apparent (Figure 4c).

4. DISCUSSION

A. Aquifer confinement

Previous works in the area of West Neck Bay treated the shallow submarine sediments as a single phreatic aquifer (O'Rourke 2000, Paulsen et al. 2001, 2004). However, the steep, vertical gradients of conductivity observed in the sediment (Figure 2) indicate that a dense layer at a depth of 20-50 cm, separates two shallow sub-aquifers, the deeper of which (typically deeper than 30-50 cm) is at least partially confined. This layer appears to separate the near shore seepage from a deeper fresh aquifer that extends farther offshore.

The presence of a confined aquifer is revealed based on the following observations. The furthest inshore excursion of high-conductivity porewater, in both the vertical and horizontal directions, at high tide coincides with the location of the dense

sediment layer, indicating that this layer provides a restriction for vertical water exchange (Figure 2). The pronounced vertical conductivity gradient in the shallow sediment layers as observed here is typical for shallow confined (or semiconfined) aquifer systems (Stieglitz, 2005). The presence of a confining unit was made evident also by means of the water level in the piezometer: the hydraulic head was significantly higher than sea level (at least 40 cm at low tide), indicating the presence of a pressurized and thus confined aquifer. If the aquifer at this location (i.e., 5 m along the transect in Figure 1a) was unconfined, then no discharge at the open top piezometer would be observed. Note that the vertical mixing zone remains at a constant location (predominantly) at low and high tide respectively, indicating that the overlying saline water does not penetrate into the underlying sediments with low conductivity signature. This is likely a result of the presence of the confining unit which is confining 'in both directions' (i.e. restricting both upward and downward flow).

B. Effect of pilings on SGD rate and salinity

Close to the pier, bulk ground conductivity at the sediment surface is low along the entire length of the pier (Figure 2), and the seepage rate is highest directly under the pier (Figure 4a). The most plausible explanation for this observed conductivity distribution and the associated seepage flux pattern is that the pilings pierce the semi-confining layer, causing a significantly elevated seepage rate driven by the hydraulic head of the associated aquifer. This could either be a result of the pilings being long enough to penetrate the (partial)confining unit, or a result of the (limited) destruction of

the confining unit during the construction of the pier. Either way, the pier-perpendicular seepage meter transect demonstrates the effect of the pier's presence on both subsurface conductivity (which rises) and on seepage rates (which fall) with distance away from the pier. Higher seepage rate is correlated with lower ground conductivity due to the observed increase of flow of fresh groundwater near the pier, which is driven by the hydraulic head in the aquifer. In an unaffected aquifer system, no such variation in conductivity or seepage rate close to a pier would be expected. Away from the pier, high bulk ground conductivity consistent with saline porewater is found considerably closer to shore (Figure 3a). This may represent aquifer and seepage condition at the site before the installation of the pier.

Previous studies document high flow rates close to the pier (Paulsen et al. 2004). This study however shows that flow rates measured in the vicinity of the pier are significantly larger than flow rate measured elsewhere in the area when directly compared to each other (Burnett et al. 2006). Along the pier little variation exists in the average discharge measured in seepage meters located 8, 11, and 15 m from the shoreline respectively. This suggests that along the pier, the impact of the piercing (or destruction) of the confining unit dominates over the commonly observed decrease in discharge with distance from the onshore hydraulic head.

The bulk ground conductivity at the sediment surface provides some indication of the origin of the discharging water. Next to the pier, where the conductivity is significantly reduced, SGD includes at least some groundwater of fresh, terrestrial origin. At 2 and 3 m away from the pier, a ground conductivity of 3.5 mS cm^{-1} and 8 mS cm^{-1} corresponds to an SGD salinity of 10 and 19 , indicating an approximate 2:1 and 1:2

ratio of fresh to saline (salt water component) groundwater discharge respectively. At 4 m away from the pier, at a ground conductivity of 9 mS cm^{-1}, a salinity of 27 was recorded, similar to the salinity of the sea water above, implying that discharge at this point is of re-circulated seawater. The discharge of this re-circulated seawater is characterized by lower seepage rates (Figure 4c). No salinity data are available from under the pier, but the ground conductivity of <0.5 mS cm^{-1} implies that the discharge here likely consists of fresh water.

In summary, by investigating bulk ground conductivity, spatial variability and origin of fresh SGD can be determined. Such investigations in themselves do not readily allow determination of the actual magnitude of fresh SGD, but the method can be used to assess how accurately the locations of seepage meters reflect the fresh groundwater discharge regime at a site, thereby assisting the improvement of SGD magnitude estimates. It is important to note that conductivity does not need to correlate with total groundwater flow at locations where salt water recirculation significantly contributes to the total groundwater flux (e.g. Li et al. 1999).

C. Anthropogenic modification of SGD

The most commonly noted effects of anthropogenic modification of SGD refer to water quality, such as an increase in nutrients and other solutes in SGD as a result of domestic or agricultural activities in the catchment of a coastal aquifer. Such modifications are expected to (and in some cases have been observed to) affect the biogeochemistry and ecology of the near-shore zone (e.g. Johannes 1980, Valiela et al.

1990, Moore 1999, Slomp and Van Capellen 2004, Bone et al. 2006). In addition seawater intrusion due to exploitation of aquifers is commonly noted in the literature (e.g. Ataie-Ashtiani et al. 1999) However, geotechnical modifications of aquifers and discharge zones such as the effect of pier pilings on discharge from confined aquifers as described here have received comparatively little attention in SGD studies to date.

Urban and industrial development modifies the coastal environment. An altered coastal hydrology may cause flow patterns of SGD comparable to those observed in regions in which natural preferential flow paths exist, such as in karstic environments (Bonacci 2001). This study provides an example of the construction of a preferential flow path for groundwater, in this case in the vicinity of the pier. There is some evidence that bulkheads may have similar effects on SGD (Rapaglia 2005). Temporal effects of such modifications remain unknown; the construction of the pier, for example, may have resulted in a systematic increase of SGD in the local setting. It is conceivable that the large number of private piers at Shelter Island has increased the total amount of SGD into West Neck Bay, instead of naturally discharging further offshore in the greater Peconic Bay system. In order to understand the full extent of groundwater discharge, and of potential anthropogenic modifications of the discharge, thermal IR imagery could be acquired during periods in which there is a distinct thermal gradient between surface and groundwater. Such IR imagery can provide useful information on the location and distribution of groundwater discharge (Mulligan and Charette 2006). Note that such remote sensing studies were outside the scope of this project.

5. Conclusion

At the study site at Shelter Island, pilings supporting a pier apparently pierced a shallow (semi)confining sediment layer, causing a comparatively high seepage rate driven by the hydraulic head of the confined aquifer, which results in a substantial increase in submarine groundwater discharge near the pier. Thus, seepage rate measurements made in the immediate vicinity of the pier (which runs perpendicular to the shoreline) cannot be considered representative for the area. This anthropogenic effect confounds the commonly observed pattern of decreasing SGD with increasing distance from shore. At this site, SGD magnitude is primarily a function of proximity to the pier.

References:

Anonymous, 2002. Submarine groundwater discharge assessment intercomparison experiment, May 17–24, 2002: Shelter Island, New York. Field report to the Intergovernmental Oceanographic Commission (Integrated Coastal Area Management Program ICAM) by SCOR/LOICZ WG112, http://ioc.unesco.org/icamNew/files/SGD%20NY%20report.pdf.

Ataie-Ashtiani, B., Volker, R. E., and Lockington, D. A. 1999. Tidal effects on sea water intrusion in unconfined aquifers. Journal of Hydrology. 216:17–31.

Bokuniewicz, H., 1980. Groundwater seepage into Great South Bay, New York. Estuarine and Coastal Marine Science. 10 (4):437–44.

Bonacci, O., 2001. Analysis of the maximum discharge of karst springs. Hydrogeology Journal. 9 (4):328–38.

Bone, S.E., Gonneea, M.E. and Charette, M.A. 2006. Geochemical cycling of arsenic in a coastal aquifer. Environmental Science and Technology. 40: 3273-3278.

Burnett, W., Chanton, J., Christoff, J., Kontar, E., Krupa, S., Lambert, M., Moore, W., O'Rourke, D., Paulsen, R., Smith, C., Smith, L., and Taniguchi, M. 2002. Assessing methodologies for measuring groundwater discharge to the ocean. EOS 83:117–23.

Burnett, W.C., Aggarwal P.K., Bokuniewicz, H., Cable, J.E., Charette, M.A., Kontar, E., Krupa, S., Kulkarni, K.M., Loveless, A., Moore, W.S., Oberdorfer, J.A., Oliveira, J., Ozyurt, N., Povinec, P., Privitera, A.M.G., Rajar, R., Ramessur, R.T., Scholten, J., Stieglitz, T., Taniguchi, M., and Turner, J.V., 2006. Quantifying submarine groundwater discharge in the coastal zone via multiple methods. Science of the Total Environment. 367 (2-3): 498-543.

Cable, J.E., Burnett, W.C., Chanton, J.P., Corbett, D.R. and Cable P.H., 1997. Field Evaluation of Seepage Meters in the Coastal Marine Environment. Estuarine, Coastal, and Shelf Science. 45: 367-375.

Cable, J.E., Martin J.B., and Jaeger J. 2006. Exonerating Bernoulli? On evaluating the physical and biological processes affecting marine seepage meters. Limnology and Oceanography Methods. 4: 172-183.

Gaswirth, S.B., Ashley, G.M. and Sheridan, R.E. 2000. Use of seismic stratigraphy to identify conduits for saltwater intrusion in the vicinity of Raritan Bay, New Jersey. Environmental Engineering Geoscience. 3:209-218.

Guswa, J., Baric, P., Carr, J., Hager, J., Rapacz, M., Schreiber, R., and Wiley R., (eds.), 1996. Hydrology and hydrogeology of urbanizing areas. St. Paul, Minn.: American Institute of Hydrology.

Johannes, R., 1980. The ecological significance of submarine discharge of groundwater. Marine Ecology Progress Series. 3:365–73.

Keller, G., and Frischknecht, F. 1966. Electrical methods in geophysical prospecting. Oxford: Pergamon Press. 535 pages.

Kermabon, A., Gehin, C., and Blavier, P. 1969. A deep-sea electrical resistivity probe for measuring porosity and density of unconsolidated sediments. Geophysics. 34: 554–71.

Kim, G., and Hwang, D. 2002. Tidal pumping of groundwater into the coastal ocean revealed by 222-Rn and CH4 monitoring. Geophysical Research Letters. 29 (14): 1678–80.

Krupa, S., Belanger, T., Heck, H., Brock, J., and Jones, B. 1998. Krupaseep: the next-generation seepage meter. Journal of Coastal Research. 25: 210–13.

Lee, D. 1977. A device for measuring seepage flux in lakes and estuaries. Limnology and Oceanography. 22: 140–47.

Li, L., Barry, D.A., Stagnitti, F. and Parlange, J.Y.,\ 1999. Submarine groundwater discharge and associated chemical input to a coastal sea. Water Resources Research. 35 (11): 3253–3259.

Moore, W.S. 1999. The subterranean estuary: a reaction zone of ground water and sea water. Marine Chemistry. 65 (1-2): 111-125.

Mulligan, A., and Uchupi, E. 2003. New interpretation of the glacial history of Cape Cod may have important implications for groundwater contamination. EOS. 84, 171 183.

Mulligan, A.E. and Charette, M.A. 2006. Intercomparison of submarine groundwater discharge estimates from a sandy unconfined aquifer. Journal of Hydrology. 327: 411-425.

Nakayama, T., Watanabe, M., Tanji, K., and Moriuka, T. 2007. Effect of underground urban structures on eutrophic coastal environments. Science of the Total Environment. In press.

O'Rourke, D., 2000. Quantifying specific discharge into West Neck Bay, Shelter Island, New York, using a three-dimensional finite-difference groundwater flow model and continuous measurements with an ultrasonic seepage meter. MSc thesis, State University of New York at Stony Brook. 88 pages.

Paulsen, R., Smith, C., O'Rourke, D., and Wong, T. 2001. Development and evaluation of an ultrasonic groundwater seepage meter, Ground Water. 39 (6): 904–11.

Paulsen R.J., O'Rourke D., Smith C.F., and Wong T.F., 2004. Tidal load and salt water influences on submarine groundwater discharge. Ground Water. 42 (7): 990-999.

Rapaglia, J., 2005. Submarine groundwater discharge into the Venice lagoon, Italy. Estuaries. 28 (5): 705-713.

Schubert, C., 1999. Groundwater flow paths and travel time to three small embayments within the Peconic Estuary, Eastern Suffolk County, New York. USGS Water-Resources Investigation Report 98-4181.

Sholkovitz, E., Herbold, C., and Charette, M. 2003. An automated dye-dilution–based seepage meter for the time series measurement of submarine groundwater discharge. Limnology and Oceanography Methods 1:16–28.

Slomp, C.P., and Van Cappellen, P. 2004. Nutrient inputs to the coastal ocean through submarine groundwater discharge: controls and potential impact. Journal of Hydrology 295 (1-4): 64-86.

Soren, J., 1978. Hydrogeologic conditions in the town of Shelter Island, Suffolk County, Long Island, New York. USGS Water Resources Investigations Report 77-77.

Stieglitz, T., 2005. Submarine groundwater discharge into the near-shore zone of the Great Barrier Reef, Australia. Marine Pollution Bulletin. 51:51-59.

Stieglitz, T., Ridd, P., and Hollins, S. 2000. A small sensor for detecting animal burrows and monitoring water conductivity. Wetlands Ecology and Management. 8:1–7.

Taniguchi, M., 2002. Tidal effects on submarine groundwater discharge. Geophysical Research Letters. 29 (12): 1561–64.

Taniguchi, M., Burnett, W., Smith, C., Paulsen, R., O'Rourke, D., Krupa, S., and Christoff, J. 2003. Spatial and temporal distributions of submarine groundwater discharge rates obtained from various types of seepage meters at a site in the northeastern Gulf of Mexico. Biogeochemistry. 66 (1-2): 35–53.

Valiela, I., Costa, K., Foreman, K., Teal, J.M., Howes, B., Aubrey, D. 1990. Transport of groundwater-borne nutrients from watersheds and their effects on coastal waters. Biogeochemistry. 10 (3): 177-197.

Figures for Chapter III

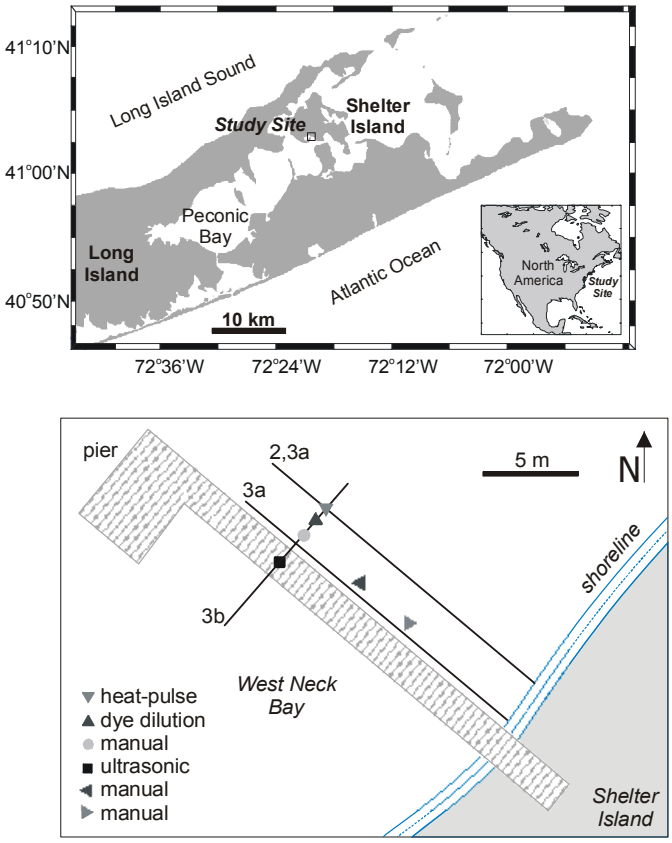

Figure 1
(a) Location map of the study site at Shelter Island.
(b) Overview of the study site, showing seepage meters (markers) and conductivity transects (lines). The respective method is indicated for each seepage meter marker, and numbers on the conductivity transects refer to the respective figure number.

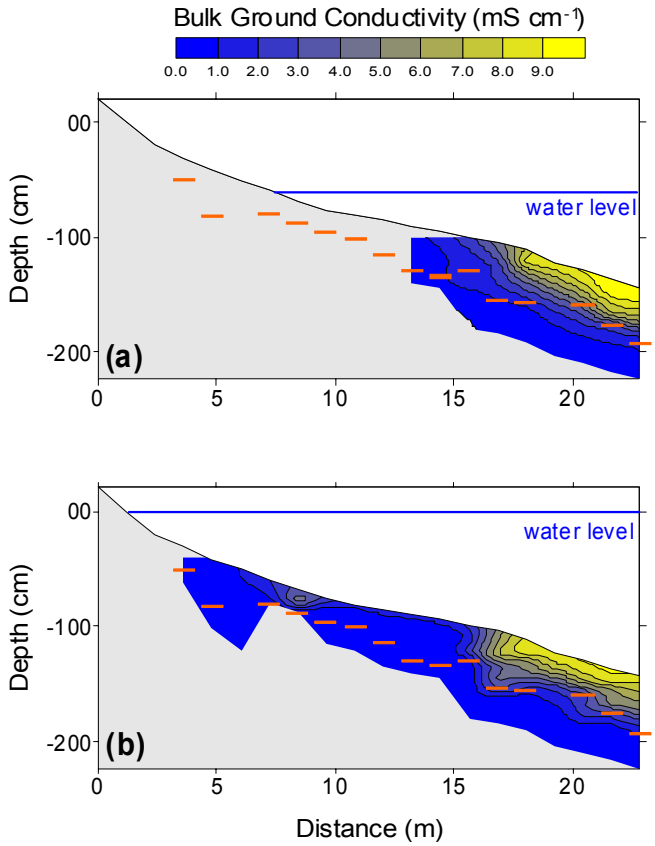

Figure 2
Bulk ground conductivity recorded along a shore-normal transect 4.3 m north of the pier at (a) low tide and (b) high tide. The origin of the axes is approximately mean high water level. The water level at the time of recording is shown. A sediment layer that was physically hard to penetrate with the conductivity probe is marked with a grey bar at each profile location, and locations of data points used in the contouring interpolation are marked with a black dot.

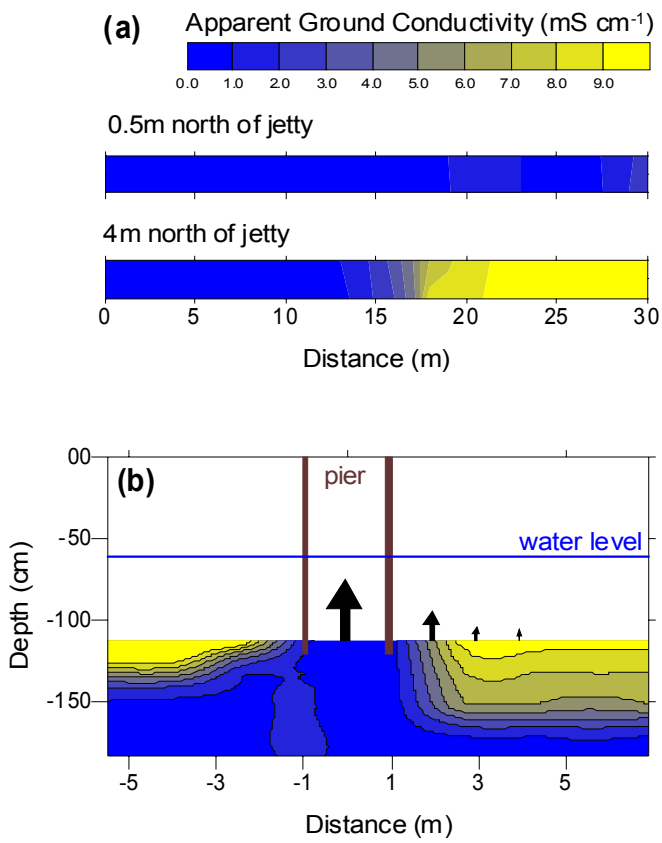

Figure 3
(a) Bulk ground conductivity at 0.5 m north of the pier (the jetty) and 4 m north of it (low tide, top 10 cm of the seabed). An increase in conductivity with increasing distance from the pier at distance > 16 m is apparent.
(b) Bulk ground conductivity along a shore-parallel transect below the pier (approximately 17 m from the mean high water level; pilings are shown in brown; length of the black arrows is approximately proportional to the average seepage flux measured at the respective location). Locations of data points used in the contouring interpolation are marked with a black dot. A decrease in seepage flow with increasing distance from the pier is apparent.

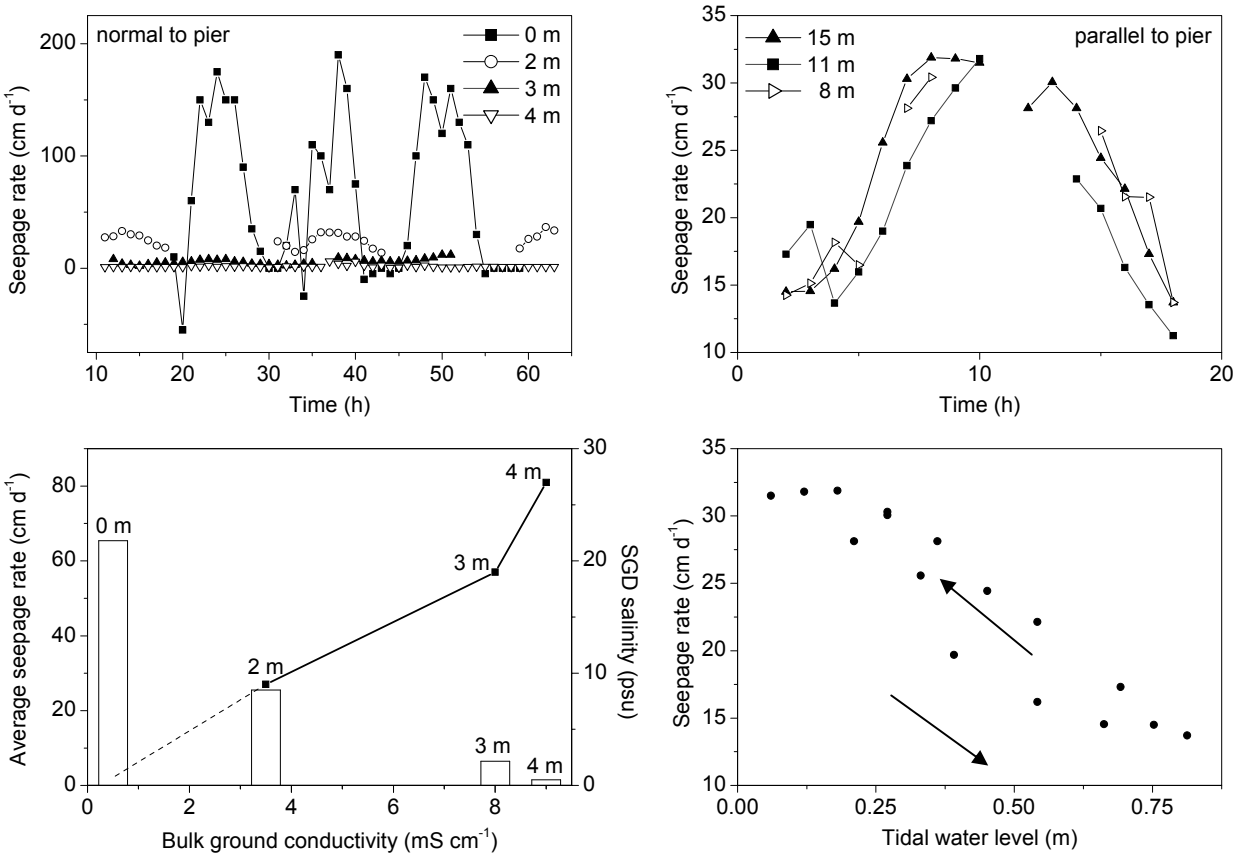

Figure 4
(a) Time series of seepage rates measured along a transect perpendicular to the pier, showing distance to the pier center (locations of the seepage meters are indicated in Figure 1b and Figure 3b).
(b) Time series of seepage rates in manual seepage meters along a transect approximately 2 m north of the pier, at a distance of 8, 11, and 15 m from shore (the symbols for the respective seepage meters are used in Figure 1b). (c) Average seepage rate (bar) and salinity (small square) in seepage meter versus bulk ground conductivity (salinity data at 0 m are not available, but anecdotal observations [taste tests] suggest a salinity close to zero, as marked with the dashed line).
(d) Seepage rate 2 m away from the pier versus tidal water level.

CHAPTER IV: The impact of groundwater advection on salinity in pore waters of permeable sediments.

1. Introduction

Much of the impetus behind the study of submarine groundwater discharge has been to determine the role the process plays in transporting chemical constituents to the coastal ocean (Johannes 1980, Capone and Bautista 1985, Capone and Slater 1990, Corbett et al. 2000, Slomp and Van Cappellen 2004). Recently, this phenomenon has been discussed extensively, but researchers have long realized the possible ecological implications of the subsea outflow of groundwater (Johannes 1980, Kohout 1966, Bokuniewicz 1980, Lee and Cherry 1978). Nutrients and other chemical constituents are often elevated in groundwater relative to surface waters (Christensen et al. 2001, Manning and Hutcheon 2003). Therefore, even if groundwater discharge does not represent a substantial proportion of the volume flux of water into the sea, it may be a primary or major input pathway for dissolved chemical constituents. In certain cases, it is likely that SGD is the main source of nutrients to coastal regions (Matson 1993). For example, nitrate supplied by SGD may cause a shift in the phytoplankton community by driving the system towards phosphate limitation, and may be responsible for harmful algal blooms (Gobler and Sanudo-Wilhelmy 2001).

To study the impact of SGD on the concentration of constituents in local areas, investigators have often attempted to determine the flow rate of SGD and multiply that volume flux by known concentrations of chemical species in wells (D'Elia et al. 1981, Oberdorfer et al. 1990). While this is helpful for comparisons, there are several problems with its quantification. Defining the proper end member can be problematic and

complicated by the fact that nutrients do not behave conservatively, and concentrations may change significantly along flow lines (Kaplan et al. 1979, Moore 1999). Improvements to this method have been made more recently, by directly measuring chemical constituents in the sediment where discharge appeared to be occurring (Charette and Allen 2006, Bone et al. 2006), but at least two difficulties remain even for conservative tracers. First, application of this method is based on the assumption that the chemical profile in the pore water and at the sediment-sea interface is invariant. However, it is yet unknown how the concentration of these constituents in the porewater may respond to temporal changes in discharge. Second, even in areas where discharge exceeds 50 cm d^{-1}, porewater in the upper few centimeters of the sediment often has a measurable salt content (Bokuniewicz et al. 2004, Rapaglia 2005). If fresh water is being advected from below, penetration of the salt into the sediment requires an efficient downward dispersion process. Whatever the mixing process is in the surficial sediments, the flux of chemical species upward across the sediment-water interface is a combination of the pore water entering the mixed layer from below and the seawater entering the mixed layer from above. The incremental chemical flux due to SGD should, therefore, not be measured at the sediment-water interface but rather at the base of the mixed layer within the sediment, especially in the presence of specific conduits which allow water to discharge from a depth below the interface as will be explained later. If we can comprehend what is happening with a conservative tracer such as salt in the vertical dimension, perhaps we can begin to understand the impact of SGD on non-conservative constituents such as nutrients.

Here we investigate the utility of the simultaneous measurement of flow rates taken with manual seepage meters and profiles of salinity in the sediment collected with a retract-a-tip piezometer to determine how these profiles change in the face of groundwater advection. In some cases, radium and nutrient concentrations were also examined.

A. Theory

There are two critical considerations when applying measurements of SGD to calculations of the fluxes of dissolved chemical species. The first is the vertical rate of advection of pore water out of the sediment, the second is the rate of dispersion downward into the sediment. The presence of salt, for example, at depth in the sediment cannot be accounted for by molecular diffusion; as in the presence of even small upward advection, molecular diffusion could not bring salt into the sediment more than a millimeter. In the absence of these processes one would expect the salinity to be zero immediately below the sediment-sea interface with even moderate rates of vertical fresh water advection, that is, SGD. Other investigators have recognized the need for a more effective mechanism for the penetration of dissolved chemical species into the sediment against upward advection (e.g. Li et al. 1999). This process is usually represented by a coefficient of dispersion, although the exact mechanism is variously described (e.g. Ullman et al. 2003).

Dispersion of salt has been oft discussed in terms of estuarine circulation and dynamics in open water (e.g. Hunkins 1981, Uncles et al. 1985, West et al. 1990). For

instance, investigators explore the impact of wind-forced circulation, turbulent mixing, and gravitational acceleration to explain how salt is able to penetrate up the estuary in the face of large discharges of freshwater (Matsukawa and Matsumura 1985). When considering a well-mixed or partially-mixed estuary, the discharge at the mouth of the estuary will have near seawater salinity but with a net magnitude equal to the fresh discharge. This is due to dispersive mixing which, if in steady state, can be represented by (adapted from Vallino and Hopkinson 1998):

$$D = (c_s * q/A) / (dc_s/dz) \quad (1)$$

where: D is dispersion, c_s is the concentration of salt (g cm^{-3}), q is the net advective discharge ($cm^3 d^{-1}$) through cross-sectional area A and dc_s/dz is the salinity gradient in the direction of the advective velocity.

A similar mixing zone occurs between fresh and salty groundwater (Moore 1999). There is no sharp boundary in this zone, but a gradient in which many important chemical reactions take place (Bone et al. 2006). In open water, the physical dispersion is a function of the advection velocity (Vallino and Hopkinson 1998). Thus, a changing rate of advection results in changes in the intensity of dispersion. Vallino and Hopkinson (1998) modified the dispersion equation to adapt to a temporally-variable down-estuary flow by increasing the dispersion parameter with increases in the net discharge. In this chapter, evidence will be presented to suggest that a similar situation may apply for groundwater and the subterranean estuary.

Many mechanisms have been suggested for the process by which salt may enter into the surficial layers of sediment (Martin et al. 2006). These include wave and tidal pumping (Li et al. 1999), density mixing (Bokuniewicz et al. 2004), changes in the

terrestrial water table (Michael et al. 2005) and bioirrigation (Martin et al. 2006) all of which are considered as components of dispersion for the purpose of this thesis. The diffusivity of salt in water is about 8.4 x 10^{-5} m^2 d^{-1} and diffusivity in a porous medium is one to two orders of magnitude less than this (Freeze and Cherry 1979). The authors further discuss that hydrodynamic or mechanical dispersion is one of the major physical processes which control the flux into and out of the sediment. This coefficient of hydrodynamic dispersion can be expressed by multiplying dispersivity with the advective velocity and adding molecular diffusion (Freeze and Cherry 1979). Gelhar (1993) gives typical dispersivity values between 0.001 and 0.01 m. Incorporating the measured values of SGD, we can calculate hydrodynamic dispersion coefficients at the sites investigated in Chapter II between 0.0001-0.02 m^2 d^{-1} (Table 2).

Cooper (1964) considered dispersion within the aquifer due to the tides. Using an equation relating the tidal range to the amplitude of the displacement of water in the in a coastal aquifer caused by the tides, he calculated typical values of dispersion up to 0.01 m^2 d^{-1} near the shoreline. Likewise, using my site-specific values for the tidal range, tidal period, porosity and hydraulic conductivity, we can calculate a dispersion coefficient at the shoreline due to tides for each of the sites described in Chapter II (Table 2). The values for these sites range from 0.02 -0.08 m^2 d^{-1} Dispersion coefficients due to the tide are expected to be higher than any due to mechanical dispersion.

Using profiles of electrical conductivity as a surrogate for salinity, Bokuniewicz et al. (2004) calculated dispersion coefficients of between 0.03 m^2 d^{-1} and 0.007 m^2 $d^{-1}$by fitting to the data a steady-state, one-dimensional solution to the advection-diffusion

equation in a semi-infinite medium with a constant salinity at the surface. Density-driven interfingering, or salt fingering, was suggested as the mechanism of dispersion. Seplow (1991) argued that salt fingering can allow for the penetration of salt into the sediment even when there is a high rate of vertical advection of water. Martin et al. (2007) also used an analytical solution to the advection-diffusion equation in conjunction with measurements of SGD and porewater salinity profiles to estimate dispersion coefficients as high as 3.4×10^{-5} m^2 d^{-1} at sites in the Indian River Lagoon, Florida. They note that the expected, mechanical hydraulic dispersion is too low to account for the observed salinity profiles in the presence of the measured SGD.

Bioturbation has also been implicated, with a dispersion estimate of 0.05 m^2 d^{-1} under the assumption that exchange occurred to a depth of 0.4 m within 46 hours (Martin et al. 2006). Vertical profiles of pore water temperature at one site (Dale and Miller 2007) showed a lag of between 0.1 and 0.3 hours cm^{-1}. The interpretation of the observed time lag in terms of conductive heat transfer in the presence of advection, yields effective dispersion coefficients between 0.02 and 0.2 m^2 d^{-1} (H. Bokuniewicz, 2007, Stony Brook University, personal communication; Table 1.).

B. Site Description

Three sites were chosen for this experiment; Peconic Bay, NY, USA, Jamaica Bay, NY, USA, and the Venice Lagoon, Italy. Jamaica Bay and Venice Lagoon were chosen as sites representative of urbanized coastal lagoons. As urbanized lagoons are under constant pressure from anthropogenic activities they often are sites at risk of

contamination from polluted groundwater discharges. Therefore it is important to understand how the advection of groundwater impacts the reactions which occur in the subterranean estuary of these systems. Both Jamaica Bay and, especially, Venice Lagoon have complex hydrogeological and aquifer characteristics, therefore Mattituck was chosen as a relatively ordinary, sandy, beach site which is in a low human impact zone.

The Peconic Bay estuary consists of a large system of bays at the east end of Long Island, NY (Figure 1a) which separate the North and South Forks of Long Island. They are open to the Atlantic Ocean to the east and have a fairly large freshwater input from the Peconic River to the west. The North Fork of Long Island has four principal freshwater flow systems, which reside in a layering of unconsolidated glacial and non-glacial deposits (Schubert et al. 2004 http://pbisotopes.ess.sunysb.edu/lig/). The south shore of the North Fork is underlain by a sequence of glacial outwash and thin (~10 m) clay confining units. These all rest upon the much thicker (~150 m) Magothy Aquifer and subsequently the Lloyd Sand Member Aquifer. Tidal range fluctuates throughout the bay from about 0.5 m to 1.5 m. In addition, studies have shown that groundwater discharge may be an important factor controlling the ecosystem structure of the bays, especially discharge seen offshore of large landfill areas near Flanders Bay (Gobler and Boniello 2003) and alongside pilings in West Neck Bay (Paulsen et al. 2004, Chapter III: Stieglitz et al. 2007). The specific site of study in the Peconic Bay is Mattituck Beach on the north shore of the bay about 12 km from the mouth of the Peconic River. The site consists of a gently sloping sandy beach with a tidal range of 0.5-0.75 m. Previous

measurements at the site have shown a tidally modulated discharge ranging from -50-+200 cm d^{-1} (unpublished data).

Jamaica Bay is a small (52 km^2) urban embayment located entirely within the boroughs of Brooklyn and Queens NYC (Figure 1b). The bay has been extensively altered by human activities such as dredging, landfill construction, and bulkhead installation (Swanson et al. 1992). It has little, if any, measurable surface water input, and almost all freshwater enters as effluent from four major sewage treatment plants (Gordon et al. 2007, Rubenstone 2007). Jamaica Bay sits atop the Upper Glacial Aquifer, a highly permeable aquifer, which is more than 210 m thick, and composed of till and outwash deposit interbedded with marine clays (Busciolano, 2002). The Upper Glacial Aquifer overlies the Jameco Aquifer which is170 m thick and is composed of fine-to-coarse gravel. The Jameco Aquifer is underlain in turn by the Magothy and Lloyd Aquifers to bedrock at a depth of 550 m (Busciolano, 2002). The majority of the bay bottom consists of a silty-clayey sediment left over from glacial outwash and salt marsh deposits; 66% of the bay is covered by marshland (Hartig et al. 2002). Meanwhile a portion of the coastline is comprised of a more permeable fine grained sand (Engelbright 1975). The specific locations chosen for this experiment in Jamaica Bay are Canarsie Pier and Canarsie Pol (Figure 1b). These locations are part of the aforementioned sandy bottom, and have gently sloping beaches (Beck et al. 2007). The Canarsie Pier site is located on the northern shore of Jamaica Bay and consists of a wide (~120 m) pier bisecting a sandy beach. All measurements were made on the east side of the pier. Canarsie Pol is the largest (96 ha) uninhabited island in Jamaica Bay and has a relief of up to 4 m. The island is covered with terrestrial vegetation and is bordered by marshes

along much of its shores to the north and east and has intermittent marshland and sandy beaches to the south and west. The mean tidal range in Jamaica Bay is about 1.5 m although there is some variation throughout the bay (Hartig et al. 2002).

The Venice Lagoon is a large (550 km^2), shallow (avg. depth 0.8 m), microtidal (~1 m) lagoon on the northwest coast of the Adriatic Sea (Figure 1c). It is an important ecosystem as its waters are home to a major fishing industry as well as host to many urban and industrial activities including the Porto Marghera Industrial zone (Belluci et al. 2002). Perhaps no lagoon in the world has been subject to a longer and more continuous history of human modification (Appendix B). The lagoon is underlain by a series of nine aquifers, some of which are artesian, with a total thickness of 1000 m (Carbognin et al. 1977). Only the uppermost aquifer is known to intercept the sea floor. The surrounding land has little, if any, relief. The lagoon's drainage basin is 1850 km^2 and has an annual average rainfall of 950 mm (Zonta et al. 2005). Previous measurements in this lagoon have shown flow rates averaging 30 cm d^{-1} in the northern lagoon and 6 cm d^{-1} in the central lagoon, with fluctuations between 0 and 200 cm d^{-1} (Rapaglia 2005).

The sites investigated for this study were both located along the western shore of the Cavallino Peninsula in the northern lagoon (Figure 1c). Both sites (Treporti to the north, and Punta Sabbioni to the south) consisted of beaches similar to those in Jamaica Bay, with Treporti consisting of silt-sand sediment and Punta Sabbioni of fine- to medium-grained sand. Both beaches were backed by artificial bulk-heads (3 m at Treporti, 1 m at Punta Sabbioni). Though both sites are located adjacent to one of the major channels in the lagoon with fast-flowing currents, they are somewhat protected

from these currents by artificial barriers (jetties and large boats that block any wind-driven currents). This site will be discussed in greater detail in Chapter V.

2. Methods

At each location, 2-5 manual seepage meters (Lee 1977) were used to determine the seepage rates. These meters consist of benthic chambers (0.25 m^2) vented to plastic bags. Water which enters the chamber displaces the water already inside the chamber into a plastic bag. Using the known volume and time, a flow rate can be determined (Bokuniewicz 1980). At each of the sites, bags were pre-filled with 500 ml of ambient water (except when samples were collected for salinity measurements) to reduce artifacts (e.g. Shaw and Prepas 1989, Libelo and MacIntyre 1994, Cable et al. 2006) and to allow for the calculation of negative flow rates (saltwater intrusion). A discussion of the error involved in the use of seepage meters is found in Appendix B. At all sites seepage meters were aligned in both shore-parallel and shore-perpendicular transects in order to examine the spatial distribution of SGD

To determine salinity profiles, a retract-a-tip piezometer (Charette and Allen 2006) was driven into the ground using a slide hammer to collect groundwater samples from different depths. The piezometer allows for multiple sample collection at intervals > 10 cm to a depth of 5 m along the same profile. The piezometer consists of a screened stainless steel tip connected to Teflon tubing. In addition, Teflon tubes attached to dedicated tips can be emplaced in the ground at pre-determined depths for an indefinite length of time. These tips have two advantages: they can be repeatedly sampled, and

they allow for the sediment and profile to reach a state of equilibrium after the perturbation caused by emplacing the tips. On two occasions, water was pumped from directly underneath the seepage meter. Here tubes attached to permanent tips placed at different depths within the sediment came through the stopper (Figure 2). Therefore, a porewater profile could be taken from sediment directly below the seepage meter simultaneous with discharge measurements. As SGD has been seen to be variable even on very small spatial scales, this was the only way to ensure collection of representative samples. This work was done in conjunction with Beck (2007); we believe this is the first attempt at this type of measurement. This is the recommended method for this type of experiment.

At the Mattituck site, a unique (Beck 2007) piezometer was used to collect samples at a much higher resolution. Briefly, a PVC pipe with porous openings every 4 cm was placed in the sediment this allowed for a quick collection of water at each depth simultaneously. In the case of Mattituck, or for those samples in which only salinity and nutrients were collected, 60 ml of water were collected after flushing the tubes with at least 30 ml of water. In this way we hope to reduce any possible mixing between depths (Beck 2007), although there is no possibility to state with certainty that the water is not mixing to a certain degree.

Samples in Jamaica Bay and Mattituck were measured immediately with a YSI version 556 conductivity, salinity and temperature meter with extra probes for measuring pH, ORP, and DO. Samples collected for nutrient (NO_{2+3}, NH_4, PO_4) analysis were acidified and then placed in ice in the field. In Venice, a YSI 30 SCT, salinity, conductivity and temperature meter was used. Within 24 hours these samples were

vacuum-filtered through 0.45 or 0.22 μm filters and frozen until analysis. Before analysis they were thawed to room temperature in darkness and the nutrients were measured on a Lachat Quikchem 8000 series auto-analyzer. Statistical analysis was done to determine the efficiency of the instrument. Samples collected for radium were filtered at a rate of less than 1 L min^{-1} through a column filled with manganese impregnated acrylic fiber. The fiber was taken to the lab, rinsed with Milli-Q water, and partially dried. Short-lived Ra (^{224}Ra) activity was measured by delayed coincidence counting (Moore and Arnold 1996).

3. Results

A. Mattituck, NY

On May 9 2006, three seepage meters were placed in the immediate vicinity of the piezometer. Though these meters were within a total area of 4 m^2, the discharge seemed to be controlled by distance from shore. There is a significant (20-50%) decrease in discharge recorded from the meter closest to shore as compared to the meter furthest from shore, although there was not much change between meters 2 and 3. The discharge had a very strong inverse correlation with tidal elevation in all three meters (Figure 3). A clear linear correlation was observed between the decrease in salinity in the meters and cumulative discharge (Figure 4). The salinity within the chambers did not decrease to zero, however, even though the cumulative SGD exceeded the volume in the head space (~12 L). The flow rate at this site varied in all three drums over a half tidal cycle, with small, negative flows recorded at high tide and flows up to 174 cm d^{-1}

recorded at low tide. Most of the discharge appeared to occur in a narrow band close to shore, consistent with the conventional wisdom, (Hubbert 1940) and, even over a short distance, SGD decreased 20-50% from the meter located closest to shore to the meter located less than 1 m further from shore. A thin shore-parallel band of the sea floor harbored high densities of the snail *Ilyanassa obsoleta*; these benthic organisms seemed to demarcate the seepage face, possibly indicating a preference to brackish salinities.

At the Mattituck site, 5 salinity profiles were taken on May 9; the last 3 are shown in Figure 5 as they were taken during periods of positive flow. The salinity in each profile decreased within the upper 60 cm of sediment from 25 at the sediment-water interface to ~1, and the salinity gradient changed with time, tide, and changing SGD. During periods of high SGD (110 cm d^{-1}), the salinity decreased rapidly between 5 and 29 cm depth and showed a monotonic, concave profile. At a lower rate of SGD (10 cm d^{-1}), the salinity at a depth of 12 cm was significantly higher then at high flow rates, and the profile was approximately linear at a flow rate of 10 cm d^{-1}. The concentrations of nutrients at Mattituck were below the detection limit of the instrument and so will not be discussed here.

B. Jamaica Bay

Seepage meters were emplaced alongside piezometer profiles at Canarsie Pier on August 23rd 2005, February 10th 2006, March 24th 2006, and May 4th 2006. Similar sampling was performed at Canarsie Pol on April 20th 2006. Among the 50 measurements made throughout these sites, the flow rates averaged less than 5 cm d^{-1}.

On August 23rd, at Canarsie Pier, there was a marked increase in discharge at maximum low tide (Figure 6a). The flow rate on this day averages 2.7 cm d^{-1} but was as high as 17.8 cm d^{-1} at low tide. The piezometer profile, which was taken before low tide, showed a uniform decrease in salinity from 25 to 16 at a depth of 200 cm (Figure 6b). No nutrient data were collected on August 23rd.

On February 10th two seepage meters were placed in about the same location as August 23rd. Flow rates were constant, averaging 1 cm d^{-1}, which could be disregarded as within the measurement error of the seepage meters (Figure 7a). One shallow (2 m) salinity profile was taken on February 10th. Though there is a great deal of variation in salinity within the upper 2 m, the overall trend suggests a decrease in salinity from 26 at the surface to 17 at depth (Figure 7b), which is similar to that seen on August 23rd. After an initial drop in salinity in the upper 40 cm, there was an increase from a salinity of 19 at 40 cm to 22 at a depth of about 100 cm.

On March 24th, the flow rate decreased from 5.3 to 2.1 cm d^{-1} as the tide rose 50 cm from the time when the first profile was taken (8:00) to the time when the third profile was collected (12:30) (Figure 8a). Average flow rates were about three times greater than February 10th. On March 24th, flow rates were collected as water was being sampled from piezometer tips emplaced directly below the seepage meter; the salinity profiles again disclosed a local, subsurface maximum with a decrease from 26 at the surface to a salinity between 16 and 20 at a depth of 10 cm (Figure 8b). Small differences between these three profiles were recorded, as the variability in salinity with depth seems to increase slightly as discharge decreases. Salinity within the chamber

remained stable (between 26-27) during the sampling period, likely because not enough water discharged into the chamber to dilute the head space.

Flow rates on May 4th at Canarsie Pier were variable ranging from 1 to 3.5 cm d^{-1} (Figure 9a). One deep (4 m) salinity profile was taken which showed an immediate decrease in salinity from 28 at the sediment surface to a salinity of 22 at 40 cm depth; this is followed by an increase to 27 at 100 cm. The upper 100 cm display almost the exact same profile as that seen on February 10th. Below 100 cm the salinity showed a fairly uniform decrease to 19 at 270 cm, and to a value of 8 at a depth of 315 cm (Figure 9b).

Seepage rates at Canarsie Pol were measured on April 20^{th,} 2006 to be between 3 and 6 cm d^{-1}, double the average SGD seen at Canarsie Pier at the same time of year (Figure 10a). The open-water salinity was about 28.8, but, over time, salinity in the seepage meters decreased to about 27 with cumulative discharge (Figure 10a). At Canarsie Pol, porewater salinity decreased almost linearly from 28.8 at a depth of 40 cm to 27.7 at 120 cm; the same salinity as was measured in the seepage meter at 11:30. This was followed by a more rapid decrease to 24 at a depth of 195 cm (Figure 10b). Salinity profiles once again suggest that dispersion is a dominant process in the upper 120 cm. In fact, the profile is approximately linear to a depth of 120 cm. Canarsie Pol, as a small island, should have a freshwater lens which mixes offshore with seawater allowing for brackish end-marker salinity. At 195 cm the salinity had dropped to 24.

At Canarsie Pier, on all dates, both PO_4 and total dissolved inorganic nitrogen (DIN; NO_3 + NO_2+NH_4) increased with depth (Figure 11). The concentration of both PO_4 and DIN at all 5 depths was consistent during three profile measurements on March

24, 2006, however, the concentration of these nutrients had decreased by about 20% at all depths from what was measured on February 10th. Below 280 cm, the concentration of both DIN and PO_4 decreased to depth. At Canarsie Pol, most depths had nutrient concentrations which were below the detection limit and so will not be discussed here.

C. The Venice Lagoon

Porewater profiles for salinity, ^{224}Ra, and nutrients were obtained coincident with seepage measurements on October 24th 2005 at Treporti and November 3rd and 10th 2005 at Punta Sabbioni (Figures 12-15). At Treporti, four seepage meters were placed along a shore-normal transect stretching 30 meters from the shore to the edge of the San Felice channel which is up to 15 m deep. Preliminary measurements made in July, 2005, gave SGD rates as high as 160 cm d^{-1}. During this sampling, six hours of measurements were made with a point taken every 30 minutes. At this site, individual measurements of rates of SGD ranged from 1.6 to 141 cm d^{-1}. Hour-to-hour variations in flow rates ranged from 15 to 90 cm d^{-1}, possibly caused by small pressure changes due to periodic wave action, and or other pulses of discharge. Because there was no systematic, temporal (e.g. tidal) variation, however, only averages are reported here. Average rates of SGD increased with distance from shore from the 1st to the 3rd meter and decreased slightly in the 4th meter (Figure 12). At Punta Sabbioni, the pore water salinity decreased from 34 to about 26 in the top 70 cm, then remained fairly constant (Figure 13a). The porewater salinity profile taken at Treporti (Figure 13c) shows a small decrease in salinity from the surface (33.9) to 30 cm (32.5) after which it increases linearly to 42 at 270 cm. The

salinity at 270 cm is much higher than either the average lagoon or open Adriatic Sea salinity. (These data will be further examined in Chapter V). Radium-224 activity at both sites increased with depth (Figures 13b and d).

At lower rates of SGD in the Venice Lagoon, a profile that suggests linear mixing was not seen as shown by the following data at Punta Sabbioni. Three seepage meters were used at the Punta Sabbioni site on November 3, and measurements were made from high to low tide over a total tidal excursion of about 90 cm. A slight, offshore increase in discharge was seen from the first to the third meter (Figure 12). However, average SGD at all three meters was low, ranging from 0.8 to 4.0 cm d^{-1}, 0.0 to 8.8 cm d^{-1} and, 2.3 to 14.7 cm d^{-1} in seepage meters SABB1, SABB2, and SABB3 respectively. On November 10th, SABB3, which had been left in place since November 3, showed flow rates between 3 and 8 cm d^{-1}. No consistent pattern in discharge with tidal variation was observed in any of the meters. Two salinity profiles were collected at Punta Sabbioni; the first was collected on November 3rd, 2005 onshore, on the beach slope. On the beach, the saturated zone was first encountered at a depth of 180 cm and had a salinity of 13.1 increasing steadily to 21.5 at a depth of 450 cm. The second profile was collected alongside SABB3 on November 10th, 2005. Here, the salinity immediately decreased from 30.6 at the surface to 25.4 at 70 cm. It then fluctuated between 25.5 and 28 to a depth of 280 cm (Figure 13a). Meanwhile ^{224}Ra increased quickly from about 10 to 580 dpm $100L^{-1}$ in the upper 60 cm, then more gradually below 60 cm to 750 dpm $100L^{-1}$ at 280 cm (Figure 13b).

DIN profiles at Treporti display a linear increase from 15 cm to a depth of 270 cm. At 15 and 30 cm the concentration of DIN is 35 μM this increases to 498 μM at 270

cm (Figure 14). The DIN correlated linearly with salinity (Figure 15). DIN and PO_4 profiles at Punta Sabbioni show no clear pattern and fluctuate with depth. However, while PO_4 shows a mid-depth maximum at Treporti, there is a consistent decrease with depth at Punta Sabbioni.

4. Discussion

A. Interpretation of the salinity profiles

Profiles at each of the sites help us begin to understand the magnitude and possible mechanisms which control dispersion. The patterns seen at Mattituck were instructive for several reasons. First, the pore water salinity within 5 cm of the sediment-water interface was invariant even though the advective flow rate (SGD) changed by an order of magnitude. In the upper few centimeters of sediment, therefore, the effective dispersion must be large enough to dominate the transport over the upward advection. Between 5 and 22 cm depth, the pore-water salinity profile did vary with the tidal modulation of SGD, suggesting that the advection flux dominates the profile when the tide was low and SGD was high. Because we assume that the advective flux does not change with depth, this implies that the dispersion process is less effective here than it is in the uppermost 5 cm of the sediment column as the salinity within the sediment decreases more rapidly, in other words, salt is not mixed down as efficiently below 5 cm. Third, the pore water salinity is again invariant at a depth of 25 cm. Assuming that the magnitude of the dispersive flux continues to decrease with depth, the maintenance of constant pore-water salinity at depth suggests that the salinity at 25 cm is the “end-

marker" salinity of the advective pore water. Fourth, even though the salinity just below the sediment-water interface remains constant at 25, the salinity within the chambers reached levels of between 14 and 19 (Figure 4), suggesting that the net flow of water entering the chambers originated at a depth of 10 or 15 cm and, somehow, resisted salinity increases (to 25) as it moved up in the sediment column to cross the sea floor. This implies that the lateral distribution of upward flow must not be uniform but rather confined to channels, columns, or preferred, vertical conduits that allow pore water from a depth of 10 or 15 cm to reach the sea floor without adjusting to the average salinity profile observed in the piezometer samples. Conceivably, salt-fingering or bioirrigation could produce this effect (Aller 2001: Figure 11.9). It is possible, however, that the seepage meters themselves served to disrupt the dispersion process in the sediment immediately below the meter, allowing for end-member porewater to reach the surface without considerable mixing.

On August 23rd in Jamaica Bay, the profiles suggest that there was very little, if any, upward advection at the time of sampling. It is likely that the dispersion process into the sediment dominated over advection, mixing salt down to at least the depth taken in this profile. The profile, however, still showed the concave form that could be generated by downward dispersion of salt superimposed on upward advection. Meanwhile on February 10th, a mid-depth maximum may be caused by intersection of preferential flow paths of higher salinity water, or may be due to stratification of sedimentary layers with different permeability in the sediment. Bioirrigation or burrow geometry is also a possible cause of this maximum, but the depth to which this layering is seen is too great for many organisms. The profile of salinity in the absence of vertical

advection and the occurrence of a subsurface maximum in salinity highlights complications in the interpretation of such data. In addition, the local maximum may point to the importance of either lateral transport or small-scale lateral variations in this vertical transport.

Each of the profiles collected on March 24th at Canarsie Pier in Jamaica Bay were also instructive for a couple of reasons. Although there was some temporal variation among the profiles, there was little change in salinity with depth below 80 cm in the upper 200 cm of sediment. This suggests to me that the effective dispersion process dominates over the process of upward advection. However, at higher rates of SGD, the variability of salinity decreased, suggesting that the advection of brackish end-marker water may help to stabilize the profile. Finally, on May 4th during the deep profile at Canarsie Pier, the variations of salinity with depth may show parts of a relic distribution from earlier situations, or that heterogeneous sediment layering and/or lateral seepage may be exerting an influence on the profile. In other words, the instantaneous discharge is unlikely to control the entire profile in this location as only 0.25 cm^3 of water are moving per hour at a flow rate of 3 cm d^{-1}.

In Canarsie Pol, salinity in the seepage meter had decreased with time as compared to the surface salinity. There must have been a mechanism, which allowed this lower salinity water to reach the surface from depth without the intervening mixing which was seen in the salinity profile . As was the case at Mattituck, the lateral distribution of upward flow at Canarsie Pol must not be uniform but rather confined to preferred, vertical conduits that allow pore water from depth to reach the sea floor without adjusting to the average salinity profile.

Evidence from the salinity, radium, and nutrient profiles in the Venice Lagoon suggest that the effective dispersion coefficient is actually controlled by the rate of advection, because linear mixing is seen where the SGD was high, but not where it was low. The linear profile of salinity from the Treporti site, under an average SGD of 50 cm d^{-1}, suggests simple mixing between the surface and the deep, high salinity/high radium end-member (Figures 13c and d). Under such high flow rates, I would expect to see a convex profile as was, in fact, seen at Punta Sabbioni. Instead, the linear curve suggests to me that, whatever the dispersion mechanism is, the dispersive flux is large enough to dominate over advection.

At Punta Sabbioni, I interpret the profiles of salinity and radium to show a deep, brackish-salinity/high-radium end member below a depth of 100 cm. Above this depth a convex profile shows the combined effects of advection and dispersion of comparable magnitude with the end-member concentrations being advected towards the surface. The rate of SGD is low, so the dispersion mechanism could not be as effective here as it was at Treporti where it was sufficiently high to control the profile even in the presence of a much greater advective flux. I conclude, therefore, that the dispersion seems to be directly related to the rate of SGD, increasing with larger seepage rates. This would be the behavior of classical, mechanical dispersion in an aquifer (Freeze and Cherry 1979). We will examine the salinity distribution in the sediment from all of these sites quantitatively in the following three sections

B. Magnitude of dispersion determined by the mass balance of salt

If one assumes that the porewater salinity profile is in steady state and that it can be represented by a linear gradient with depth in the sediment, the profile can be used with the measured SGD to estimate the dispersion coefficient. The mass of salt in a volume of sediment with porewater salinity S_o and porosity Φ is $\Phi S_o/1000$**.** For example, a porewater salinity of 27 corresponds to a mass concentration of 0.027 grams of salt per cubic centimeter of water. In sediment of porosity 0.5 with porewater salinity at the sediment water interface of 27, there would be 0.0135 grams of salt per cubic centimeter of sediment. Assuming that the salinity gradient is linear and that the salinity reaches zero at a depth z_1, then the gradient is $\Phi S_o/1000z_1$. Continuing the example above, if the pore water salinity gradient is such that the salinity is zero at a depth, z_1, of 540 centimeters, the gradient is -0.0135/540 grams of salt per centimeter cubed of sediment per centimeter depth, or $-2.5*10^{-5}$ g cm^{-4}. Now in the presence of an upward advective (volume) discharge of porewater, or SGD, the advective velocity (ω)of the porewater is SGD/Φ and the rate at which salt is flushed from the sediment is:

$$\Phi S_o (\text{SGD}/\Phi)/1000 \text{ or, } S_o\text{SGD}/1000. \quad (2)$$

For my example, if the SGD is 4 cm d^{-1} (1.5 cubic centimeters of water per square centimeter per day) then, assuming a porosity of 0.5, three centimeters of the sediment would be flushed every day carrying out 8*0.0135 or 0.108 grams of salt per square centimeter per day. To maintain steady-state, this same amount of salt must be brought down into the sediment by dispersion; so the dispersion coefficient must equal the advective daily loss of salt divided by the mass concentration gradient of salt per unit volume of sediment, or,

$$1000S_o\mathrm{SGD}/(1000S_o\Phi/z_1), \text{ or } \mathrm{SGD}z_1/\Phi \text{ or } \omega z_1 \quad (3)$$

In the case of my example, this is 0.43 m^2 d^{-1}. If the deep, end-member salinity is not zero, but, instead, some value S_2 reached at a depth z_2, then the dispersion coefficient is

$$\mathrm{SGD}z_2S_o/(S_o-S_2) \quad (4)$$

where z is zero at the sediment water interface.

For the data taken at Canarsie Pier with an average SGD of 1.5 cm d^{-1}(Figure 16), the dispersion coefficient was calculated to have been 0.16 and 0.17 m^2 d^{-1}. Applying the same method to the profile of salinity measured at Canarsie Pol, assuming a zero salinity groundwater end-member and using the average SGD flow of 3.5 cm d^{-1}, yields a dispersion coefficient of 0.84 m^2 d^{-1}. Alternatively, if all but the last two points at 120 and 195 cm in the slope are disregarded, the dispersion coefficient decreases to 0.45 m^2 d^{-1}, but this may be an overestimate because it seems to me that the "end-member salinity" may be too high due to the likely occurrence of a freshwater lens below the island. In Venice, if I assume that the end-member salinity is 26 at Punta Sabbioni and 42 at Treporti, then both sites have a profile in which the salinity changes by 8 over a depth of 285 cm. Because of the difference in SGD, the dispersion coefficients were calculated to be 0.23 m^2 d^{-1} and 2.8 m^2 d^{-1} in Punta Sabbioni and Treporti respectively. Previous estimates of dispersion coefficients range from 0.0001 to 0.2 m^2 d^{-1} (Table 1). Apart from the dispersion coefficient found at Treporti, coefficients were, in general within the range, or slightly higher than those measured elsewhere.

Unlike Jamaica Bay and Venice, however, Mattituck had large temporal variation in SGD, ranging from -10 to 174 cm d^{-1}. Though the end points of the profile are invariant (Figure 5), the shape of the profile seemed to be affected by the flow rates.

Using the expression $D = SGDz_0/\Phi$, the dispersion coefficient at Mattituck ranged up to 0.8 $m^2\ d^{-1}$ depending on the value of SGD.

C. Magnitude of dispersion: steady-state, one-dimensional analytical solutions:

1. A "slab" solution (Martin et al. 2007).

The steady-state, one-dimensional equation governing the advection-dispersion of salt (S) is:

$$0 = \omega \partial S/\partial z - D\partial^2 S/\partial z^2 \quad (5)$$

Where ω, as before, is SGD/Φ. To describe measured, porewater salinity profiles, Martin et al. (2007) applied this relationship to mixing in a slab of sediment, with an upper and lower limit in which the salinity of the porewater changes. They assumed that mechanical, hydraulic dispersion was operative within the slab. In the sediment above the slab, bioturbation was actively mixing the sediment. The salinity on the lower boundary was taken to be the asymptotic salinity deep in the sediment column. The solution of Martin et al. (2007) to equation 5 is:

$$S(z) = \frac{1}{1-\exp\left(\frac{\omega}{D}L\right)}\left\{S_L\left[1-\exp\left(\frac{\omega}{D}z\right)\right] + S_u\left[\exp\left(\frac{\omega}{D}\right)Z - \exp\left(\frac{\omega}{D}L\right)\right]\right\} \quad (6)$$

where S is salinity, ω is the advective velocity of porewater, D is the dispersion coefficient, L is the lower limit of the salinity profile, S_L is the salinity at the lower limit, z is the depth of sample, and S_u is the salinity at the upper limit of the salinity profile. Using a diffusion coefficient 0.9 x 10^{-6} $m^2\ d^{-1}$ (which is molecular diffusion from modified for sediment tortuosity using a formulation in the literature and a porosity of

0.45) of they calculated SGD rates which were more than an order of magnitude lower than SGD measured directly using seepage. Alternatively, to reproduce the measured SGD rates, a much larger dispersion coefficient would be needed. This conclusion is consistent with both earlier investigators at other sites and with my results.

I applied equation 6 to my data determine the dispersion coefficient from SGD rates measured simultaneously with porewater salinity profiles. Figures 17a-c shows the results of this relationship at Jamaica Bay, Mattituck, and Venice respectively. In Jamaica Bay, I was able to largely reproduce the curves at Canarsie Pier and Canarsie Pol using dispersion coefficients of 0.3 and 0.5 $m^2\ d^{-1}$ respectively (Figure 17a). In Mattituck, the high-flow profile could be well represented using a dispersion coefficient of 0.84 $m^2\ d^{-1}$ (Figure 17b). The low- flow profile was more difficult to replicate due to negative flow rates, or salt water intrusion depressed the profile below a linear mixing line, still I was able to calculate a diffusion coefficient of 0.015 $m^2\ d^{-1}$ (Figure 17b). At Treporti in the Venice Lagoon, a dispersion coefficient of 3.0 $m^2\ d^{-1}$ was needed to match the profile of salinity in the face of a high SGD rate, which is similar to the coefficient calculated using the salt balance (Figure 17c). At Punta Sabbioni, on the other hand, the dispersion coefficient was much lower (0.04 $m^2\ d^{-1}$) using this method than when using the mass balance. With this method, I was able to reproduce the curve which may explain the discrepancy as compared to assuming a linear mixing profile (Figure 17c). I was also able to calculate a dispersion coefficient of 0.15 $m^2\ d^{-1}$ (Figure 17d) for Brazil using data from a salinity profile collected near seepage meter SD6 (Oberdorfer et al. 2007). All of the calculated diffusion coefficients are much higher

than those calculated by Martin et al. (2007) but correspond well with the coefficients I calculated using the mass balance method.

2. Exploration of the relationship between BGC and SGD as explained by dispersion coefficients; a steady-state, one-dimensional, semi-infinite analytical solution.

Although a slab-solution as suggested by Martin et al. (2007) may be more appropriate in some situations (e.g. Mattituck) or, perhaps, in layered sediment, there is no *a priori* reason to prefer it and I choose to further this discussion relating BGC to SGD through dispersion with a slightly different expression. In order to explain the physical significance of the empirical parameters used to relate BGC to SGD (Chapter II, equation 1), and to simplify the mathematics, I considered a steady-state, one-dimensional, semi-infinite analytical solution to the advection-dispersion equation, I will demonstrate later that in these applications the slab-solution is practically indistinguishable from that for a semi-infinite sediment column. The distribution of the concentration of salt $S(z)$, with depth in the sediment, assuming a constant salinity, S_o, at the surface, ($z = 0$) is then governed by:

$$F = S\omega - D\frac{\partial s}{\partial z} \tag{7}$$

or $$\frac{D}{\omega}\frac{\partial s}{\partial z} = S - \frac{F}{\omega} \tag{8}$$

Where F is a constant flux of salt, ω is the advective velocity of porewater, and D is the dispersion coefficient. Note that, in the sediment column, the convention is to have z

increasing downward from the surface, so a value of ω greater than zero is in the downward direction. Because the convention for SGD is to have SGD greater than zero (positive), in the upward direction ω = -SGD/Φ, where Φ is porosity. The boundary conditions for the advection-diffusion equation in a semi-infinite medium are: $S=S_o$ at $z=0$ and S remains finite as $z\rightarrow\infty$. If I change the variables such that:

$$\vartheta = (S - \frac{F}{\omega}) \tag{9}$$

then:

$$\frac{\partial \vartheta}{\partial z} = \frac{\partial (S - \frac{F}{\omega})}{\partial z} = \frac{\partial S}{\partial z}, \text{ since F/ω is a constant} \tag{10}$$

So, in terms of the new variable:

$$\frac{D}{\omega}\frac{\partial \vartheta}{\partial z} = \vartheta \tag{11}$$

With the boundary conditions: $\vartheta = (S_o - F/\omega)$ at $z=0$ and ϑ remains finite as $z\rightarrow\infty$. The solution to this equation is:

$$\vartheta = \left(S_o - \frac{F}{\omega}\right)\exp\left(\frac{\omega}{D}z\right) \tag{12}$$

Substituting relationship (11) into (12)

$$\frac{D}{\omega}\frac{\partial \vartheta}{\partial z} = \frac{D}{\omega}\left(S_o - \frac{F}{\omega}\right)\left(\frac{\omega}{D}\right)\exp\left(\frac{\omega}{D}z\right) \tag{13}$$

$\vartheta = (S_o - F/\omega)$ at $z=0$ as required and, if SGD is upwards (in the negative z direction), ω is a value less than zero so, ϑ remains finite as $z\rightarrow\infty$, as required. F is the constant flux of

salt, not water, so if the end-member salinity of the porewater advecting into the system is zero, then F can be taken as zero. Figure 18 shows that in Jamaica Bay this equation (12) and (5) essentially yield the same distribution; their differences are not great enough to be resolved in the data. Integrating over the upper one-meter of sediment and converting salinity to conductivity by the empirical equation (Manheim et al. 2004):

$$S = 7.042 * \left(\frac{10}{\sigma_w}\right)_{-1.0233} \tag{14}$$

we have: $$\sigma_{b\ (avg.)} = 1/z_o \int_o^{zo} \Phi^m \sigma_w e^{-0.977(\Phi)(\mathrm{SGD})/D\ z}\, dz \tag{15}$$

Where σ_b is the bulk ground conductivity as measured by the conductivity logger, σ_w is the interstitial water conductivity, and the exponent (m) is a characteristic of the sediment matrix and refer to the effect tortuosity will have on the bulk ground conductivity of the sediment. If the upward advection of groundwater is of fresh groundwater (zero salinity) I would expect F=0 and the relationship between BGC and SGD reduces to:

$$=\Phi^{-m}\sigma_w D/z_o(0.977)\mathrm{SGD}\ [1-e^{-(0.977(\Phi)SGD/D)\ zo}] \tag{16.}$$

This simpler relationship, therefore allows us to extrapolate SGD values from BGC, which would be advantageous because it requires less labor to collect BGC data than to take many accurate SGD measurements, and it is more feasible to cover a large area as discussed in Chapter II. If we insert different values of D (dispersion coefficient), assuming a average depth (z_0) of 1 m, a porosity (Φ) of 0.5 and an exponent

(*m*) of 1.2, we are able to largely reproduce the correlation between SGD and BGC at the various sites (Figure 19), in a way similar to figure 12 in Chapter II. The correlation at Shelter Island, Cockburn Sound, Flamengo Bay and Mauritius correspond to dispersion coefficients of 0.05, 0.09, 0.21, and 0.38 $m^2\ d^{-1}$ respectively (Table 2.)

D. Characteristics of dispersion

In each of the salinity profiles described in this chapter, salt penetrates into the sediment regardless of the flow. Molecular diffusion of salt through the pore water is entirely insufficient to move salt downward against even a small upward advection, so other, more efficient mixing processes must be operative. At Mattituck, salt penetration occurred as deep as 25 cm even though the upward advection was as high as 174 cm d^{-1}. The data suggest that the depth, to which salt can penetrate into the sediment, is dependent on flow, as is demonstrated in equation 16 which has SGD in the denominator. For example, in all of the Jamaica Bay sites, saline water was observed to depths of at least 100 cm, and often much deeper (i.e. 350 cm in Canarsie Pier). However, in Mattituck, which has a much higher average flow rate, the salinity is close to zero at 25 cm. At each of these locations, non-zero salinity end members at depth in the sediment most likely indicate the influence of large-scale recirculation of sea water (10's to 100's of meters). While strong salinity gradients in the upper meter of sediment would be indicative of downward dispersion of salt from the sediment-water interface on a small scale (1 m), I can envision the presence of a deep, constant salinity end member

as indicative of the recirculation of sea water on a scale much larger than the size of the devices I have been using to make these measurements.

Several candidates have been implicated as effective dispersion mechanisms for downward mixing from the sediment-water interface. These all tend to occur over small scales and include mechanical hydraulic dispersion, salt-fingering, wave or tidal dispersion, and bioirrigation. Any or all of the proposed mechanisms could be active at any particular site. A comparison of various estimates of the dispersion coefficients calculated here (Table 2) showed that mechanical hydraulic dispersion is insufficient to explain the porewater salinity distributions in all cases. This same conclusion was reached by Martin et al. (2007) in the Indian River Lagoon. Theoretically, tidal mixing would seem to be of the appropriate magnitude to explain the salinity distributions at Cockburn Sound, Shelter Island, and in Mattituck under low SGD, but the other situations required even more effective mechanisms of dispersion. My results showed that characteristics of the process would include dispersion that increases with increasing flow rate. Mechanical hydrodynamical dispersion has this characteristic, but, with the information I have available, appears to be of insufficient magnitude. The dispersion might also vary in intensity; being greatest in the top few centimeters of the sediment column and lowest (zero?) at a depth of about 25 cm, for example, at Mattituck. At Treporti, in the Venice lagoon, gravitational convection or salt fingering could not have been the dispersion mechanism because the porewater salinity at depth was greater that that at the sediment-water interface giving a stable, porewater density profile. The rapid dispersion implied by the linear salinity gradient could have been due to bioirrigation or, less likely, by mechanical hydraulic dispersion. In this case, I would favor the latter

because of the high SGD, which as shown in equation 4 must increase dispersion to maintain the profile. In addition, the profile goes to a depth of 2.8 m, which is much larger than normally seen in benthic sediments (Aller 2001).

In Chapter II, an empirical relationship between bulk ground conductivity (BGC) and SGD measured from seepage meters was observed at four sites Cockburn Sound, Shelter Island, Ubatuba, Brazil, and Mauritius. Tidally-averaged SGD vs. BGC (Figure 19) shows variations in the curves among the 4 sites. The difference in curves between sites is most likely due to variation in the dispersion of salt downward and the formation factor of the sediments. In this interpretation, Shelter Island has the lowest vertical dispersion. Dispersion at Ubatuba is higher than Shelter Island, while dispersion at Mauritius is highest. Cockburn Sound would require a vertical dispersion slightly higher than at Shelter Island but less than what is found at Ubatuba or Mauritius. For the use of BGC as a proxy for SGD, values of the vertical dispersion of salt is critical, as it controls the depth to which salt can penetrate downward into the sediment against an upward advection of (fresh) groundwater.

E. A comment on the ecological implications of dispersion

Nutrient profiles collected at Canarsie Pier showed a persistent, nonlinear increase in dissolved inorganic nitrogen and phosphate with depth (Figures 11a, b). On both February 10 and March 24, 2006 the profiles of both displayed an exponential increase with depth. Nutrient concentrations were slightly higher on February 10 then March 24, although SGD was 50% lower on February 10. This may have been caused

by a change in the nutrient concentration of the source water, but it could also be the result of biologically-mediated processes. Although there is no clear process evident in our results, Ullman et al. (2003) proposed that at Cape Henlopen, Delaware (a sandy beachface) nutrient concentrations in the porewater must be regulated by a combination of dispersive mixing between the saline and fresh-water end-members as well as diagenetic input or removal. Although the investigators discount the possibility of advection, nutrient profiles are likely to be affected by this change and, therefore, care should be taken to make measurements of nutrient concentrations in the porewater during periods of both high and low flow.

The DIN profile at Treporti in the Venice Lagoon (Figure 14) is harder to explain. The profile is essentially the same as the salinity profile (Figure 15) and suggests linear mixing between the surface and a depth of almost 3 m. This occurs in the face of an average upward advection of 50 cm d^{-1}. At flow rates of this magnitude there may not be sufficient time for biological processes to greatly affect the profile as the water and associated nutrients are discharged quickly. Instead hydrodynamic dispersion which is enhanced by advection seems to be the dominant process, allowing low nutrient surface water to be mixed down into the sediment.

Nutrient concentrations were below the detection limit in the Mattituck site. However salinity measurements suggest that the magnitude of SGD affects the salinity profiles. If the same process occurs for nutrients this must be accounted for when examining the role of SGD on the discharge of nutrients into the coastal zone.

Higher rates of advection serve to decrease the concentration of nutrients in the sediment due to dispersive mixing of lower nutrient surface water down into the

sediment. On the other hand, SGD may transport porewater with high nutrient concentrations towards the surface water before removal processes can occur. If preferred, vertical conduits exist in the sediment, as interpreted from my salinity results at Mattituck and Jamaica Bay, nutrient concentrations from the base of such channels may be rapidly brought to the sediment-water interface, bypassing intervening, microbiological processing. Because of the non-conservative nature of nutrients and the lack of data at the Mattituck site it is, unfortunately, hard to quantify the effect SGD, both constant and dynamic, has on the profiles of nutrients in the sediment. This process is, thus, not yet fully understood and further investigation is required to constrain the situation.

V Conclusions

In coastal environments, investigators should expect SGD to show large spatial and temporal variability which will alter chemical gradients in the porewater and vertical dispersion coefficients might exceed 3 $m^2 d^{-1}$. Evidence from salinity profiles made at several locations suggests that the shape of porewater profiles is dependent upon the rate SGD as well as the mechanism of vertical dispersion. Measurements of rates of SGD, as well as porewater salinity profiles and their changes, have utility in studying the still unresolved mechanisms of downward dispersion. Increasing advection increases the efficiency of mixing through hydrodynamical dispersion between surficial waters and the deep end-member. In other cases, the dispersive mechanism may involve small-scale preferred pathways for vertical transport, such as would be the case for bioirrigation and

gravitational convection or salt-fingering which are simulated dispersion but may really be considered as a source of advection.

Profiles of conductivity (or salinity) in the sediment could be used to extrapolate seepage meter measurements to a larger area. With knowledge of how dispersion processes work, which could be obtained through laboratory testing, one may be able to define the correlation between SGD and pore water profiles to a greater extent, thus increasing the utility of comparing BGC and SGD data.

Investigations of this sort are hampered by the resolution in both time and space of the various methods as well as by the time lags needed for profiles to reach equilibrium with observed conditions. In addition, depending on the mechanism of dispersion, it is possible that the presence of the seepage meters themselves may alter the dispersion and hence, influence the porewater profiles at the point of measurements. These issues must be topics of future research.

References:

Aller R.C. 2001. Transport and reactions in the bioirrigated zone. In: The Benthic Boundary Layer. New York. Oxford University Press. 404 pages.

Ataie-Ashtiani, B., Volker, R. E., and Lockington, D. A. 1999. Tidal effects on sea water intrusion in unconfined aquifers. Journal of Hydrology. 216: 17–31.

Beck A.J. 2007. Submarine groundwater discharge (SGD) and dissolved trace metal cycling in the subterranean estuary and coastal ocean. PhD Thesis. Stony Brook University. 308 pages.

Beck A.J. Rapaglia J.P. Cochran J.K. and Bokuniewicz H.B. 2007. Radium mass-balance in Jamaica Bay, NY: Evidence for a substantial flux of submarine groundwater. Marine Chemistry. In Press.

Belluci, L. G., Frignani, M., Paolucci, D. and Ravanelli, M. 2002. Distribution of Heavy Metals in Sediments of the Venice Lagoon: the role of the Industrial area. The Science of the Total Environment. 295: 35-49.

Bokuniewicz H. 1980. Groundwater Seepage into Great South Bay, New-York. Estuarine and Coastal Marine Science. 10 (4): 437-444.

Bokuniewicz H., Pollock M., Blum J., and Wilson R. 2004. Submarine groundwater discharge and salt penetration across the sea floor. Groundwater. 42: 983-989.

Bone, S.E., Gonneea, M.E., and Charette, M.A. 2006. Geochemical cycling of arsenic in a coastal aquifer. Environmental Science and Technology. 40: 3273-3278.

Brusseau, M., L., 1993. The influence of solute size, pore water velocity, and intraparticle porosity on solute dispersion and transport in soil. Water Resources Research. 29(4) 1071-1080.

Busciolano, R., 2002. Water Table and the Potentiometric-Surface Altitudes of the Upper Glacial, Magothy and Lloyd Aquifers on Long Island, New York, in March-April 2000, with a Summary of Hydrogeologic Conditions. Water-Resources Investigations Report 01-4165, United States Geological Survey.

Cable, J.E., Martin J.B., Jaeger J. 2006. Exonerating Bernoulli? On evaluating the physical and biological processes affecting marine seepage meters. Limnology and Oceanography Methods. 4: 172-183.

Capone D.G. and Bautista M.F. 1985. A groundwater source of nitrate in nearshore marine sediments. Nature. 313: 214-216.

Capone D.G., and Slater J.M. 1990. Interannual patterns of water table height and groundwater derived nitrate in nearshore sediments. Biogeochemistry. 10: 277-288.

Carbognin, L., Gatto, P., and Mozzi, G., 1977. Guidebook to Studies of Land Subsidence Due to Ground-Water Withdrawal. IAHS-AISH 121: 65-81

Charette, M.A., and Allen M.C. 2006. Precision groundwater sampling in coastal aquifers using a direct push shielded screen well-point system. Groundwater Monitoring and Remediation. 26 (2): 87-93.

Christensen, T.H., Kjeldsen, P., Bkerg, P.L., Jensen, D.L., Christensen, J.B., Baun, A., Albrechtsen, H.J., and Herom, G. 2001. Biogeochemistry of landfill leachate plumes. Applied Geochemistry. 16: 659-718.

Cooper, H.H. 1964. A hypothesis concerning the dynamic balance of freshwater and saltwater in a coastal aquifer in H.H. Cooper, F.A. Kohout, H.R. Henry, and R.E.

Glover, Sea water in coastal aquifers, U.S. Geological Survey Water Supply Paper 1613-C;C1-C12.

Corbett, D.R., Dillon, K., and Burnett, W. 2000. Tracing groundwater flow on a barrier island in the northeast Gulf of Mexico. Estuarine, Coastal, and Shelf Science. 51: 227-242.

Dale, R.K. and Miller, D.C. 2007. Spatial and temporal patterns of salinity and temperature at an intertidal groundwater seep. Estuarine, Coastal, and Shelf Science. 72 (1-2): 283-298.

D'Elia, C.F., Webb, K.L., and Porter, J.W. 1981. Nitrate-rich groundwater inputs to Discovery Bay, Jamaica – A significant source of N to local coral reefs. Bulletin of Marine Science. 31 (4): 903-910.

Englebright, S. 1975. Jamaica Bay: A case study of geo-environmental stress. NYS Geological Association Guidebook, 47th Annual Meeting. 279-291.

Freeze, R.A., and Cherry, J.A. 1979. *Groundwater*. Prentice Hall Inc., Englewood Cliffs, NJ, 604 p.

Gelhar L. 1993. *Stochastic Subsurface Hydrology*. Prentice Hall Inc., Englewood Cliffs, NJ. 390 p.

Gobler, C.J., and Sañudo-Wilhelmy, S.A. 2001. Temporal variability of groundwater seepage and Brown Tide Blooms in a Long Island Embayment. Marine Ecology Progress Series. 217: 299-309.

Gobler, C.J., and Boniello, G.E. 2003. Impacts of anthropogenically influenced groundwater seepage on water chemistry and phytoplankton dynamics within a coastal marine system. Marine Ecology Progress-Series. 255: 101-114.

Gordon, A., Huber, B., and Houghton, R., 2007. Temperature, Salinity and Currents in Jamaica Bay. Jamaica Bay Ecosystem Research and Restoration Team (JABERRT) Final Report, Vol. 1: p51-53.

Hartig, E.K., Gorntz, V., Kolker, A., Mushacke, F., and Fallon, D. 2002. Anthropogenic and climate change impacts on salt marshes of Jamaica Bay, New York City. Wetlands. 22 (1): 71-89.

Hubbert, M.K. 1940. The theory of ground water motion. Journal of Geology. 48 (8): 785-944.

Hunkins, K. 1981. Salt dispersion in the Hudson Estuary. Journal of Physical Oceanography. 11: 729-738.

Johannes, R.E. 1980. The ecological significance of the submarine discharge of groundwater. Marine Ecolological Progress Series. 3: 365-373

Kaplan, W., Valiela, I., and Teal, J.M. 1979. Denitrification in a salt marsh ecosystem. Limnology and Oceanography. 24 (4): 726-734.

Kohout, F.A. 1966. A neglected phenomenon of coastal hydrology. Hydrology. 26: 391-413.

Lee, D.R. 1977. A device for measuring seepage flux in lakes and estuaries. Limnology and Oceanography. 22 (1): 140-147.

Lee, D.R., and Cherry, J.A., 1978. A field exercise on groundwater flow using seepage meters and minipiezometers, Journal of Geological Education. 27: 6-10.

Li, L., Barry, D.A., Stagnitti, F., and Parlange, J.Y. 1999. Submarine groundwater discharge and associated chemical input to a coastal sea. Water Resources Research. 35: 3253-3259.

Libelo, E.L., and MacIntyre, W.G. 1994. Effects of surfacewater movement on seepage-meter measurements of flow through the sediment-water interface. Applied Hydrogeology. 4: 49-54.

Manheim, F.T. Krantz, D.E. and Bratton, J.F. 2004b. Studying ground water under Delmarva coastal bays using electrical resistivity. Ground Water. 42 (7): 1052-1068.

Manning, D.A.C., and Hutcheon, I.E. 2003. Distribution and mineralogical controls on ammonium in deep groundwaters. Applied Geochemistry. 19: 1495-1503.

Martin, J.B., Cable, J.E., Jaeger, J., Hartl, K., and Smith C.G. 2006. Thermal and chemical evidence for rapid water exchange across the sediment water interface by bioirrigation in the Indian River Lagoon, Florida. Limnology and Oceanography. 51 (3): 1332-1341.

Martin, J.B., Cable, J.E., Smith C., Roy M., and Cherrier J. 2007. Magnitudes of submarine groundwater discharge from marine and terrestrial sources: Indian River Lagoon, Florida. Water Resources Research. 43: W05440, doi: 10.1029/2006WR005266.

Matson, E.A. 1993. Nutrient flux through soils and aquifers to the coastal zone of Guam (Mariana Islands). Limnology and Oceanography. 38 (2): 361-371.

Matsukawa, Y., and Matsumura, S. 1985. Peculiar dispersion of salt by wind-driven fluctuations in the stratified water near the coast. Journal of Oceanography. 41 (3): 176-180.

Michael, H.A., Mulligan, A.E., and Harvey, C.F. 2005. Seasonal Oscillations in water exchange between aquifers and the coastal ocean. Nature. 436: 1145-1148.

Moore, W.S. 1996. Large groundwater inputs to coastal waters revealed by Ra-226 enrichments. Nature. 380: 612-614.

Moore, W.S. 1999. The subterranean estuary: a reaction zone of ground water and sea water. Marine Chemistry. 65 (1-2): 111-125.

Moore, W.S., and Arnold, R. 1996. Measurement of Ra-223 and Ra-224 in coastal waters using a delayed coincidence counter. Journal of Geophysical Research-Oceans. 101: 1321-1329.

Oberdorfer, J.A., Valentino, M.A., and Smith, S.B. 1990. Groundwater contribution to the nutrient budget of Tomales Bay, California. Biogeochemistry. 10: 199-216.

Oberdorfer, J.A., Charette, M.A., Allen, M., Martin, J.B., and Cable, J.E. 2007. Hydrogeology and geochemistry of near-shore submarine groundwater discharge at Flamengo Bay, Ubatuba, Brazil. Estuarine, Coastal, and Shelf Science. submitted.

Paulsen, R.J., O'Rourke, D., Smith, C.F., and Wong, T.F. 2004. Tidal load and salt water influences on submarine groundwater discharge. Ground Water. 42 (7): 990-999.

Rapaglia, J. 2005. Submarine groundwater discharge into the Venice lagoon, Italy. Estuaries. 28 (5): 705-713.

Roychoudhury, A.N. 2001. Dispersion in unconsolidated aquifer sediments. Estuarine, Coastal, and Shelf Science. 53: 745-757.

Rubenstone, J. 2007. Stable Isotope Evidence for Water Mass Mixing in Jamaica Bay. Jamaica Bay Ecosystem Research and Restoration Team (JABERRT) Final Report, Vol. 1: p54-59.

Schubert, C.E., Bova, R.E., and Misut, P.E. 2004. Hydrogeologic framework of Long Island's North Fork, Suffolk County, NY. Abstract to the 11th annual meeting of Long Island Geologists. Stony Brook, NY. 17 April 2004.

Seplow, M.S. 1991. The influences of groundwater seepage on the pore water salinity of Great South Bay. M.S. Thesis State University of New York at Stony Brook.

Shaw, R.D. and Prepas, E.E. 1989. Anomalous, short-term influx of water into seepage meter. Limnology and Oceanography. 34 (7): 343-351.

Slomp, C.P., Van Cappellen, P. 2004. Nutrient inputs to the coastal ocean through submarine groundwater discharge: controls and potential impact. Journal of Hydrology. 295 (1-4): 64-86

Stieglitz T., Rapaglia J., and Krupa S. 2007. An effect of pier pilings on near-shore submarine groundwater discharge from a confined aquifer. Estuaries. In press.

Swanson, R.L., West-Valle, A.S., and Decker, C.J., 1992: Recreation vs. Waste Disposal: The Use and Management of Jamaica Bay: Long Island History Journal, v.5, no.1, pp. 21-24.

Ullman, W.J. Chang, B. Miller, D.C. and Madsen, J.A. 2003. Groundwater mixing, nutrient diagenesis, and discharge across a sandy beachface, Cape Henlopen, Delaware (USA). Estuarine Coastal and Shelf Science. 57: 539-552.

Uncles, R.J., Elliot, R.C.A., and Weston, S.A. 1985. Dispersion of salt in a partly mixed estuary. Estuaries. 8 (3): 256-269.

Vallino, C.S. and Hopkinson, J.J. 1998. Estimation of dispersion and characteristic mixing times in Plum Island Sound estuary. Estuarine, Coastal, and Shelf Science. 46: 333-350.

West, J.R., Uncles, R.J., Stephens, J.A., and Shiono, K. 1990. Longitudinal dispersion processes in the Upper Tamar Estuary. Estuaries. 13 (2): 118-124.

Zonta, R., Cochran, J.K., Collavini, F., Costa, F., Scattolin, M., and Zaggia, L. 2005. Sediment and heavy metal accumulation in a small canal, Venice, Italy. Aquatic Ecosystem Health & Management. 8 (1): 63-71.

Tables for Chapter IV

Table 1. Dispersion coefficients ($m^2 d^{-1}$) in groundwater systems

DISPERSION COEFFICIENT	REFERENCE	COMMENT
0.01	Cooper 1964	Tidal mixing
0.001-0.07	Brusseau 1993	Pore size and advective velocity
0.0084-0.042	Ataie-Ashtiani et al. 1999	Tidal mixing
0.0001-0.01	Roychoudhury 2001	Pore size and advective velocity
0.007-0.03	Bokuniewicz 2004	Density driven mixing/salt fingering
0.05	Martin et al. 2006	Bioturbation
0.02-0.2	Bokuniewicz per com 2007*	Calculated by convective heat transfer

*Using data from Dale and Miller 2007, he calculated these coefficients.

Table 2. Calculated dispersion coefficients, in $m^2 d^{-1}$, using different techniques described in this chapter.

Location	Hydrodynamical Dispersion (Freeze and Cherry 1979)	Tidal Mixing (Cooper 1964)	salt balance	Analytical (slab) solution (Martin et al. 2007)	Analytical solution for the BGC-SGD relationship
Cockburn Sound	0.0002-0.001	0.08	*	*	0.09
Shelter Island	0.0007-0.006	0.07	*	*	0.05
Flamengo Bay, Brazil	0.0004-0.003	0.03	0.15#	0.15#	0.21
Mauritius	0.002-0.02	0.02	*	*	0.38
Canarsie Pier	0.00004-0.0003	0.04	0.16	0.3	**
Canarsie Pol	0.00009-0.0008	0.04	0.46	0.5	**
Mattituck Low SGD	0.00002-0.0001	0.06	0.01	0.015	**
Mattituck High SGD	0.002-0.02	0.06	0.84	0.84	**
P. Sabbioni, Venice	0.00009-0.0008	0.05	0.23	0.04	**
Treporti, Venice	0.001-0.01	0.05	2.8	3.0	**

Hydrodynamical dispersion is calculated as a function of the advection velocity. Tidal mixing was calculated using the technique from Cooper (1964) with site specific tide data. Explanation of the calculation of the dispersion coefficients in the other three columns are found within the discussion section of this chapter.

*****No profiles of salinity were taken at these sites and therefore dispersion coefficients from both the salt balance method and the slab solution could not be calculated.
******No BGC data was collected at these sites.
from data collected by Oberdorfer et al. 2007

Figures for Chapter IV

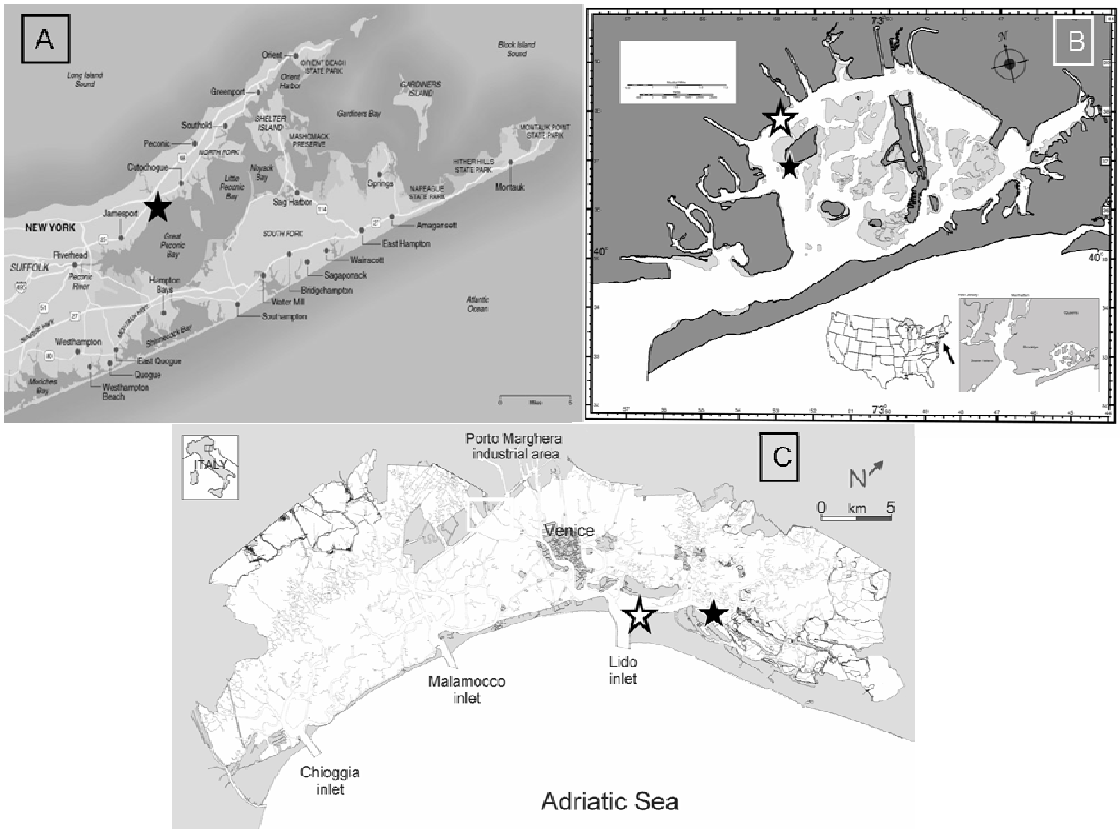

Figure 1A. Peconic Bay, NY. Mattituck site is represented by the star. 1B. Jamaica Bay, NY. Canarsie Pier is represented by the hollow star while Canarsie Pol is represented by the filled star. 1c. The Venice Lagoon, the hollow star corresponds to Punta Sabbioni, the filled star corresponds to Treporti.

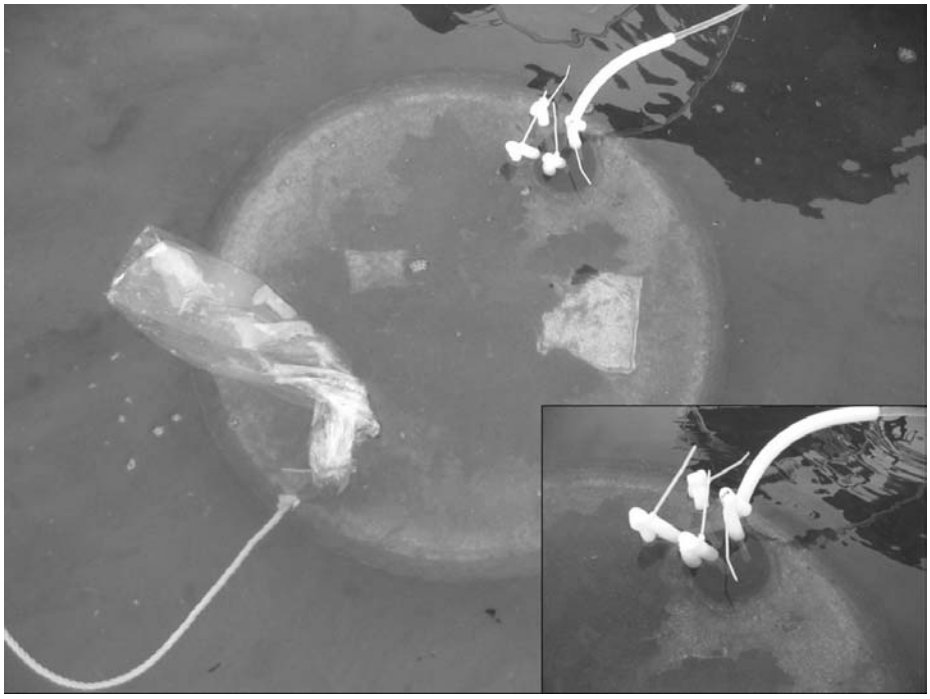

Figure 2. Design of seepage meter with tubes attached to dedicated tips coming up through the stopper.

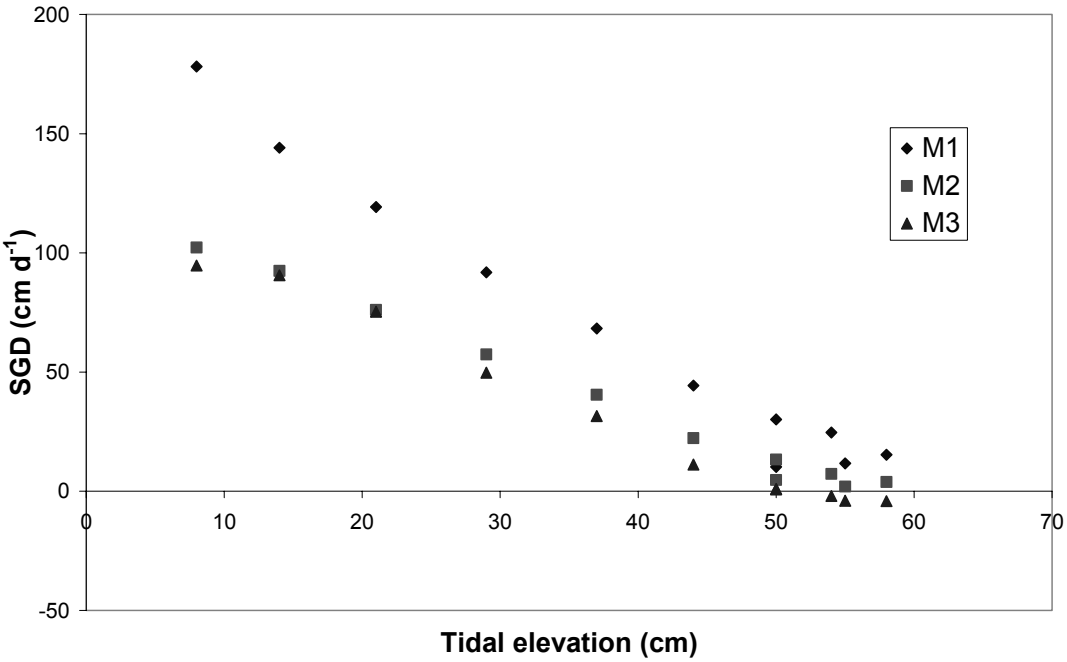

Figure 3. Correlation between SGD rate and tidal elevation at Mattituck for all three seepage meters. M1 is located closest to shore (approximately 5 m from the low tide shoreline), M2 is 50 cm further from shore than M1, and M3 is 50 cm past M2.

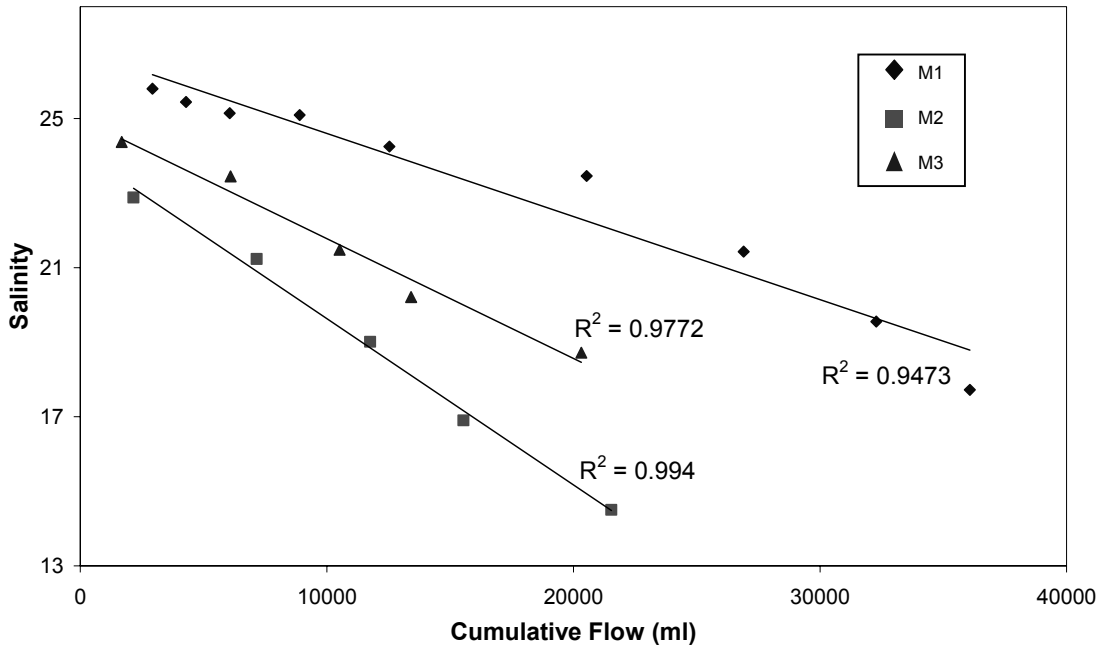

Figure 4. Salinity vs. cumulative discharge in the three Mattituck meters

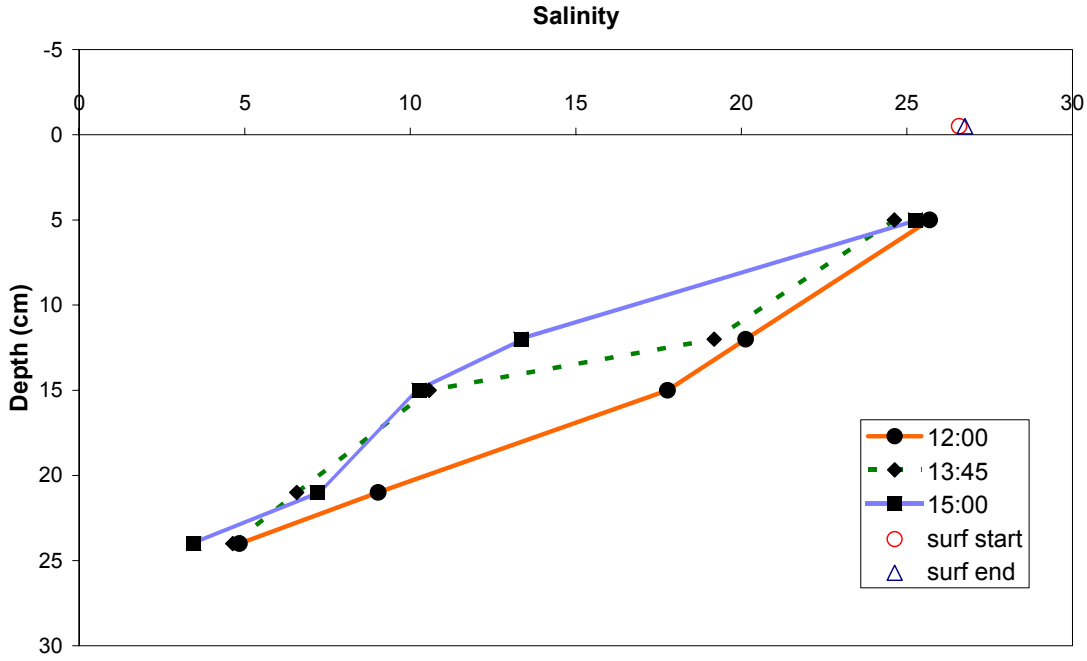

Figure 5. Salinity profiles at Mattituck on May 9th. The salinity in the open water just above the sediment water interface was 26. The 12:00 profile corresponds to an average flow rate of 10 cm d^{-1}. The 13:45 profile corresponds to an average flow rate of 50 cm d^{-1}. The 15:00 profile corresponds to an average flow rate of 110 cm d^{-1}. The profile changed from approximately linear one to one concave upward as SGD increased

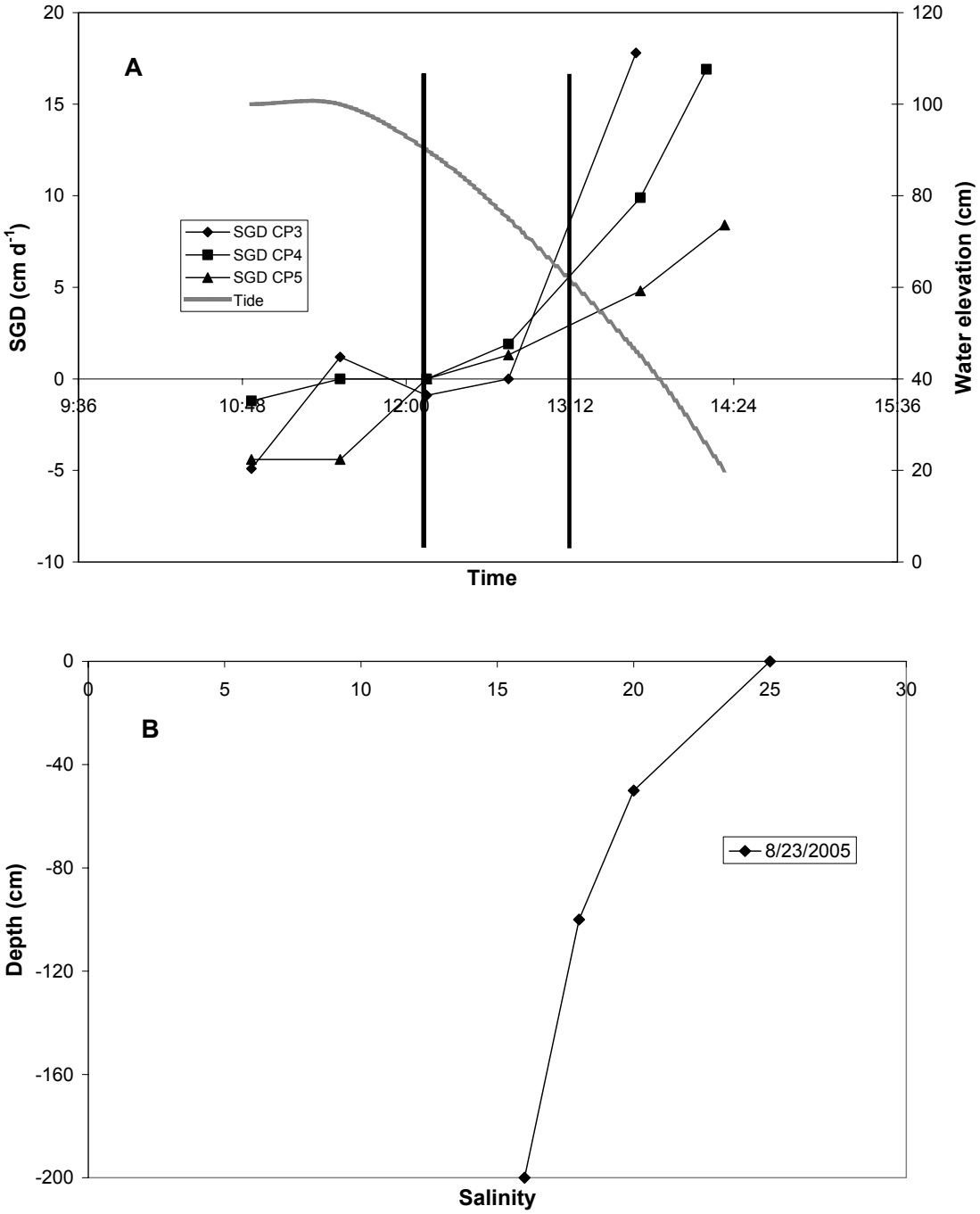

Figure 6a. SGD vs. tidal elevation on August 23rd 2005 at Canarsie pier Jamaica Bay. Approximate collection time of corresponding profile of salinity demarcated by two thick black lines 6b. Corresponding profile of salinity in the sediment. The two lines designate the period in which the salinity profile was measured

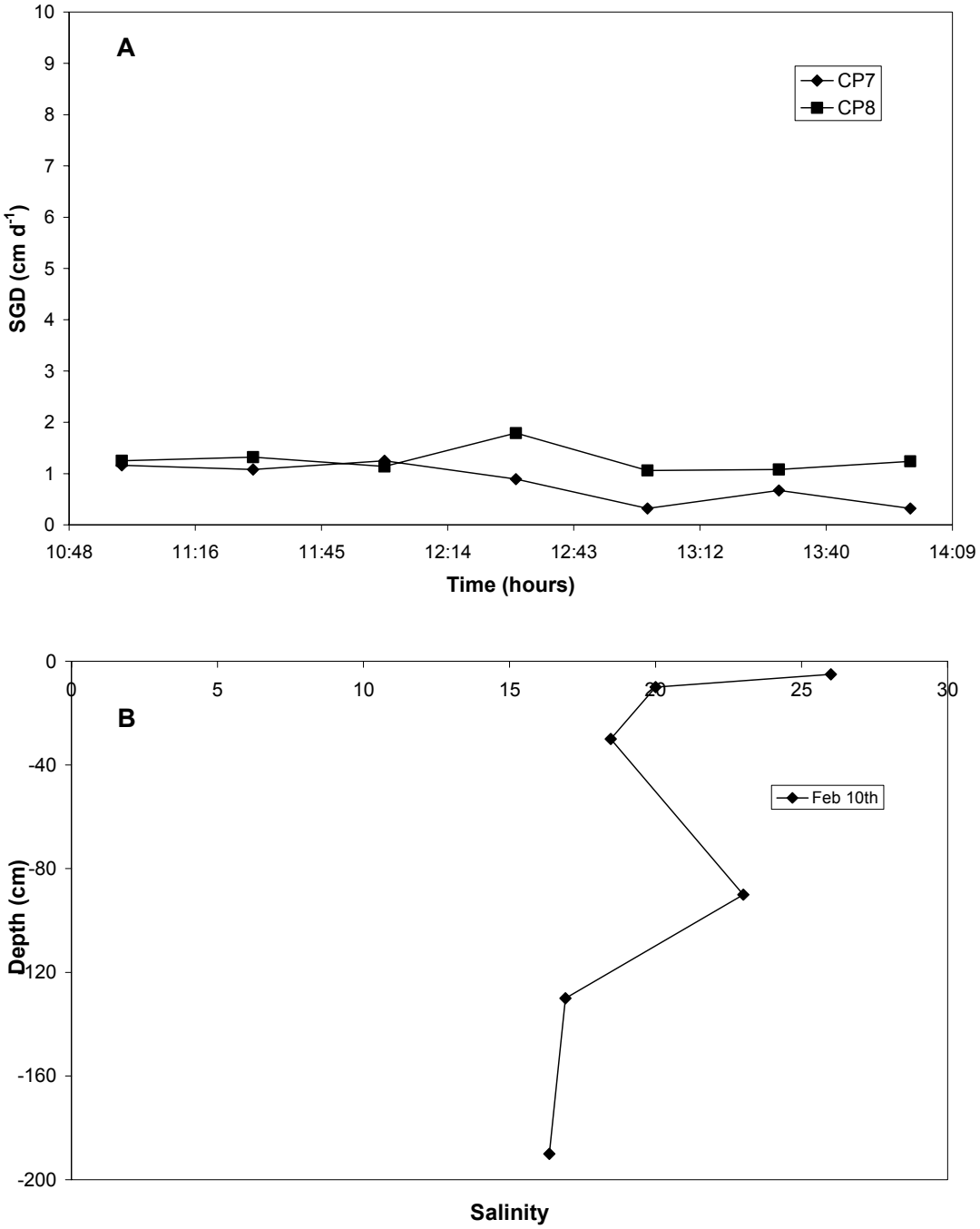

Figure 7a. SGD in two seepage meters at Canarsie Pier on February 10th, 2006. SGD averaged 1 cm d^{-1} and can be considered as zero or within the measurement error of the seepage meters. b. Corresponding profile of salinity in the sediment located in between the two seepage meters.

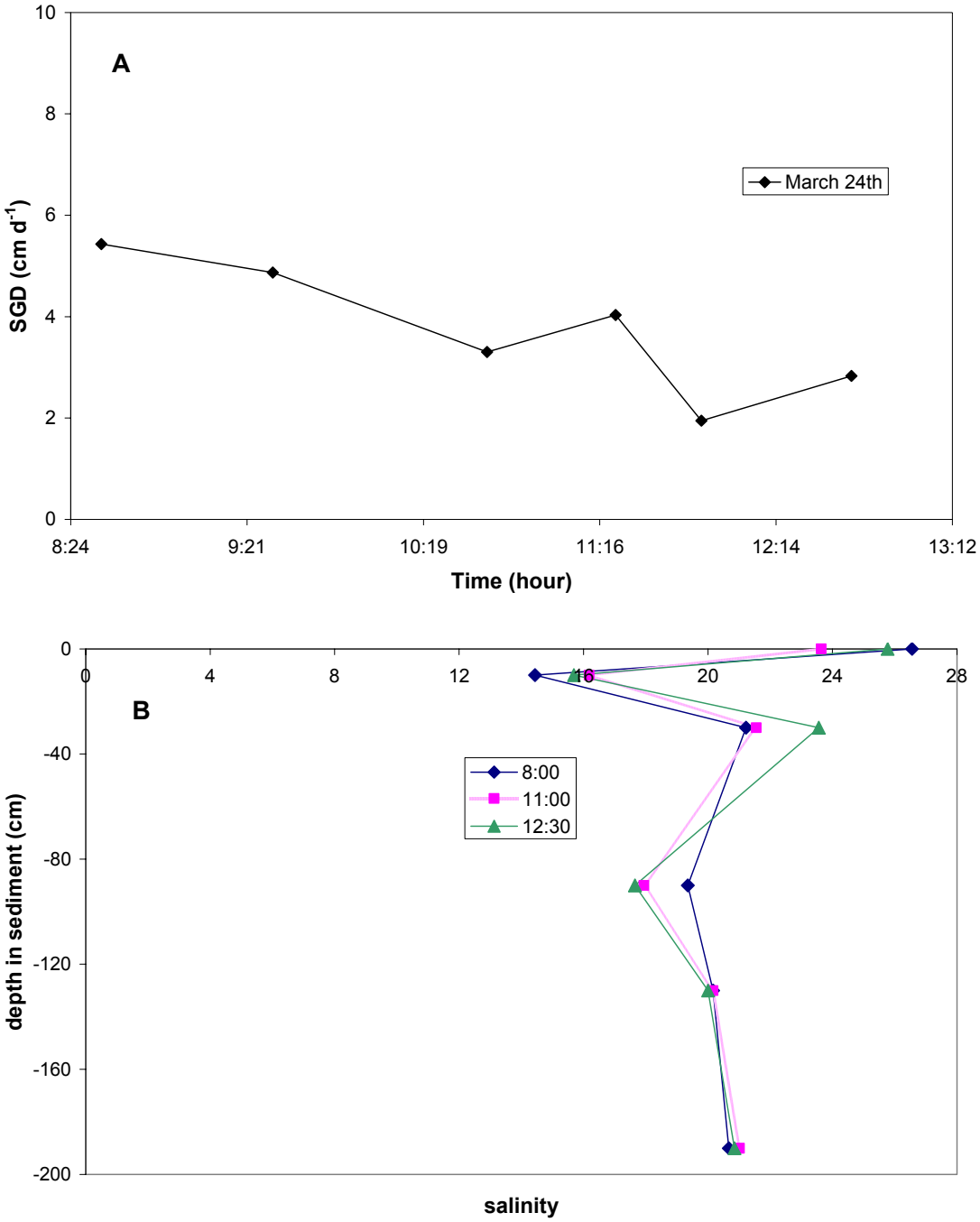

Figure 8a. SGD at Canarsie Pier over a dedicated piezometer on March 24th, 2006. 8b. salinity profiles directly under the seepage meter on March 24th. Each profile shows a subsurface maximum at about 30 cm.

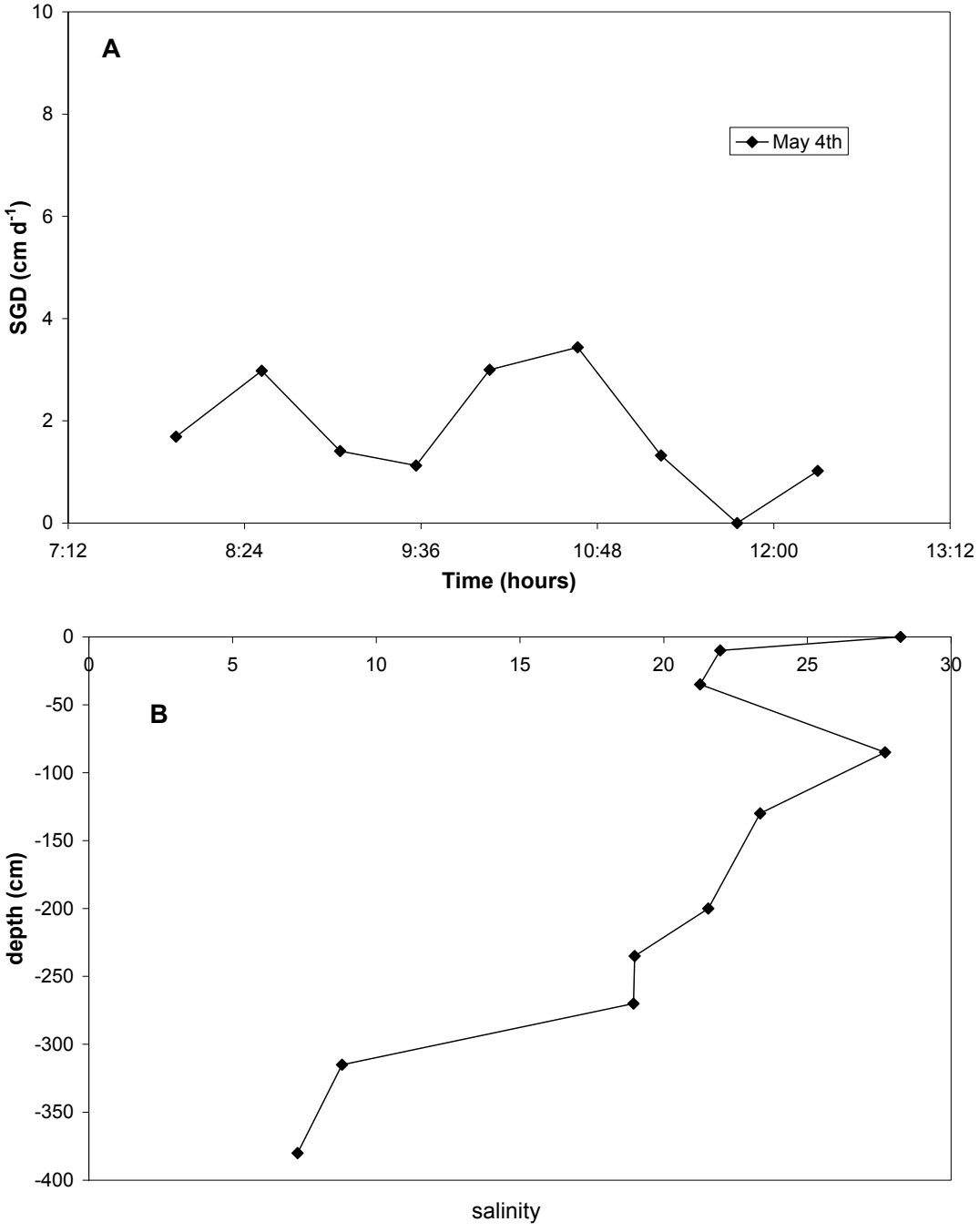

Figure 9a. SGD vs. time at Canarsie Pier on May 4th 2006. 9b. Corresponding profile of salinity in the sediment.

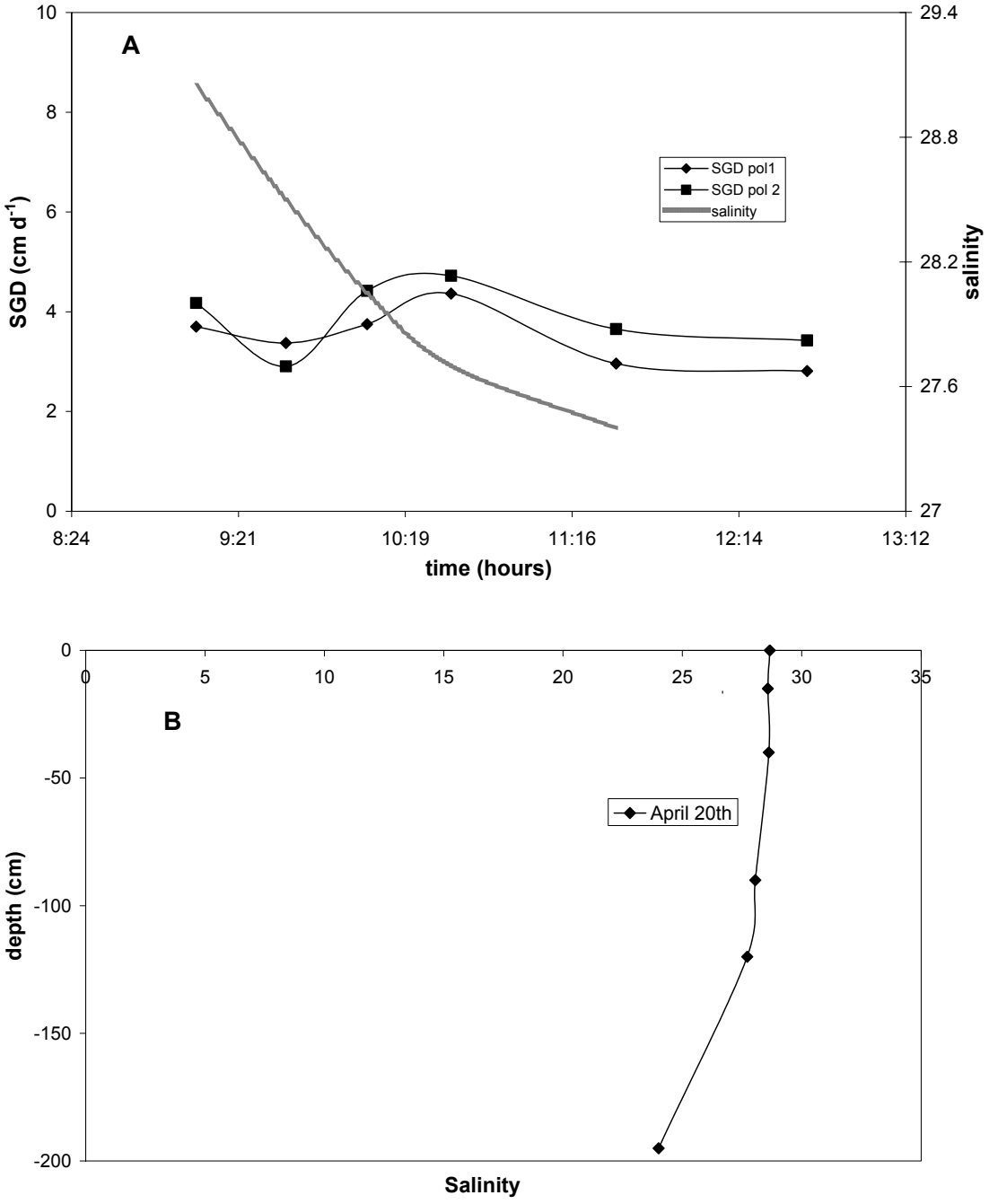

Figure 10a. SGD vs. tidal elevation at Canarsie Pol collected on April 20th 2006. Solid line shows the variation of salinity with time in the seepage meter 10b. Corresponding profile of salinity in the sediment located in between the 2 seepage meters

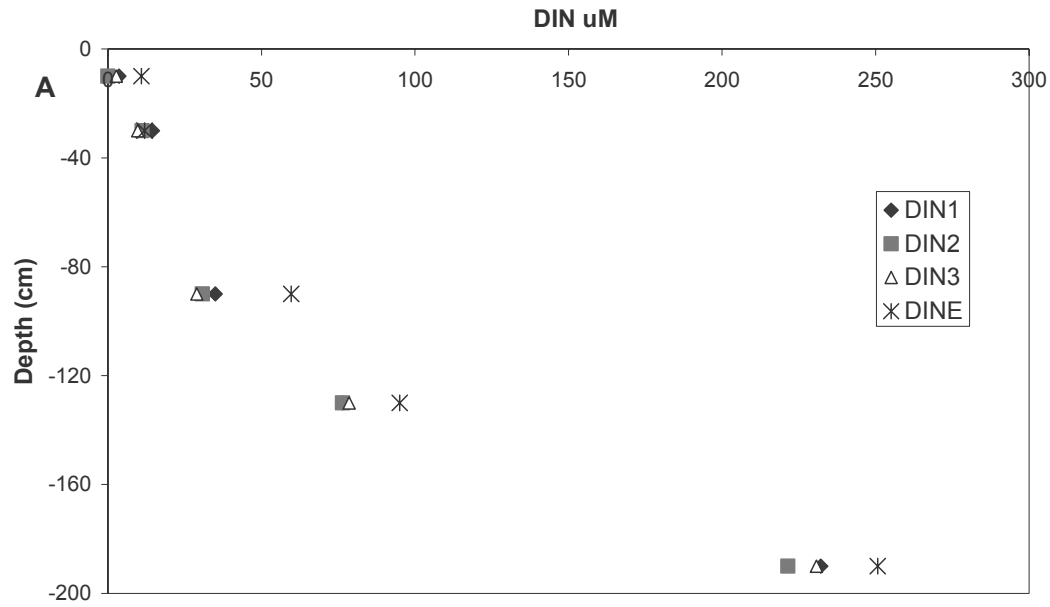

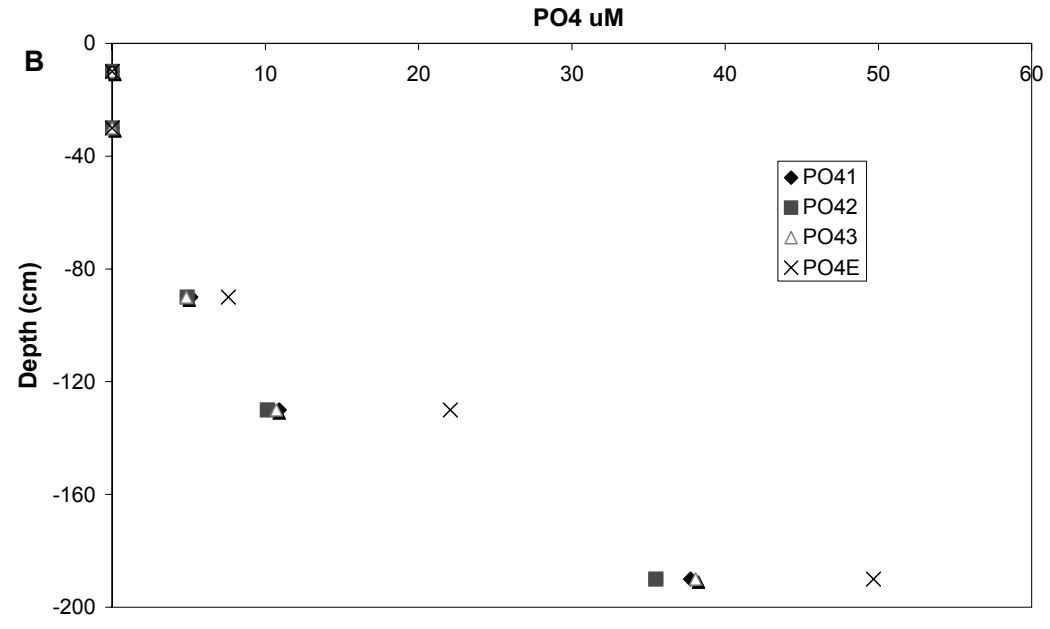

Figures 11A and B. Profiles of dissolved inorganic nitrogen (DIN) and PO_4 at Canarsie Pier. The diamond, square, and triangle profiles were taken at 8:00, 11:00, and 12:30 on March 24th respectively. The X profiles were taken on February 10th.

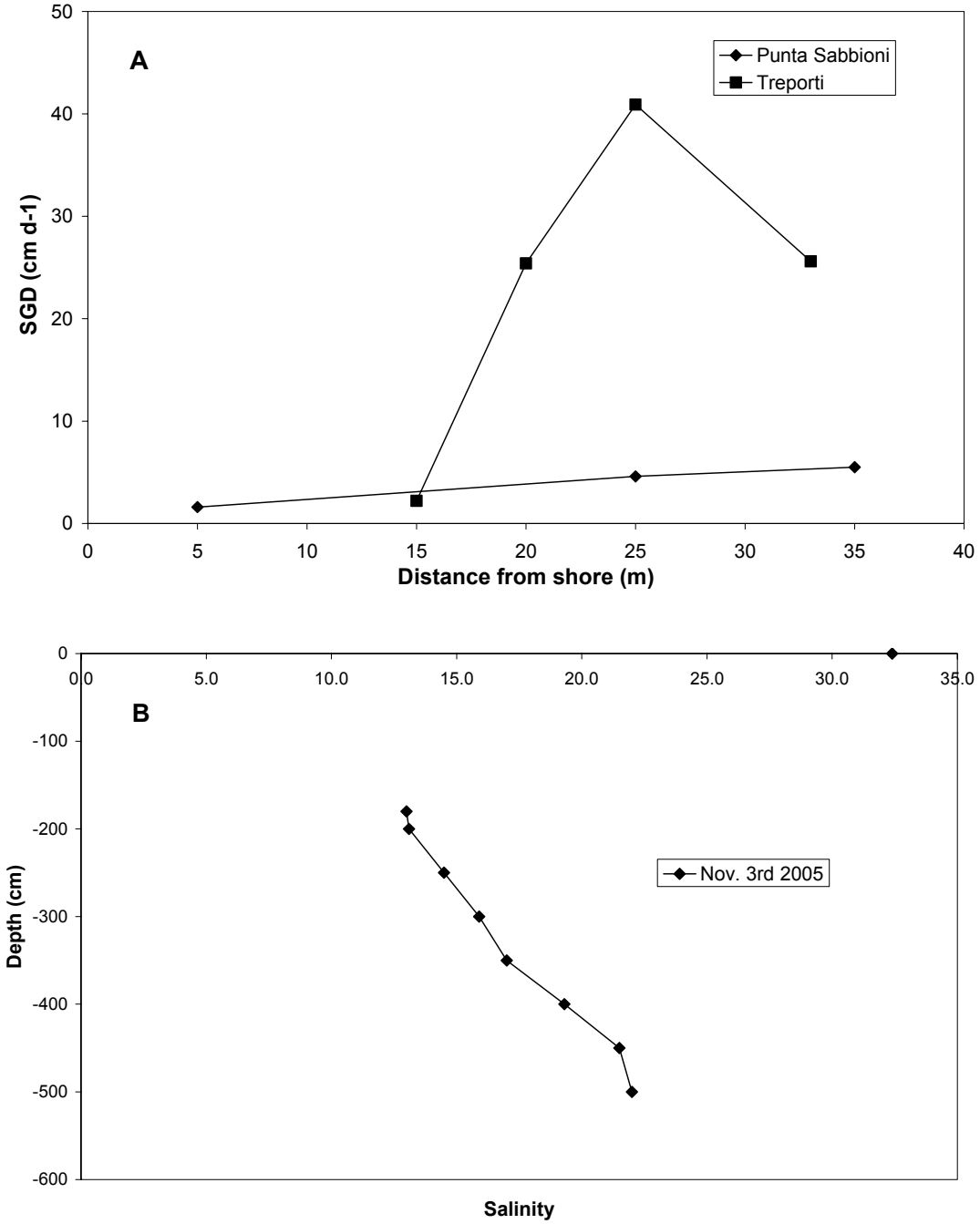

Figure 12a. Average SGD vs. distance from shore at two locations in the Venice Lagoon. 12b. salinity profile measured at Punta Sabbioni.

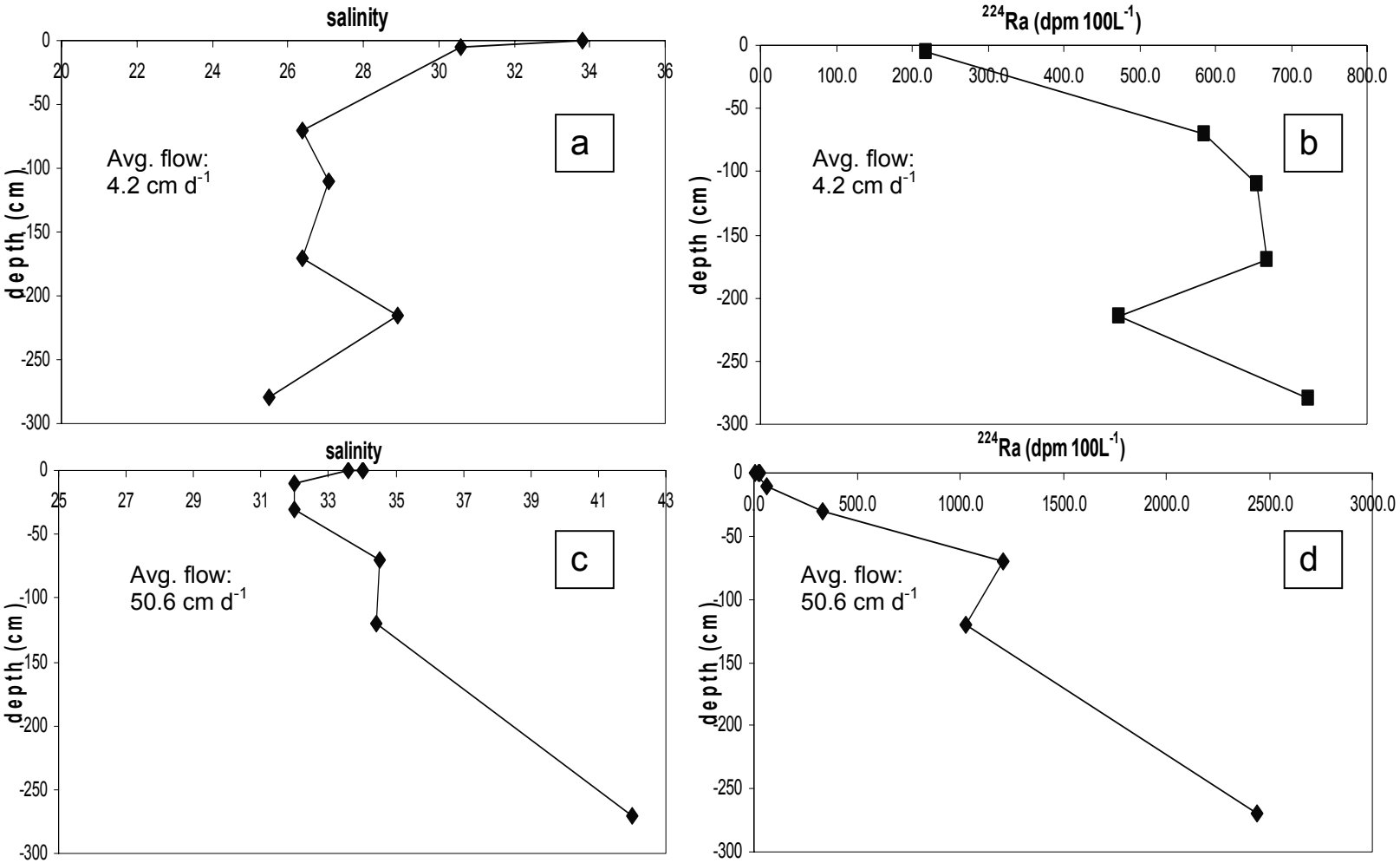

Figure 13 Salinity (a) and 224-Ra (b) porewater profiles at Punta Sabbioni on November 10th, 2005 and salinity (c) and 224-Ra (d) at Treporti on October 24th, 2005.

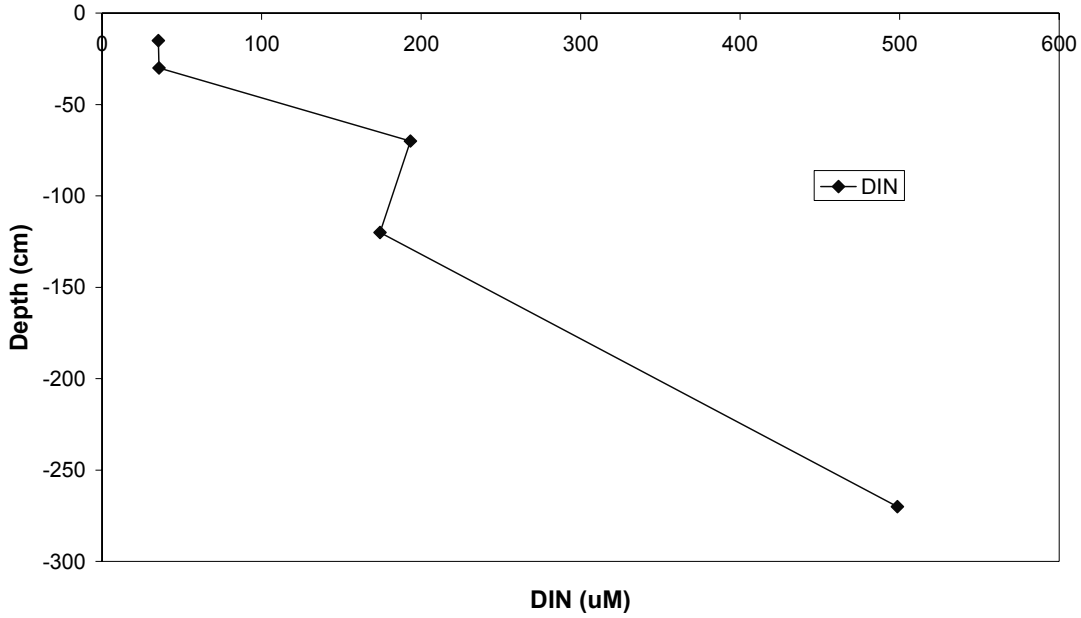

Figure 14. Profile of DIN in the sediment at Treporti.

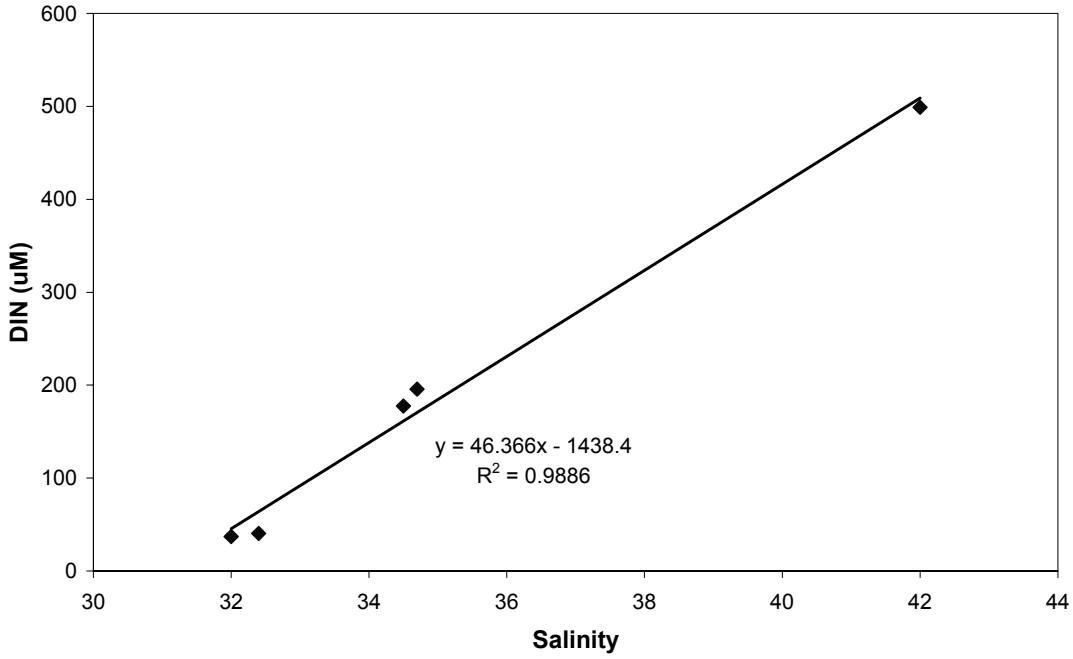

Figure 15. Correlation between salinity and DIN in the pore water at Treporti.

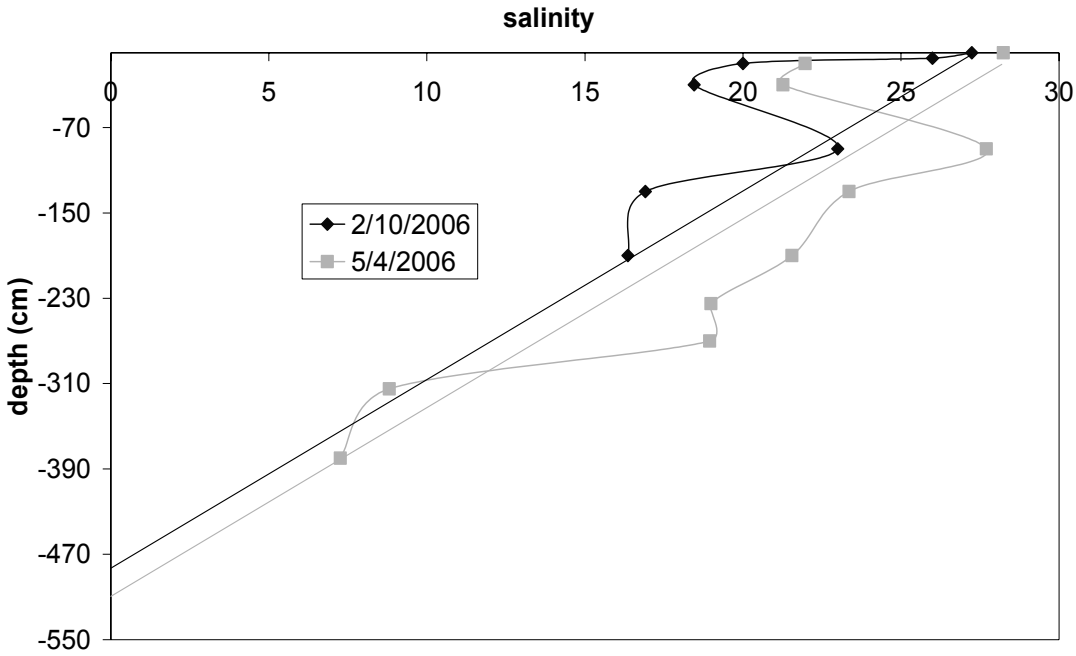

Figure 16. Shallow and deep profiles of salinity in Canarsie pier taken on February 10th (Figure 7b) and May 4th 2006 (Figure 9b.) respectively. The straight line extends the observed trend to a (hypothetical) zero-salinity end member at depth

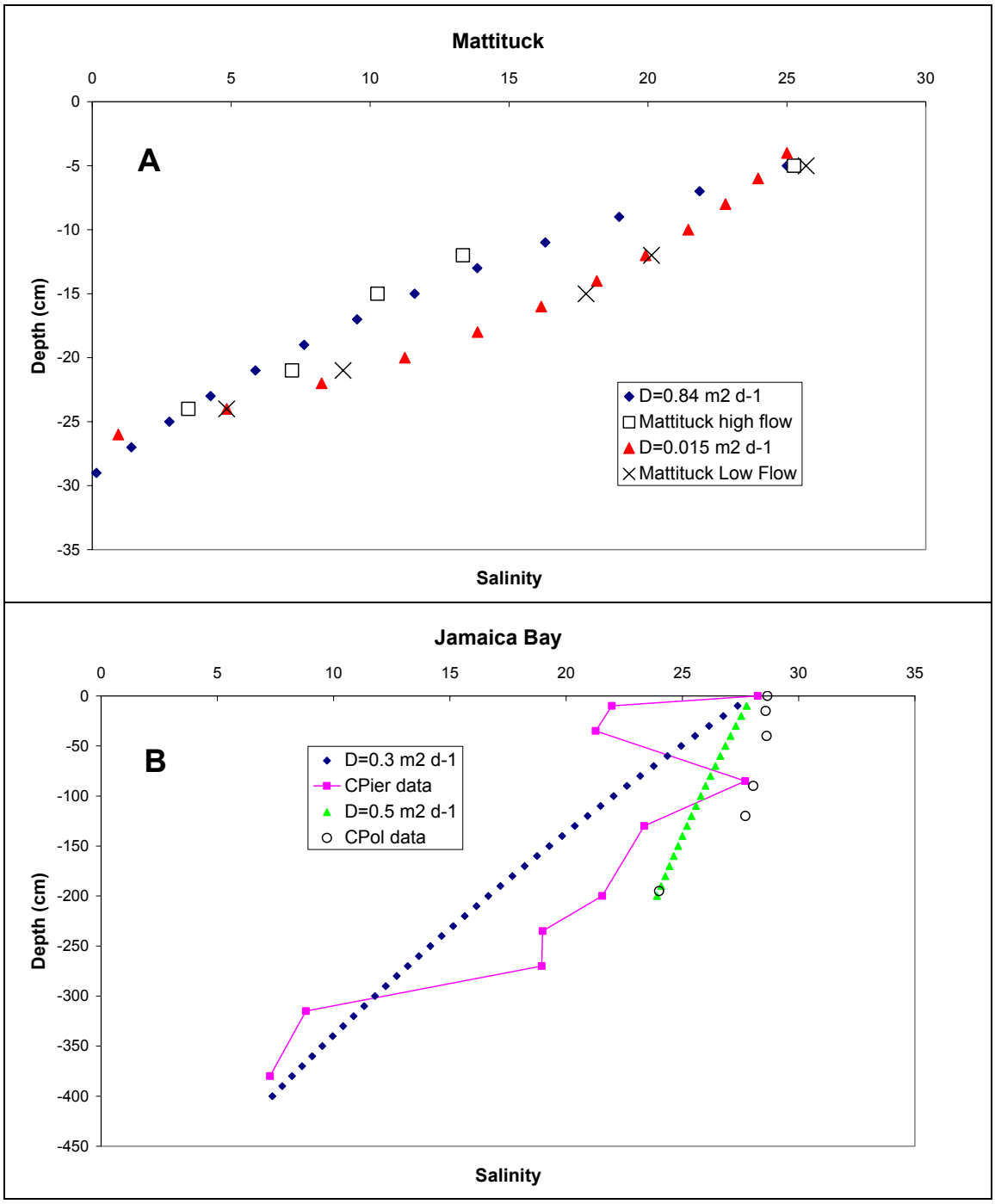
Mattituck
A
Depth (cm)
Salinity
D=0.84 m2 d-1
Mattituck high flow
D=0.015 m2 d-1
Mattituck Low Flow
Jamaica Bay
B
Depth (cm)
Salinity
D=0.3 m2 d-1
CPier data
D=0.5 m2 d-1
CPol data

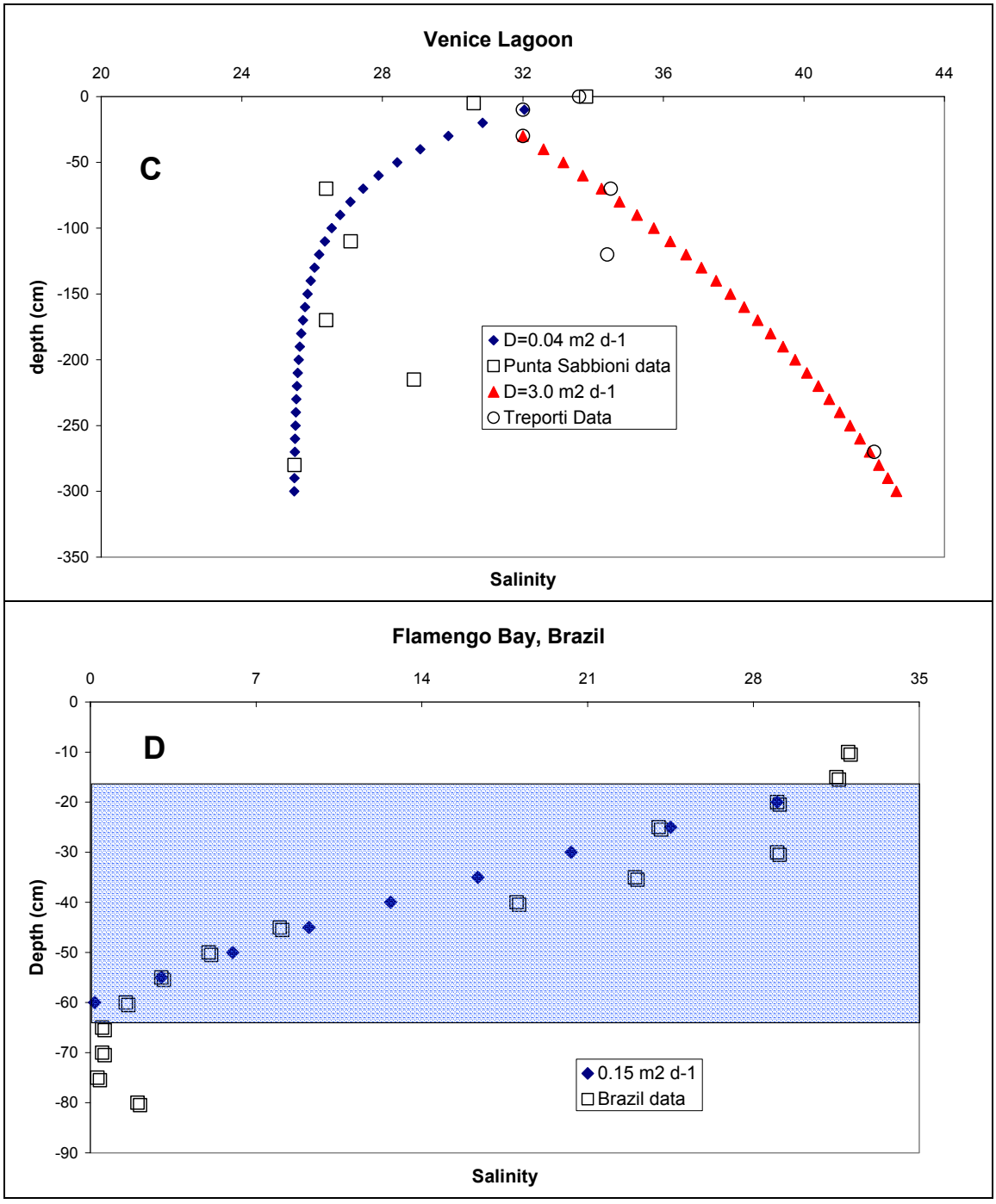

Figure 17. A. Profiles of salinity and matching dispersion coefficients during high and low flow regimes at the Mattituck site. B. Profiles of salinity and matching dispersion coefficients at both Jamaica Bay sites. C. Profile of salinity and matching dispersion coefficient at both Venice Lagoon sites. D. Profile of salinity and matching dispersion coefficient for the slab highlighted in blue for the Brazil data from Chapter II. All coefficients were determined using the relationship described in Martin et al. 2007.

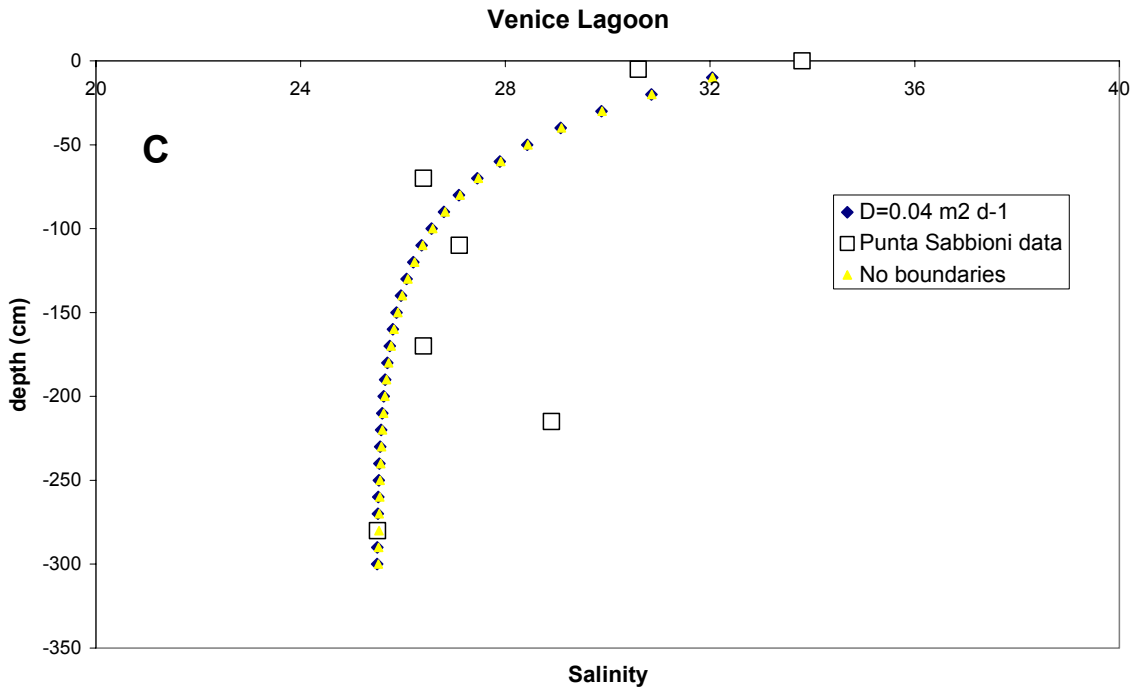

Figure 18. Relationship between the two methods used for determining dispersion coefficients in the Venice Lagoon

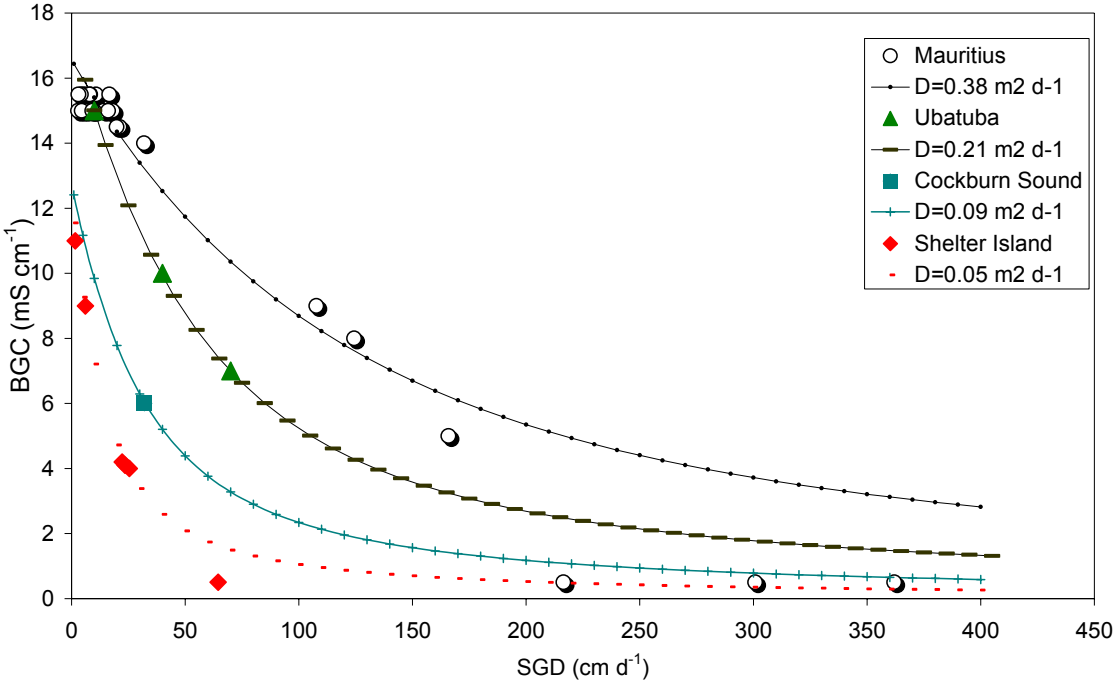

Figure 19. Relationship between BGC and SGD utilizing information from equation 14. With this equation one can determine dispersion coefficients that best fit the curves and attempt to show which mechanism discussed in table 1 controls the relationship. The most likely possibilities are porosity and hydraulic conductivity but further data needs to be compiled to make definitive statements.

CHAPTER V: A Previously Undocumented Source of Water Into Venice Lagoon, Italy[2]

1. Introduction

The flow of groundwater beneath barrier islands has been cited as a possible pathway for salt water and chemical exchange between a protected embayment and the open sea (Bokuniewicz and Pavlik 1990, Corbett et al. 2000, 2002, Windom et al. 2006). When other sources of exchange are limited, the movement of water beneath a barrier island may also present a substantial input of nutrients such as nitrate to the open ocean (Corbett et al. 2002) and has even been considered to be a major source of iron into the south Atlantic Ocean (Windom et al. 2006). In this chapter I investigate the movement of water beneath the barrier islands and sand spits of the Venice Lagoon, Italy, and show that it may be a significant source of both salt water and other compounds into the lagoon.

The Venice Lagoon presents an excellent opportunity to study the impact of anthropogenic modifications on the advection of groundwater beneath a barrier formation, because, within a decade, the tidal barriers of the Modulo Sperimentale Elettrodinamico "MOSE" Project will periodically enclose this embayment In most cases the difference in elevation between the sea and the lagoon will be 20 cm or less. In the worst case scenario (1966) the water elevation was 194 cm. Because complementary works, such as the raising of pavement in the city should function until an elevation of 110 cm the relative difference in 1966 would have been 84 cm

[2] An abbreviated version of this chapter has been prepared for publication in Proceedings of the 2007 International Association of Hydraulic Research's 2007 conference on Engineering Structures in the Coastal Environment (Rapaglia 2007). This version will, most likely, be submitted to Science of the Total Environment

(http://www.salve.it/it/soluzioni/f_acquealte.htm). If you add the IPCC forecast of an increase in local sea level of 60 cm over the next 100 years the difference would still be less than 1.5 m even in the worst-case scenario. This difference in pressure may serve to increase the flow of water underneath the barrier island, driving water of marine origin into the Venice Lagoon (Windom et al. 2006).

Anthropogenic impacts on submarine groundwater discharge (SGD) signature into coastal lagoons have been previously investigated and deemed important in several diverse settings. Three examples include: 1) the drilling of pilings through an apparent confining layer creating conduits for discharge in Shelter Island, NY (Chapter III; Stieglitz et al. 2007); 2) the paving of surfaces and building of underground urban structures may reduce groundwater discharge in Japan but also serve to decrease the quality of groundwater, therefore increasing the importance of the water which does discharge (Nakayama et al. 2007); 3) the dredging of channels for navigation may intercept confining layers of aquifers allowing for an increase of SGD into the Venice Lagoon (Rapaglia 2005).

Even if most of the water exchange through a barrier island is of a marine origin, processes take place within the sediment which can make this flow very important to the biogeochemistry of the back-barrier lagoon. Moore (1999) suggested that the zone of interaction between fresh groundwater and saline water which enters into the sediment resembles an estuary, and, therefore, coined the term “subterranean estuary” to describe this zone. Later investigators suggested that the subterranean estuary is a zone of great importance because the chemical reactions that take place when salt and fresh water mix have important implications for both the benthic ecosystem and that of the overlying

body of water (e.g. Charette and Sholkovitz 2006, Charette and Allen 2006, Beck et al. 2007). Although the flow of water underneath a barrier island is effectively a re-circulation of salt water from the sea to the lagoon, the chemistry of this water will likely be impacted as it comes into contact with both sediment particles and the freshwater lens. Hence when it discharges into the lagoon it may import constituents such as nitrates into a lagoon.

Here we use data from manual seepage meters (Lee 1977) to determine flow rates in two locations along the Cavallino Peninsula, Venice Lagoon. Based on these measurements, in conjunction with sediment salinity profiles taken with a retract-a-tip piezometer, and available tidal data, I estimated the potential subsurface exchange between the Adriatic and the lagoon.

A. Previous Work

Submarine groundwater discharge is a pathway for exchange beneath barrier islands (Bokuniewicz and Pavlik 1990, Corbett et al. 2002, Windom et al. 2006). The driving impetus for this flow has been suggested to be the temporary difference in water elevation between the embayment and the sea (Vacher 1988, Bokuniewicz and Pavlik 1990). Conceptually speaking, when the sea level elevation is greater on one side of the island then the other, there is a hydraulic gradient towards the lower elevation. This difference in elevation causes a deformation of the Ghyben-Herzberg freshwater lens towards the side of higher elevation causing a higher pressure head on the high sea level side (Vacher 1988). This pressure head causes water to intrude into the saturated saline

aquifer, which, although water is slightly compressible, forces water to move throughout the aquifer and, eventually discharge on the other side of the island. There is a time lag between intrusion and discharge but it is not because the water must move all the way across the island, rather it is time for the pressure to transmit from one side to the other, and is partially dependent on the transmissivity of the aquifer. A good review of the theoretical process of the Ghyben-Herzberg relation and the two sea-level problem is found in Vacher (1988).

In Fire Island, NY, it was argued that a difference in elevation of just a few centimeters between the Atlantic Ocean and Great South Bay would significantly affect the flow beneath the barrier island (Bokuniewicz an Pavlik 1990). The authors measured the difference in head (water elevation) between the bay and the ocean by running long hoses from the groundwater divide, located at the highest dune, to both the Atlantic and Great South Bay. The tubes were filled with water and a difference in head of a few centimeters could be seen. Simultaneously discharge into Great South Bay was measured using conventional manual seepage meters, and a positive correlation was seen between flow out of the bay and elevation difference between the bay and the ocean. A difference of only a few centimeters of head could drive a flow of $\geq$20 cm d^{-1} (Bokuniewicz and Pavlik 1990). As these head differences are in constant fluctuation and are dependent on many variables, such as tidal variation and wave-set-up, most of the discharge at this site consists of a re-circulation of sea water, however, when water passes through sediment the chemistry of the water is fundamentally changed.

In the Gulf of Mexico, the flow of conservative tracers was used to determine the discharge rate and direction of flow across a barrier island (Corbett et al. 2000). In this

study, the authors used a well field to measure both hydraulic gradients as well as monitor the dispersion/movement of a dye tracer to determine both the hydraulic conductivity and estimated discharge. Hydraulic conductivities ranged from 20-180 m d^{-1} and the estimated discharge was 2-8 x 10^6 m^3 yr^{-1}. (Corbett et al. 2000) suggest that, if one can establish the discharge of groundwater across the barrier islands, they may also begin to understand the flux of nutrients into coastal waters. Following this investigation, (Corbett et al. 2000) attempted to reconcile the problem of the flux of nutrients by performing a mass balance of nutrients into Appalachiola Bay. They measured nutrients in wells downfield from septic systems and on site sewage disposal systems, and concluded that groundwater discharge was a significant source of nutrients, particularly phosphate, into the surrounding waters. However, this source was less than expected due to aerobic respiration of nutrients as there was an immediate decrease in nitrogen concentration away from the septic system. They suggest that septic tanks and other sewage systems be placed at least 50 m away from the mean high tide line (Corbett et al. 2002).

In 2003 and 2004, (Windom et al. 2006) looked at the possible role that SGD across a barrier island plays in iron enrichment in the southern Atlantic Ocean (Windom et al. 2006). The Patos Lagoon in southern Brazil is a large lagoon whose only outlet to the sea is a small inlet on the southern end. Contribution from freshwater discharges as well as wind can force the lagoon to be up to 3 m higher than the ocean on the other side of a 240 km long barrier sand spit. Windom et al. (2006) hypothesized that the flow of water into the ocean was driven by the elevation difference, though the system was far from simple due to some artesian pressure. The authors, using a combination of radium

measurements to show the large amount of excess radium in the nearshore zone and profiles of salinity along the beach suggested that there was a large discharge of fresh water coming into the ocean from the lagoon (Windom et al. 2006). The discharge showed that the lagoon was a large, if not primary source of reduced iron in the southern Atlantic Ocean. As iron, when reduced, is one of the more important nutrients, they theorize that this flow of groundwater is responsible for the large amount of biological production taking place in this zone. SeaWiFS satellites show a high concentration of chlorophyll-a off the coast of the Patos Lagoon (Windom et al. 2006).

Though few scientists have specifically investigated the impact of urban modification on the flow of groundwater, some studies have shown that humans do affect the flow of groundwater and associated chemicals into coastal zones (Rapaglia 2005, Nakayama et al. 2007, Stieglitz et al. 2007). Rapaglia (2005) suggested that the SGD in Venice could be affected by dredging activities, which may have pierced confining layers of aquifers, or highly permeable layers which serve as conduits for discharge. In addition, the emplacement of bulkheads (raising the local elevation) along the shoreline of the industrial zone may have changed the hydrology of the zone allowing for an immediate response to precipitation events. Chapter III of this thesis showed that the emplacement of pier pilings into West Neck Bay, NY apparently pierced a semi-confining layer creating conduits of high discharge. Nakayama et al. (2007) used the NICE groundwater flow model to argue that sewage pipes, seashore concrete dikes and embankments have changed the hydrology in and around the city of Tokyo, Japan. They argued that these structures actually diminish groundwater flowing into Tokyo Bay, thereby raising the local groundwater table.

It is likely there are many more impacts of anthropogenic modification on local hydrological networks and thus SGD, but with current technology and understanding of this process, it is difficult to make quantitative statements about the impact of change. Here I will discuss how the permeable fill material of a former inlet may present a large, high conductivity, conduit of water transport through the barrier peninsula of Cavallino in the Venice Lagoon. I will then investigate the possible impact of the "MOSE" project and how it may serve to increase the flow of saline groundwater and associated nutrients into the lagoon.

B. Site Description

The Venice Lagoon is a large (550 km^2), shallow (average depth of 0.8 m), lagoon on the northeast coast of Italy (Figure 1). The lagoon is characterized by an asymmetrical semi-diurnal tide with a range between 0.3 m at neap and 1.2 m at spring tides. Over 200 islands dot the surface of the lagoon including 118 of which comprise the city of Venice itself. As of the 2000 census, the population of the city of Venice was 70,000 with perhaps another 30,000 inhabiting the other islands. In addition to the islands, marshes cover about 20% of the lagoon floor with most marshland concentrated in the northern third of the lagoon (IKONOS satellite images 2001). During extreme low tide events, as much as 40% of the lagoon may be exposed to the air. Some natural and man-made channels greater than ten meters deep bisect the lagoon. Natural channels were formed from previous river courses or tidal channels, and all deep channels are now maintained by an active dredging program.

The northern third of the lagoon is dominated by silt- and clay-sized sediments apart from the areas which are exposed to fast currents in or bordering deep channels. The central third of the lagoon is characterized mainly by silt-sized sediments, while the southern third has the coarsest sediments apart from the fringing marshlands to the west (Tagliapietra and Guerzoni 2006). Sand dominates the sediment near the inlets.

The lagoon is bordered on the north and west by the Italian mainland, which in this area is characterized by low-lying agricultural and industrial sites, with one major urban settlement comprising roughly 200,000 inhabitants. the Dolomite mountains lie 50 km to the north and are a major source of water into the pressurized aquifer system (Carbognin et al. 1977). The lagoon is connected to the Adriatic Sea through three inlets named, from north to south, the Lido, the Malamocco, and the Chioggia. The Lido is the largest of the three inlets, and about half of the tidal prism passes through it (Luca Zaggia 2007, CNR Venice, personal communication). The lagoon is separated from the Adriatic Sea, from north to south, by the barrier peninsula of Cavallino, the barrier island of Lido, the barrier island of Pellestrina, and the barrier peninsula of Chioggia. Cavallino is the largest of the barriers, about 20 km long, 4 km wide at its largest point, and its average elevation is about 2.5 m above sea level with a maximum elevation greater than 5 m. All of the barriers are underlain primarily with fine- to coarse-grained sands, and the beaches are, generally, gently sloping, fine-sand beaches. As evidenced by the numerous groins found along the coastline (Ravera 2000), erosion is a major problem for the entire northwestern Adriatic coast. The only exception is the southern half of the Cavallino Peninsula where sand transported by the longshore currents accumulates against northern jetty of the Lido Inlet causing active accretion.

The particular sites of study for this investigation are located along the edge of the San Felice Canal about 1 km and 6 km north of the Lido Inlet, respectively. The main site (6 km from the inlet) borders an area known as Treporti. The Treporti site is located adjacent to a promontory of Cavallino where two major collectors intersect; the S. Felice and the Burano canals. The S. Felice canal is an especially deep (up to 25 m) natural canal which may have comprised the former river bed of the second largest river in Italy, the Piave. Cores taken at this site revealed a thin (~0.1 m), sandy layer lying above a fine-grained silt layer of at least 0.4 m. The upper few centimeters were exposed to both fairly strong surface currents (up to 0.2 m s^{-1}) and periodic wave action from the large passenger boats which docked nearby every 30 minutes. At the time of the experiment the site was relatively tranquil with a narrow beach (~5 m) backed by a steep man-made slope up to an elevation of 3 m. The slope was covered with natural vegetation. At the time of writing, however, this site had been completely altered for the development of a marina (Figure 2.). Historical maps of the Venice Lagoon circa 1700 A.D. show that a former, large inlet connected the lagoon to the Adriatic Sea near the Treporti site (Figure 3). Anecdotal evidence suggests that this inlet was in-filled with gravel and sand material and then overlain with sand and silt. This is most likely the case as the gravel would resist erosion more than sand or silt (Hiscock 2005). Unfortunately no records could be found as to the depth and breadth of this fill, and the overlying sediment is likely to have changed over the centuries.

The second site, Punta Sabbioni, is located closer to the inlet and is also along the S. Felice canal and therefore is periodically exposed to fast currents as well as waves from the large boats which pass by every so often. The beach here slopes gently

downwards to the water before flattening out for an extent of 20 m. Beyond 20 m the sediment drops quickly into the canal. A 0.5 m core at this site revealed a 30 cm layer of fine sand and silt, underlain by a layer of medium grained sand.

Previous measurements in the northern lagoon showed a large flow of groundwater into the lagoon, with an average of 16-20 cm^3 crossing a square centimeter of the sea floor daily (*e.g.*, 20 cm d^{-1}) (Rapaglia 2005, Garcia-Solsona et al. 2007). Discharge of this magnitude could not be forced by the water table hydraulic gradient (as most of the land surrounding the northern lagoon is below sea level) and must be driven from elsewhere. Artesian conditions from a nine-tiered aquifer system may be driving the flow. In addition, salinity measurements within the sampling devices suggest that the source of much of the water must be re-circulated water from the lagoon itself. This has been seen at other locations as well (e.g. Moore 1996, Li et al. 1999).

C. The Modulo Sperimentale Elettrodinamico "MOSE" Project

The Venice Lagoon has been subject to an increasing occurrence of damaging floods over the last 50 years. Due to subsidence caused by groundwater extraction and the relative sea level rise, the city has lost 23 cm to mean sea level since 1900 (Barbero et al. 2004). The frequency of flooding in this city, which is a UNESCO world heritage site, has quadrupled since the beginning of the 20th century. In order to combat this problem, the authorities of Venice have chosen to build movable barriers which are being emplaced in the bottom of the lagoon's three inlets. When ready, these barriers would rise pneumatically from the sediment anytime extreme flooding (>110 cm

http://www.salve.it/it/soluzioni/f_acquealte.htm) is forecast (about 10 times a year). They will then be lowered into the sea once the water level has subsided. This controversial project has been dubbed the "MOSE" Project.

The movable barriers are a novel design, one intended to have as little visual impact on the area as possible. Currently, much of the sea floor has been dredged in the three inlets and they are in the process of emplacing the barriers. In addition, they have also straightened the channels and created an artificial island in the middle of the Lido (the largest) Inlet. These modification have already had an appreciable impact on the current velocity and may be changing the response time to the tidal forcings, thereby changing the amount of time the sea is elevated relative to the lagoon and vice-versa.

2. Methods

Submarine groundwater discharge measurements were made using benthic chambers, which are commonly utilized in SGD experiments (Lee 1977, Bokuniewicz 1980, Shaw et al. 1990, Libelo and McIntyre 1994, Cable et al. 1997, 2006, Rapaglia 2005, Burnett et al. 2006). Briefly, the severed top of a 55 gallon steel drum (0.25 m^2) is inserted open-end into the sediment. The drum is vented, through a small nozzle, to a plastic bag, which allows room for expansion. A second, larger, hole is drilled into the top of the drum which allows for the passage of water thereby facilitating the ability to emplace or remove the chamber from the sediment. When in the sediment a rubber stopper is fitted into the hole. Using the collection volume and time, we can calculate a flow rate which is reported in cm d^{-1} (cm^3 cm^{-2} d^{-1}). Three to four seepage meters were

placed in both shore parallel and shore normal transects in both sites. Salinity of water in the seepage meters was measured using a YSI SCT 30 meter or a HYDROLAB 5000 series multiparameter probe.

Seepage meters have been criticized as being susceptible to artifacts which may cause errors in the estimation of flow rates. Some of these processes include: an anomalous input of water as the drum settles into the sediment, or due to suction caused by placing an empty bag on the seepage meter (Shaw and Prepas 1989, Shaw et al. 1990); input of water into the bag when emplaced in an area of fast currents due to pressure changes described by the Bernoulli Effect (Shinn et al. 2002), and the effect of bioturbation (Martin et al. 2006). However, if one is aware of these issues, they can be mitigated by carefully inserting the chamber into the ground, pre-filling the bags with a certain volume of water, and placing a bucket over the bag to reduce pressure effects (Cable et al. 1997, 2006). Although currents could cause a flow of water into the seepage meters (Huettel et al. 1996, Shinn et al. 2002), flow induced by a Bernoulli Effect would not drive a flow rate of 275 cm d^{-1} (Cable et al. 2006). In addition, qualitative observations of current velocities showed no association to the patterns of discharge seen at this location. Seepage meters are generally considered reliable in the face of moderate to large flow rates (above 5 cm d^{-1}; Bokuniewicz et al. 2004), and have been known to agree well with other methods of measuring SGD (Burnett et al. 2006).

An AMS gas-vapor probe was utilized to collect pore water profiles in the sediment at both sites. This probe has previously been considered a suitable method for collecting high resolution profiles (Charette and Allen 2006, Bone et al. 2006). The probe, which has a stainless steel retractable tip to minimize contamination, can collect

samples every 10 cm to a depth of 5m (or more pending ease of insertion into the sediment). For the purposes of this investigation samples were taken every 0.25 to 0.5 m, in order to sample the transition in salinity with depth. Water was pumped into a polyethylene bottle using a standard hand pump. The water was measured using either YSI SCT 30 meter or a HYDROLAB 5000 series multi-parameter recorder.

Tidal data collected by the regional Venice government was utilized to determine the difference in water elevation between the lagoon and the sea. One of the tidal gauges is located within 500 m of the Treporti site, while Punta Sabbioni elevation was estimated from tidal elevations recorded at three nearby sites. In the open sea, it is unlikely that there is any significant change in water elevation caused by the tide between the National Research Council's Adriatic platform (located 10 km east of the Lido Inlet) and the Adriatic facing beaches of Cavallino which are 12 km across open water from the platform. In fact, there is no change in water level elevation recorded between the research platform and the entrance to the Lido Inlet (Community of Venice website http://www2.comune.venezia.it/maree/real.asp).

3. Results

Rates of SGD were measured at Treporti on July 6, October 24, November 2, and November 3, 2005 and on July 15, 2006. Flow rates were highly variable both temporally and spatially and ranged from 0 to 141 cm d^{-1}, averaging 36 cm d^{-1} (Table 1). Flow rates as great as this are not often found where unconfined aquifers intersect the sea (Bokuniewicz 1980, Stieglitz 2005), without the presence of a large water table

hydraulic gradient. In previous experiments, in seemingly similar settings an offshore decrease in SGD was found (Bokuniewicz 1980) and/or a negative correlation of SGD with tidal elevation (e.g. Paulsen et al. 2004). At Treporti, this pattern was not seen, however here SGD was directly correlated with difference in elevation between the lagoon and the sea (Figure 4). This correlation is very strong in seepage meter Treporti (4) but is much weaker in the other two seepage meters recorded during this period, perhaps due to a time lag between the tidal phase and discharge. If a time lag of 1.5 hours between the tidal elevation and corresponding discharge is considered, the correlation improves in the two devices closest to shore but weakens in the seepage meter furthest from shore (Treporti 4). Difference in head between the sea and lagoon have been known to a drive a flow beneath barrier islands (e.g., Bokuniewicz and Pavlik 1990). It is likely, however, that this process is enhanced by a conduit of high permeability to allow for the measured flow rates.

In each of the seepage meters there is a very weak negative correlation between current (represented by change in tidal height over the measurement period) and SGD (Figure 5). This inverse relationship is strongest in seepage meter TREP2, which is closest to shore, and, therefore, should be least affected by the current. In any case, the data from each seepage meter suggest that the current is not driving flow, thereby providing evidence that the Bernoulli Effect is not an important factor in the SGD at this site.

Measurements also were made at Punta Sabbioni on November 4 and 10, 2005, October 25, 2006, and March 6, 2007. Flow rates were much lower in Punta Sabbioni than in Treporti, not exceeding 9 cm d^{-1} and averaging 3.3 cm d^{-1}. At this site a negative

correlation between tidal elevation and SGD was present in most samples (Figure 4). On November 10, there was no correlation between tide and SGD, but data were only collected for 3 hours. On each of the other days data were collected for at least 6 hours. Only data from the seepage meters placed furthest from the shore are shown as they have the longest continuous series of data collection (other seepage meters were exposed at low tide) (Figure5). Unlike the situation at Treporti, there was no significant correlation with elevation difference between the lagoon and the sea at Punta Sabbioni.

At Treporti, salinity in the seepage meters increased from 33.8 to 35.0 with cumulative discharge. In Punta Sabbioni, on the other hand, there was a small decrease in salinity in each of the seepage meters from 35.0 to 34.0 with increasing discharge. However, it is important to note that less than 5 liters of total water passed through the seepage meters in Punta Sabbioni, or less than 25% of the head space.

Salinity in the sediment in Treporti was measured on November 2, 2005. After an initial drop relative to the overlying water in the upper 0.3 m, it increased linearly with depth (Figure 6). The surface salinity was 34.1 during the sampling period. The salinity decreased to 32.6 at 0.1m and 32.4 at 0.3 m. Below 0.3 m, the salinity increased linearly to 42.0 at a depth of 2.7 m. In Punta Sabbioni, on November 4th, the situation was different. The profile was taken at the elevation of mean high tide, however, no water could be extracted until a depth of 1.8 m because of the sediment matrix. At this depth, water with a salinity of 13.1 was found. Salinity then increased linearly to 22.2 at a depth of 0.5 m, still significantly lower than the ambient salinity of 32.6, perhaps signifying the presence of a freshwater lens.

A profile of porewater salinity was taken further offshore (in the vicinity of the deepest seepage meter) on November 10, 2005. Here salinity dropped within the upper 5 cm from 33.0 to 30.2. Salinity continued to drop to 26.4 at 70 cm and then fluctuated between 25.5 and 28.9 over the next 2 m (Figure 6). At this distance from shore (~30 m) it is possible that the freshwater lens has little effect on the overall salinity.

4. Discussion

A. Explanation of high discharge rates at Treporti.

The behavior of the seepage at Treporti is difficult to explain. If it was driven by the onshore, water-table hydraulic gradients, it is unclear why it did not follow the expected tidal patterns of discharge based on tidal height (Taniguchi 2002), and why the discharge pattern was so different from Punta Sabbioni, a seemingly similar location. If the discharge was driven by artesian pressure from below, daily variation would likely be less because an artesian condition would not be expected to change substantially on short-time scales. In addition, artesian input would be expected to cause a decrease in salinity with cumulative discharge within the chamber instead of the increase seen in Treporti.

Perhaps a difference in elevation between the Adriatic and the lagoon could explain the patterns seen at Treporti. Indeed, flow rates into the lagoon near Treporti increase when the Adriatic is at a higher elevation than the lagoon (Figure 4). The correlation is strongest in the device located furthest from shore. Here, we are dealing with differences in water elevation of less than 0.2 m between the two bodies of water,

however the difference could be as much as 0.35 m for a short period of time on any day (Figure 7). Notably, the flow rates can be marginally positive even though the elevation difference is negative, this suggests that there is a lag in response time (seen in two chambers) between discharge and elevation differences, perhaps due to the influence of the hydraulic gradient of the freshwater lens under the barrier. Still, it remains likely that there are periods of water intrusion into the sediment when the elevation in the lagoon is much higher than in the sea.

Two other pieces of evidence support the hypothesis that there is a flow of salt water under the barrier at this location. The first is the indication of the existence of a former inlet located adjacent to the current Treporti site. Maps dated from the 1200's to 1700's show a large former inlet which cut through the barrier in this area. In fact, there were as many as six, or more inlets into the Venice Lagoon that no longer exist today. These inlets were often artificially filled with loose gravel and sand and other permeable materials. If this were to be the case, even though they are now likely covered by several meters of deposited silt and sand, they could serve as permeable conduits for large volume exchange between the sea and lagoon. It is unlikely that a small difference in elevation could cause such a large flow into the lagoon unless the hydraulic conductivity of the barrier was very high. According to Darcy's Law:

$$q = -k\, dh/dl \qquad (1).$$

where q is the specific discharge in m d^{-1}, k is the conductivity in m d^{-1} and dh/dl is the hydraulic gradient (unit-less). If maximum discharge is 1 m d^{-1} corresponding to a dh of only 0.2 m, and the width of the barrier is 4000 m then k must be 2 x 10^4 m d^{-1}. This conductivity is very high and could only be explained by a major conduit of discharge.

Secondly, although the salinity profile at Punta Sabbioni (Figure 6) suggests the presence of a thin freshwater lens below the beach (common of barrier beaches), measurements in Treporti almost immediately rise to Adriatic salinity and even higher. Punta Sabbioni, which is characterized by low discharge negatively correlated with tidal elevation (Figure 5) and a salinity profile suggesting the presence of a freshwater lens, could be considered typical of the inland side of a barrier landform. Treporti can not be characterized in the same way. The discharge is too large and variable to be driven by a small water table hydraulic gradient, and the pore water profile shows an increase to open Adriatic salinity with depth.

B. Possible impacts of the "MOSE" Project

When considering the hydrogeology of a dam, flow beneath the dam is dependent on the difference in head from the upstream to the downstream portion of the dam. This difference in head will drive a flow of water through the soil, if possible, from one side to the other. The majority of the water will flow along the path of least resistance or conduits of high permeability. When closed, the barriers can also be considered as a type of dam which temporarily leads to an artificially perched body of water alongside a variably permeable coastline.

According to descriptions of the "MOSE" Project, the barriers will be raised only about ten times a year, for short times (6-24 hours) (http://www.salve.it/it/soluzioni/f_acquealte.htm). However, in this period there will be a large difference in elevation between the sea and lagoon as the water piles up against

the shorelines of the barrier lands before subsiding. These barriers will be raised when the water elevation reaches 110 cm above msl. During the largest flood, which took place in 1966, flood waters reached 194 cm creating a difference of more then 80 cm. However during the typical flood the elevation difference would be less than 40 cm (Figure 8). Still, the role of the "MOSE" barriers on both the water and contaminant flow into the Venice Lagoon must be reconsidered.

The tidal prism in the lagoon has been calculated as:

$$V_p = Q_{avg} * t \quad (2)$$

where: V_p = the tidal prism (m^3), Q_{avg} = average discharge $m^3\ s^{-1}$, t = time (s). From the known peak discharge of 20,000 $m^3\ s^{-1}$ (Gačić et al. 2002) the prism is calculated as 6.0 x 10^8 m^3. To determine the impact on the SGD estimate that the barriers may have on the flow through the barrier islands we will assume that (a) the barriers are closed for a full day; (b) the average elevation difference is 0.20 m between the Adriatic and the lagoon, thereby driving an average flow of 1 m d^{-1} (as suggested by the measurements described in the Section 3); (c) each of the former inlets (n=6) are similar conduits of about 500 m width, and (d) the discharge occurs within a maximum distance of 50 m from the shoreline. We can estimate the total discharge through these conduits as:

$$Q = q * \sum A_{(n)} \quad (3)$$

where Q = total discharge ($m^3\ d^{-1}$), q = specific discharge ($m^3\ m^{-2}\ d^{-1}$), A = discharge area of each inlet (m^2). Under normal flood circumstances the difference in elevation would be about 10 cm this would drive a flow of 100 cm d^{-1} or 1 m d^{-1} into the lagoon (Table 2) (Figure 8). The discharge is, thus, calculated to be 0.97 x 10^5 $m^3\ d^{-1}$ or .02% of the tidal prism. Though a discharge of this magnitude is likely important, it is low

compared to both the mean annual river discharge (3.1×10^6 m^3 d^{-1}) and previously estimated SGD rates (up to 6.4×10^7 m^3 d^{-1}) in the lagoon. This may be the case for the first few years of use, but with the current pattern of sea level rise and local subsidence, it is quite possible that the barriers will be raised much more frequently and for longer duration in the decades to come. If the maximum elevation difference is close to 1 m (as in the 1966 flood), instead of 0.10 m, or the gates stay closed longer, the exchange would increase proportionately (Table 2.). For instance, extrapolating the discharge curve seen in seepage meter Treporti 4 (Figure 4) to a 1 meter elevation difference would lead to a discharge of 665 cm d^{-1} (6.65 m d^{-1}) causing a volume flux of water of 9.5×10^5 $m^3 d^{-1}$ into the lagoon. Also, it is possible that a large elevation difference between the sea and the lagoon could drive exchange beneath all parts of the barrier lands as they are made up of a permeable, if much less so, sandy sediment. If, for example there is an average discharge of 8 cm d^{-1} within 50 m from the shore along the entire 30 km of coastline, which is possible as suggested by the discharge at Punta Sabbioni and in previous work (Bokuniewicz and Pavlik 1990), the total discharge would be 1.2×10^5 $m^3 d^{-1}$.

At this juncture the evidence for exchange beneath the barrier is sparse, but such an exchange is not without precedent. In addition, in terms of the Treporti data, it is the only process that could explain the patterns seen in the flow rate. It is likely that the strength of the correlation is affected by other processes, such as current induced discharge, local water table forcing, etc., but that the overarching force appears to be the tidal elevation difference between the sea and the lagoon. Unfortunately the Treporti site has been modified during the construction of a new marina (Figure 2). Sites of other

former inlets have yet to be evaluated but further data from these sites may serve as evidence for the theories supplied above.

C. Ecological significance of the transport of water through barrier islands

The flow of groundwater into the sea is now considered to be an important source of nutrients and pollutants into the coastal zone (e.g. Johannes 1980, Valiela et al. 1990, Slomp and Van Capellen 2004). Water from terrestrial aquifers often shows high levels of nutrients (from agricultural activities) or metals (from industries). Some investigators have shown that flow beneath a barrier island can be contaminated in the case of the presence of septic and other waste water systems on the island (Corbett et al. 2000). Most of the waste produced on the barrier lands of Venice is treated in septic systems or discharged into surface water bodies (small streams, channels) without treatment. In Cavallino, there are several hectares comprising agricultural faculties. The groundwater beneath the Venice Lagoon has been previously measured and seen to have elevated nitrate and chloride levels (Di Sipio et al. 2006). High levels of dissolved inorganic nitrogen (1.2-44 mg L^{-1}) and phosphate (0.03-1.9 mg L^{-1}) were measured in the saline water below the peninsula of Cavallino (Table 3, Figure 9: unpublished data 2006). Assuming the concentration of dissolved inorganic nitrogen does not change along the flow path and the discharge driven into the Venice Lagoon by the closed barriers during a normal flood (10 cm difference in elevation) is 0.97 x 10^5 m^3 d^{-1} we would have a flux of nitrogen equal to the concentration in the discharging groundwater multiplied by the volume flux of water. This would lead to a volume flux into the lagoon totaling 110-

4300 kg d^{-1} and 3-180 kg d^{-1} of nitrogen and phosphate respectively (Table 3). In comparison to the direct discharge of untreated effluents by the city of Venice and nutrient inputs by the rivers of the drainage basin this source may not be important for the overall nutrient concentration of the lagoon (Collavini et al. 2005). However it would significantly affect the local nutrient loading and may be important for nearby salt marsh ecosystem processes.

Even if the average water elevation difference between the Adriatic and the open sea is negligible, this process can change the water chemistry and contaminant concentration that occurs when it intrudes into and discharges from the sediment. As salt water enters into the sediment reactions take place in the subterranean estuary which can allow for the desorption of chemicals into the pore water. These chemicals can then be transported along the flow path and discharge into either the lagoon or the sea. Ergo, the import of this movement of water is not only for the hydrological balance of the lagoon but for the ecological processes occurring in the lagoon as well.

5. Conclusion

The "MOSE" Project is one of the largest and, perhaps most controversial, public works projects in the history of Europe. A large effort has and will continue to go into the study of the impacts of this project on the Venice Lagoon. One phenomenon that deserves attention is potential enhancement of the exchange of water under the lands separating the lagoon from the Adriatic Sea. Evidence suggests that a difference in elevation between the sea and the lagoon may drive an exchange of water under the

barrier islands, especially where former inlets have been in-filled with highly permeable materials. Although the quantity of discharge is small when compared with other SGD to the lagoon, the "MOSE" barriers, when closed, will enhance and prolong the presence of a hydraulic gradient across the barrier lands from the sea to the lagoon. This hydraulic gradient drives water through these conduits. In addition, when salt water enters sediment, its composition will change, often becoming more contaminated. Such a situation could represent a new source of pollution into the lagoon, specifically in the case of Cavallino where high nutrient concentrations are found in the groundwater, though it must be noted that the flushing of seawater with low nutrient concentrations may serve to "clean" the groundwater in the years to come. It remains, however, that the evidence for this flow needs to be strengthened and much more data need to be collected to determine if this is an issue which should be addressed. Either way this presents an exciting opportunity to study the impact of a major anthropogenic alteration on the movement of water through land.

References:

Barbero, A.S., Albani, A.D., and Bonardi, M. 2004. Ancient and modern salt marshes in the lagoon of Venice. Palaeography, Palaeoclimatology, and Palaeoecology. 202: 229-244.

Beck, A.J., Tsukamoto, Y., Tovar-Sanchez, A., Huerta-Diaz, M., Bokuniewicz, H., and. Sanudo-Wilhelmy, S.A. 2007. Importance of geochemical transformations in determining submarine groundwater discharge-derived trace metal and nutrient fluxes. Applied Geochemistry. 22: 477-490.

Bokuniewicz, H. 1980. Groundwater Seepage into Great South Bay, New-York. Estuarine and Coastal Marine Science. 10 (4): 437-444.

Bokuniewicz, H., and Pavlik, B. 1990. Groundwater seepage along a barrier island. Biogeochemistry. 10: 257-276.

Bokuniewicz, H.J., Pollock, M., Blum, J., and Wilson, R. 2004. Submarine groundwater discharge and salt penetration across the sea floor. Ground Water. 42: 983-989.

Bone, S.E., Gonneea, M.E., and Charette, M.A. 2006. Geochemical cycling of arsenic in a coastal aquifer. Environmental Science and Technology. 40: 3273-3278.

Burnett, W.C. Aggarwal, P.K., Bokuniewicz, H., Cable, J.E., Charette, M.A., Kontar, E., Krupa, S., Kulkarni, K.M., Loveless, A., Moore, W.S., Oberdorfer, J.A., Oliveira, J., Ozyurt, N., Povinec, P., Privitera, A.M.G., Rajar, R., Ramessur, R.T., Scholten, J., Stieglitz, T., Taniguchi, M., and Turner, J.V. 2006. Quantifying submarine groundwater discharge in the coastal zone via multiple methods. Science of the Total Environment. 367 (2-3): 498-543.

Cable, J.E., Burnett, W.C., Chanton, J.P., Corbett, D.R. and Cable, P.H., 1997. Field Evaluation of Seepage Meters in the Coastal Marine Environment. Estuarine, Coastal, and Shelf Science. 45: 367-375.

Cable, J.E., Martin, J.B., and Jaeger, J. 2006. Exonerating Bernoulli? On evaluating the physical and biological processes affecting marine seepage meters. Limnology and Oceanography Methods. 4: 172-183.

Carbognin, L., Gatto, P., and Mozzi, G., 1977 Guidebook to Studies of Land Subsidence Due to Ground-Water Withdrawal, *IAHS-AISH* n 121, 65-81.

Charette, M.A., and Sholkovitz, E.R. 2006. Trace element cycling in a subterranean estuary: Part 2. Geochemistry of the pore water. Geochimica et Cosmochimica Acta. 70 (4): 811-826.

Charette, M.A., and Allen M.C. 2006. Precision groundwater sampling in coastal aquifers using a direct push shielded screen well-point system. Groundwater Monitoring and Remediation. 26 (2): 87-93.

Collavini F, Bettiol C, Zaggia L, Zonta R. 2005. Pollutant loads from the drainage basin to the Venice Lagoon (Italy). Environmental International 31:939– 47.

Corbett, D.R., Dillon, K., and Burnett, W. 2000. Tracing groundwater flow on a barrier island in the northeast Gulf of Mexico. Estuarine, Coastal, and Shelf Science. 51: 227-242.

Corbett, D.R., Dillon, K., Burnett, W., and Schaefer, G. 2002. The spatial variability of nitrogen and phosphorus concentration in a sand aquifer influenced by onsite sewage treatment and disposal systems: a case study on St. George Island, Florida. Environmental Pollution. 117: 337-345.

Di Sipio, E., Galgaro, A., and Zuppi, G.M. 2006. New geophysical knowledge of groundwater systems in Venice estuarine environment. Estuarine, Coastal, and Shelf Science. 66 (1-2): 6-12.

Gačić, M., Kovačević, V., Mazzoldi, A., Paduan, J., Arena, F., Mancero Mosquera, I., Gelsi, G., and Arcari, G. (2002). "Measuring Water Exchange between the Venetian Lagoon and the Open Sea". Eos Transactions. 83 (20), 217-222.

Garcia-Solsona, E., Masqué, P., Cochran, J.K., Garcia-Orellana, J., Rapaglia, J., Beck, A., Zaggia, L., Collavini, F., and Bokuniewicz, H. 2007. Estimating submarine groundwater discharge into the northern Venice Lagoon, Italy by using the radium quartet. Marine Chemistry. Submitted.

Hiscock, K. 2005. *Hydrogeology: Principles and Practice*. Blackwell Publishing, England, 408p.

Huettel, M., Ziebis, W., and Forster, S. 1996. Flow-induced uptake of particulate matter in permeable sediments. Limnology and Oceanography. 41: 2 309-322.

Johannes, R.E. 1980. The ecological significance of the submarine discharge of groundwater. Marine Ecological Progress Series. 3: 365-373.

Lee, DR. 1977. A device for measuring seepage flux in lakes and estuaries. Limnology and Oceanography. 22 (1): 140-147.

Li, L., Barry, D.A., Stagnitti, F. and Parlange, J.Y., 1999. Submarine groundwater discharge and associated chemical input to a coastal sea. Water Resources Research. 35 (11): 3253–3259.

Libelo, E.L., and Macintyre, W.G. 1994. Effects of Surface-Water Movement on Seepage-Meter Measurements of Flow Through the Sediment Water Interface. Applied Hydrology. 4 (94): 49-54.

Martin, J.B., Cable, J.E., Jaeger, J., Hartl, K., and Smith C.G. 2006. Thermal and chemical evidence for rapid water exchange across the sediment-water interface by bioirrigation in the Indian River Lagoon, Florida. Limnology and Oceanography. 51 (3): 1332-1341.

Moore, W.S. 1999. The subterranean estuary: a reaction zone of ground water and sea water. Marine Chemistry. 65 (1-2): 111-125.

Nakayama, T., Watanabe, M., Tanji, K., and Moriuka, T. 2007. Effect of underground urban structures on eutrophic coastal environments. Science of the Total Environment. In press.

Rapaglia, J., 2005. Submarine groundwater discharge into the Venice lagoon, Italy. Estuaries. 28 (5): 705-713.

Ravera, O. 2000. The Lagoon of Venice: the result of both natural factors and human influence. Journal of Limnology. 59 (1): 19-30.

Shaw, R.D., and Prepas, E.E. 1989. Anomalous, short-term influx of water into seepage meter. Limnology and Oceanography. 34 (7): 343-351.

Shaw, R.D., Shaw, J.F.H., Fricker, H., and Prepas, E.E., 1990. An Integrated Approach to Quantify Groundwater Transport of Phosphorous to Narrow Lake, Alberta. Limnology and Oceanography 35 (4): 870-886.

Shinn, E.A.; Reich, C.D. and Hickey, T.D. 2002. Seepage meters and Bernoulli's revenge. Estuaries. 25(1): 126-132.

Slomp, C.P., and Van Cappellen, P. 2004. Nutrient inputs to the coastal ocean through submarine groundwater discharge: controls and potential impact. Journal of Hydrology. 295 (1-4): 64-86.

Stieglitz, T. 2005. Submarine groundwater discharge into the near-shore zone of the Great Barrier Reef, Australia. Marine Pollution Bulletin. 51: 51-59.

Stieglitz, T., Rapaglia, J., and Krupa, S. 2007. An effect of pier pilings on near-shore submarine groundwater discharge from a confined aquifer. Estuaries and Coasts. In Press.

Tagliepietra, D., and Guerzoni, S., eds. 2006. Atlante Della Laguna. Venice, Italy.

Taniguchi, M. 2002. Tidal effects on submarine groundwater discharge into the ocean. Geoophysical Research Letters. 28(12): 1561-1565.

Vacher H.L. 1988. Ground water in barrier islands-theoretical analysis and evaluation of the unequal sea level problem. Journal of Coastal Research. 4(1): 139-148.

Valiela, I., Costa, K., Foreman, K., Teal, J.M., Howes, B., and Aubrey, D. 1990. Transport of groundwater-borne nutrients from watersheds and their effects on coastal waters. Biogeochemistry. 10 (3): 177-197.

Windom, H.L., Moore, W.S., Felipe, L., Niencheski, H., and Jahnke, R.A. 2006. Submarine groundwater discharge: a large, previously unrecognized source of dissolved iron into the southern Atlantic Ocean. Marine Chemistry. 102: 252-266.

Tables for Chapter V:

Table 1. Seepage meter measurements in Treporti

Location	Date	Seepage Meter	**SGD (cm d^{-1})**
TREPORTI	11/2/2005	TREP 1	**1.7**
TREPORTI	11/2/2005	TREP 1	**1.9**
TREPORTI	11/2/2005	TREP 1	**1.8**
TREPORTI	11/2/2005	TREP 1	**3.7**
TREPORTI	11/2/2005	TREP 1	**2.1**
TREPORTI	11/2/2005	TREP 2	**56.1**
TREPORTI	11/2/2005	TREP 2	**50.8**
TREPORTI	11/2/2005	TREP 2	**34.9**
TREPORTI	11/2/2005	TREP 2	**17.9**
TREPORTI	11/2/2005	TREP 2	**16.0**
TREPORTI	11/2/2005	TREP 2	**8.5**
TREPORTI	11/2/2005	TREP 2	**7.5**
TREPORTI	11/2/2005	TREP 2	**11.3**
TREPORTI	11/3/2005	TREP 2	**42.6**
TREPORTI	11/3/2005	TREP 2	**39.2**
TREPORTI	11/3/2005	TREP 2	**23.0**
TREPORTI	11/3/2005	TREP 2	**31.6**
TREPORTI	11/3/2005	TREP 2	**39.1**
TREPORTI	11/3/2005	TREP 2	**33.0**
TREPORTI	11/3/2005	TREP 2	**29.6**
TREPORTI	11/3/2005	TREP 2	**38.8**
TREPORTI	11/2/2005	TREP 3	**78.3**
TREPORTI	11/2/2005	TREP 3	**67.7**
TREPORTI	11/2/2005	TREP 3	**76.5**
TREPORTI	11/2/2005	TREP 3	**89.0**
TREPORTI	11/2/2005	TREP 3	**85.5**
TREPORTI	11/2/2005	TREP 3	**81.9**
TREPORTI	11/2/2005	TREP 3	**37.6**
TREPORTI	11/2/2005	TREP 3	**6.7**
TREPORTI	11/3/2005	TREP 3	**141.1**
TREPORTI	11/3/2005	TREP 3	**106.6**
TREPORTI	11/3/2005	TREP 3	**115.0**
TREPORTI	11/3/2005	TREP 3	**120.4**
TREPORTI	11/3/2005	TREP 3	**72.8**
TREPORTI	11/3/2005	TREP 3	**29.0**
TREPORTI	11/3/2005	TREP 3	**15.5**
TREPORTI	11/3/2005	TREP 3	**67.4**
TREPORTI	11/3/2005	TREP 3	**90.7**
TREPORTI	11/2/2005	TREP 4	**39.3**
TREPORTI	11/2/2005	TREP 4	**16.9**
TREPORTI	11/2/2005	TREP 4	**20.8**
TREPORTI	11/3/2005	TREP 4	**95.5**
TREPORTI	11/3/2005	TREP 4	**17.8**
TREPORTI	11/3/2005	TREP 4	**92.7**

TREPORTI	11/3/2005	TREP 4	**63.4**
TREPORTI	11/3/2005	TREP 4	**60.7**
TREPORTI	11/3/2005	TREP 4	**60.4**
TREPORTI	11/3/2005	TREP 4	**4.6**

Table 2. Values of theoretical volume flux of water into the Venice Lagoon pending different elevation between the sea and the lagoon when the inlets are closed with barriers.

Tidal elevation diff. from sea to lagoon (cm)	Flow rate (cm d^{-1})	Theoretical volume flux into the lagoon (10^5 m^3 d^{-1})	Frequency of event (n yr^{-1})**
10	65	0.97	9
20	130	1.9	3
30	200*	2.8	0.8
40	265*	3.8	0.3
50	330*	4.7	0.2
60	400*	5.7	0.07
70	465*	6.6	0.02
80	530*	7.6	0.01
90	600*	8.6	0.01
100	665*	9.5	0.001

The frequency of events is listed in the last column.
*these are theoretical estimates based on the extrapolation of results measured
**The frequency of events is based on data collected from the Community of Venice website http://www2.comune.venezia.it/maree/storic_val.asp

Table 3: Values of DIN and PO4 in the saline groundwater below the peninsula of Cavallino near the site under investigation (unpublished data 2006).

Cavallino Sample #	DIN (mg L^{-1})	PO_4 (mg L^{-1})	DIN Flux (kg d^{-1})*	PO_4 flux (kg d^{-1})*
1	6.8	0.7	660.2	65.3
2	12.1	0.4	1175.3	35.9
3	1.9	0.0	181.3	0.0
4	4.4	0.2	430.9	21.2
5	10.7	0.9	1041.6	85.1
6	33.8	1.6	3276.4	157.5
7	1.5	0.1	146.0	10.0
8	6.9	0.6	668.0	54.7
9	38.2	1.5	3707.1	148.2
10	44.3	1.9	4298.3	183.9
11	1.2	0.2	112.5	15.9
12	1.3	0.1	129.6	14.5
13	1.4	0.2	139.5	15.3

* The nutrient flux estimates are based on the volume flux of water estimated for the most common flooding events (10 cm difference) as seen in table 1.

Figures for Chapter V:

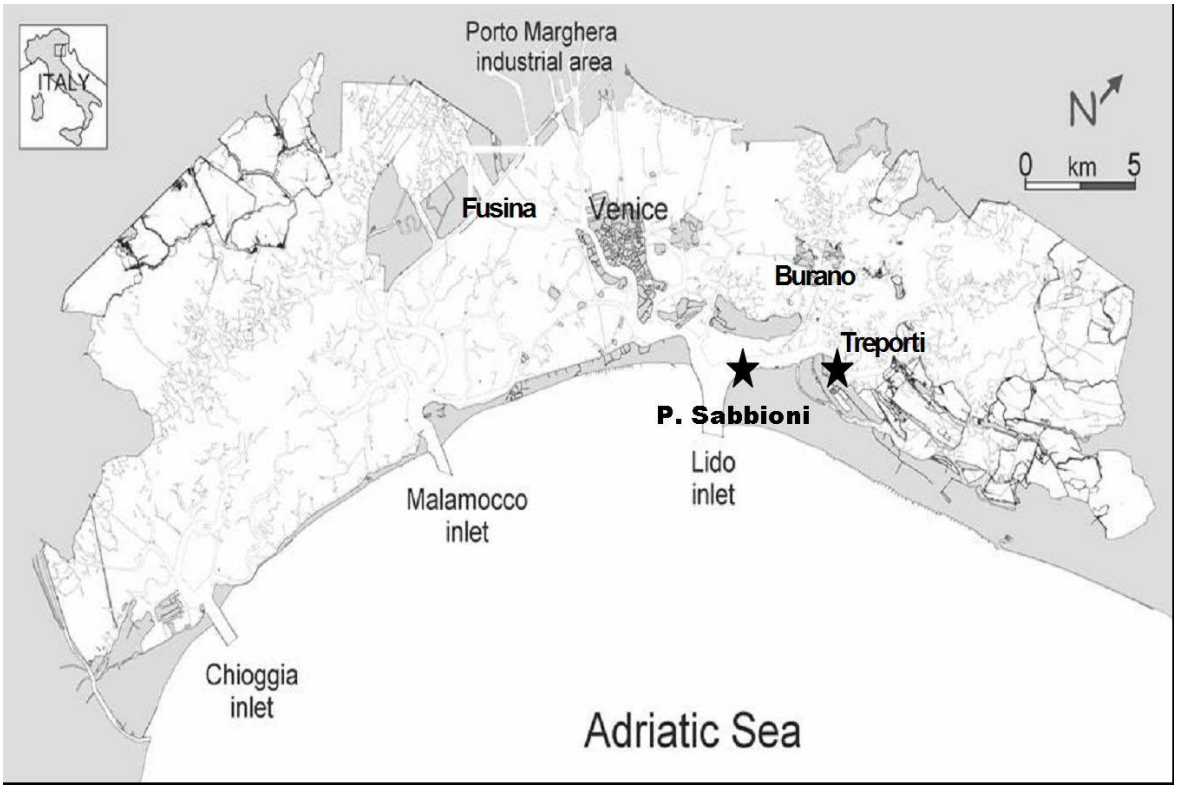

Figure 1. Map of the Venice Lagoon.

Figure 2. Photo of the construction work at the new marina near Treporti. Previously, this was a gently sloping hill with a small sandy beach back towards the building.

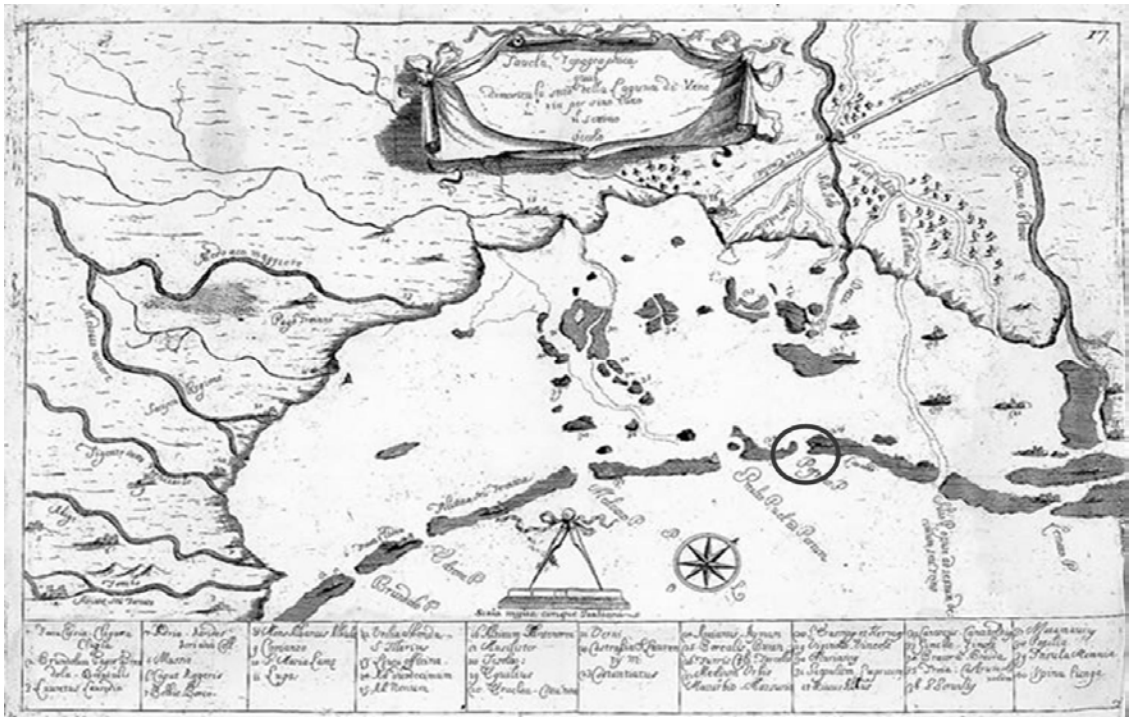

Figure 3. Historic Map of the Venice Lagoon. Drawn around the year A.D. 1600. The former inlet located at the present day Treporti site is circled.

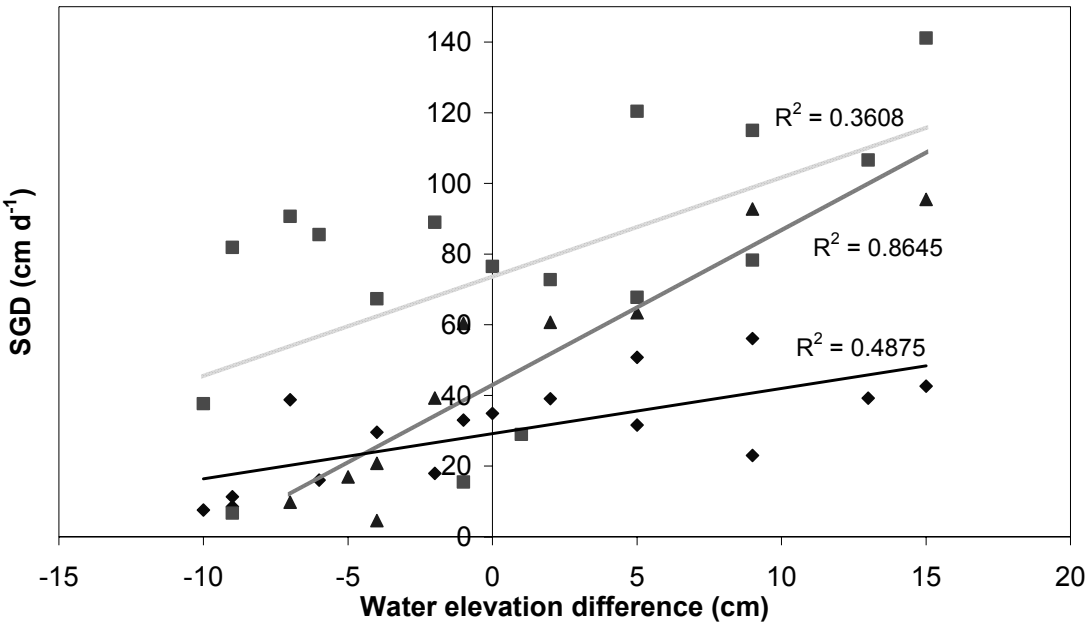

Figure 4. Correlation between discharge flow rates and water elevation difference from measurements made in three seepage meters on separate days in Treporti. A positive elevation difference means that the Adriatic is higher than the Venice Lagoon.

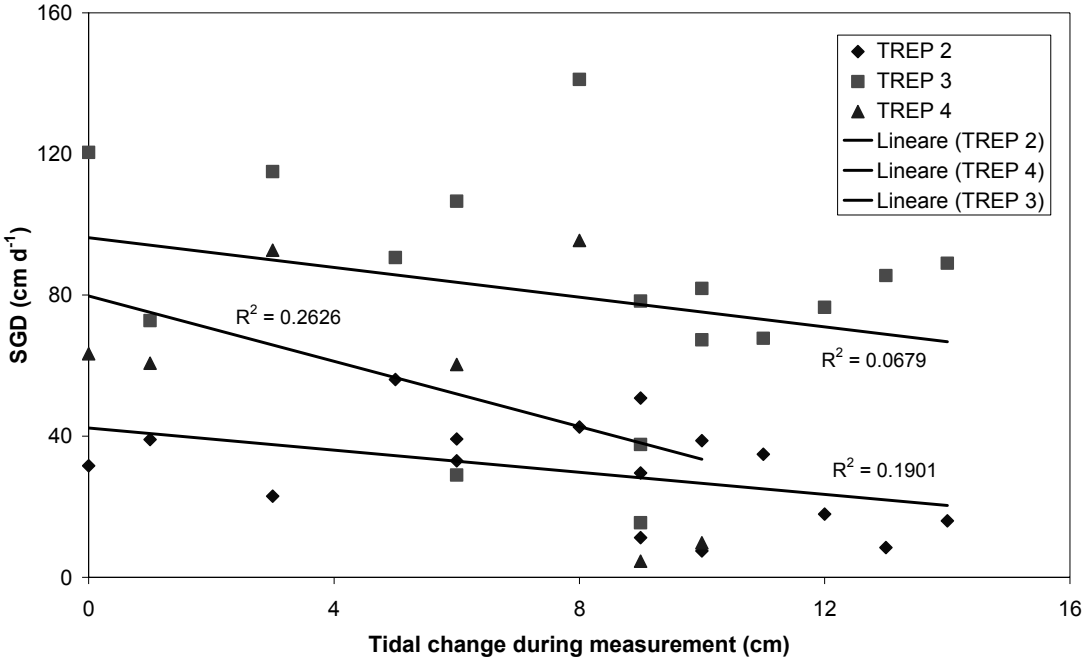

Figure 5. Correlation between SGD and tidal elevation at Punta Sabbioni on three sampling days. In general there is negative correlation with tidal height.

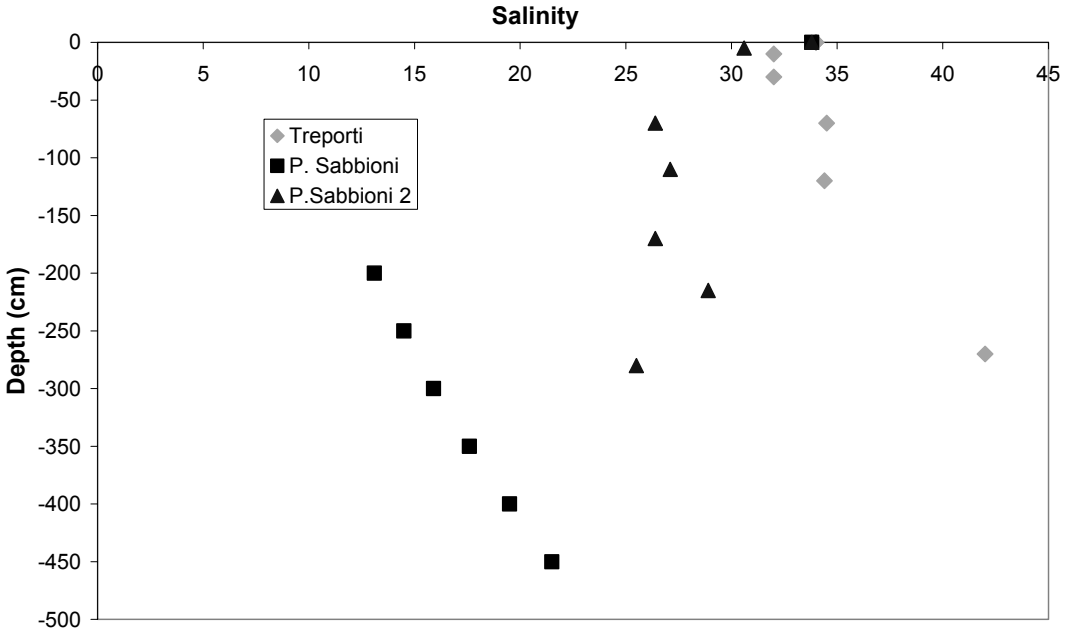

Figure 6. Porewater profiles of salinity at Treporti and Punta Sabbioni

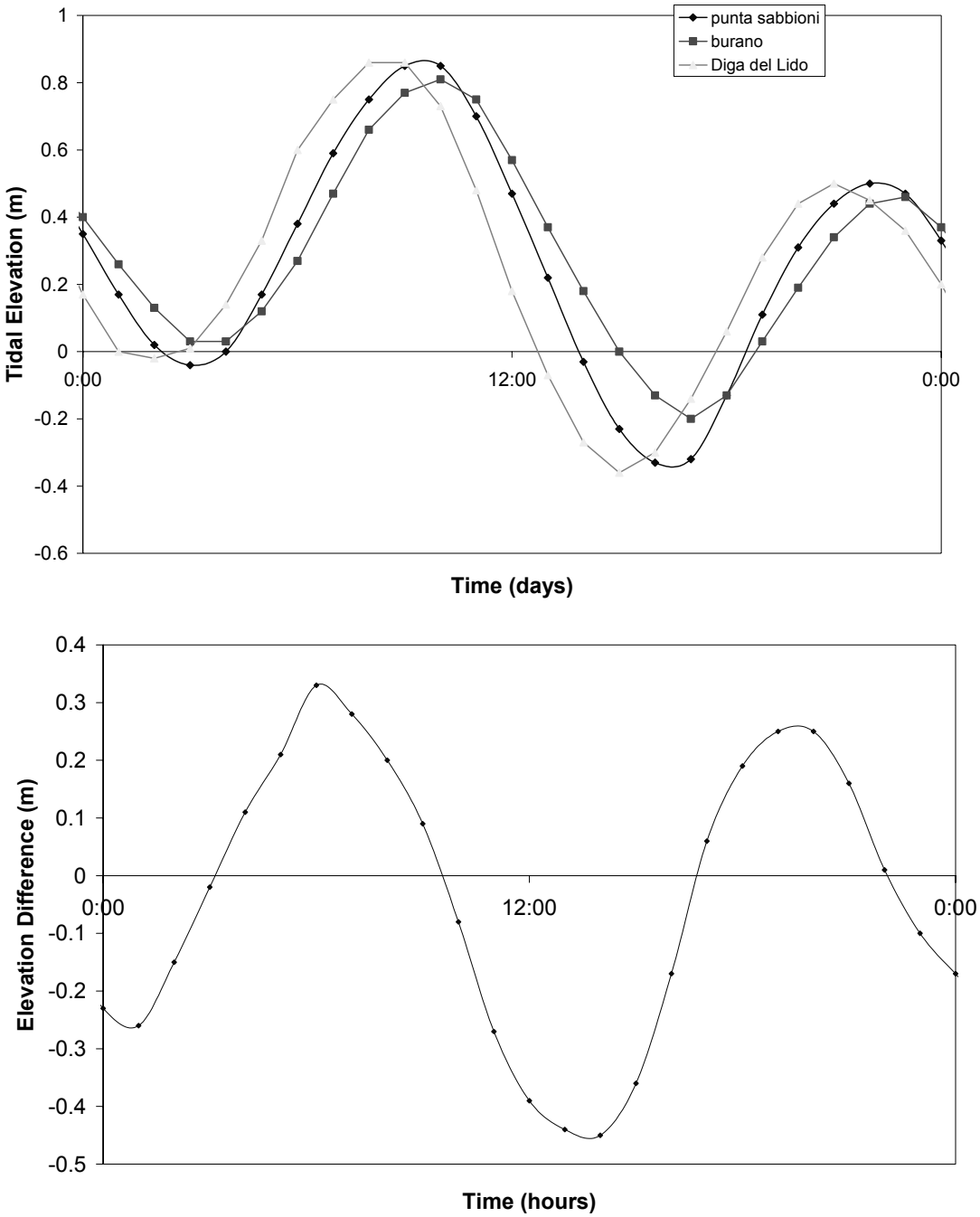

Figure 7. A. Typical tidal cycle at three measuring locations in the Venice Lagoon. Diga del Lido is located at the opening of the Lido Inlet and has essentially the same tidal signal as the CNR platform located 10 km offshore. B. The difference in elevation between the sea and the lagoon. Positive difference means that the sea is elevated above the lagoon. The Burano station is located 1 km west of Treporti (Figure 1). Data utilized from the Comune di Venezia Centro Maree.

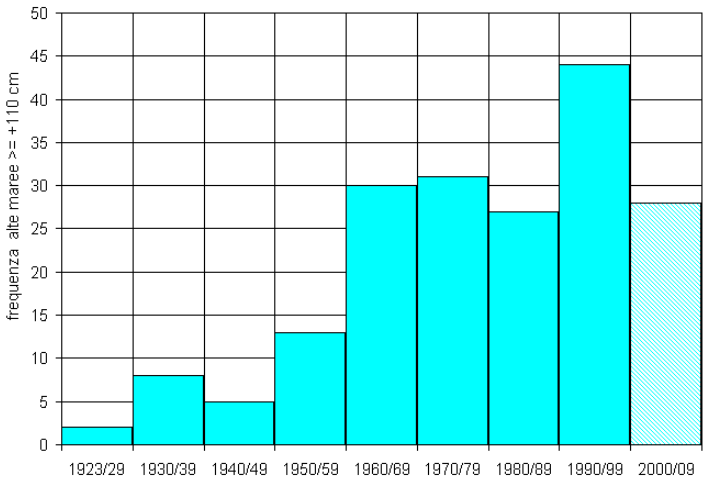

DISTRIBUZIONE DECENNALE delle alte maree >=+110 cm, registrate dal mareografo di Punta della Salute - Venezia, dal 1923 al 2005.

Figure 8. Increase in the frequency of flood events in the Venice Lagoon over the last 9 decades. http://www2.comune.venezia.it/maree/storic_val.asp

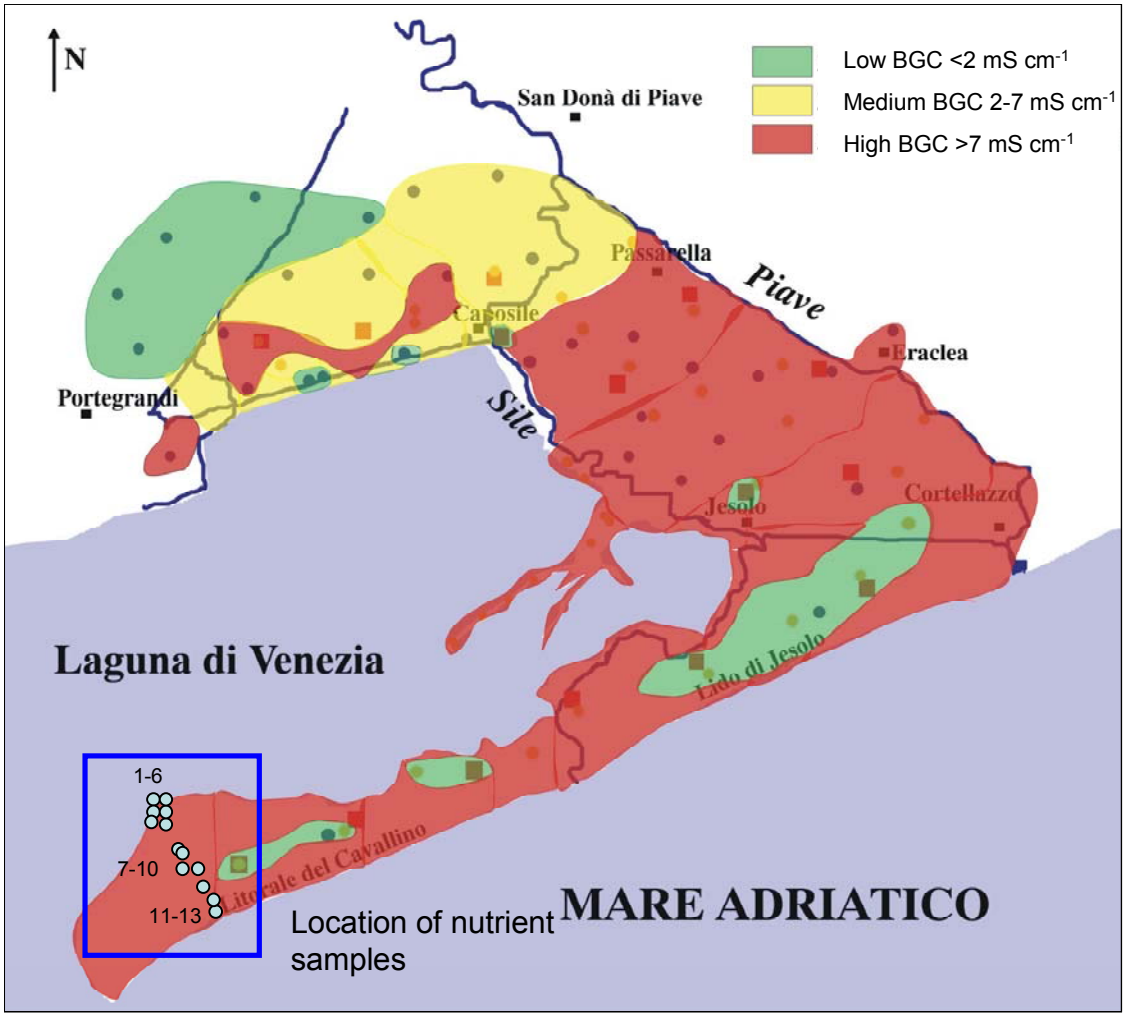

Figure 9. Distribution of BGC beneath the barrier peninsula of Cavallino and the land to the north of the lagoon. Blue circles represent the locations of nutrient samples discussed in this chapter. Map courtesy of Eloisa Di Sipio (unpublished data).

CHAPTER VI. SUMMARY AND FUTURE WORK

A. Overview of the main objectives of the thesis

After three decades of research, many improvements have been made in the study of submarine groundwater discharge (SGD) (Taniguchi et al. 2002, Burnett et al. 2006). Investigators have estimated SGD in different areas both directly (point measurements) and indirectly (through the use of tracers and models). Still much doubt remains about how to accurately quantify SGD, and, therefore, an intercalibration exercise was initiated (Burnett et al. 2006). These experiments, in some of which I have participated, have led to the ideas in this thesis.

It became apparent, after the Shelter Island experiment, that to understand SGD on a large scale, we must first look at processes on a small scale. Recently one of the major focuses of SGD research has shifted to understanding the processes that are taking place within the sediment of the discharge zone. Moore (1999) suggested that the zone where fresh groundwater mixes with interstitial seawater was a “subterranean estuary”. He hypothesized that in this zone many processes take place which fundamentally change the composition of the water before it discharges into the coastal zone. With this in mind, one could no longer state that the flux of non-conservative constituents is the concentration of those constituents in an onshore well multiplied by the discharge.

Researchers began to realize that the best way to understand the impact of the submarine groundwater discharge was to examine the processes taking place in the sediment (Bone et al. 2006, Charette and Sholkovitz 2006, Martin et al. 2006). In this thesis, I attempt to reconcile some of the processes that are occurring in the sediment by looking at a comparison between SGD and bulk ground conductivity (BGC) in Chapters

II, III, and IV. Therein, the relationship between BGC and fresh SGD suggests that the discharge of groundwater as well as other mechanisms of dispersion must have an effect on the distribution of salinity in the sediment. A further investigation the utility of using BGC to better understand the quantity and quality of the SGD signature in coastal areas was discussed.

In Chapter IV of this thesis, I investigated how the profile of salinity in the sediment was affected by the rate of advection as well as mechanisms of dispersion. Researchers use in situ measurements to understand the flux of contaminants into coastal zones, however, until now, these investigations considered only a constant rate of advection or no advection at all (e.g. Charette and Allen 2006). In this chapter, I investigated the relationship between SGD and sediment characteristics, including how a changing rate of advection (e.g. tidally induced) might affect the profiles of salinity and perhaps other constituents in the sediment. This is important when considering how to quantify the flux of these constituents. It seems that the rate of advection may significantly affect the porewater chemical concentration (such as the salt concentration, the concentration of nutrients, and possibly heavy metals as well) and, therefore, investigators should be aware of this impact when researching constituent transport by SGD. In this chapter, I also described certain processes that allow salt to intrude into the sediment and how the intrusion is impacted by the rate of advection itself. Somewhat surprisingly, it seemed, increasing positive vertical advection increased the penetration of salt into the sediment through hydrodynamical dispersion in some locations. This process lends evidence to the idea that this zone is a subterranean “estuary” as the process of dispersion has been frequently studied in fluvial estuaries, and is considered a

major process controlling mixing in these estuaries. Dispersion is also mentioned in Chapter IV as a cause of the site-specific discrepancies in the relationship between BGC and SGD and the utility of using BGC to estimate SGD. Thus, it has been deemed very important to further understand the process of dispersion and how it affects sediment properties.

The final objective of this thesis was to determine how anthropogenic modifications to the environment may change SGD signatures and the possible impact of these modifications on both small-scale sediment profiles and, in turn, larger ecosystems. In Chapter III, I investigated how the drilling of pier pilings through a confining layer of an aquifer created a major conduit of discharge. In the immediate vicinity of the pilings the porewater was noticeably freshened by the discharge of fresh groundwater from below, meanwhile further away from the pier the groundwater was saline. There was a very strong inverse correlation between pore water conductivity and discharge at this site.

A combination of seepage measurements and porewater profiles have helped establish the idea that there may be a large exchange of saline groundwater through the barrier lands separating the Venice Lagoon from the Adriatic Sea. In Chapter V, I discussed how the in-filling of a former inlet presented a high conductivity conduit of groundwater transport below the barrier islands of the Venice Lagoon. In addition, I examined one of the possible implications of a major project intended to protect the city of Venice and her lagoon from rising waters which consistently inundate the city. It is possible that when the barriers of the famed “MOSE” project are closed there will be a

transport of water from the sea to the lagoon driven by the hydraulic gradient, which is established when the elevation of the sea is high as compared to the lagoon.

B. A closer look at the intercomparison experiment, and how to utilize the knowledge obtained

As is often the case in science, the intended objectives of a project were only partially achieved, but, in the meantime, results from the project have led to the re-evaluation of data and, in turn, unforeseen conclusions. The intercomparison project was designed to see how different techniques compared when measuring SGD in the same location (Burnett et al. 2001). In addition, the experiments were meant to determine whether certain techniques were more apt for use in different hydrogeological settings. Unfortunately, in most cases, the objective of the experiment was confounded by situations which led to an over-or-under estimation of SGD by certain techniques. In Cockburn Sound, the majority of the discharge was located in the intertidal zone and, therefore, difficult to measure using conventional seepage meters (Taniguchi et al. 2003). In Sicily, seepage meters were useless in the face of large waves in the basin, and integrated tracers could not be compared to seepage meter measurements (Burnett and Dulaiova 2006). In Shelter Island, the presence of pier pilings which had pierced a confining layer produced significant small scale spatial variability in SGD (Stieglitz et al. 2007), and in Mauritius a large submarine spring dominated the SGD and caused an under-estimation of discharge by the integrative tracers radium and radon (Bokuniewicz et al. 2007).

In some cases the estimates measured by the different methods did not agree within an order of magnitude (Burnett et al. 2006). In addition, many of the expected patterns, often seen in SGD, were not witnessed. For example, patterns such as correlation with tidal elevation and an offshore decrease in SGD were frequently confounded by the fact that the discharge was controlled by other natural and anthropogenic factors.

One of the more promising methods that came out of this project has been the simultaneous use of conventional seepage meters to measure directly SGD and BGC to determine the location of this discharge. In many cases a relationship between SGD and BGC was established, and, therefore, BGC measurements could be used to estimate SGD, in order to obtain a better estimate of SGD within a large area.

When designing an experiment to understand the role of SGD into a system, both of these methods should be considered. As described in this thesis, often, the measurement of SGD was not inherently designed to compare directly these two methods. Thus, the preferred approach would be to take BGC measurements in an attempt to locate sites of fresh and salty pore water. Once these locations have been found, seepage meters should be emplaced in both zones in order to determine if there is a disparity of discharge driven by the advection of fresh water. If this is the case, the BGC study could be expanded. Measurements of BGC should be taken as frequently as possible, while continuously measuring the flow using seepage meters in the sites of high and low BGC. If the rate of SGD varies within the seepage meters over time, BGC measurements should be made in and around these seepage meters as the flow varies in order to better understand how the rate of advection itself is controlling the BGC

distribution. In addition, ground-truthing of BGC measurements should be done as often as possible, by using a piezometer to draw water from the sediment in zones of different BGC values in order to determine how well the measurements correspond to actual salinity values, and to determine if the differences seen in the measured BGC are caused by salinity or matrix dynamics. In addition, physical characteristics of the site may aide in the understanding of this relationship and, if it can be determined what combination of these parameters determine the relationship, qualitative statements as to the discharge may be expanded to many coastal areas.

Other methods tested in these intercomparison experiments are useful in the study of SGD and should be, when possible, utilized alongside BGC and seepage meter measurements. Unfortunately, the use of measuring the concentration or activity of naturally occurring tracers to integrate discharge often requires a large amount of funding which may not be available for coastal zone managers. One of the benefits of the two methods described in this thesis is that both methods are relatively simple to use and very cheap to make. Therefore the utility of this comparison may be possible with little funding as well.

C. SGD and its impact on a small scale, what we have learned, and where to go from here

This thesis discussed some of the processes associated with the discharge of groundwater on a small scale, specifically within the sediment. SGD has been seen, in this thesis and many other studies, to be variable on small spatial and temporal scales

(e.g. Bokuniewicz 1980). Therefore, the factors that control SGD must also be investigated at this scale because many of the processes that control the ecosystem, such as primary production, could be affected by discharges on this scale. This is important in the understanding of the discharge of not only water but its associated constituents as well. This thesis investigated the process of dispersion and how this process may be controlling the profile of salt in interstitial water. Under the influence of diffusion alone salt could not penetrate into the sediment deeply into the sediment, especially in the face of upward advection. In many of the investigated sites, however, salt was able to penetrate deep into the sediment even in the face of large upward advection. I hypothesized that dispersion may allow for this penetration of salt in all sites. The processes of density-mixing, tidal and wave pumping, bioirrigation and others likely control this process. In addition, the character of the sediment itself is very important in controlling how salt may disperse into the sediment. As is seen in fluvial estuaries, the dispersion seems to be controlled by the rate of advection itself and, therefore, will likely change with changing rates of advection, which occur frequently.

This thesis discusses how dispersion is site-specific and makes some inferences as to the factors which control it. However, it should be taken as a preliminary body of work. Specific experiments should be designed both in the laboratory and in the field to determine the rate of dispersion in the sediment. In the laboratory one could set up a tank to test the impact of: 1) type of sediment, 2) density of overlying water, 3) rate of upward advection, 4) tidal elevation changes, and 5) bioirrigation. In the field, it will be more difficult to isolate one factor in the process of dispersion, but reconnaissance work could be used to find sites of high and low discharge, different types of sediment,

different local benthic fauna, etc. to determine what are the dominant factors in dispersive processes.

Once we gain a greater understanding of the factors that impact dispersion we can infer how different processes control the flux of constituents into the body of water from the sediment. We may then also be able to state, with greater accuracy, the ecological significance of SGD.

D. Understanding of anthropogenic modification on the SGD signature of coastal lagoons

The study of SGD came about in order to better understand the hydrological balance of drainage basins. Soon investigators began to realize that SGD can have a significant ecological impact on those systems. One of the goals of the study of SGD is to alert managers and the public to the possible implications of this discharge, thus enabling them to make informed decisions regarding the modification or protection of their ecosystems.

Recently, however, we have begun to realize that the modifications we are making affect the discharge of groundwater and its associated constituents in coastal waters (e.g. Nakayama et al. 2007). In a previous manuscript, I discussed the possibility that dredging channels and creating bulkheads along shorelines may have significantly changed the SGD process in the Venice Lagoon (Rapaglia 2005). In this thesis I investigated the effects of drilling pier pilings through confining layers, increasing natural discharge into West Neck Bay, NY. In addition, I returned to the Venice Lagoon

in order to examine the possible impact of the emplacement of large barriers at the bottom of the three inlets to safeguard the city of Venice from future flooding. I discussed how the difference in water elevation between the sea and the lagoon when the barriers are closed, may drive a significant flow of water beneath the barrier beaches and into the lagoon.

Future work regarding both the study of SGD as well as projects which are based on the impact of the input of SGD should account for anthropogenic modification. From the source of groundwater flowing to the sea, both the flow and the composition of groundwater encounters human inputs' from physical barriers of flow, such as the foundation of buildings to the input of chemicals from fertilizers and pesticides (Swartz et al. 2006). In addition, recently, other discharges such as industrial plant effluent are flowing into groundwater recharge zones. We must first understand how modifications to the hydrological character of an area affect discharge. If this is possible, better decisions may be made in the future regarding which type of modification will have the best possible outcome when considering all aspects of an ecosystem. In this thesis I have provided some examples of important modifications, but there are many others. The only way to know for sure is to make measurements in a site before and after modification is complete. Unfortunately, if problems do occur, it is often too late to remedy the situation. Perhaps the easiest way to determine the impact of a project is to model what the flow will be like when the modifications are done, or to model what the natural situation would be like without these modifications. Every now and then there is the possibility to measure the SGD signature before and after modification takes place. In the case of the Venice Lagoon, we are fortunate to be involved in the measurement of

SGD as the tidal barriers mentioned in Chapter V are being emplaced to separate the lagoon from the sea.

Over the last three decades, the study of SGD has gone from a fledgling subject to an important scientific field. We have learned much and made many improvements in our techniques. Still, this is a complex process and there remains a great deal to study before we can make accurate statements concerning both the flow of water across the sediment-sea interface and the flux of its associated constituents. This thesis has attempted to clarify some of the processes which affect SGD on a small-scale as well as to determine the impact of human modification in order to increase our understanding of the importance of this process in local, regional, and global systems.

References

Bokuniewicz, H. 1980. Groundwater Seepage into Great South Bay, New-York. Estuarine and Coastal Marine Science. 10 (4): 437-444.

Bokuniewicz, H. Rapaglia, J. and Beck A. 2007. Submarine Groundwater Discharge from a Volcanic Island: A case study of Mauritius Island. International Journals of Oceans and Oceanography. In Press.

Bone, S.E., Gonnea, M.E., and Charette, M.A. 2006. Geochemical cycling of arsenic in a coastal aquifer. Environmental Science and Technology. 40: 3273-3278.

Burnett, W. C. and Dulaiova, H. 2006. Radon as a tracer of submarine groundwater discharge into a boat basin in Donnalucata, Sicily. Continental Shelf Research. 26: 862-873.

Burnett, W.C., Taniguchi, M. and Oberdorfer, J. 2001. Measurement and significance of the direct discharge of groundwater into the coastal zone. Journal of Sea Research 46 (2): 109-116.

Burnett, W.C. Aggarwal, P.K., Bokuniewicz, H., Cable, J.E., Charette, M.A., Kontar, E., Krupa, S., Kulkarni, K.M., Loveless, A., Moore, W.S., Oberdorfer, J.A., Oliveira,

J., Ozyurt, N., Povinec, P., Privitera, A.M.G., Rajar, R., Ramessur, R.T., Scholten, J., Stieglitz, T., Taniguchi, M., and Turner, J.V., 2006. Quantifying submarine groundwater discharge in the coastal zone via multiple methods. Science of the Total Environment. 367 (2-3): 498-543.

Charette, M.A., and Sholkovitz, E.R.2006. Trace element cycling in a subterranean estuary: Part 2. Geochemistry of the pore water. Geochimica et Cosmochimica Acta. 70 (4): 811-826.

Charette, M.A., and Allen, M.C. 2006. Precision groundwater sampling in coastal aquifers using a direct push shielded screen well-point system. Groundwater Monitoring and Remediation. 26 (2): 87-93.

Martin, J.B., Cable, J.E., Jaeger, J., Hartl, K., and Smith, C.G. 2006. Thermal and chemical evidence for rapid water exchange across the sediment-water interface by bioirrigation in the Indian River Lagoon, Florida. Limnology and Oceanography 51 (3): 1332-1341.

Moore, W.S. 1999. The subterranean estuary: a reaction zone of ground water and sea water. Marine Chemistry. 65 (1-2): 111-125.

Nakayama, T., Watanabe, M., Tanji, K., and Moriuka T. 2007. Effect of underground urban structures on eutrophic coastal environments. Science of the Total Environment. In press.

Rapaglia, J., 2005. Submarine groundwater discharge into the Venice lagoon, Italy. Estuaries. 28 (5):705-713.

Stieglitz, T., Rapaglia, J., and Krupa, S. 2007. An effect of pier pilings on near-shore submarine groundwater discharge from a confined aquifer. Estuaries. In press.

Swartz, C.H. Reddy, S., Benotti, M.J., Yin, H., Barber, L.B., Brownawell, B.J., and Rudell, R.A., 2006. Steroid estrogens, nonylphenol ethoxylate metabolites, and other wastewater contaminants in groundwater affected by a residential septic system on Cape Cod, MA. Environmental Science and Technology. 40. 4894-4902.

Taniguchi, M.; Burnett, W.C., Cable J.E., and Turner. J.V. 2002. Investigation of submarine groundwater discharge. Hydrological Processes. 16: 2115-2129.

Taniguchi, M., Turner, J.V., and Smith, A. 2003 Evaluations of groundwater discharge rates from subsurface temperature in Cockburn Sound, Western Australia. Biogeochemistry. 66:111–24.

APPENDIX A: ALL SEEPAGE METER MEASUREMENTS USED IN THIS THESIS

LOCATION	DATE	DEVICE	TIME	VOLUME	**SGD**	SALINITY
SHELTER ISLAND	05/20/02	SM1	10:54	1280	**24.0**	12
SHELTER ISLAND	05/20/02	SM1	14:17	1600	**30.0**	13
SHELTER ISLAND	05/20/02	SM1	15:09	1518	**28.5**	12
SHELTER ISLAND	05/20/02	SM1	16:02	1090	**20.4**	15
SHELTER ISLAND	05/20/02	SM1	16:41	872	**16.4**	15
SHELTER ISLAND	05/21/02	SM1	16:53	1390	**26.1**	
SHELTER ISLAND	05/21/02	SM1	17:27	1180	**22.1**	
SHELTER ISLAND	05/21/02	SM1	18:08	870	**16.3**	
SHELTER ISLAND	05/22/02	SM1	7:29	550	**10.3**	
SHELTER ISLAND	05/22/02	SM1	8:11	760	**14.3**	
SHELTER ISLAND	05/22/02	SM1	8:52	780	**15.1**	11.5
SHELTER ISLAND	05/22/02	SM1	9:29	840	**18.2**	10.4
SHELTER ISLAND	05/22/02	SM1	10:07	850	**16.5**	9.3
SHELTER ISLAND	05/22/02	SM1	11:24	1500	**28.1**	6.8
SHELTER ISLAND	05/22/02	SM1	12:01	1623	**30.4**	6.5
SHELTER ISLAND	05/22/02	SM1	17:18	1410	**26.4**	*1.6*
SHELTER ISLAND	05/22/02	SM1	17:54	1150	**21.6**	17
SHELTER ISLAND	05/22/02	SM1	18:29	1100	***21.5***	
SHELTER ISLAND	05/22/02	SM1	19:08	780	**13.7**	
SHELTER ISLAND	05/23/02	SM1	12:10	3180	**29.8**	
SHELTER ISLAND	05/23/02	SM1	13:04	2240	**33.2**	7
SHELTER ISLAND	5/20/2002	SM2	10:57	1510	**26.5**	6
SHELTER ISLAND	5/20/2002	SM2	11:55	1620	**29.4**	10
SHELTER ISLAND	5/20/2002	SM2	13:18	1542	**28.9**	11
SHELTER ISLAND	5/20/2002	SM2	14:05	1460	**27.4**	10
SHELTER ISLAND	5/20/2002	SM2	15:00	1260	**23.6**	12
SHELTER ISLAND	5/20/2002	SM2	15:50	1050	**19.7**	13
SHELTER ISLAND	5/20/2002	SM2	16:31	960	**18.0**	15
SHELTER ISLAND	5/21/2002	SM2	12:35	1640	**30.8**	
SHELTER ISLAND	5/21/2002	SM2	14:43	1730	**32.4**	
SHELTER ISLAND	5/21/2002	SM2	15:33	1510	**26.5**	
SHELTER ISLAND	5/21/2002	SM2	16:12	1310	**24.6**	
SHELTER ISLAND	5/21/2002	SM2	16:51	1200	**21.8**	
SHELTER ISLAND	5/21/2002	SM2	17:30	1090	**19.2**	
SHELTER ISLAND	5/21/2002	SM2	18:11	820	**14.9**	
SHELTER ISLAND	5/22/2002	SM2	7:32	830	**17.3**	
SHELTER ISLAND	5/22/2002	SM2	8:55	970	**19.5**	15.6
SHELTER ISLAND	5/22/2002	SM2	9:33	680	**13.7**	13.5
SHELTER ISLAND	5/22/2002	SM2	10:07	880	**16.0**	11.7
SHELTER ISLAND	5/22/2002	SM2	10:47	980	**19.0**	11.2
SHELTER ISLAND	5/22/2002	SM2	11:26	1230	**23.9**	10

SHELTER ISLAND	5/22/2002	SM2	12:04	1500	**27.2**	9
SHELTER ISLAND	5/22/2002	SM2	12:40	1580	**29.6**	8.8
SHELTER ISLAND	5/22/2002	SM2	13:16	*1640*	***31.8***	8.8
SHELTER ISLAND	5/22/2002	SM2	16:00	850	**17.7**	*2.8*
SHELTER ISLAND	5/22/2002	SM2	16:43	1220	**22.9**	10.7
SHELTER ISLAND	5/22/2002	SM2	17:20	1030	**20.7**	
SHELTER ISLAND	5/22/2002	SM2	17:57	870	**16.3**	
SHELTER ISLAND	5/22/2002	SM2	18:29	650	**13.5**	
SHELTER ISLAND	5/22/2002	SM2	19:08	580	**11.3**	
SHELTER ISLAND	5/23/2002	SM2	12:20	1770	**15.1**	4
SHELTER ISLAND	5/23/2002	SM2	13:09	1700	**22.8**	10
SHELTER ISLAND	5/23/2002	SM2	13:47	1300	**26.1**	
SHELTER ISLAND	5/23/2002	SM2	15:33	1900	**26.7**	8
SHELTER ISLAND	5/23/2002	SM2	16:25	1430	**26.0**	
SHELTER ISLAND	5/20/2002	SM2	11:00	1770	**28.5**	8
SHELTER ISLAND	5/20/2002	SM2	12:01	1450	**27.2**	11
SHELTER ISLAND	5/20/2002	SM2	12:40	1540	**28.9**	10
SHELTER ISLAND	5/20/2002	SM2	13:26	1410	***26.4***	10
SHELTER ISLAND	5/20/2002	SM2	14:12	1430	**26.8**	14
SHELTER ISLAND	5/20/2002	SM2	15:05	1260	***22.9***	15
SHELTER ISLAND	5/20/2002	SM2	15:54	980	**18.4**	15
SHELTER ISLAND	5/20/2002	SM2	16:34	900	**16.9**	17
SHELTER ISLAND	5/21/2002	SM3	11:52	1460	**27.4**	
SHELTER ISLAND	5/21/2002	SM3	12:39	1510	**28.3**	
SHELTER ISLAND	5/21/2002	SM3	13:19	1760	**33.0**	
SHELTER ISLAND	5/21/2002	SM3	13:54	1607	**30.1**	
SHELTER ISLAND	5/21/2002	SM3	14:46	1550	**29.1**	
SHELTER ISLAND	5/21/2002	SM3	15:26	1720	**28.5**	
SHELTER ISLAND	5/21/2002	SM3	16:09	1320	**24.8**	
SHELTER ISLAND	5/21/2002	SM3	16:50	1280	**21.8**	
SHELTER ISLAND	5/21/2002	SM3	17:32	1180	**20.1**	
SHELTER ISLAND	5/21/2002	SM3	18:14	1040	**18.3**	
SHELTER ISLAND	5/22/2002	SM3	7:35	1100	**23.8**	
SHELTER ISLAND	5/22/2002	SM3	8:17	1060	**19.9**	
SHELTER ISLAND	5/22/2002	SM3	8:59	670	**14.5**	14.8
SHELTER ISLAND	5/22/2002	SM3	9:36	750	**14.6**	14
SHELTER ISLAND	5/22/2002	SM3	10:14	950	**16.2**	12.6
SHELTER ISLAND	5/22/2002	SM3	10:50	1080	**19.7**	12.1
SHELTER ISLAND	5/22/2002	SM3	11:29	1410	**25.6**	11.1
SHELTER ISLAND	5/22/2002	SM3	12:06	1670	**30.3**	10.1
SHELTER ISLAND	5/22/2002	SM3	12:41	1700	**31.9**	10.2
SHELTER ISLAND	5/22/2002	SM3	13:20	1810	**31.8**	9.1
SHELTER ISLAND	5/22/2002	SM3	13:53	1680	**31.5**	10
SHELTER ISLAND	5/22/2002	SM3	15:29	1500	**28.1**	10.2
SHELTER ISLAND	5/22/2002	SM3	16:07	1550	**30.1**	10.1
SHELTER ISLAND	5/22/2002	SM3	16:48	1550	**28.1**	10.1

SHELTER ISLAND	5/22/2002	SM3	17:23	1260	**24.4**	
SHELTER ISLAND	5/22/2002	SM3	18:00	1220	**22.1**	
SHELTER ISLAND	5/22/2002	SM3	18:34	800	**17.3**	
SHELTER ISLAND	5/22/2002	SM3	19:08	560	**13.7**	
SHELTER ISLAND	5/23/2002	SM3	12:30	1850	**17.6**	7
SHELTER ISLAND	5/23/2002	SM3	13:13	2030	**26.0**	11
SHELTER ISLAND	5/23/2002	SM3	13:50	1600	**30.0**	14
SHELTER ISLAND	5/23/2002	SM3	14:36	2100	***28.1***	13
SHELTER ISLAND	5/23/2002	SM3	15:17	2220	**36.7**	13
SHELTER ISLAND	5/23/2002	SM3	15:50	1610	***30.2***	14
SHELTER ISLAND	5/23/2002	SM3	16:25	2030	**33.6**	
MAURITIUS	3/19/2005	M1	15:31	1520	**34.2**	
MAURITIUS	3/19/2005	M1	16:08	3120	**70.2**	
MAURITIUS	3/19/2005	M1	16:36	3140	**147.2**	
MAURITIUS	3/19/2005	M1	16:57	6730	**180.3**	
MAURITIUS	3/19/2005	M1	17:23	4000	**204.5**	
MAURITIUS	3/19/2005	M1	17:36	6920	**278.0**	
MAURITIUS	3/19/2005	M1	17:59	7260	**185.6**	
MAURITIUS	3/20/2005	M1	9:17	4240	**159.0**	
MAURITIUS	3/20/2005	M1	9:41	1100.00	**14.4**	
MAURITIUS	3/20/2005	M1	10:24	7240	**62.7**	
MAURITIUS	3/20/2005	M1	11:29	6050	**148.0**	
MAURITIUS	3/20/2005	M1	11:57	7060	**361.0**	
MAURITIUS	3/20/2005	M1	12:14	7300	**178.5**	
MAURITIUS	3/20/2005	M1	12:40	6700	**145.0**	
MAURITIUS	3/20/2005	M1	13:06	7320	**216.7**	
MAURITIUS	3/20/2005	M1	13:30	13040	**174.6**	
MAURITIUS	3/20/2005	M1	14:12	6840	**202.5**	
MAURITIUS	3/20/2005	M1	14:31	12680	**182.9**	
MAURITIUS	3/20/2005	M1	15:10	13080	**319.9**	
MAURITIUS	3/20/2005	M1	15:45	9940	**279.6**	
MAURITIUS	3/20/2005	M1	16:09	13000	**228.5**	
MAURITIUS	3/20/2005	M1	16:42	7040	**360.0**	
MAURITIUS	3/20/2005	M1	16:54	9500	**267.2**	
MAURITIUS	3/20/2005	M1	17:14	7540	**124.7**	
MAURITIUS	3/22/2005	M1	14:02	4570	**321.3**	5.00
MAURITIUS	3/22/2005	M1	14:12	5200	**225.0**	5.00
MAURITIUS	3/22/2005	M1	14:30	2780	**312.8**	5
MAURITIUS	3/22/2005	M1	16:25	3660	**411.8**	5
MAURITIUS	3/22/2005	M1	17:38	2480	**279.0**	5
MAURITIUS	3/19/2005	M2	15:30	1200	**28.1**	
MAURITIUS	3/19/2005	M2	16:05	660	**14.9**	
MAURITIUS	3/19/2005	M2	16:32	1240	**22.5**	
MAURITIUS	3/19/2005	M2	17:04	2940	**28.0**	
MAURITIUS	3/20/2005	M2	9:18	1370	**18.3**	
MAURITIUS	3/20/2005	M2	10:00	920	**13.6**	
MAURITIUS	3/20/2005	M2	10:38	1600	**14.1**	

MAURITIUS	3/20/2005	M2	11:42	2070	**17.4**	
MAURITIUS	3/20/2005	M2	12:49	2400	**14.7**	36
MAURITIUS	3/20/2005	M2	14:21	1500	**22.8**	35
MAURITIUS	3/20/2005	M2	14:59	2190	**12.7**	
MAURITIUS	3/20/2005	M2	16:36	1100	**11.5**	35
MAURITIUS	3/20/2005	M2	17:30	1340	**16.4**	36
MAURITIUS	3/19/2005	M3	15:33	1416	**28.4**	
MAURITIUS	3/19/2005	M3	16:10	2500	**52.1**	
MAURITIUS	3/19/2005	M3	16:40	1440	**24.5**	
MAURITIUS	3/19/2005	M3	17:13	5760	**55.9**	
MAURITIUS	3/20/2005	M3	9:19	5680	**91.3**	
MAURITIUS	3/20/2005	M3	9:56	4620	**72.2**	
MAURITIUS	3/20/2005	M3	10:32	6600	**68.8**	
MAURITIUS	3/20/2005	M3	11:26	1600	**56.3**	
MAURITIUS	3/20/2005	M3	11:27	7140	**121.7**	
MAURITIUS	3/20/2005	M3	12:00	6800	**225.0**	
MAURITIUS	3/20/2005	M3	12:34	6360	**162.6**	
MAURITIUS	3/20/2005	M3	12:56	4980	**147.4**	
MAURITIUS	3/20/2005	M3	13:15	7000	**93.8**	22
MAURITIUS	3/20/2005	M3	13:57	7140	**91.3**	22
MAURITIUS	3/20/2005	M3	14:59	9400	**160.2**	
MAURITIUS	3/20/2005	M3	15:45	5770	**154.6**	
MAURITIUS	3/20/2005	M3	16:14	11500	**202.1**	20
MAURITIUS	3/20/2005	M3	16:46	8900	**156.4**	22
MAURITIUS	3/20/2005	M3	17:31	6920	**176.9**	21
MAURITIUS	3/19/2005	M4	16:16	940	**14.7**	
MAURITIUS	3/19/2005	M4	16:56	1020	**14.3**	
MAURITIUS	3/19/2005	M4	17:40	800	**10.5**	
MAURITIUS	3/19/2005	M4	18:14	1380	**22.8**	
MAURITIUS	3/20/2005	M4	10:23	2240	**22.5**	
MAURITIUS	3/20/2005	M4	11:20	2330	**23.4**	
MAURITIUS	3/20/2005	M4	12:25	4520	**56.5**	
MAURITIUS	3/20/2005	M4	13:46	2840	**20.0**	36
MAURITIUS	3/20/2005	M4	15:17	3440	**21.7**	36
MAURITIUS	3/20/2005	M4	16:20	2600	**23.2**	37
MAURITIUS	3/20/2005	M4	17:05	1840	**23.0**	37
MAURITIUS	3/20/2005	M4	17:55	1920	**21.6**	36
MAURITIUS	3/22/2005	M4	12:57	2000	**16.8**	36
MAURITIUS	3/22/2005	M4	14:10	1700	**18.4**	35
MAURITIUS	3/22/2005	M4	15:31	1880	**16.0**	36
MAURITIUS	3/22/2005	M4	16:43	2460	**19.2**	36
MAURITIUS	3/22/2005	M4	17:17	840	**13.9**	36
MAURITIUS	3/20/2005	M5	9:52	740	**11.9**	
MAURITIUS	3/20/2005	M5	10:27	1270	**12.3**	
MAURITIUS	3/20/2005	M5	11:25	1540	**15.2**	
MAURITIUS	3/20/2005	M5	12:23	2000	**12.9**	36
MAURITIUS	3/20/2005	M5	13:50	1650	**10.7**	35

MAURITIUS	3/20/2005	M5	15:17	1460	**12.4**	
MAURITIUS	3/20/2005	M5	16:35	1240	**20.5**	37
MAURITIUS	3/20/2005	M5	17:15	400	**5.0**	37
MAURITIUS	3/22/2005	M5	11:53	1780	**16.1**	35
MAURITIUS	3/22/2005	M5	13:21	1560	**17.2**	35
MAURITIUS	3/22/2005	M5	14:23	1500	**12.1**	36
MAURITIUS	3/22/2005	M5	15:33	2100	**16.4**	36
MAURITIUS	3/22/2005	M5	16:48	1160	**20.4**	36
MAURITIUS	3/20/2005	M6	11:11	7050	**123.9**	
MAURITIUS	3/20/2005	M6	11:43	7900	**277.7**	
MAURITIUS	3/20/2005	M6	11:57	7460	**262.3**	
MAURITIUS	3/20/2005	M6	12:08	7050	**283.3**	
MAURITIUS	3/20/2005	M6	12:22	6100	**490.2**	
MAURITIUS	3/20/2005	M6	12:30	7620	**214.3**	
MAURITIUS	3/20/2005	M6	13:18	6520	**111.1**	6
MAURITIUS	3/20/2005	M6	13:53	13560	**173.4**	5
MAURITIUS	3/20/2005	M6	14:39	14200	**199.7**	5
MAURITIUS	3/20/2005	M6	15:37	11000	**412.5**	5
MAURITIUS	3/20/2005	M6	15:52	13540	**292.9**	
MAURITIUS	3/20/2005	M6	16:25	13160	**264.4**	
MAURITIUS	3/20/2005	M6	17:00	10400	**307.9**	5
MAURITIUS	3/20/2005	M6	17:27	11200	**190.9**	5
MAURITIUS	3/20/2005	M6	17:55	19480	**304.4**	
MAURITIUS	3/22/2005	M6	11:49	26000	**365.6**	7
MAURITIUS	3/22/2005	M6	13:17	3420	**384.8**	
MAURITIUS	3/22/2005	M6	14:00	3720	**414.4**	6
MAURITIUS	3/22/2005	M6	15:05	3740	**420.8**	5
MAURITIUS	3/22/2005	M6	16:25	3660	**411.8**	5
MAURITIUS	3/22/2005	M6	17:40	3640	**409.5**	4
MAURITIUS	3/20/2005	M7	10:55	940	**10.2**	
MAURITIUS	3/20/2005	M7	11:47	1220	**4.3**	37
MAURITIUS	3/20/2005	M7	14:25	1000	**15.2**	36
MAURITIUS	3/20/2005	M7	15:02	1850	**11.4**	
MAURITIUS	3/20/2005	M7	16:34	930	**9.0**	36
MAURITIUS	3/20/2005	M7	17:32	960	**14.6**	37
MAURITIUS	3/20/2005	M8	11:03	1600	**17.3**	
MAURITIUS	3/20/2005	M8	11:55	2210	**36.6**	
MAURITIUS	3/20/2005	M8	12:29	470	**2.2**	27
MAURITIUS	3/20/2005	M8	14:27	800	**11.8**	36
MAURITIUS	3/20/2005	M8	16:32	3220	**28.8**	36
MAURITIUS	3/20/2005	M8	17:35	1300	**22.2**	36
MAURITIUS	3/21/2005	M9	17:47	840	**7.6**	
MAURITIUS	3/22/2005	M9	6:30	380	**10.2**	37
MAURITIUS	3/22/2005	M9	6:56	1100	**2.5**	
MAURITIUS	3/22/2005	M9	11:00	1060	**8.3**	36
MAURITIUS	3/22/2005	M9	12:18	1120	**7.4**	36

MAURITIUS	3/22/2005	M9	13:45	760	**5.9**	37
MAURITIUS	3/22/2005	M9	14:59	850	**7.2**	38
MAURITIUS	3/22/2005	M9	16:07	500	**5.5**	36
MAURITIUS	3/23/2005	M9	10:14	1440	**11.4**	36
MAURITIUS	3/23/2005	M9	11:26	2450	**21.5**	37
MAURITIUS	3/23/2005	M9	13:24	1750	**6.5**	36
MAURITIUS	3/23/2005	M9	15:58	1420	**5.9**	
MAURITIUS	3/22/2005	M10	11:07	970	**11.9**	
MAURITIUS	3/22/2005	M10	11:54	640	**6.8**	35
MAURITIUS	3/22/2005	M10	12:48	880	**7.9**	36
MAURITIUS	3/22/2005	M10	13:52	220	**1.0**	35
MAURITIUS	3/22/2005	M10	15:58	320	**2.5**	
MAURITIUS	3/22/2005	M11	12:13	850	**5.8**	36
MAURITIUS	3/22/2005	M11	13:38	950	**7.5**	36
MAURITIUS	3/22/2005	M11	14:50	1200	**8.0**	35.5
MAURITIUS	3/22/2005	M11	16:15	980	**11.5**	35.5
MAURITIUS	3/22/2005	M12	12:15	430.00	**2.9**	36
MAURITIUS	3/22/2005	M12	13:41	420	**2.9**	38
MAURITIUS	3/22/2005	M13	11:40	7950	**75.8**	22
MAURITIUS	3/22/2005	M13	12:45	6000	**116.4**	20
MAURITIUS	3/22/2005	M13	13:24	6450	**213.4**	20
MAURITIUS	3/22/2005	M13	14:06	6000	**146.7**	11
MAURITIUS	3/22/2005	M13	15:00	2340	**239.3**	10
MAURITIUS	3/22/2005	M13	16:25	1620	**182.3**	8
MAURITIUS	3/22/2005	M13	17:33	1660	**186.8**	10
MAURITIUS	3/22/2005	M14	11:12	3430	**96.5**	
MAURITIUS	3/22/2005	M14	12:10	4000	**150.0**	22
MAURITIUS	3/22/2005	M14	12:29	3600	**126.6**	20
MAURITIUS	3/22/2005	M15	12:20	3160	**355.5**	5.5
MAURITIUS	3/22/2005	M15	13:20	3000	**368.4**	5
MAURITIUS	3/23/2005	M16	10:17	560	**4.8**	36
MAURITIUS	3/22/2005	M16	11:25	1300	**6.4**	37
MAURITIUS	3/22/2005	M16	13:19	440	**3.6**	38
MAURITIUS	3/22/2005	M16	14:40	640	**4.7**	
MAURITIUS	3/22/2005	M16	16:20	1020	**5.0**	36
MAURITIUS	3/23/2005	M17	10:30	1220	**5.2**	36
MAURITIUS	3/23/2005	M17	12:46	750	**4.4**	36
MAURITIUS	3/23/2005	M17	14:30	1370	**8.5**	
MAURITIUS	3/23/2005	M17	16:09	1430	**6.7**	36
MAURITIUS	3/23/2005	M18	10:35	3000	**15.2**	35
MAURITIUS	3/23/2005	M18	12:30	2630	**13.3**	36

MAURITIUS	3/23/2005	M18	14:25	2000	**10.6**	
MAURITIUS	3/23/2005	M18	16:14	2360	**12.1**	36
MAURITIUS	3/24/2005	M18	10:27	1020	**11.3**	35
MAURITIUS	3/24/2005	M18	11:21	620	**9.7**	35
MAURITIUS	3/24/2005	M18	11:59	830	**15.6**	35
MAURITIUS	3/24/2005	M18	12:31	950	**14.4**	35
MAURITIUS	3/23/2005	M19	10:45	7200	**45.5**	36
MAURITIUS	3/23/2005	M19	12:20	6310	**35.1**	38
MAURITIUS	3/23/2005	M19	14:13	6350	**29.0**	
MAURITIUS	3/23/2005	M19	4:22	5000	**30.9**	36
MAURITIUS	3/23/2005	M19	17:56	420	**47.3**	
MAURITIUS	3/24/2005	M19	10:12	2340	**25.8**	37
MAURITIUS	3/24/2005	M19	11:09	1270	**25.5**	35
MAURITIUS	3/24/2005	M19	11:42	2110	**34.9**	35
MAURITIUS	3/24/2005	M19	12:18	820	**12.8**	35
MAURITIUS						
MAURITIUS	3/23/2005	M20	12:02	4350	**22.4**	38
MAURITIUS	3/23/2005	M20	13:59	6500	**25.0**	
MAURITIUS	3/23/2005	M20	16:29	3000	**19.4**	36
MAURITIUS	3/24/2005	M20	10:23	850	**10.4**	36
MAURITIUS	3/24/2005	M20	11:12	620	**10.0**	35
MAURITIUS	3/24/2005	M20	11:51	830	**14.1**	35
MAURITIUS	3/24/2005	M20	12:26	650	**11.1**	32
MAURITIUS	3/24/2005	M21	10:10	910	**10.0**	35
MAURITIUS	3/24/2005	M21	11:04	650	**11.4**	35
MAURITIUS	3/24/2005	M21	11:39	460	**5.9**	35
MAURITIUS	3/24/2005	M21	12:15	610	**9.3**	35
MAURITIUS	3/21/2005	B1	10:06	640	**12.4**	36
MAURITIUS	3/21/2005	B1	10:36	230	**3.2**	
MAURITIUS	3/21/2005	B1	11:20	160	**2.6**	
MAURITIUS	3/21/2005	B1	11:57	-270	**-4.5**	
MAURITIUS	3/21/2005	B1	12:35	-440	**-8.3**	
MAURITIUS	3/21/2005	B1	13:07	0	**0.0**	
MAURITIUS	3/21/2005	B1	13:39	470	**4.8**	
MAURITIUS	3/21/2005	B1	14:34	430	**9.0**	
MAURITIUS	3/21/2005	B1	15:02	0	**0.0**	
MAURITIUS	3/21/2005	B1	15:34	60	**0.7**	
MAURITIUS	3/21/2005	B1	16:28	940	**11.5**	
MAURITIUS	3/22/2005	B1	7:09	6250	**18.1**	
MAURITIUS	3/21/2005	B2	10:07	170	**3.2**	
MAURITIUS	3/21/2005	B2	10:38	-310	**-4.1**	
MAURITIUS	3/21/2005	B2	11:22	-150	**-2.3**	
MAURITIUS	3/21/2005	B2	12:01	280	**4.4**	
MAURITIUS	3/21/2005	B2	12:40	370	**7.4**	
MAURITIUS	3/21/2005	B2	13:42	380	**4.5**	
MAURITIUS	3/21/2005	B2	14:33	200	**4.5**	

MAURITIUS	3/21/2005	B2	15:00	280	**4.6**	
MAURITIUS	3/21/2005	B2	15:36	520	**5.5**	
MAURITIUS	3/21/2005	B2	16:31	0	**0.0**	
MAURITIUS	3/22/2005	B2	7:10	2070	**6.1**	
MAURITIUS	3/21/2005	B3	10:09	570.00	**10.7**	
MAURITIUS	3/21/2005	B3	10:41	1200.00	**16.1**	
MAURITIUS	3/21/2005	B3	11:25	1400.00	**20.7**	36
MAURITIUS	3/21/2005	B3	12:04	1130.00	**17.2**	36
MAURITIUS	3/21/2005	B3	12:45	780.00	**15.7**	
MAURITIUS	3/21/2005	B3	13:15	920.00	**18.5**	
MAURITIUS	3/21/2005	B3	13:43	1270.00	**17.0**	
MAURITIUS	3/21/2005	B3	14:27	1400.00	**21.9**	36
MAURITIUS	3/21/2005	B3	15:04	400.00	**6.8**	36
MAURITIUS	3/21/2005	B3	15:37	1400.00	**14.3**	
MAURITIUS	3/21/2005	B3	16:44	880.00	**21.5**	
MAURITIUS	3/22/2005	B3	7:12	6320.00	**19.1**	
MAURITIUS	3/21/2005	B4	10:12	540	**3.9**	
MAURITIUS	3/21/2005	B4	11:33	4140	**17.3**	
MAURITIUS	3/21/2005	B4	13:52	1060	**5.2**	
MAURITIUS	3/21/2005	B4	15:29	20	**0.1**	
MAURITIUS	3/22/2005	B4	7:17	2350	**7.6**	
MAURITIUS	3/21/2005	B5	10:12	540	**3.9**	
MAURITIUS	3/21/2005	B5	11:33	4140	**17.3**	
MAURITIUS	3/21/2005	B5	13:52	1060	**5.2**	
MAURITIUS	3/21/2005	B5	15:29	20	**0.1**	
MAURITIUS	3/22/2005	B5	7:17	2350	**7.6**	
CANARSIE PIER	8/23/2005	CP3	10:52		**-4.9**	31
CANARSIE PIER	8/23/2005	CP3	11:31		**1.2**	30
CANARSIE PIER	8/23/2005	CP3	12:09		**-0.9**	31
CANARSIE PIER	8/23/2005	CP3	12:45		**0.0**	30
CANARSIE PIER	8/23/2005	CP3	13:41		**17.8**	30
CANARSIE PIER	8/23/2005	CP4	10:52		**-1.2**	30
CANARSIE PIER	8/23/2005	CP4	11:31		**0.0**	29
CANARSIE PIER	8/23/2005	CP4	12:09		**0.0**	27
CANARSIE PIER	8/23/2005	CP4	12:45		**1.9**	28
CANARSIE PIER	8/23/2005	CP4	13:43		**9.9**	28
CANARSIE PIER	8/23/2005	CP4	14:12		**16.9**	30
CANARSIE PIER	8/23/2005	CP5	10:52		**-4.4**	30
CANARSIE PIER	8/23/2005	CP5	11:31		**-4.4**	26
CANARSIE PIER	8/23/2005	CP5	12:09		**0.0**	30
CANARSIE PIER	8/23/2005	CP5	12:45		**1.3**	28
CANARSIE PIER	8/23/2005	CP5	13:43		**4.8**	31
CANARSIE PIER	8/23/2005	CP5	14:20		**8.4**	30
CANARSIE PIER	2/10/2006	CP7	11:00		**1.2**	
CANARSIE PIER	2/10/2006	CP7	11:30		**1.1**	

CANARSIE PIER	2/10/2006	CP7	12:00		**1.3**	
CANARSIE PIER	2/10/2006	CP7	12:30		**0.9**	
CANARSIE PIER	2/10/2006	CP7	13:00		**0.3**	
CANARSIE PIER	2/10/2006	CP7	13:30		**0.7**	
CANARSIE PIER	2/10/2006	CP7	14:00		**0.3**	
CANARSIE PIER	2/10/2006	CP8	11:00		**1.3**	
CANARSIE PIER	2/10/2006	CP8	11:30		**1.3**	
CANARSIE PIER	2/10/2006	CP8	12:00		**1.1**	
CANARSIE PIER	2/10/2006	CP8	12:30		**1.8**	
CANARSIE PIER	2/10/2006	CP8	13:00		**1.1**	
CANARSIE PIER	2/10/2006	CP8	13:30		**1.1**	
CANARSIE PIER	2/10/2006	CP8	14:00		**1.2**	
CANARSIE PIER	3/24/2006	CP9	8:34		**5.4**	
CANARSIE PIER	3/24/2006	CP9	9:30		**4.9**	
CANARSIE PIER	3/24/2006	CP9	10:40		**3.3**	
CANARSIE PIER	3/24/2006	CP9	11:22		**4.0**	
CANARSIE PIER	3/24/2006	CP9	11:50		**1.9**	
CANARSIE PIER	3/24/2006	CP9	12:39		**2.8**	
CANARSIE PIER	5/4/2006	CP10	7:26	90	**1.7**	
CANARSIE PIER	5/4/2006	CP10	7:57	180	**3.0**	
CANARSIE PIER	5/4/2006	CP10	8:31	80	**1.4**	
CANARSIE PIER	5/4/2006	CP10	9:04	60	**1.1**	
CANARSIE PIER	5/4/2006	CP10	9:34	160	**3.0**	
CANARSIE PIER	5/4/2006	CP10	10:04	220	**3.4**	
CANARSIE PIER	5/4/2006	CP10	10:40	80	**1.3**	
CANARSIE PIER	5/4/2006	CP10	11:15	0	**0.0**	
CANARSIE PIER	5/4/2006	CP10	11:45	60	**1.0**	
CANARSIE POL	4/20/2006	POL1	8:29	250	**3.7**	29.05
CANARSIE POL	4/20/2006	POL1	9:08	180	**3.4**	28.5
CANARSIE POL	4/20/2006	POL1	9:39	180	**3.8**	28.05
CANARSIE POL	4/20/2006	POL1	10:06	225	**4.4**	27.7
CANARSIE POL	4/20/2006	POL1	10:35	300	**3.0**	27.4
CANARSIE POL	4/20/2006	POL1	11:32	330	**2.8**	
CANARSIE POL	4/20/2006	POL2	8:36	230	**4.2**	
CANARSIE POL	4/20/2006	POL2	9:08	160	**2.9**	
CANARSIE POL	4/20/2006	POL2	9:39	220	**4.4**	
CANARSIE POL	4/20/2006	POL2	10:07	235	**4.7**	
CANARSIE POL	4/20/2006	POL2	10:35	370	**3.7**	
CANARSIE POL	4/20/2006	POL2	11:33	420	**3.4**	
TREPORTI	11/2/2005	TREP 1	11:20	90	**1.7**	
TREPORTI	11/2/2005	TREP 1	11:51	100	**1.9**	
TREPORTI	11/2/2005	TREP 1	12:22	120	**1.8**	
TREPORTI	11/2/2005	TREP 1	13:01	150	**3.7**	
TREPORTI	11/2/2005	TREP 1	13:25	70	**2.1**	
TREPORTI	11/2/2005	TREP 2	11:21	2980	**56.1**	34.9

TREPORTI	11/2/2005	TREP 2	11:52	2700	**50.8**	34.9
TREPORTI	11/2/2005	TREP 2	12:23	2350	**34.9**	34.7
TREPORTI	11/2/2005	TREP 2	13:02	730	**17.9**	34.8
TREPORTI	11/2/2005	TREP 2	13:26	1050	**16.0**	35
TREPORTI	11/2/2005	TREP 2	14:04	300	**8.5**	34.7
TREPORTI	11/2/2005	TREP 2	14:25	400	**7.5**	34.7
TREPORTI	11/2/2005	TREP 2	14:55	100	**11.3**	
TREPORTI	11/3/2005	TREP 2	9:12	1660	**42.6**	33.9
TREPORTI	11/3/2005	TREP 2	9:34	2500	**39.2**	34.1
TREPORTI	11/3/2005	TREP 2	10:10	1100	**23.0**	34.1
TREPORTI	11/3/2005	TREP 2	10:37	1680	**31.6**	34.3
TREPORTI	11/3/2005	TREP 2	11:07	2700	**39.1**	34.4
TREPORTI	11/3/2005	TREP 2	11:46	1520	**33.0**	34.5
TREPORTI	11/3/2005	TREP 2	12:12	2096	**29.6**	34.5
TREPORTI	11/3/2005	TREP 2	12:42	2060	**38.8**	34.5
TREPORTI	11/2/2005	TREP 3	11:21	4300	**78.3**	34.9
TREPORTI	11/2/2005	TREP 3	11:53	3600	**67.7**	34.8
TREPORTI	11/2/2005	TREP 3	12:24	5150	**76.5**	34.8
TREPORTI	11/2/2005	TREP 3	13:03	4100	**89.0**	34.8
TREPORTI	11/2/2005	TREP 3	13:30	5150	**85.5**	34.7
TREPORTI	11/2/2005	TREP 3	14:05	2900	**81.9**	34.7
TREPORTI	11/2/2005	TREP 3	14:25	2000	**37.6**	34.6
TREPORTI	11/2/2005	TREP 3	14:56	450	**6.7**	
TREPORTI	11/3/2005	TREP 3	9:12	5500	**141.1**	34.1
TREPORTI	11/3/2005	TREP 3	9:34	6420	**106.6**	34.1
TREPORTI	11/3/2005	TREP 3	10:10	5500	**115.0**	34.4
TREPORTI	11/3/2005	TREP 3	10:37	6400	**120.4**	34.5
TREPORTI	11/3/2005	TREP 3	11:07	1160	**72.8**	34.7
TREPORTI	11/3/2005	TREP 3	11:16	1540	**29.0**	34.7
TREPORTI	11/3/2005	TREP 3	11:46	740	**15.5**	34.7
TREPORTI	11/3/2005	TREP 3	12:13	3460	**67.4**	34.7
TREPORTI	11/3/2005	TREP 3	12:42	5460	**90.7**	34.4
TREPORTI	11/2/2005	TREP 4	14:02	1600	**39.3**	34.4
TREPORTI	11/2/2005	TREP 4	14:26	900	**16.9**	34.5
TREPORTI	11/2/2005	TREP 4	14:56	1400	**20.8**	
TREPORTI	11/3/2005	TREP 4	9:32	4060	**95.5**	34.1
TREPORTI	11/3/2005	TREP 4	9:56	820	**17.8**	34.2
TREPORTI	11/3/2005	TREP 4	10:23	4600	**92.7**	34.2
TREPORTI	11/3/2005	TREP 4	10:53	2470	**63.4**	34.3
TREPORTI	11/3/2005	TREP 4	11:15	3440	**60.7**	34.5
TREPORTI	11/3/2005	TREP 4	11:47	2780	**60.4**	34.5
TREPORTI	11/3/2005	TREP 4	12:13	244	**4.6**	34.5
TREPORTI	11/3/2005	TREP 4	12:43	260	**9.8**	34.4
PUNTA SABBIONI	11/4/2005	SABB1	10:21	-50	**-0.8**	34.8

PUNTA SABBIONI	11/4/2005	SABB1	10:55	40	**0.7**	35
PUNTA SABBIONI	11/4/2005	SABB1	11:28	100	**1.9**	35
PUNTA SABBIONI	11/4/2005	SABB1	11:58	60	**1.3**	35
PUNTA SABBIONI	11/4/2005	SABB1	12:35	106	**2.2**	34.6
PUNTA SABBIONI	11/4/2005	SABB1	13:02	155	**2.3**	34.6
PUNTA SABBIONI	11/4/2005	SABB1	13:40	210	**4.0**	34.7
PUNTA SABBIONI	11/4/2005	SABB1	14:10	0	**0.0**	34.7
PUNTA SABBIONI	11/4/2005	SABB1	14:42	108	**2.0**	34.7
PUNTA SABBIONI	11/4/2005	SABB1	15:12	80	**1.6**	34.7
PUNTA SABBIONI	11/4/2005	SABB1	15:40	140	**2.6**	34.7
PUNTA SABBIONI	11/4/2005	SABB1	16:10			
PUNTA SABBIONI	11/4/2005	SABB2	10:22	0	**0.0**	35
PUNTA SABBIONI	11/4/2005	SABB2	10:56	80	**1.4**	35
PUNTA SABBIONI	11/4/2005	SABB2	11:28	310	**5.8**	35
PUNTA SABBIONI	11/4/2005	SABB2	11:59	300	**4.7**	34.9
PUNTA SABBIONI	11/4/2005	SABB2	12:36	155	**3.4**	
PUNTA SABBIONI	11/4/2005	SABB2	13:02	240	**3.6**	34.7
PUNTA SABBIONI	11/4/2005	SABB2	13:41	196	**3.8**	34.7
PUNTA SABBIONI	11/4/2005	SABB2	14:11	100	**1.8**	34.7
PUNTA SABBIONI	11/4/2005	SABB2	14:42	460	**8.7**	34.7
PUNTA SABBIONI	11/4/2005	SABB2	15:12	300	**6.0**	34.7
PUNTA SABBIONI	11/4/2005	SABB2	15:40	360	**6.8**	34.7
PUNTA SABBIONI	11/4/2005	SABB2	16:11	450	**8.8**	34
PUNTA SABBIONI	11/4/2005	SABB3	10:22	850	**14.1**	35
PUNTA SABBIONI	11/4/2005	SABB3	11:03	330	**6.7**	35
PUNTA SABBIONI	11/4/2005	SABB3	11:31	750	**13.7**	34.9
PUNTA SABBIONI	11/4/2005	SABB3	12:03	650	**9.9**	34.8
PUNTA SABBIONI	11/4/2005	SABB3	12:40	240	**5.2**	34.7
PUNTA SABBIONI	11/4/2005	SABB3	13:06	140	**2.3**	34.7
PUNTA SABBIONI	11/4/2005	SABB3	13:42	176	**3.4**	34.7
PUNTA SABBIONI	11/4/2005	SABB3	14:11	220	**4.0**	34.7
PUNTA SABBIONI	11/4/2005	SABB3	14:42	310	**5.8**	34.7
PUNTA SABBIONI	11/4/2005	SABB3	15:12	260	**5.2**	34.7
PUNTA SABBIONI	11/4/2005	SABB3	15:40	180	**3.3**	34.7
PUNTA SABBIONI	11/4/2005	SABB3	16:12	390	**7.9**	34.3
PUNTA SABBIONI	11/4/2005	SABB3	16:40	140	**2.5**	34.3
PUNTA SABBIONI	11/10/2005	SABB3	13:14	200	**204.8**	
PUNTA SABBIONI	11/10/2005	SABB3	13:45	180	**177.4**	
PUNTA SABBIONI	11/10/2005	SABB3	14:17	160	**151.8**	29.3
PUNTA SABBIONI	11/10/2005	SABB3	14:47	160	**146.6**	29.3
PUNTA SABBIONI	11/10/2005	SABB3	15:20	780	**689.2**	29.7

APPENDIX B: DISCUSSION OF ERROR IN SGD MEASUREMENTS MADE USING SEEPAGE METERS.

Generally the actual measurement error associated with use of the seepage meters (that is the area covered by the device, the time the collection bags are left on and the volume recovered) is small <2.5 % (Zeitlin 1980, Cable et al. 2006). However, variations in seepage caused by external mechanisms may be as great as 20% and has been found to be even higher in some cases (Shinn et al. 2002). Zeitlin (1980) performed an analysis on errors in seepage meter measurements and determined that the causes of variability are: technical and measurement error (<2.5%), permeability and bioturbation differences in the sediment (~10%), differences in sea level on various time scales (e.g. waves, tides, seasonal density variation) (~20%), viscosity differences in the sediment, etc.

One way to look at the error in the SGD measurement is to attempt to duplicate and replicate measurements. Duplication of measurements involves the use of multiple seepage meters simultaneously measuring SGD located right next to each other. Replication of measurements involves the use of one seepage meter taking measurements at short intervals and seeing how well they correspond. If there is little error (variability) then the measurements when plotted against each other should fall in a one to one line with a slope that goes through zero. Zeitlin (1980) found that 50% of the duplicate measurements and 70% of the replicate measurements fell within a variation of less than 20%.

In the data described within this thesis, data collected in Jamaica Bay, Shelter Island, and Mattituck can be seen as duplicate measurements (Figures 1-3), while data collected in Mauritius, which were repeated in short intervals of time, can be treated as

replicate measurements (Figure 4). In both Shelter Island and in two sites in Jamaica Bay, there was a very good correlation between rates measured in both meters, with y-intercepts close to the origin. In addition, the duplicate measurements were also consistent, especially so for the data collected in Mattituck. The trend of the duplicate measurements at Mattituck had a y-intercept of zero and displayed the same temporal pattern. Only Mauritius is shown to examine the replication of measurements, as the time interval for all other sites is too long to separate error from common temporal variation in discharge. In Mauritius measurements were made every 5 minutes and, therefore temporal variation should not have been the cause of discrepancies in discharge.

After calculating a mean and variance for each pair of measurement, a standard deviation can be calculated for the pooled data. Excluding one set of measurements (Mattituck 1 vs. 2; Figure 3) because the variance showed a strong linear correlation to the mean, the pooled standard deviation was 9.0 cm d^{-1} on a pooled mean of 73.2 cm d^{-1} (Figure 5), or +/- 12%. For the one set of data (Mattituck 1 vs. 2) that showed a linear trend between the standard deviation and the mean, the standard deviation was 35% of the mean. These values are similar to the values estimated by Zeitlin from data taken only in Great South Bay, NY.

Zeitlin M. 1980. Variability and Predictability of Submarine Groundwater Flow into a Coastal Lagoon, Great South Bay, NY. Master's Thesis. State University of New York at Stony Brook. 110 pages.

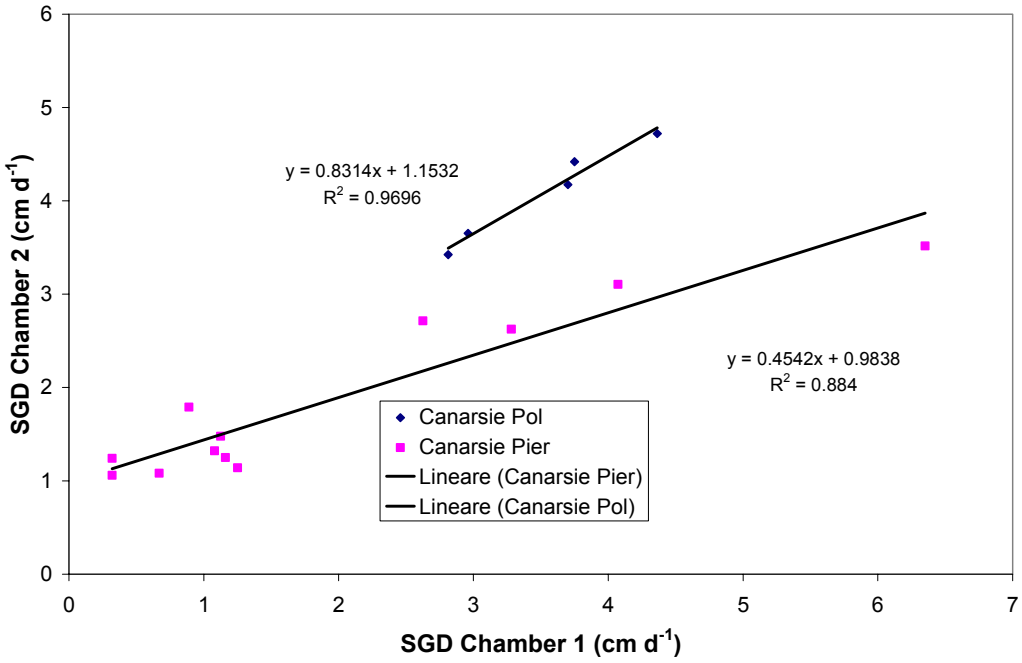

Figure 1. Duplicate measurements at two sites in Jamaica Bay

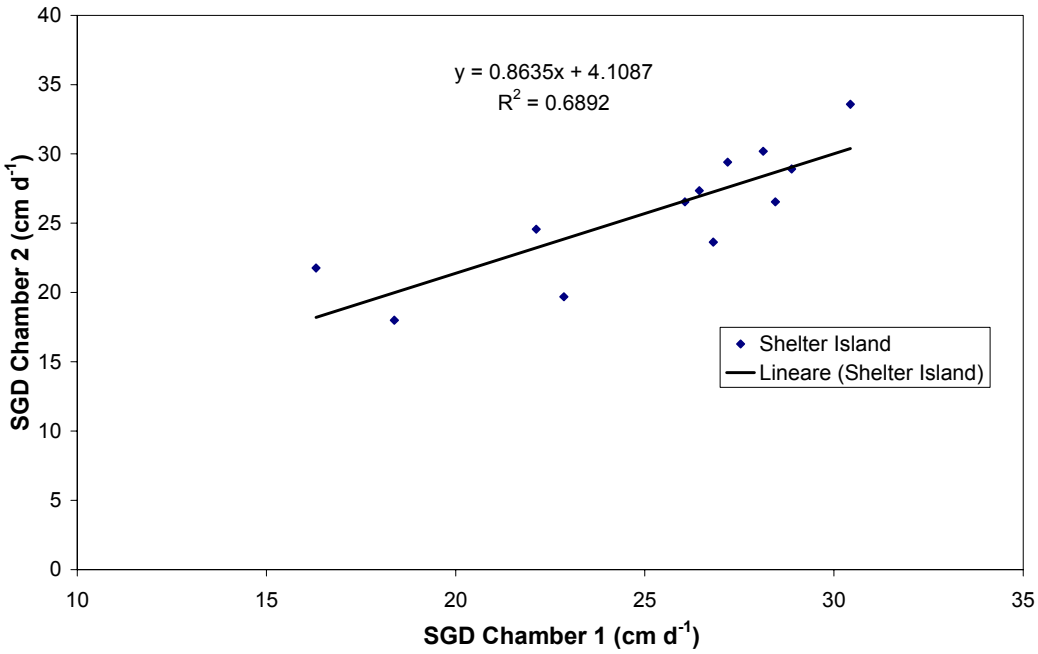

Figure 2. Duplicate measurements at Shelter Island

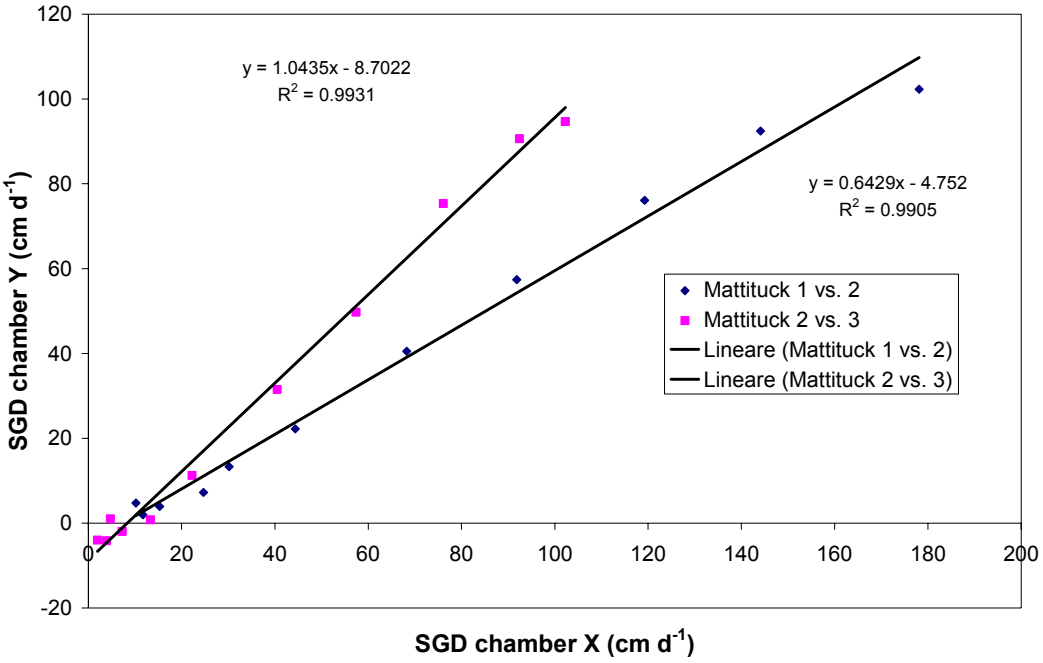

Figure 3. Duplication of seepage at Mattituck NY. The Blue dots represent the relationship between seepage meters M1 and M2, meanwhile the pink squares represent the relationship between M2 and M3.

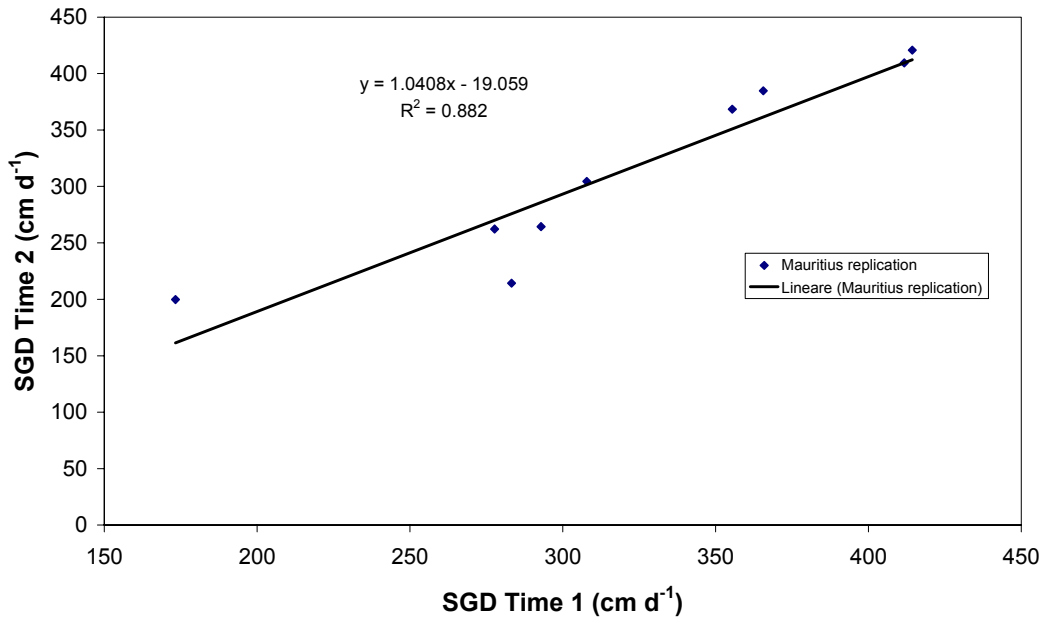

Figure 4. Time replication of SGD measurements at Mauritius, each measurement taken for 5 minutes immediately after one another.

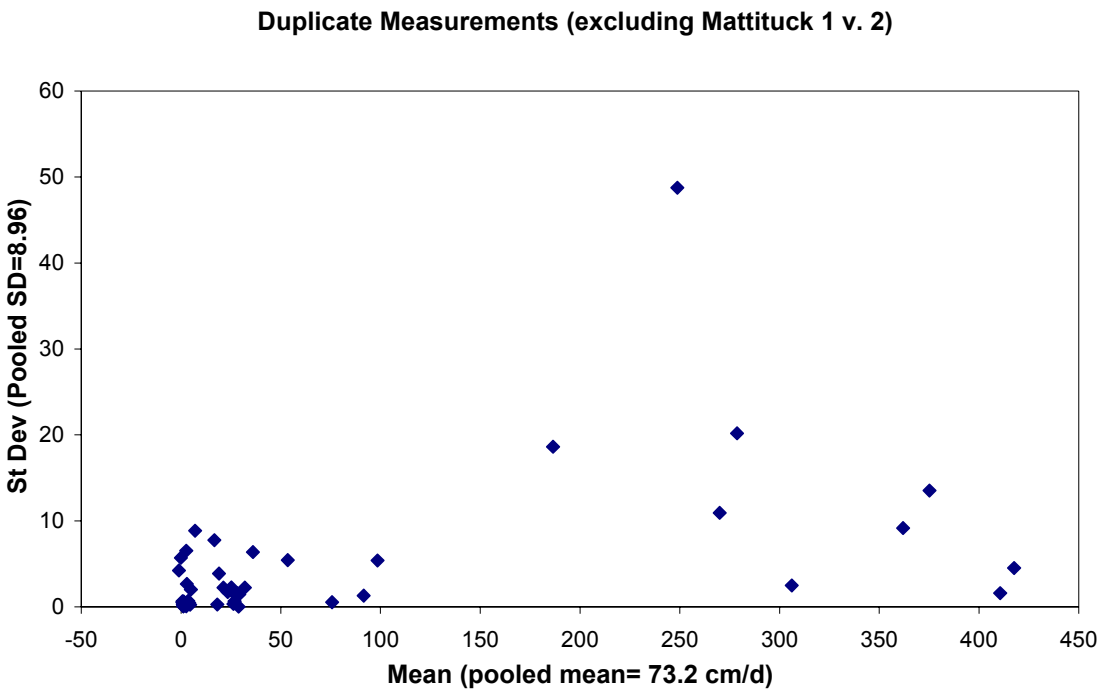
Duplicate Measurements (excluding Mattituck 1 v. 2)
St Dev (Pooled SD=8.96)
Mean (pooled mean= 73.2 cm/d)
60
50
40
30
20
10
0
-50
0
50
100
150
200
250
300
350
400
450

Figure 5

APPENDIX C: EVOLUTION OF THE VENICE LAGOON AS SEEN THROUGH MAPS. www.salve.it [3]

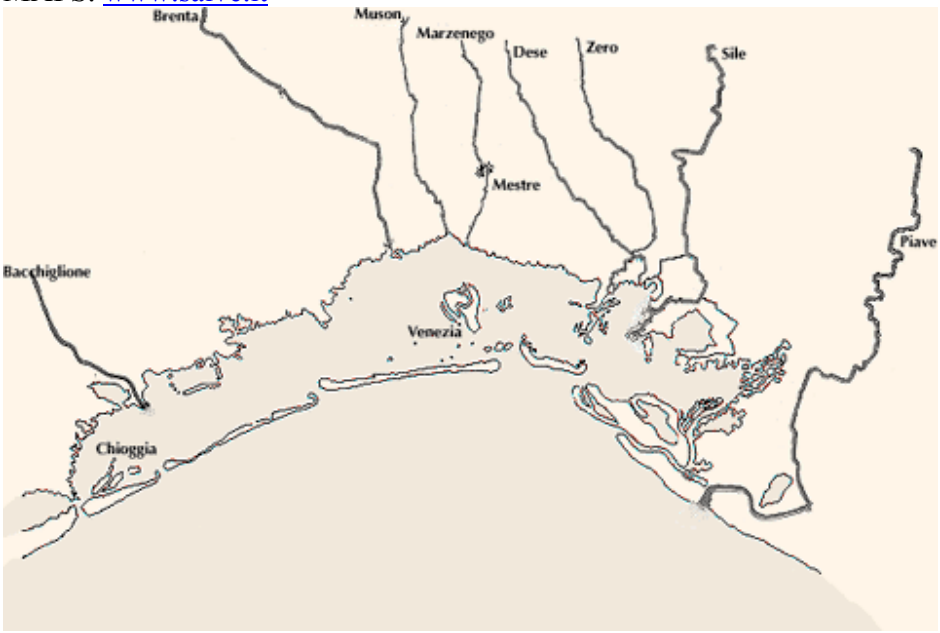

1300 AD: the lagoon before major anthropogenic modification

1350: Beginning of the diversion of major rivers

[3] Maps copied with permission from the SALVE website. www.salve.it.

1400: Diversion of the Brenta River further south. In put of sand into the Cavallino littoral zone.

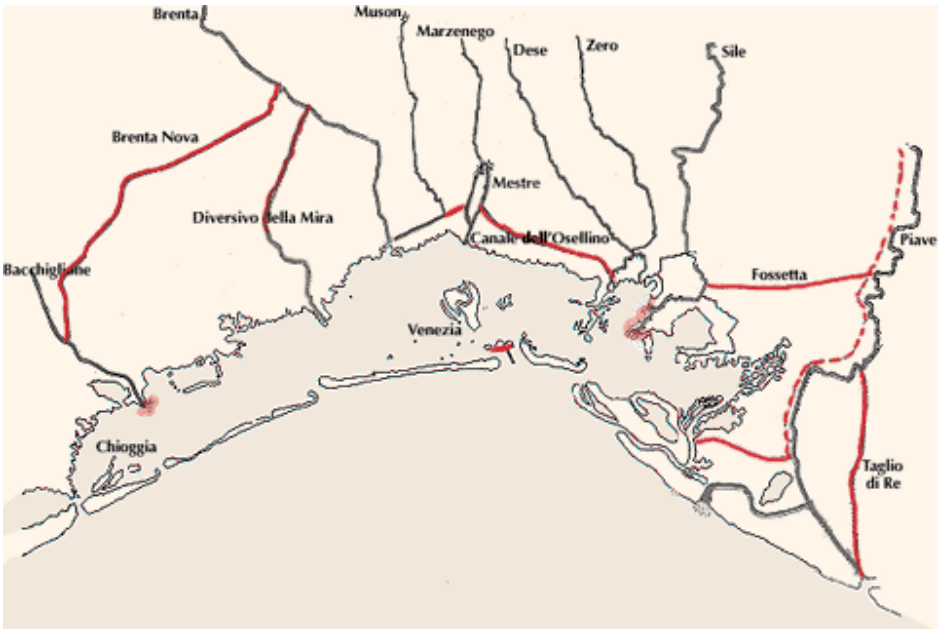

1500: Diversion of Brenta River further south and the Piave River out of the lagoon. Fortification of the Lido inlet.

1550: Diversion of the Brenta River out of the lagoon. Dredging of a deep navigation channel from the Malamocco inlet to the city.

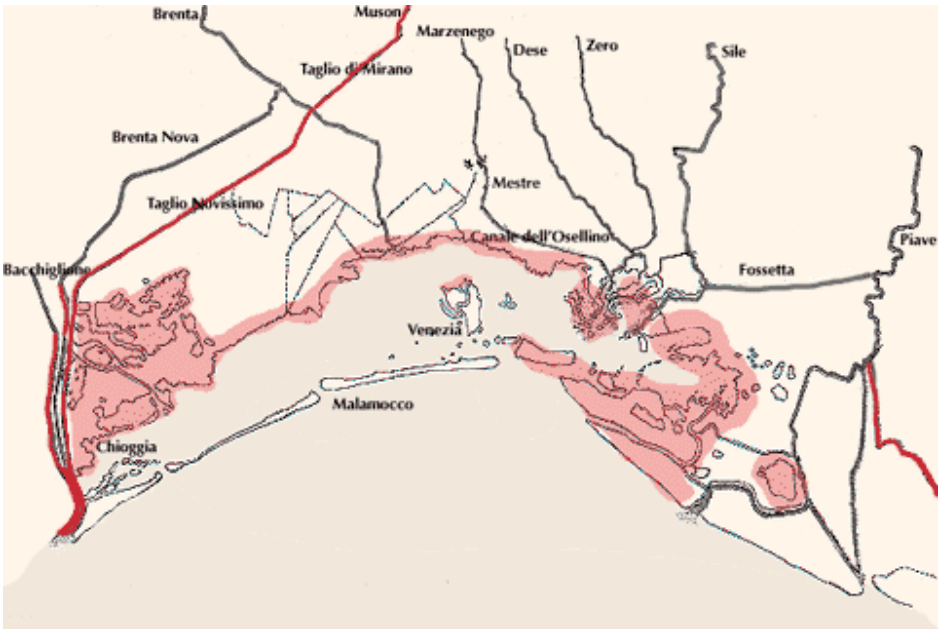

1600: Emplacement of sand and other sediment around the lagoon to stabilize its borders

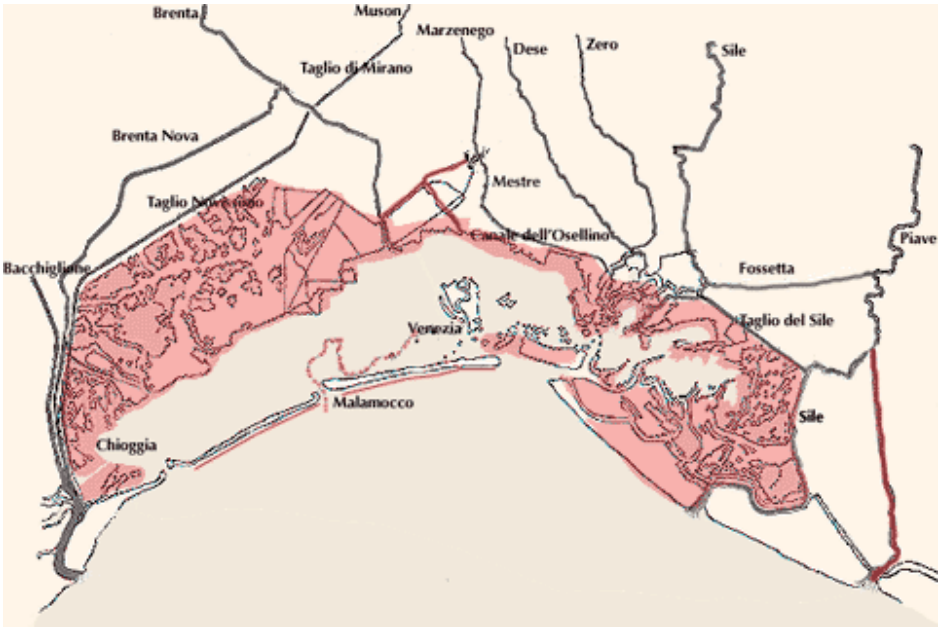

1700: Emplacement of bulkheads among much of the lagoons islands and surrounding land

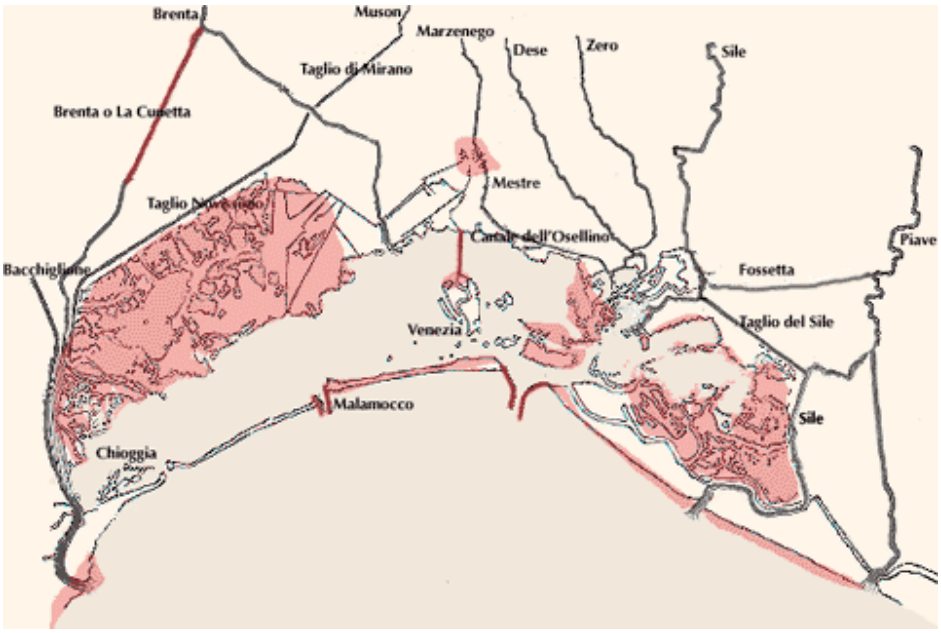

1800: Replenishment of beaches and construction of the railroad bridge to Venice

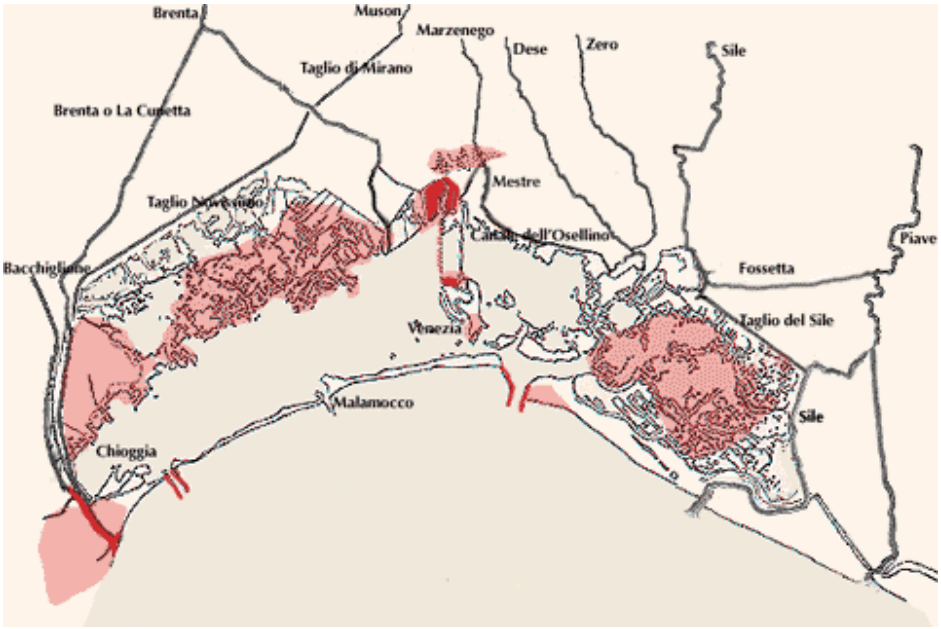

1900: Emplacement of large jetties to permanently fix the position of the inlets. Beginning of the creation of the industrial zone

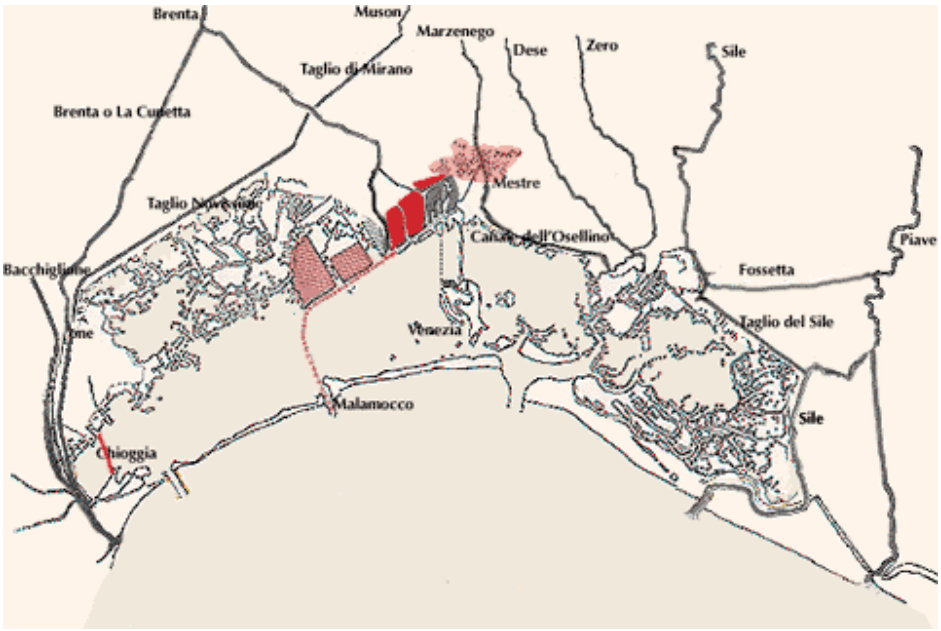

Today: Finishing the Porto Marghera Industrial Zone, dredging of the deep Malamocco-Marghera transport canal, and as of today the “MOSE” project